AN EXPLORATION OF BIOCHEMISTRY INCLUDING BIOTECHNOLOGY, STRUCTURAL CHARACTERIZATION, DRUG DESIGN, AND CHROMATOGRAPHIC ANALYSES

A Dissertation
Presented to
The Academic Faculty

By

Kristi Lee Burns

In Partial Fulfillment
Of the Requirements for the Degree
Doctor of Philosophy in Chemistry and Biochemistry

Georgia Institute of Technology

May 2007

AN EXPLORATION OF BIOCHEMISTRY INCLUDING BIOTECHNOLOGY, STRUCTURAL CHARACTERIZATION, DRUG DESIGN, AND CHROMATOGRAPHIC ANALYSES

Approved by:

Dr. Sheldon W. May, Advisor
School of Chemistry and Biochemistry
Georgia Institute of Technology

Dr. James C. Powers
School of Chemistry and Biochemistry
Georgia Institute of Technology

Dr. Donald F. Doyle
School of Chemistry and Biochemistry
Georgia Institute of Technology

Dr. Stanley H. Pollock
Department of Pharmaceutical Sciences
Mercer University

Dr. Leslie T. Gelbaum
School of Chemistry and Biochemistry
Georgia Institute of Technology

Date Approved: [September 28, 2006]

for my husband, Mark Thomas Carlson, who agreed that staying in school and becoming fake doctors together would be a cool idea.

ACKNOWLEDGEMENT

I would like to express my thanks to my advisor, Dr. May, for his constant support and encouragement. I owe a special debt of gratitude for the many hours he spent with me developing my writing; I hope a few of those many lessons shine through in this work. I particularly appreciate his seemingly infinite patience and willingness to allow me to develop into a solid laboratory researcher, especially during the early years when he must have been convinced that I would break each and every piece of equipment in his laboratory. I would like to thank Dr. Charlie Oldham, who taught me far more than just how to fix every piece of broken equipment. He taught me day in and day out, with patience and sometimes frustrated with a bright red face. Charlie, you are a rare gem, thank you.

I would also like to thank my undergraduate advisor, Dr. Elena Rybaka-Akimova, who taught me about the sheer joy and love of science, and that there is no stronger driving force in the universe than positive reinforcement. I would like to thank Dr. Williams for seeing 'something' in me and always backing me up behind closed doors.

I am very grateful for the constant intellectual and emotional support provided by my many lab mates. I would like to thank my many lab mates, Jennifer Lane, Maggie Gunnerson, Tiffany Huang, Veronica De Silva, Jeremy Thompson, Michael 'Misha' Lubarsky, Nadia Bogouslouvsky, Kelly 'KJ' Dennison, Josh Sasine,

and Di Wu for the many lessons you all have taught me. Michael Foster, who honed my thinking skills, always pushing me to think quicker, faster, more in depth, and always with a sense of humor.

Finally, I would like to thank family without whom I could never have achieved my goals.

We thank the National Textile Center for partial support of the PHB and iso-CoA work and the National Science Foundation Grant # BIR-9306392 for partial funding of the solution NMR spectrometers.

TABLE OF CONTENTS

LIST OF TABLES

LIST OF FIGURES

LIST OF SYMBOLS AND ABBREVIATIONS

AcCoA	acetyl coenzyme A
AcAcCoA	acetoacetyl-CoA
ATP	adenosine triphosphate
CDB	1-(carboxymethyl)-3,5-diphenyl-2-methylbenzene
CNP	2’,3’-cyclic-nucleotide 3’-phosphodiesterase
CoA	free coenzyme A
COSY	correlation spectroscopy
COX	cyclooxygenase
DCW	dry cellular (cell) weight
DMSO	dimethyl sulfoxide
DTNB	Ellmann’s reagent, 5,5'-dithiobis(2-nitrobenzoic acid)
EBSELEN	2-phenyl-1,2-benzisoselenazole-3(2H)-one
EDC	1-ethyl-3-(3-dimethylaminopropyl) carbodiimide
EDTA	ethylenediaminetetraacetic acid
EGF	epidermal growth factor
ELISA	enzyme-linked immunosorbent assay
EPPS	4-(2-Hydroxyethyl)piperazine-1-propanesulfonic acid
GI	gastrointestinal
GSH	glutathione, reduced form
GSSG	glutathione, oxidized disulfide dimer form
HBCoA	β-hydroxybutyryl-CoA

hCNP-CF	human brain 2′,3′-cyclic-nucleotide 3′-phosphodiesterase
HMQC	heteronuclear multiple quantum correlation
HOMePAES	[(±)1-(4′-hydroxyphenylthio)-2-aminopropane] hydrochloride
HOMePAESe	1-(4′-hydroxyphenylseleno)-2-aminoethane
HPLC	high performance liquid chromatography
IC_{50}	inhibition constant at 50 percent
LB media	Luria-Bertani media
MDB	1-methanesulfonamide-3,5-diphenyl benzene
MS	mass spectrometry
MST	methylsulfone terphenyl
MRM	multiple reaction monitoring
NADPH	reduced β-nicotinamide-adenine dinucleotide phosphate
$NADP^+$	oxidized β-nicotinamide-adenine dinucleotide phosphate
NMR	nuclear magnetic resonance
NSAID	non-steroidal anti-inflammatory drugs
OD_{600}	optical density (absorbance) at a wavelength of 600 nanometers.
PAES	[2-(phenylthio)ethylamine] hydrochloride
PAESe	1-(phenylseleno)-2-aminopropane.
PGHS	prostaglandin H synthase
PHB	poly-(β)-hydroxybutyric acid
PMSF	phenylmethanesulfonyl fluoride
RP-HPLC	reversed phase high performance liquid chromatography
SDS	sodium dodecyl sulfate

TBAHS	tetrabutylammonium hydrogen sulfate
TCEP	triscarboxyethyl phosphine

SUMMARY

This thesis has several topics, which we list here and then summarize in more detail. The topics are:

I. POLY-(BETA)-HYDROXYBUTYRIC ACID

A. ANALYSIS OF THE IN VITRO BIOSYNTHESIS OF POLY-(BETA)-HYDROXYBUTYRIC ACID

B. DESIGN AND OPTIMIZATION OF A POLY-(BETA)-HYDROXYBUTYRIC ACID EDUCATIONAL LABORATORY

II. ISO-COENZYME A: THE FIRST STRUCTURAL CHARACTERIZATION, ENZYMATIC ANALYSIS, AND REGIOSELECTIVE SYNTHESIS

III. RATIONAL DESIGN AND ANALYSIS OF NOVEL SELECTIVE PROSTAGLANDIN SYNTHASE-2 NON-STEROIDAL ANTIINFLAMMATORY DRUGS FOR THE TREATMENT OF INFLAMATION

IV. SELENIUM REDOX CYCLING IN THE PROTECTIVE EFFECTS OF ORGANOSELENIDE-ANTIOXIDANTS AGAINST PEROXYNITRITE-INDUCED DNA DAMAGE

Poly-(β)-hydroxybutyric acid (PHB) is a biodegradable, thermoplastic biopolyester produced as a carbon-energy storage source by bacteria that are challenged by nutrient limitation. While production of PHB for industrial applications is generally accomplished via fermentation, *in vitro* enzymatic synthesis can be an attractive alternative. We now report a detailed analysis of the *in vitro* biosynthesis of PHB using the three-enzyme system from *Cupriavidus necator*. We have developed quantitative HPLC

methodology which resolves CoA, acetyl-CoA, acetoacetyl-CoA, and β-hydroxybutyryl-CoA with baseline resolution and then utilized this methodology to elucidate the fluctuations in metabolite concentrations and the effect of each individual enzyme on the overall system. The experimental results were then used to design the first kinetic model for *in vitro* PHB biosynthesis. All previous modeling studies of PHB production have been designed to analyze *in vivo* biosyntheses, typically in bacteria but also in yeast and plants. Our results can therefore serve as a basis for further development of the potential of *in vitro* enzymatic syntheses of polyesters as a compliment to the more widely used approach of *in vivo* production of these polymers.

Iso-coenzyme A (iso-CoA) is an isomer of coenzyme A (CoA) in which the monophosphate is attached to the 2′-carbon of the ribose ring. While iso-CoA was first reported in 1959 by Khorana and coworkers to be a byproduct of the chemical synthesis of CoA, relatively little literature attention has been focused on iso-CoA or on acyl-iso-CoA compounds. We now report, in chapters 6 through 10, the first structural characterizations of iso-CoA, acetyl-iso-CoA, acetoacetyl-iso-CoA, and β-hydroxybutyryl-iso-CoA using MS, MS/MS, and homo- and hetero-nuclear NMR analyses. All previous characterizations of the structure of iso-CoA have been based on chromatographic analyses, which ultimately rest on comparisons with the degradation products of CoA and NADPH, or have been based on assumptions regarding enzyme specificity. We

describe HPLC methodology to separate the isomers of several iso-CoA-containing compounds with baseline resolution. We also report here the first examples of iso-CoA-containing compounds acting as substrates in enzymatic acyl-transfer reactions. Finally, we describe a simple synthesis of iso-CoA from CoA, which utilizes β-cyclodextrin to produce iso-CoA with high regioselectivity. We also demonstrate a plausible mechanism, which accounts for the existence of up to 18% of the iso-CoA isomers in commercial preparations of CoA-containing compounds. Considering that approximately 9% of all classified enzymes utilize CoA or acyl-CoA substrates, we anticipate that these results will provide the necessary methodology and impetus for investigating iso-CoA compounds as potential pseudosubstrates or inhibitors of the more than 350 known CoA-utilizing enzymes.

In Chapters 11 through 13 we report that phenylaminoethyl selenide compounds protect DNA from peroxynitrite-mediated single-strand breaks (1). Moreover, these organoselenium compounds protect DNA more effectively than their sulfur analogues. Additionally, the ability of glutathione to enhance the protective effects of the selenium-containing compounds against peroxynitrite-induced DNA damage suggests that a selenium redox cycle, in which the peroxynitrite-generated selenoxide is recycled back to a selenide via glutathione, has been established. The mechanism of protection against peroxynitrite mediated DNA damage was investigated by HPLC for the selenium- and corresponding sulfur-containing compounds. HPLC analysis

shows that phenylaminoethyl selenides are quickly oxidized by peroxynitrite forming selenoxides as the sole selenium-containing product. Moreover, in the presence of reduced glutathione, the selenide to selenoxide ratio was higher suggesting the establishment of a glutathione-mediated catalytic redox cycle. Phenylaminoethyl sulfide (PAES) was, likewise, shown to react slowly with peroxynitrite to form a small quantity of the sulfoxide as the main product but no redox cycle could be established with the sulfur analogues (1). Finally, the unique chemistry of the reaction between peroxynitrite and HOMePAES was investigated using HPLC and HPLC/MS.

Finally, in chapter 14, we report the development of novel CDB derivatives, which are selective COX-II inhibitors. A series of compounds were assayed with an in vitro colorimetric inhibitor screening and with a whole blood ELISA screening and the results indicate that MST is a selective inhibitor of COX-II.

AN EXPLORATION OF BIOCHEMISTRY INCLUDING BIOTECHNOLOGY, STRUCTURAL CHARACTERIZATION, DRUG DESIGN, AND CHROMATOGRAPHIC ANALYSES

VOLUME I

By

Kristi Lee Burns

CHAPTER 1

PHB Introduction

A Brief History of Enzyme Catalysis. Enzymes are nature's catalysts. These proteins catalyze a rich variety of metabolic transformations, doing so with very high catalytic rates under mild conditions, and with high regioselectivity and stereospecificity. Given the vast potential of enzymes, it seems obvious that societies would foster development of this technology. Indeed, enzymatic reactions have been exploited for millennia by cultures which use bacterial enzymes to ferment milk into yogurt and kefir, yeast enzymes to bake and brew, the enzyme rennin from stomachs of ruminant animals for cheese production, and even proteases from fruits like papaya (papain) and pineapple (bromelain) to tenderize meat (2).

Modern enzyme technology. Modern enzyme technology dates to the 1833 partial isolation of an amylase enzyme, diastase, by Payen and Persoz (3). The slow advance of enzyme technology through the rest of the 19th and early into the 20th century laid the foundation for the leaps in enzyme biotechnology of the last 50 years. Early advances of particular note include Berzelius's 1835 (4) general theory of catalysis and Kuhne's 1878 coinage of the descriptive term 'enzyme' (from the Greek 'en' for in and 'zyme' for yeast). Despite Kuhne's apparently deliberate coinage, he did not prove that enzymes were distinct entities

from the yeast from whence they came and this contention remained unproven until 1897 when the Buchner brothers generated ethanol from glucose using a cell-free yeast extract. Theoretical advances like the 1894 publication of Emil Fisher's lock-and-key hypothesis proved just as important in advancing enzymology as the more tangible crystallization of the first enzyme, Jack Bean urease, by Sumner in 1926, which led to his determination that enzymes were proteins (4).

Enzymes in Industrial Biotechnology. The use of enzymes in industrial biotechnology can be traced back to Christian Hansen's 1874 industrial scale saline extraction of chymosin from calf stomachs (5), which was used for cheese production. This was shortly followed by Japanese scientist Jokichi Takamine's development of an industrial scale isolation of takadiastase, a well-known fungal amylase. Takamine's 1894 patent was the first for enzymology and this important enzyme was critical to the early structural determinations of sugar-containing compounds including CoA, NAD(P)H, and DNA (5).

Despite the 19th and early 20th century advances in enzyme biotechnology the commercial potential for enzymes was not fully explored or implemented in earnest until after the close of the Second World War. In the leather industry, trypsin-containing pancreatic extracts were first developed in 1917, but these extracts did not replace the disgusting historical practice of using pigeon and dog excrement in the leather bating process

until after WWII (5). The detergent industry finally grasped the full potential of enzymes in the late 50's and early 60's with the development of Alcalase, a pH stable (pH 8-10) microbial alkaline protease, which was successfully incorporated into commercial laundry detergents. The starch industry also flourished from innovations like the use of fungal amylases for syrup production in the 1950's, amyloglucosidases—which could entirely hydrolyze starch to glucose—in the 1960's, and glucose isomerases (glucose to fructose) in the 1970's. By combining the action of these enzymes, in the 1980's, the starch industry successfully developed a process for producing high fructose corn syrup from starch (5); this has remained the starch industry's most dominant sweetener with a global annual sales topping 1 billion.

Industrial Enzymes the Second Revolution. The advances in molecular biology and genetic engineering of the 1980's prompted a second 'revolution' in the industrial enzyme sector which facilitated the generation of the first recombinant enzyme, Lipolase®, which was released in 1987 as a detergent additive (6). More recent advances center around protein engineering which can employ rational design techniques, like site-directed mutagenesis, which led to Novozyme's development of a bleach-stable detergent enzyme—Everlase® (7). Another recent engineering methodology is the non-rational technique of directed evolution (8), which Diversa Corp. (9) employed to optimize a

xylanase enzyme so that it is stable at temperatures in excess of 90°C (10).

Rationale for the use of Industrial Enzymes. There are numerous reasons that enzymes are considered highly attractive for industrial syntheses (11-14). Enzymes are well known for the capacity to catalyze reactions under very rapid rates with exquisite selectivity; thus, generating fewer unwanted side effects, less by-products and lower product clean-up costs than with traditional syntheses (14). Enzymes are often able to function under pH, temperature and pressure, and solvent conditions that are amenable to life. Furthermore, enzymes derived from extremophiles or via genetic modification can efficiently catalyze reactions under conditions extreme to life; this type of enzymatic reactions can be exploited for energy savings and pollution prevention. Unlike many chemical biocatalysts, which are often made of heavy transition metals or toxic compounds, enzymes themselves are non-toxic and biodegradable to the environment; thus, eliminating at least one potentially expensive waste stream (5,11-13,15).

Enzymes are now an integral part of the industrial biotechnology sector. As of 2003 the global sales of industrial enzymes were estimated at $2.3 billion with 35% in detergents, 28% in food applications, 17% in agriculture/feed, 10% in textile processing, and the remaining 10% divided among paper/pulp,

leather, synthesis of fine/bulk chemicals, personal care, and fuel industries (2,16). The classic rationale in favor of employing enzymes in industrial synthesis is their exquisite regio- and enantio-selectivity. However, a paradigm shift is occurring within industry to an emphasis on industrial sustainability.

White Biotechnology. Sustainability, with regard to industrial biotechnology, refers to specifically integrating the traditionally disparate industrial objectives of increasing market shares, engaging in environmentally sustainable practices, and promoting socially acceptable practices, into a single harmonious triad. This general trend has led to the development of the term white (or industrial) biotechnology, a phrase recently coined by the 2003 European Association for Bioindustries (EuropaBio) Conference (16). White biotechnology refers to all bio-based sustainable industrial chemistry and is distinguished from plant-based (green) or medical-based (red) biotechnologies (16). White biotechnology has been high on international agendas over the past few years as evinced by several recent publications by the OCED (17,18), EuropaBio (19), SusChem, (20)—a dedicated website for the European Technology Platform for Sustainable Chemistry containing representatives from many of the major European chemical manufactures—and the Road Map for Biomass Technologies in the United States (21,22).

Development of a sustainable bio-based economy that uses eco-efficient bioprocesses and renewable bio-resources is considered a "key strategic challenge for the 21st century" by the 30 nation consortium of the OECD (the Organization for Economic Cooperation and Development) (17,18). White biotechnology, which is critical to this initiative, encompasses the entire sphere of bio-based products, including utilization of bio-feedstock and the development of microbial bioreactors, and enzyme biotechnology obviously plays a critical role in this rapidly developing field.

A classic example of the potential of white-enzyme biotechnology to alleviate environmental concerns while increasing company profit margins was developed and implemented by the Mitsubishi-Rayon Co (22). In this case, the immobilized enzyme nitrile hydratase has replaced the two previous techniques, which used either a copper catalyst or sulfuric-acid hydrolysis to synthesize acrylonitrile from acrylamide (22). The nitrile hydratase process decreases reaction temperatures, increases single-pass conversion rates to 100%, eliminates the need for product concentration, and decreases energy and CO_2 emissions 5 fold (11). In this instance, enzyme technology has created a more efficient and environmentally friendly process, decreased production costs, and increased the resulting bottom line.

White Biotechnology in the Pharmaceutical Industry. The pharmaceutical industry is increasingly incorporating white and enzyme biotechnology into their syntheses because in this industry high enzyme costs are easily offset by the high profit margins of the pharmaceuticals. In certain situations, enzyme specificity can be used in enantioselective syntheses in order to avoid undesirable byproducts, which may pose a public health risk. The lessons learned from the tragic side effects of one of the thalidomide isomers prompted the FDA's current stance of pushing pharmaceutical companies to identify and market only the active enantiomer of a drug (23). Marketing only the active isomer reduces the risk of unintended and potentially dangerous side effects.

Additionally, enzyme biotechnology will likely be exploited in the pharmaceutical industry's latest tactic of patenting single isomeric forms of drugs, which were previously marketed as isomeric mixtures, in order to maintain patent and marketing exclusivity. To date, so called chiral switch drugs, which include Nexium—the S enantiomer of Prilosec, Lexapro—the S enantiomer of Celexa, Focalin—the R,R diasteriomer of Ritalin, and Xyzal—the R enantiomer of Zyrtec, have been generated via chiral syntheses and purifications, but new selective enzyme technologies are on the horizon (24,25).

The pharmaceutical industry also utilizes enzyme biotechnology for the design of syntheses, which increase efficiency by decreasing the number of synthetic steps, reduce

costs by eradicating or downsizing the use of expensive chiral precursors, and eliminating costly and complex downstream isomer purifications. DSM has been enzymatically synthesizing cephalexin on an industrial scale for several years (26). In this case, an in house immobilized penicillin G acylase enzyme (27,28), called Assemblase 7500 (26), was developed which catalyzes the conversion of D-phenylglycine amide and 7-amino desacetoxy cephalosporanic acid to the cephalosporin analog, cephalexin (26,29). In this instance, the careful design of the immobilized enzyme has increased the efficiency of downstream processing (26). An immobilized enzyme with a density less than water was designed which can be removed easily by skimming the immobilized enzyme off the top of the reaction solution in which the product has precipitated and sunk to the bottom (26). The commercial chemo-enzymatic production of cephalexin is preferred over the traditional 10-step chemical method because it uses less input chemicals, obviates the need for hazardous solvents like phosphorous pentachloride and dichloromethane; this reduces the waste stream (19,30). Overall, DSM's enzyme process reduces materials used and energy consumption by 65% and reduces overall costs by 50% (19).

White-Enzyme Biotechnology Increases Product Value. Enzyme biotechnology has the potential to add value to products while increasing profit margins and protecting the environment. In the textile industry, tremendous advances have been achieved by

employing enzymes in the fabric polishing process (6,12,31,32). This process, known as bio-polishing, imparts a softness to fabrics that lasts multiple washing cycles; the traditional chemical processes last only a few washes and have a higher environmental impact (12). In a related process, enzymes like cellulose (31,32) are being used to achieve the 'stone-washed' appearance of denim without the use of pumice stones, which are a non-renewable mined resource. The economic rationale for using enzymatic bio-stoning instead of pumice stones is not immediately apparent since enzyme costs are roughly equivalent pumice stones. However, a complete economic accounting clearly indicates that enzymes are more cost effective when considering that the enzymatic bio-stoning decreases damage to fabrics, product variation, rejected fabrics, reduces wear and tear on washing machines, eliminates stone storage and disposal costs, manual labor for de-stoning and removing pumice grit from garments, and increases machine space for garments instead of stones (12).

Green Chemistry. Green chemistry is a major component of sustainable industry and white biotechnology (14). The term green chemistry was coined over 10 years ago (33) and is defined as the design, development and implementation of chemicals, processes and products that reduce or eliminate the use or generation of substances hazardous to human health and the environment (33-35). The 12 principles of green chemistry laid out by the US Environmental Protection Agency (35,36), listed in

Table 1, clearly indicate the intimate connection between enzyme biotechnology and green chemistry .

Indeed, the 2005 Presidential Green Chemistry Challenge Award for Alternative Synthesis Pathways was presented to Novazyme and the Archer Daniels Midland Company for their joint development and commercialization of NovaLipid™ an enzymatic process for interesterification of vegetable oils using Lipozyme® (37,38). This enzymatic process positively affects human health by replacing partially hydrogenated vegetable oils with interesterified oils, which contain higher polyunsaturated fatty acid levels and no unhealthy trans-fats. Additionally, this process benefits the environment by eliminating certain byproducts, waste streams, and several harsh chemicals, and by increasing product yields from edible oil resources (37,38). This technology will likely be quite desirable to the food industry because of the new FDA mandate requiring that manufacturers list trans fatty acids on the Nutrition Facts panel of foods and some dietary supplements (39).

Table 1. 12 Principles of Green Chemistry Developed by the U.S. Environmental Protection Agency (35,36).

1	**Prevent waste**	Design chemical syntheses to prevent waste, leaving no waste to treat or clean up.
2	**Design safer chemicals and products**	Design chemical products to be fully effective, yet have little or no toxicity.
3	**Design less hazardous chemical syntheses**	Design syntheses to use and generate substances with little or no toxicity to humans and the environment.
4	**Use renewable feed stocks**	Use raw materials and feed stocks that are renewable rather than depleting. Renewable feedstocks are often made from agricultural products or are the wastes of other processes; depleting feedstocks are made from fossil fuels (petroleum, natural gas, or coal) or are mined.
5	**Use catalysts, not stoichiometric reagents**	Minimize waste by using catalytic reactions. Catalysts are used in small amounts and can carry out a single reaction many times. They are preferable to stoichiometric reagents, which are used in excess and work only once.
6	**Avoid chemical derivatives**	Avoid using blocking or protecting groups or any temporary modifications if possible. Derivatives use additional reagents and generate waste.
7	**Maximize atom economy**	Design syntheses so that the final product contains the maximum proportion of the starting materials. There should be few, if any, wasted atoms.
8	**Use safer solvents and reaction conditions**	Avoid using solvents, separation agents, or other auxiliary chemicals. If these chemicals are necessary, use innocuous chemicals.
9	**Increase energy efficiency**	Run chemical reactions at ambient temperature and pressure whenever possible.
10	**Design chemicals and products to degrade after use**	Design chemical products to break down to innocuous substances after use so that they do not accumulate in the environment.
11	**Analyze in real time to prevent pollution**	Include in-process real-time monitoring and control during syntheses to minimize or eliminate the formation of byproducts.
12	**Minimize the potential for accidents**	Design chemicals and their forms (solid, liquid, or gas) to minimize the potential for chemical accidents including explosions, fires, and releases to the environment.

Green Plastics. Green plastics, named after the green chemistry movement and interchangeably called bio-based plastics/polymers, are defined as any or all polymers produced in a manner consistent with green chemistry (40). Green plastics include polymers that are synthesized from agricultural and petroleum feed stocks, and may or may not be degradable, biodegradable, or compostable (40,41). Once only a fledgling enterprise, green plastics are currently growing into a mature international industry.

Petrochemically Derived Green Plastics. Perhaps the most liberal use of the green plastics classification applies to the traditional petrochemically derived polymers, which are synthesized using the principles of green chemistry. An excellent example of this type of green chemistry is the Ultimer Process that was developed by the Nalco chemical company and was awarded the 1999 Presidential Green Chemistry Award in the Alternative Solvents/Reaction Chemistry category (42). The Ultimer process utilizes an aqueous dispersion polymerization technique to generate water stable colloids of acrylamide polymers. This technique eliminates the use of hydrocarbon solvents and surfactants, utilizes a byproduct of nylon synthesis that would otherwise be treated as industrial waste, generates a product of higher quality then the chemical process, and therefore is more cost efficient (42).

Biopolymers are Green Plastics. Likely the most narrowly defined category of green plastics are known as biopolymers,

which are polymeric substances that are specifically formed in a biological system (43). Bioplastics have been organized into eight classes as follows: polynucleotides (DNA, RNA); polyamides (peptides and proteins including enzymes, silk, keratin, and collagen); polysaccharides (starch, glycogen, cellulose, chitin); polyisoprenes (rubbers and some gels); lignin (the phenolic polymer that acts as the cementing matrix in wood); polyphosphates (believed to be involved in signal transduction); poly-β-hydroxyalkanoic acids or PHAs (PHB, PHBV); and the newly discovered polythioesters (44).

Classifications of Other Green Plastics. Many green polymers do not fit into the previously discussed categories of biopolymers or green petrochemical plastics. These green plastics may be derived from fossil fuels or agricultural feedstocks, produced chemosynthetically or biologically, and may be degradable, biodegradable or compostable. Various organizations have established controlled scientifically verifiable standards for classifying the characteristics of degradable, biodegradable, and compostable plastics; the ASTM terminology and standards are listed in Table 2 (45-48). We note that even the historic petrochemically derived plastics , including nylon-66, polyethylene, and polypropylene, can disintegrate over time via chemical and photochemical mechanisms and sheer forces, and under certain conditions these polymers can eventually decay into a friable powder; however this process

requires decades to years, which disqualifies these polymers as readily degradable or green (49,50).

Table 2. ASTM Terminology and Definitions (45,46).

Polymer	A substance consisting of molecules characterized by the repetition (neglecting ends, branch junctions, and other minor irregularities) of one or more types of monomeric units.
Plastic	A material that contains as an essential ingredient one or more organic polymeric substances of large molecular weight, is solid in its finished state, and, at some stage in its manufacture or processing into finished articles, can be shaped by flow.
Degradable plastic	A plastic designed to undergo a significant change in its chemical structure under specific environmental conditions, resulting in a loss of some properties that may be measured by standard methods appropriate to the plastic and the application in a period of time that determines its classification.
Biodegradable plastic	A degradable plastic in which the degradation results from the action of naturally occurring microorganisms such as bacteria, fungi, and algae.
Compostable plastic	A plastic that undergoes degradation by biological processes during composting to yield carbon dioxide, water, inorganic compounds, and biomass, at a rate consistent with known compostable materials and leaves no visible, distinguishable or toxic residue. • A plastic product is considered to have demonstrated satisfactory disintegration if after 12 weeks in a controlled composting test, no more than 10% of its original dry weight remains after sieving on a 2.0-mm sieve. • A plastic product is considered to demonstrate a satisfactory rate of biodegradation by achieving [60% or 90% depending on polymer composition] conversion to carbon dioxide within [a 180 days or 365 for radiolabeled materials] • A plastic product can demonstrate satisfactory terrestrial and aquatic safety if it [has] concentrations of regulated heavy metals less than 50% of those prescribed for sludges or composts in the country where the product is sold, and the germination rate and the plant biomass of the sample composts [have] no less than 90% of the corresponding blank composts for two different plant species.

The physical characteristics of degradable and biodegradable polymers are a direct result of the chemical structure of the polymer and are not dependent on the polymer feedstock or the production method (40,41,51). Consequently, there are degradable compostable plastics that are chemically synthesized from fossil fuels and even biopolymers that do not biodegrade or that degrade so slowly that they are considered non-degradable (37,38,47). Poly (ε-caprolactone) is a classic example of a polymer that is biodegradable, compostable and synthesized chemically from fossil fuels (40,51-53).

Compostability of Green Polymers. Polymers can be officially classified as compostable if they fit the ASTM standards, listed in Table 2, which require the polymer to degrade or biodegrade to a non-toxic indistinguishable residue within a specified time period (45,46). Oddly, the somewhat arbitrary ASTM time limits for compostable polymers cause leaves and wood to be classified as non-compostable. Consequently, the cellulose and lignin found in wood and leaves represent brilliant examples of polymers that are considered biodegradable but not compostable, without further processing (41,54). ASTM's composting standards can also create limitations for industrial polymers regarding polymer thicknesses, composition, and additives.

Poly-(β)-mercaptopropionate: the non-biodegradable biopolymer. Steinbuchel and coworkers (55) recently reported the first non-biodegradable biopolymer, poly-(β)-mercaptopropionate.

This polythioester did not biodegrade in soil, compost and activated sludge microcosms or when placed in 74 different environmental samples containing bacteria and fungi. The polythioester class of biopolymers were very recently discovered by Steinbuchel and coworkers and are considered unnatural biopolymers which can only be produced as homopolymers by engineered *E. coli* (55). The authors suggest that the lack of biodegradation observed with poly-(β)-mercaptopropionate might be because microorganisms capable of hydrolyzing the thioester linkage have not evolved in nature (55). This example highlights the importance of the chemical structure of the polymer in the ability to biodegrade.

The Effect of Antioxidants on Polymer Biodegradation. Polymer additives can also affect the ability of polymers to degrade or biodegrade. Cis-poly(isoprene) is biodegradable whether it is produced naturally by the rubber tree or chemically from petrochemical feed stocks; however, antioxidants additives in the polymer will prevent biodegradation of cis-poly(isoprene) which will then require decades to degrade (51). Additives that prevent biodegradation can also occur naturally as in the case of tannins in certain trees like the sequoia which retard microbial growth to such an extent that the trees require centuries to biodegrade (51).

The Effect of Pro-oxidants on Polymer Degradation: Oxo-(bio)degradable Polymers. Another class of polymers, which seemingly hover on the razor edge of green plastics, are the oxo-

(bio)degradable and photo-(bio)degradable plastics (51,56-59). Two well accepted mechanisms for biodegradation of polymers are hydro-biodegradation and oxo-biodegradation (56). Hydro-biodegradation pertains primarily to polymers containing heteroatom linkages, such as polyesters and polyamides, while oxo- and photo-biodegradation concerns non-hydrolysable polymers like the polyolefins (56). The natural biopolymers lignin, rubber and humus degrade via oxo-biodegradation; typically lignin degrading fungi such as white rot fungi promote biodegradation possibly by employing lignin peroxidases, manganese-dependendent peroxidases, and laccases to promote oxidative biodegradation (54).

Oxo-biodegradable plastics are produced either by adding pro-oxidants (56,58) or by omitting anti-oxidants that are usually added to traditional petrochemical polymers. Indeed, the polymer industry has spent considerable effort in the development of anti-oxidant additives that prevent oxo-biodegradation and produce highly stable polymers; unfortunately, this excellent stability is now known to create end-of-life disposal problems (56). Oxo-biodegradable plastics exhibit nearly identical properties to the traditional petrochemically derived polymers, which are already entrenched in the world market. The potential promise of these polymers is to create plastics with industrially desirable characteristics and to prevent the end-of-life problems for landfills and marine environments.

Research is currently underway to create oxo-degradable polymers that are programmed to degrade after a given time period, or only under certain conditions (56). Oxo-biodegradable plastics could be marketed to farmers for programmed-life mulching plastics that prevent erosion and degradation of soil in fallow fields but degrade in time for planting (56). Currently, Symphony Plastics markets oxo-biodegradable plastics for producing bags and sacs. A closely related class of green polymers is the photo-biodegradable polymers, which have additives that accelerate degradation when exposed to light. It is likely that polymers with both pro-oxidative and pro-photo-biodegradative properties are being developed (56).

The arguments against pro-degradative polymers focus on the potential toxicity of the oxidants and photosensitive additives; this is of particular interest for composting environments (41). Moreover, the polymer additive must remain stable and soluble during process of polymer oxo-biodegradation. As oxo-biodegradation occurs polymers often pass through a gel phase which can alter the solubility or stability of the polymer additive; if a reduction in additive solubility occurs the additive may be partitioned out of the polymer which will render the polymer inert to further biodegradation (48). Recent biometric studies of CO_2 formation have confirmed that bioconversion of polyethylene is viable; moreover, the observation of greater than 60% mineralization within 180 days suggests that these polymers are viable applicants for

compostable plastics (48,56). The long term effects of microscopic polymer particles and bioconversion of polymers on microorganisms remains to be determined.

The Cost of Traditional Plastics on Waterways. The boom of the plastics industry in most first world countries, including the US, Europe and Japan, over the past 40 years has largely contributed to today's 'disposable' economy and serious environmental dilemmas regarding solid waste management and disposal (60). Waterways are historic sites for dumping solid wastes including plastics, which unfortunately are particularly recalcitrant to degradation in marine environs. Recently, the detrimental effect of traditional plastics on marine environments has received substantial interest (61-66).

It has come to light that enormous swaths of the oceans contain alarmingly high levels of plastics, which apparently accumulate in certain areas due to oceanographic convergences and eddies known as gyres (62). The North Pacific central gyre, has an abundance and mass of neustonic [floating in the surface film of water] plastic approximately 3 and 7 fold higher, respectively, than that recorded anywhere else in the pacific ocean (61,66). Generations of poor solid waste management may have created more than unattractive beachscapes (61,62) and entanglement or suffocation hazards for marine life (61,64). The microscopic friable powders which traditional recalcitrant polymers can form have recently been shown to be present in

marine samples and incorporated into single celled marine organisms (63). The accumulation of plastics and potentially toxic additives in marine environments have as yet unknown consequences, which includes the potential for bioaccumulation of toxins as larger species feed on 'plastic-laden' microorganisms (63,66).

Plastics Filling Landfills. Plastics also contribute a substantial and unnecessary quantity of landfill waste. In New York City plans are currently under development to ship the 50,000 tons of solid waste that are generated each day to southern and western states (67). Low plastic prices have resulted in an influx of cheaply made 'disposable' plastic products that are intended for limited use before disposal. These type of products, rising populations, and the extremely slow decomposition of plastics have created solid waste disposal problems (68). Serious solid waste disposal problems have lead to the creation of packaging waste disposal laws such as the Extended Producer Responsibility (EPR) laws, which place some of the waste disposal costs on the product manufacturer (69). Take-back laws are a type of EPR law in which consumers may return product packaging to the manufacturer (often in the store) in order to avoid consumer-end disposal costs (69).

Government-mandated Recycling Systems. Government-mandated recycling systems can increase environmental awareness and

consumer desire for biodegradable products. Japan has invested heavily in biodegradable polymers as part of a goal to create a closed-loop no waste economy; this is particularly important because of Japan's high population density on a small isolated land mass (70,71). In Germany the Duales System Deutschland AG (DSD AG) which was founded in the 1991, is probably the most stringent EPR-type system in the world (72). The DSD provides two options for manufactures and retailers: 1.) to 'take-back' sales packaging for reuse or recycling, typically in the store, or 2.) pay a fee toward Germany's privately run collection and reprocessing system known as Der Grune Punkt (The Green Dot), in which a green dot is placed on the item, which can then be disposed of at central locations or via curbside recycling (72).

The Green Dot. Germany's Green Dot system has resulted in recycling rates that far exceeded the legislated mandates (73). The Green Dot has been adopted by 24 countries world wide; 5 of these countries now have recycling rates in excess of 50%, as shown in Figure 1 (73). These recycling rates are substantially better than in the US where recycling rates are currently about 28% (74). Successful government-regulated recycling systems other than the Green Dot have been developed in non-EU countries including Great Britain, Canada, Australia, and Japan. Critics of Germany's Green Dot system cite antitrust issues regarding the single private DSD Company, problems including creating a glut of recyclables with out the infrastructure to convert these materials into useful products or energy, and general program

confusion (72). Moreover, the Green Dot system does not necessarily promote environmentally responsible practices since all 'green' products—such as certain biodegradable plastics—are not necessarily included; this is in part because legislation does not keep pace with biotechnology (72).

Figure 1. Material Recycling Quota (in %) Reached in European Countries. Reproduced from Braunegg *et al* (73).

Oil Reserves Affect the Future of Polymer Production. In the U.S. approximately 10% of output from crude-oil refineries is used in the industrial production of polymers (75). World wide oil supplies are limited resources, and the US Energy Information Administration conservatively estimates that conventional oil resources will peak in the year 2044 and will be significantly depleted in another 25 years, as shown in Figure 2 (76). While estimate dates for peak oil are notoriously inaccurate, often shifting forward as predicted dates approach, and peak oil production depends heavily on future technologies, estimates of this sort clearly underscore the finite nature of world oil resources and the importance of investing in alternative bio-based feed stocks for polymer production (76). The U.S. Departments of Agriculture and Energy estimate that the U.S. is capable of generating one billion tons of annually-renewable biomass feed stocks each year (77).

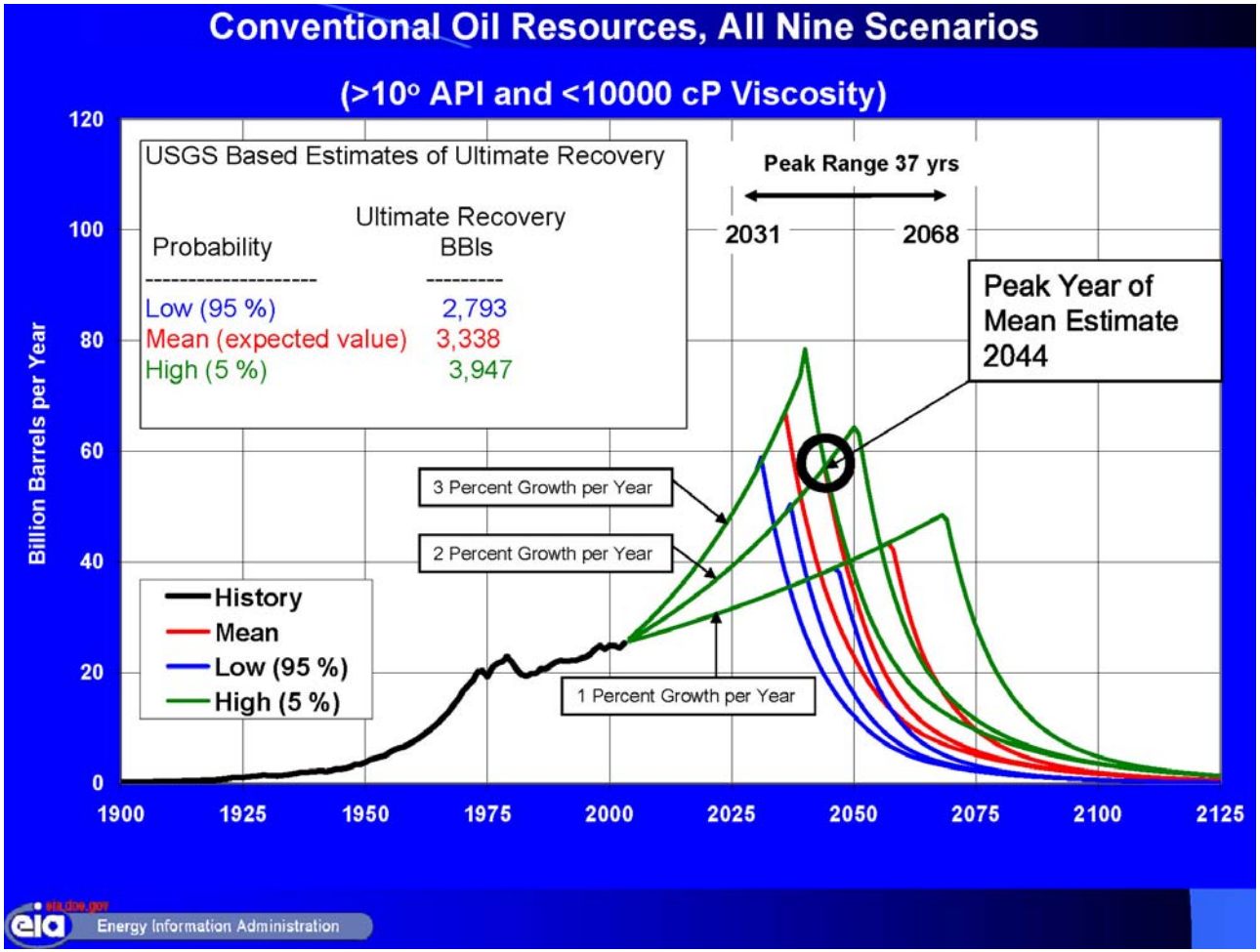

Figure 2. Estimate of World Wide Peak Oil Production. Reproduced from Caruso (76).

Today's high oil prices and the national dependence on foreign oil may provide further incentives for developing polymers from bio-based feed stocks (78). The current climb in crude oil prices has substantially increased the market prices of petrochemically derived polymers. This provides an opportunity for agriculturally derived biopolymers, which are becoming increasingly cost competitive with traditional polymers.

Oil supplies and prices are also highly dependent on the world economy and political situations. Indeed, the current US administration has stated that reducing dependence on foreign oil is a matter of economic and national security (78). On Aug 9th 2005 the US Energy Policy Act of 2005 was signed (78). The bill suggests doubling funding for renewable feed stocks, including cellulosic biomass for bio-fuels and other products by 2008 (78). However, the bill does little in the short term to reduce US oil consumption or increase use of biomass-based biopolymers since no mandates are suggested that would boost energy production from renewable feed stocks (79). Moreover, many critics suggest that the bill lacks focus (79), especially when considering that a NAS study was commissioned on converting motor vehicle trips to bicycle trips (80).

Are Biopolymers Sustainable? Can biotechnology move us toward a sustainable society? This question, proposed in 1999, by Gerngross (81) in a Nature Biotechnology paper, of the same name, has created an enduring controversy amongst the scientific

community and general media. In this paper Gerngross shows that the production of 1 kg of PHA requires 2.39 kg of fossil fuels whereas only 2.36 kg is required for polystyrene synthesis (81). While the difference in fossil fuel requirements between the two polymers is only 0.13 kg, Gerngross makes the critical argument that PHA production combusts the entire 2.36 kg of fossil fuels, whereas only 1 kg of fossil fuels are burned in the manufacture of polystyrene with the balance sequestered in the polystyrene itself. Consequently, Gerngross suggests that fermentation-derived PHA polymers provide no advantage over petrochemical polymers with respect to sustainability (81).

In 2001, Gerngross and colleagues at Monsanto Company, Ecobalance, Inc., and Cereon Genomics (82) published a study which showed no difference in greenhouse gas emissions between the production of polyethylene via petrochemical means and PHB produced from corn that was genetically engineered to contain PHA; this was consistent with Gerngross' previous publication (81). While the calculations and conclusions drawn by Gerngross' 1999 publication (81) are not in doubt, the comprehensiveness of the study parameters have been reevaluated in more recent literature reports with intriguing results.

Gerngross' 2001 publication (81) indicated that the greenhouse gas emission profile was greatly improved for PHA over polyethylene when corn stover (the mature, cured stalks of grain with the ears removed) was used as a fuel source which replaced, in part, fossil fuels. The energy source for biopolymer

production is critical to these types of analyses since alternative fuel sources like corn stover, wind, water, and solar energy can drastically alter the energy profile and increase the attractiveness of PHA production from an energy and greenhouse gas emissions standpoint. Considering that each corn plant typically produces only two ears of corn, using the huge quantities of corn silage for energy production seems obvious. Indeed, biomass energy is commonly used as a fuel source in other agricultural industries such as the sugar industry which regularly uses sugar cane bagasse to fuel sugar extraction (82,83). However, the Corn Belt states currently use a disproportionate quantity of coal for electricity generation; this is a result of tradition and a lack of infrastructure, which if remedied could substantially increase the efficiency of biopolymer production from corn (82). On the other hand, there is no particular reason that the energy derived from corn stover must be used for producing agriculturally-derived biopolymers; instead this energy could be applied to the production of petrochemically-derived polymers, which would further depress the cost of this type of polymer (82).

Doi and coworkers (84) published a 2003 study which contradicted Gerngross' previous conclusions and indicated that PHA produced via by bacterial fermentation of the renewable carbon resource, soybean oil, could have markedly lower energy consumption and carbon dioxide greenhouse gas emissions than typical petrochemical polymers (84). In 2005, Kim and Dale (85)

published a painstakingly thorough assessment of PHA derived from no-tilled corn. The authors suggest that the disparity between the conclusions of the Gerngross (81,82) and the Doi (84) studies result from differential approaches to allocating parameters in the corn wet milling process, PHA fermentation yields, and the operational data in the PHA fermentations and recovery.

Specifically, Kim and Dale (86) suggest that the Gerngross analysis (81,82) failed to account for the environmental burden of converting corn grain to dextrose and byproducts, and that the study by Doi and Coworkers (84) did not consider soil nitrogen and carbon dynamics in the agricultural ecosystem. Kim and Dale (85) conclude that by using today's technology there is no significant advantage to PHA production over polystyrene. However, the authors suggest that corn grain based PHA is more favorable than polystyrene in terms of global warming and non-renewable energy concerns (85). Moreover, technologies expected to be available in 2-3 years, which improve fermentation efficiency and recovery of bacterial bioreactor derived PHA (85,87), such as an integrated production system, can substantially reduce the environmental impacts of PHA, excepting eutrophication. The integrated production system discussed in the publication uses corn stover and the corn grain for dextrose production and lignin-rich residues are used to generate the steam and electricity needed for the PHA fermentation process; however, the technology for PHA from corn stover is not currently available on a commercial basis (85,87).

One intriguing study suggests that PHA production could be produced in an economically advantageous manner when integrated with sugar and ethanol production in the Brazilian sugar cane industry (83). Apparently, the 1970's oil crisis prompted the Brazilian government to combine sugar mills with distilleries for the integrated production of sugar and ethanol; thus, an extensive milling infrastructure was built which generates such an energy excess, by incinerating bagasse, that sugarcane processing is actually energetically self-sufficient. Consequently, integrating PHA production as a percentage of the Brazilian sugar cane milling/ethanol generating process could add a high profit margin product, PHA, to the relatively low priced sugar sales, and with minimal infrastructure alteration (83).

So how can we answer the question that Gerngross proposed in his 2000 Scientific American article entitled "How Green are Green Plastics" (75)? After all currently available data is considered, Gerngross' (75,81,82) dismissal of fermentation-derived PHA polymers as an environmentally sustainable alternative to petrochemical polymers clearly needs to be reconsidered; however, PHA is not a clear winner either (84,85). Agriculturally derived biopolymers may indeed be green under the appropriate carefully controlled and well-studied conditions. Industrial plants must be designed with considerations that incorporate location, to reduce agricultural transportation costs, crop and land maintenance issues like no-tillage systems need be evaluated, and renewable energy sources must be employed

(85). Perhaps, the best answer to Gerngross' question may be that the 'greenness' of a polymer, like many commercial products, greatly depends upon the particular characteristics of a given polymer, which are governed by the chemical structure, the polymer growth and cultivation conditions, the efficiency of industrial plant design, the current market conditions, and the governmental and cultural mandates and practices.

Natureworks PLA. In April of 2002, Cargill-Dow officially opened the first global-scale plastic resin manufacturing facility, which is capable of producing 300,000 metric tons of Natureworks PLA each year (88). The Natureworks products shown in Table 3 are polymer resins and fibers which are biodegradable, and synthesized from lactic acid derived from annually renewable resources (89). As shown in Figure 3 (90), Natureworks PLA is generated when starch, obtained from corn kernel endosperms, is enzymatically converted to dextrose which is used as a feed stock for bacterial fermentations that generate lactic acid; this lactic acid then undergoes dehydration to lactides which are chemically polymerized to PLA (89-91).

Table 3. Structure of Commercial Bio-Based or Green Polymers and the Monomer Constituents.

Polymer Name & Trademark	Company	Monomer(s)	Polymer Structure
PHB	Metabolix BP/ Innovene ADM	β-Hydroxybutyric acid 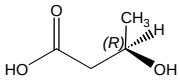	Poly-(β)-hydroxybutyric acid 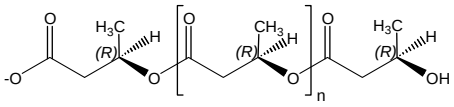
PHB(V) BioPol	Metabolix	β-Hydroxybutyric acid 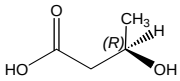 β-hydroxyvaleric acid 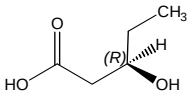	BioPol Poly-(β)-hydroxybutyric-*co*-valeric acid 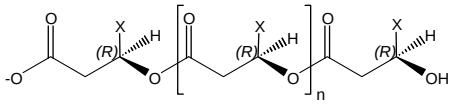 X=CH_3; CH_2CH_3
PHB(HHx) Nodax	P & G Kaneka	β-Hydroxybutyric acid 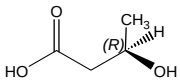 β-hydroxyhexanoic acid 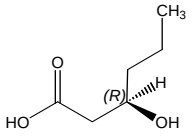	Nodax Family Poly-(β)-hydroxybutyric-*co*-hexanoic acid 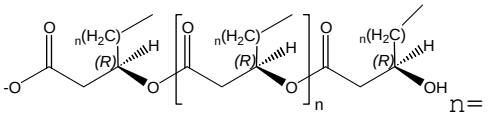 n= 2-12
Natureworks PLA	Cargill	Lactic acid 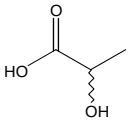	Polylactic acid 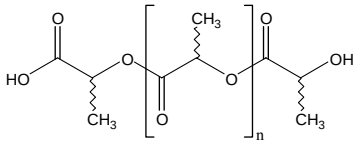
Ecoflex	BASF	1,4-butanediol 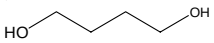 Adipic Acid 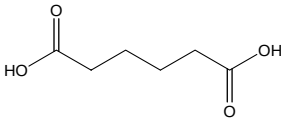 Terephthalic Acid 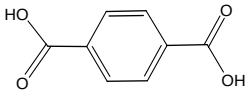	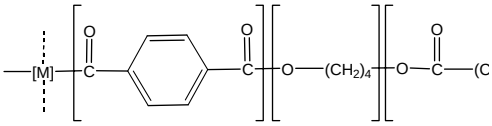 M: e.g., monomers with a branching and chain extension effect (92)

Table 3 Continued

MaterBi	Novamont	ε-caprolactone 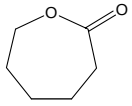 α-D-glucose 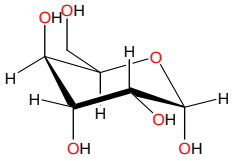	Mater-Bi are composites often containing: Poly-(ε)-caprolactone 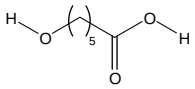 Starch: Comprised of amylase, a mostly linear polymer of α-(1→4)-D-glucose, and amylopectin (shown below), a non-random α-(1→6) branched amylase polymer 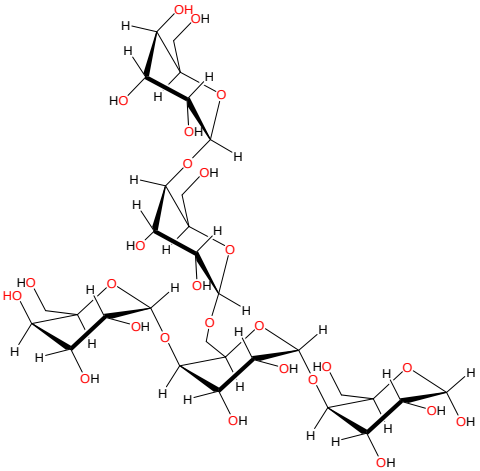
3GT Sorona	Dupont	1,3-propanediol 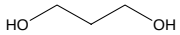 Terephthalate Moiety 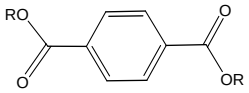 R=H or CH_3	poly(trimethylene terephthalate) PPT; 3GT 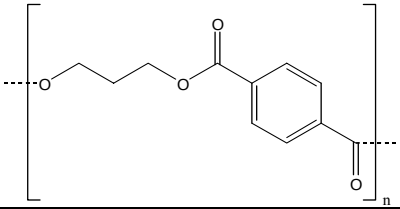

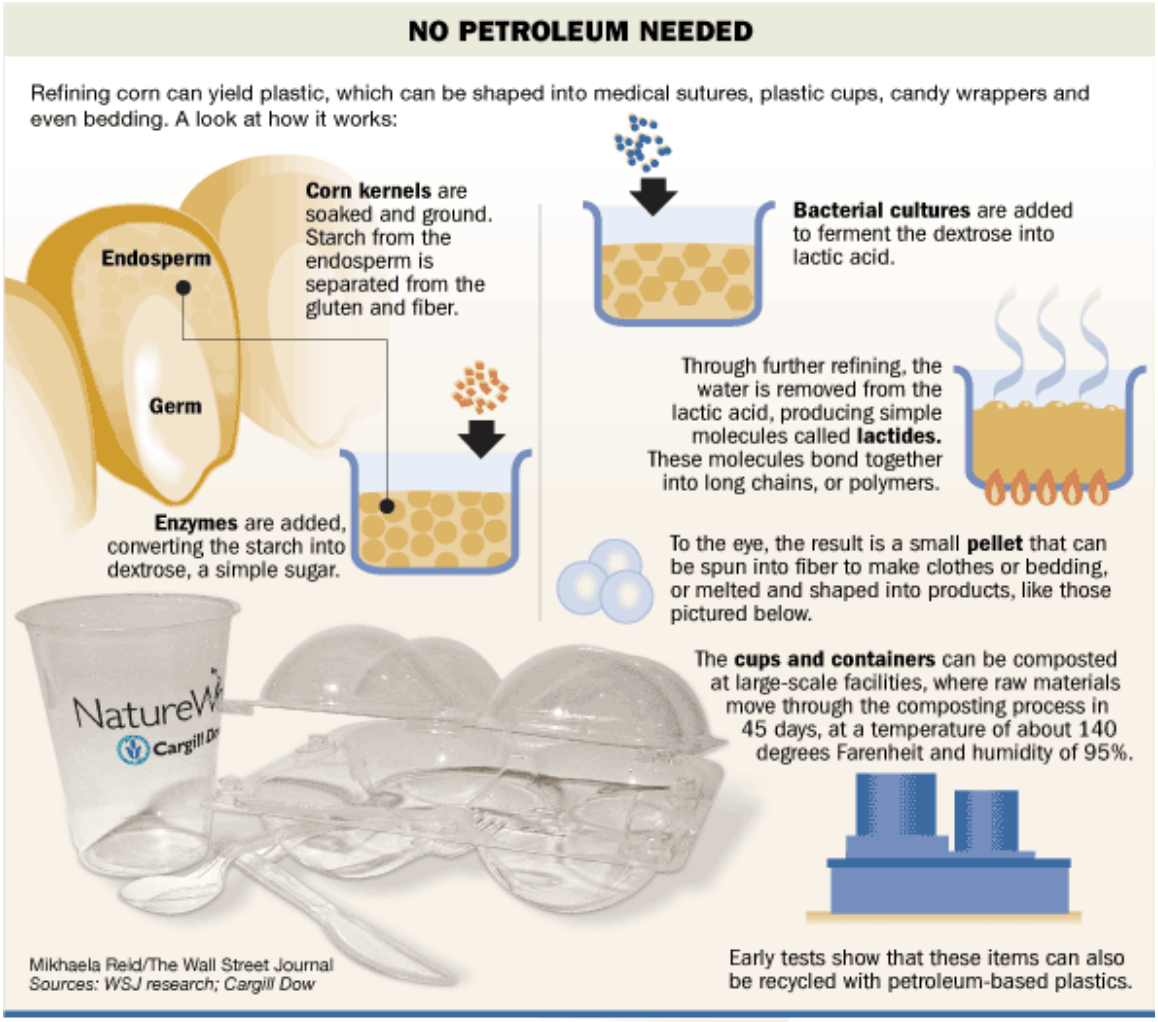

Figure 3. Industrial Synthesis of Natureworks PLA. Reproduced from Herrick (90).

Properties of PLA. PLA has properties similar to polystyrene with respect to gloss, clarity, temperature stability and processability while its flavor and odor barrier properties and resistance to grease and oil are similar to PET (91). PLA has GRAS (Generally Regarded As Safe) Status for food packaging since PLA decomposes to lactic acid at levels that are well below those deemed safe for consumption (89). PLA is heat sealable at temperatures lower than polypropylene and polyethylene. Different formulations affect rigidity and flexibility, and copolymerization can greatly affect PLA properties (89). The stereochemistry of PLA significantly affects the products crystallinity (89,91). Since various bacterial strains produce different lactic acid isomers or ratios of isomers, the crystallinity of the final PLA can be controlled during the fermentation stage by careful selection of bacterial strains. Indeed, blends of the stereoisomers often have better mechanical properties than isotactic PLA polymers. By modifying the stereochemical blend and therefore the resultant crystallinity PLA can be processed on most conventional machinery including blown film, extrusion, thermoforming, and injection molding. Furthermore, polymer branching can be induced by reacting PLA with hydrogen peroxide in order to make PLA amenable to extrusion coating of paper for drinking cup applications (89,91,93).

The Green Possibilities for PLA. How green is PLA? Cargill-Dow published a Life Cycle Assessment (LCA) study in 2003, which reported that their first generation PLA production

system consumes 22-55% less energy from fossil fuels than do petrochemical polymers (94). Moreover, by implementing plans for energy generation from wind power and biomass, PLA could consume up to an outstanding 90% less energy than conventional petrochemical polymers (94). However, the authors fail to discuss the very same issue that Gerngross raised regarding the greenness of PHAs. As shown in Figure 4 (94), unlike petrochemical polymers which sequester a large portion of fossil fuels in the polymer itself , 100% of the fossil fuels required to produce PLAs are burned and generate greenhouse gasses. Consequently, when comparing the consumption of fossil fuels for energy production with concomitant greenhouse gas production, we see that PLA production burns more fossil fuels than HIPS, GPPS, LDPE, PET-SSP, PP or PET-AM. Moreover, PLA is only truly advantageous with respect to fossil fuel expenditure when its energy requirements are derived from wind and biomass; these technologies are not currently available. The study also analyzed greenhouse gas emissions for global climate change effects and found that PLA was better than most polymers and equal to PP and LDPE. In addition, employing biomass and wind energy for the remaining energy balance requirements could effectively 'close the loop' on carbon related to energy generation, and yield a negative greenhouse gas impact for PLA pellets. The potential for PLA to act as a greenhouse gas sink is not feasible with any petrochemically derived polymer (94).

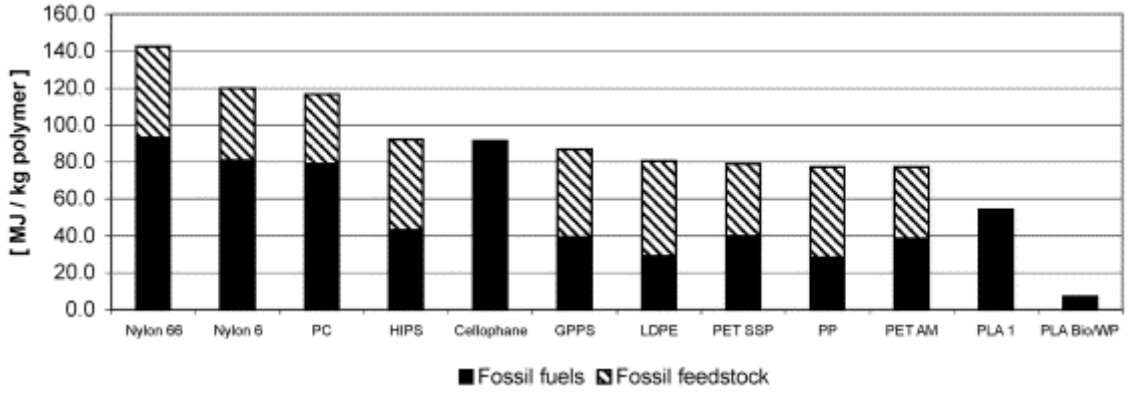

Figure 4. Fossil Energy Requirement for some Petroleum Based Polymers and PLAs. The cross-hashed parts of the bars represent the fossil energy used as chemical feedstock (the fossil resource to build the polymer chain). The solid part of each bar represents the gross fossil energy use for the fuels and operations supplies used to drive the production processes. PC, polycarbonate; HIPS, high impact polystyrene; GPPS, general purpose polystyrene; LDPE, low density polyethylene; PET SSP, polyethylene terephthalate solid state polymerization (bottle grade); PP, polypropylene; PET AM, polyethylene terephthalate, amorphous (fibers and film grade); PLA1, polylactide (first generation); PLA B/WP, (polylactide, biomass/wind power scenario). Reproduced from Vink *et al* (94).

Cargill-Dow's Joint PLA Venture is Dissolved. "Customers are not willing to pay a premium for environmentally friendly polymers." This statement, made by Andrew N. Livers, president and CEO of Dow Chemical, during a conference call to analysts, was in response to questions regarding Dow's decision to withdraw from Cargill-Dow, a 50-50 joint venture between Cargill, Inc and Dow Chemical (95) for the development and marketing of NatureWorks PLA. Early in January 2005, Dow contributed 170 million to Cargill-Dow and transferred its 50% interest in the joint venture back to Cargill, Inc. in return for a release from its commitments regarding Cargill-Dow's debt obligations (96). This news came as a shock to the burgeoning bioplastics industry despite attempts by both companies to downplay the news, and Cargill's public commitment to the future of PLA (97). As the world's largest privately owned company and corn merchant, Cargill, Inc. has the solid financial wherewithal, backing, and assets to see the newly renamed Natureworks PLA company to success (97).

Cargill Supports Natureworks PLA. Natureworks PLA has yet to be in the black, and it is this slow movement toward profitability in addition to the slower than expected development of the bioplastics industry that appears to have been the motivating force behind Dow's retreat (98). Developing a new plastics market takes time, and Dow may have miscalculated just how long it would take to build the PLA market to a level that would bring a return on investments (97,98). Poor management and

company leadership may also have hindered the market advancement of PLA (88). In 2003, Kathleen Bader was appointed CEO of Natureworks PLA to bring the company into focus and into the black (88,98). Initial restructuring included eliminating research into frivolous product lines like developing biodegradable PLA products to replace golf tees and tea bags, (products that are already biodegradable), reducing the number of projects from 16 to just 2 (packaging and fibers), and reducing polymer production costs by producing fewer but larger batches of PLA in order to reduce expensive startup costs (88).

Natureworks PLA becomes Cost Competitive. Natureworks PLA now sells for less than $1 U.S. per pound and is cost competitive with PET (88). Moreover, with the cost of oil today spiking to records of greater than $70 U.S. per barrel, the cost advantage of PLA over PET is increasing (88,90). Wild Oats, an organic food store that switched to PLA packaging, has seen deli sales rise by more than 15 percent, in large part due to customer acceptance of their eco-packaging; moreover, the company has been buffered from soaring oil prices and now pays 3-5 percent less for their eco-friendly packaging (88,90,99). Cargill reports that for every $5 increase per barrel of oil, PLA gains a 'penny-a-pound' advantage over PET, and they further maintain that PLA will remain cost competitive even if oil-prices drop back to the mid-$20s per barrel (88,90).

Problems with Market Acceptance. Despite the potential economic and environmental attributes of PLA, market acceptance

of biopolymers has been less than stellar and Bader, CEO of NatureWorks PLA, has yet to land a major national contract (88). PLA is a hard sell because many companies refuse to believe that a plastic, which decomposes at 140 C under composting conditions, could withstand normal storage in facilities in the Deep South. While it is true that PLA water bottles will get tiny bubble-like imperfections after storage for 8 months, Bader insists that no one wants to drink 8 month old water (88). Surprisingly, PLA has hit a nerve with eco-friendly retailers, such as Patagonia, which refused PLA products on the basis that some of the feed stock could be from corn that is genetically engineered (88).

Ecoflex. In April 2005, BASF announced plans to nearly double production of Ecoflex by opening a second plant in Schwarzheide, GE capable of producing 6,000 m.t./year, which brings BASF's Ecoflex capacity up to 14,000 m.t./year (100-102). Ecoflex is a biodegradable, aliphatic-aromatic copolyester of adipic acid, terephthalic acid, and 1,4-butanediol derived from petrochemical or bio-based feed stocks (40), as shown in Table 3. Since its introduction in 1998, Ecoflex has become the leading synthetic biodegradable material on the world market. This popularity is due in large part to its good thermoplastic properties, which are comparable to LDPE. Ecoflex can be used in starch blends or alone in flexible films and is used in the packaging and flexible films sectors in products like disposable packaging, paper coating, shopping bags, and agricultural

sheeting (103). BASF's decision to increase production comes on the heals of the recently passed amendment to the German Packaging ordinance, which now exempts all biodegradable packaging from the DSD recycling fee until 2012, irrespective of the material basis. Since Ecoflex is now included in the exemption to the DSD Fee, BASF expects the demand for Ecoflex to rise and the plant, expected to go online in 2006, will enable BASF to meet market demand (103).

Mater-Bi. Another major international manufacturer of biodegradable plastics is Novamont of Italy, the producers of Mater-Bi, a family of starch-based resins that typically contain greater than 60% starch with the remainder being some other biodegradable material(s), often poly-ε-caprolactone (53,89,104), as shown in Table 3. The Mater-Bi family of resins is used in a wide range of applications including compostable thin films for shopping bags, mulching, packaging and hygiene (105). Mater-Bi can be thermotransformed to make non-transparent hard trays for fresh food packaging, and extrusion technology can be employed to make nets for fruits and vegetables. Injection molding of Mater-Bi is used to produce cutlery and antistatic combs and some Mater-Bi foams are biodegradable and water soluble for use in packaging. One example is a Mater-Bi resin containing 60% starch and 40% poly-ε-caprolactone, which has properties similar to LDPE, and can therefore be handled on conventional film blowing equipment with only minor adjustments (89,106). Poly-ε-

caprolactone serves to provide added strength and water resistance to the Mater-Bi line of products (41). Recently, Novamont joined with Goodyear to develop Mater-Bi™ Biofiller which is produced from maize starch to act as a biofiller for use in tire mixtures (107). In September 2004, Novamont acquired EastarBio, the copolyester business and technology platform of Eastman Chemical Company (107).

Sorona. In 2000, Dupont™ unveiled Sorona® a family of poly(trimethylene terephthalate), PTT, also called 3GT polyesters (108). Unlike the historically dominant 2GT polymers, including polyethylene terephthalate (PET) which are synthesized from ethylene glycol (2G) and terephthalic acid monomers, 3GT polymers are comprised of 1,3-propanediol (3G) and terephthalic acid monomers (109). While the attractive physical properties of 3GT polymers have been known for years, this polymer class was not previously marketable due to difficulties with polymer processing requirements and purity, and the high cost of 1,3-propanediol. The Sorona® polymers are being targeted primarily as fibers for the textile and apparels market but also have applications in fibers, plastics, film, and engineering components (109). Currently the Sorona® polymers are not biodegradable because Dupont claims that this is undesirable for their target market; however, the company states that Sorona® polymers can easily be designed with biodegradability in mind if a market becomes available (110).

The 1,3-propanediol used to synthesize Sorona® polymers is currently obtained from non-renewable resources. However, in 1995 Dupont teamed up with Genencor Inc. (111) and in 2003 Dupont was awarded the Presidential Green Chemistry Challenge Award in the Alternative Solvents and Reaction Conditions Category for developing the microbial production of 1,3-propanediol (112). As shown in Figure 5, the microbial production of 1,3-propanediol has been accomplished by genetically engineering a pathway into *E. coli*, which effectively generates 1,3-propanediol from the glycerol produced during glucose metabolism (113).

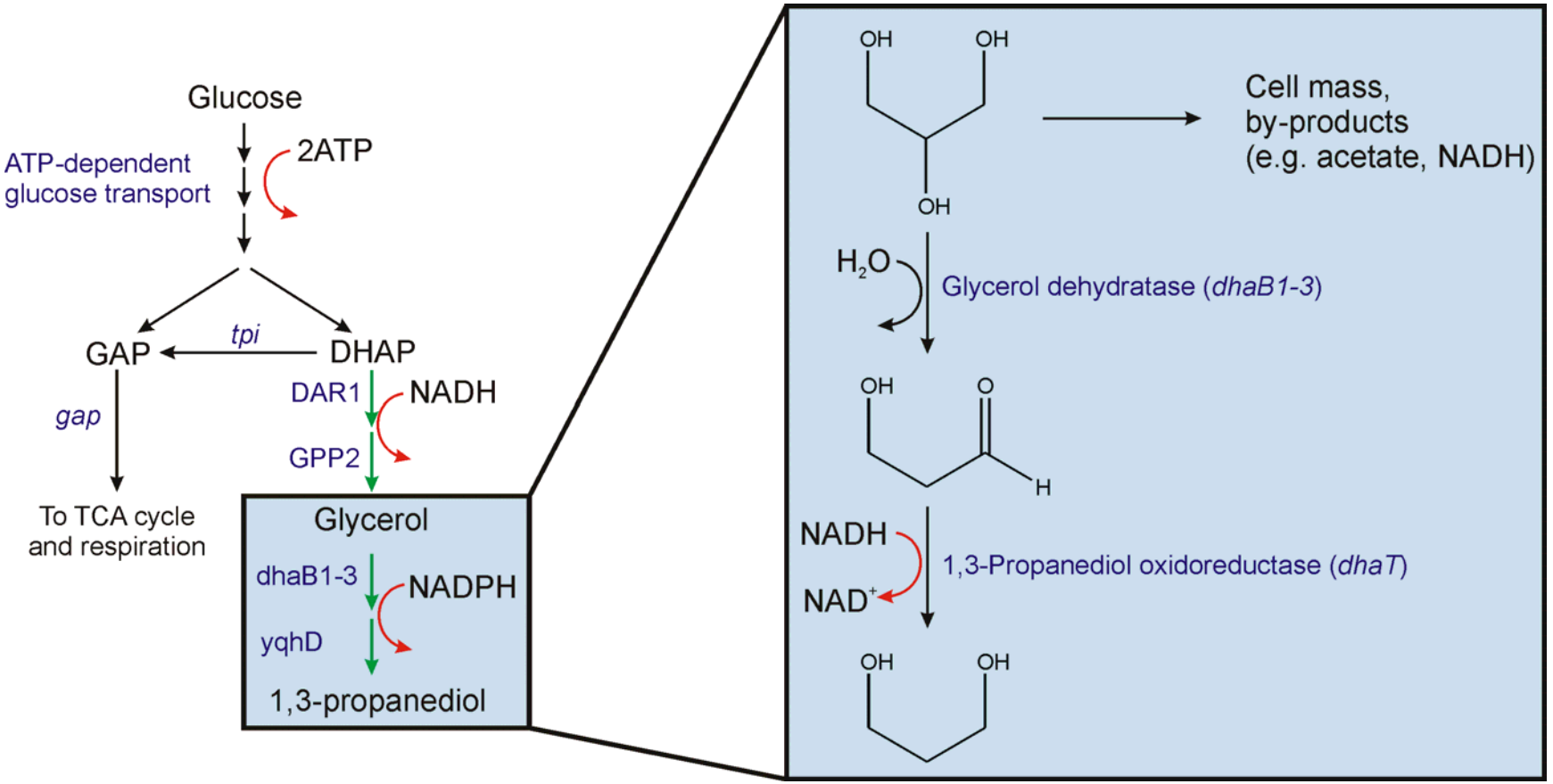

Figure 5. Metabolic Engineering and Pathways for the Microbial Production of 1,3-Propanediol in *E. coli*. Abbreviations are as follows: DAR1, glycerol 3-phosphate dehydrogenase; GPP2, glycerol 3-phosphate phosphatase; dhaB1-3, glycerol dehydratase; yqhD, dhaT, a known 1,3-propanediol oxidoreductase in bacteria that performs this type of reaction; yqhD, a previously uncharacterized 1,3-propanediol oxidoreductase endogenous to *E. coli* shown to have a higher activity than dhaT; gap, glyceraldehydes 3-phosphate dehydrogenase; tpi, triosephosphate isomerase. Modified from Nakamura *et al* (113).

Poly-β-hydroxyalkanoates. Poly-β-hydroxyalkanoates (PHAs) are a relatively large class of biodegradable polyesters produced by certain bacteria as a reserve source of carbon and reducing potential, and are typically generated when the bacteria undergoes an environmental stress such as nutrient deficiency. Over 150 different hydroxyalkanoic acids have been reported in the literature as monomers for PHAs (114). Poly-β-hydroxybutyric acid (PHB), shown in Table 3, discovered near the turn of the 20th century, was the first identified and characterized PHA (115,116). PHB is the simplest, most widely studied of the PHA biopolymers, and is a thermoplastic with characteristics similar to polypropylene or polyethylene (89). PHB can be extruded, spun into fibers, molded, or made into films. As a homopolymer, PHB is considered too brittle for most commercial applications (115); however, PHB copolymers which typically contain hydroxyalkanoic acid monomers such as valerate [PHB-(V), BioPol] (116) or hydroxyhexanoate [PHB-HHx, Nodax] (117), have significantly more attractive mechanical properties for the commercial market (89,116).

The History of PHB. Early literature accounts of PHB date as far back as the late 1800's, but it was Maurice Lemoinge in 1923 who first identified and characterized the biopolymer present in *Bacillus subtilis* and *Bacillus megabacterium* that would later be known as PHB (115). During the period from 1923 to 1927, Lemoinge showed that autolysates of *B. subtilis* in distilled water contained an acidic compound, which was

eventually identified as the same compound as that found in the urine of diabetics, β-hydroxybutyric acid (118). During this period, Lemoinge proposed the existence of so-called 'macromolecules' as high molecular weight molecules to a very skeptical audience. Over the next decades, Lemoinge and coworkers continued to publish studies on PHB, which they termed 'lipide-β-hydroxbutyrique'. Indeed, it appears that Lemoinge's nomenclature relegated studies of PHB to relative obscurity; because, while PHB was well known among microbiologists and even included in early textbooks, PHB was classified as a lipid instead of a macromolecule or polyester (118). Consequently, the significance of PHB and Lemoinge's theories regarding macromolecular structure did not reach the wider scientific community; thus, the 1953 Nobel Prize in Chemistry was awarded to Hermann Staudinger for his discoveries in the field of macromolecular chemistry (119). PHB would remain veiled until its nearly simultaneous rediscovery by two independent laboratories, in the US and Great Brittan, in 1958 and 1959 (116).

W.R. Grace Company Attempts Commercialization of PHB. The first attempt to commercialize PHB was undertaken by W.R. Grace Company of Maryland in 1960 (89,116). Researchers at the company proposed that PHB's stereoregular, isotactic nature and its 180 C melting point, which is near that of polypropylene, might confer PHB with mechanical properties that could compete effectively with polyolefins, with biodegradability as an added benefit.

Initially, large test batches of PHB were produced for molded plastics and absorbable sutures with the bacteria, *Rhizobium*, which was reported to generate up to 58% of its dry cell weight as PHB. Two years later, W. R. Grace Company abandoned this project citing poor thermal stability of the PHB as the rationale for abandoning the project. In 1964, Webber and Baptist published a summary of their research at W.R. Grace Company entitled 'Bacteria Produce Polyester Thermoplastic'; this was one of the first publications on this subject to reach the wider polymer chemistry community (89,116).

ICI Commercializes PHB. The homopolymer PHB has a high melting point of 180 C and undergoes slow crystallization to form large spherulitic structures, which impart brittleness and undesirable mechanical properties for molded plastics and films. PHB's high melting point also makes it venerable to thermal degradation via ester pyrolysis during melt processing. Application of nucleating agents and careful handling can significantly improve the final mechanical properties of PHB; consequently, Imperial Chemical Industries of Great Britain (ICI) was able produce small items, like golf teas, from PHB using extrusion molding.

ICI Commercializes the PHB Copolymer BioPol. ICI began developing BioPol a PHA biopolymer for market in 1975 (120). BioPol, shown in Table 3, is a copolymer designated PHB(V), which contains β-hydroxybutyric acid and β-hydroxyvalaric acid monomers. Research at ICI showed that the random copolymer,

PHB(V), had a lower melting point than the homopolymer; this results in advantageous mechanical properties that are intermediate between polypropylene and polyvinylchloride. The PHB(V) copolymer, trademarked BioPol, could be processed into blown film, cast film, calendered (pressed between rollers or plates in order to smooth and glaze into thin into sheets) and be made into bottles by injection and extrusion blow molding (89).

In 1982, ICI introduced BioPol to market; this was in the wake of the 1970's oil crisis in which, like today, high oil prices had made non-petroleum based biopolymers economically attractive (120). BioPol was produced by commercial scale fermentation of *W. eutrophus* H16 (now *Cupriavidus necator*), a bacterial strain acquired from Schlegel who had reported high levels of PHB accumulation in this strain in the 1950's. Indeed, it was later shown that the H16 strain could generate up to 80% of its dry cell weight as PHB(V) when cultured on glucose (89,116). The rate of biodegradation of BioPol ranged from a few days for very thin cast films to nine months for shampoo bottles under anaerobic sewage conditions (89). By 1991, ICI's BioPol market was successful; Wella of Germany was using PHB to manufacture biodegradable shampoo bottles, and ICI expanded production from 25 tons/year to 300 tons/year with expectations to open a commercial-sized plant with a 10,000 ton capacity by 1996 (89,116).

Other Companies Attempt PHB Commercialization. It comes as no surprise that by 1991 several other companies were also

marketing small quantities of PHB (89). Seibu Gas Company, also produced PHB using an autotrophic strain of the bacteria *C. necator* which generated PHB using CO_2 as a feedstock (89). Another enterprise, a state owned subsidiary of Petrochemie Danube of Austria, called btF mbH, produced 20 tons of PHB per year for use in controlled release drug delivery systems. PHB has been shown to be biocompatible, although it decomposes extremely slowly in the human body. btF mbH produced PHB using the bacteria *A. Latus* which generates PHB during the active growth phase; this is in contrast to most PHB producing bacteria which must undergo two-phase culture wherein the bacteria is first cultured under optimal growth conditions in order to reach the desired biomass and PHB production is then induced by nutrient depravation.

ICI's Success with PHB. Although the price for BioPol was 30 times greater than polypropylene, ICI's BioPol enterprise was profitable; by 1992, production had reached 600,000 lb/year in the UK, and hair care products in blow-molded bottles with injection-molded caps were successfully marked in North America. Expanded production for larger markets consistently deflated production costs for BioPol until market prices reached $8-10 U.S. per pound in the early 1990's, and ICI anticipated that their planned expansion would drive prices down to about $4 U.S. per pound.

The Commercial Fall of BioPol. In 1993, ICI transferred BioPol to Zeneca Bio Products, one of ICI's spin off units, and

ICI exited the biopolymer field (89). Zeneca Bio Products was expected to continue ICI's plans of opening a 10,000 ton capacity plant in 1995 (121). However, in 1996 Monsanto acquired the BioPol trademark and all patent rights from Zeneca Bio Products. Monsanto continued to market BioPol, even producing credit cards for Greenpeace in 1997. Disposable cups, planters, cutlery, compost bags, packaging for personal care products, fish nets, and disposable razors numbered among the products made from BioPol (89). Monsanto was also heavily involved in studies to genetically engineer plants for PHB production, and initial results were promising, with one Arabidopsis plant reported to contain 14% PHB (122,123). However, the possibility of creating stable, viable plants capable of producing PHB in quantities high enough for economical polymer recovery was simply too distant for Monsanto. Consequently, in 1998 Monsanto announced the end of BioPol production, research and development. This marked the end of commercial PHA production (89).

Metabolix Obtains Monsanto's Interests in PHB. In May of 2001, Metabolix, a small startup company founded by Oliver Peoples of MIT, acquired all of Monsanto's interests and rights to BioPol (124). In 2005, Metabolix won the Presidential Green Chemistry Challenge Small Business Award for their progress toward producing PHAs in both bacterial bioreactors and in plant tissues (38,42). Reports indicate that genetically engineered *E. coli* bacteria can generate up to 95% of their dry cellular weight as PHB (125). A high yield of PHB in the intracellular bacterial

granules is economically important because the generated PHB must be separated and purified from non-PHB bacterial cell matter in a process that is often time consuming, solvent intensive, and expensive. Currently, Metabolix claims that their PHB production methodology will be cost competitive with traditional petrochemically-derived polymers (105).

The Future of Commercial PHB. In November 2004, Archer Daniels Midland Company (ADM) and Metabolix announced the establishment of a 50:50 joint venture and plans to open a 50,000 ton per year production facility for manufacturing PHB products including film, coated paper, and molded goods from engineered bacteria (126,127). Additionally in March 2005, Metabolix announced a two-year collaboration with Innovene, the new olefin and derivative subsidiary of BP, to develop switchgrass biopolymer technology (127,128). Metabolix is attempting to genetically engineer switchgrass for PHA production. Switchgrass (*Panicum virgatum*) also known as Panic grass, is one of the hardy perennial grasses that populate the Tallgrass Prairie ecosystem of North America. Reaching heights of 6 feet, Switchgrass, which is often harvested for hay, may potentially yield large quantities of biopolymer and biomass (129). Abundant quantities of biomass could be used as a cheep, energy efficient, annually renewable source of energy for fueling the recovery of PHB from the grass. This is similar to the technique of using bagasse to fuel sugar plants (83), and may prove critical to reducing PHB production costs.

Nodax. Nodax is a family of PHA copolymers that are being developed by Proctor & Gamble and Kaneka, which are composed of β-hydroxybutyric acid and medium chain length β-hydroxyalkanoic acid monomers (117) as shown in Table 3. The mechanical properties of PHAs are highly dependent on the monomer structure. Medium chain length β-hydroxyalkanoic acids are generally defined as having between 6 and 16 carbon units and are differentiated from short chain length β-hydroxyalkanoic acids, which have less than 5 carbon units (130). Copolymers containing the β-hydroxybutyric acid and β-hydroxyhexanoic acid monomers, which generate PHB(Hx), are the simplest group of PHAs in the Nodax family. Other monomers used in the Nodax family include β-hydroxyoctanoic acid, to generate PHB(O), and β-hydroxydecanoic acid, PHB(D) (117). While relatively small percentages of the medium chain length β-hydroxyalkanoic acid monomers are incorporated into the final Nodax copolymer, the material properties can be substantially different from the PHB monomer (117), as illustrated by the data shown in Table 4 (131). Several grades of Nodax are being prepared for market; these are classified according to molecular weight, the constituent monomers, and the percentage of the medium chain length monomer incorporated into the final polymer. This strategy offers a wide array of mechanical properties and provides the Nodax family of biopolymers with exceptional commercial market flexibility (117).

Table 4. Physical Properties of Various PHA in Comparison with Conventional Plastics. Reproduced from Chen *et al* (131).

Samples	Tm (1C)	Tg (1C)	Tensile strength (Mpa)	Elongation at break (%)
PHB	177	4	43	5
P(HB-co-10% HV)	150	---	25	20
P(HB-co-20% HV)	135	---	20	100
P(HB-co-10% HHx)	127	-1	21	400
P(HB-co-17% HHx)	120	-2	20	850
Polypropylene	170	---	34	400
Polystyrene	110	---	50	—

HB: 3-hydroxybutyrate; HV: 3-hydroxyvalerate; HHx: 3-hydroxyhexanoate

Chemical Synthesis of Nodax. Recently, Proctor & Gamble and Kaneka reported the development of a chemical ring-opening polymerization of the Nodax polymers (117). All other commercial PHA polymers have been produced via fermentation biosynthesis because biofermentations ensure formation of an isotactic polymer. The isotactic character of biologically-produced PHAs is critical to the physical, mechanical, and thermochemical properties. However, Proctor & Gamble and Kaneka have developed chemical PHA syntheses that produce satisfactorily isotactic polymers by using the catalyst/initiator, ethylzine isopropoxide, and highly enantiomerically enriched lactone monomers for the ring opening polymerization of β-lactones as shown in Figure 6 (117) .

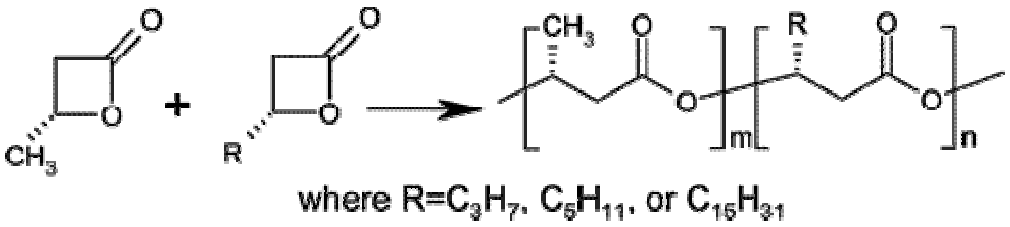

Figure 6. Chemical Synthesis of Nodax Polymer. Reproduced from (117)

A biofermentation process has also been developed for the synthesis of the Nodax family of biopolymers. Although there are slight differences between the synthetically and biologically

derived polymers, due to their differing degrees of isotacticity, the synthetic reaction does produce good yields (117). Proctor & Gamble and Kaneka are currently evaluating bio-production sites for developing and commercializing the Nodax family of biopolymers in the U.S., Europe, and Asia (132).

In Vitro Enzymatic Syntheses. While production of PHB for industrial applications is generally accomplished via industrial scale bioreactors, *in vitro* enzymatic synthesis is an attractive alternative for several reasons. *In vitro* polymer production obviates the necessity for polymer extraction from bacterial cells. Another consideration is that polymer synthesis within cells is subject to limitations related to the cellular uptake and possible toxicity of substrates, which limits the range of polymers that can be produced *in vivo* (133,134). In contrast, the enzymes used by *C. necator* in the biosynthesis of PHB accept a wide variety of alternative substrates, thus making possible *in vitro* production of novel homopolymers or copolymers. It has also been suggested that the physical size of the polymer produced during *in vitro* syntheses is not restricted by the physical size of the bacterial cell, as is the case with biofermentations (44). Indeed, reports indicate that in some cases PHB polymer produced *in vitro* has a higher molecular weight than polymer generated *in vivo* (44,135). In addition to potentially increasing polymer chain length, *in vitro* PHA syntheses may also allow for better control of polymer

polydispersity. As mentioned previously, bacterial biosyntheses of PHB by *C. necator* require a two-phase fermentation process. In the first phase, large quantities of bacteria are accumulated under optimal conditions, and then a secondary nutrient-limiting fermentation is required for polymer accumulation. *In vitro* syntheses eliminate the need for the initial growth phase prior to polymer accumulation. Finally, with *in vitro* syntheses the quantities and selection of enzymes and substrates can be carefully controlled, intricately manipulated, analyzed, and even modeled to better understand PHB production in both *in vitro* and *in vivo* systems (136).

Enzymatic Production of PHB in C. necator. PHB is produced in many bacteria, including *C. necator*, via a pathway consisting of three enzymes as shown in Figure 7. The first enzyme, β-ketothiolase, catalyzes the Claisen ester condensation of two acetyl-CoA molecules, producing one CoA and one acetoacetyl-CoA molecule. Acetoacetyl-CoA is then utilized by the NADPH-dependent enzyme, acetoacetyl-CoA reductase, to produce β-hydroxybutyryl-CoA. Finally, PHB synthase catalyzes the polymerization of β-hydroxybutyryl-CoA, forming PHB and releasing CoA. *In vivo* this PHB synthesis pathway is highly regulated by CoA product inhibition, $NADPH/NADP^+$ ratios, and acetyl-CoA availability (137).

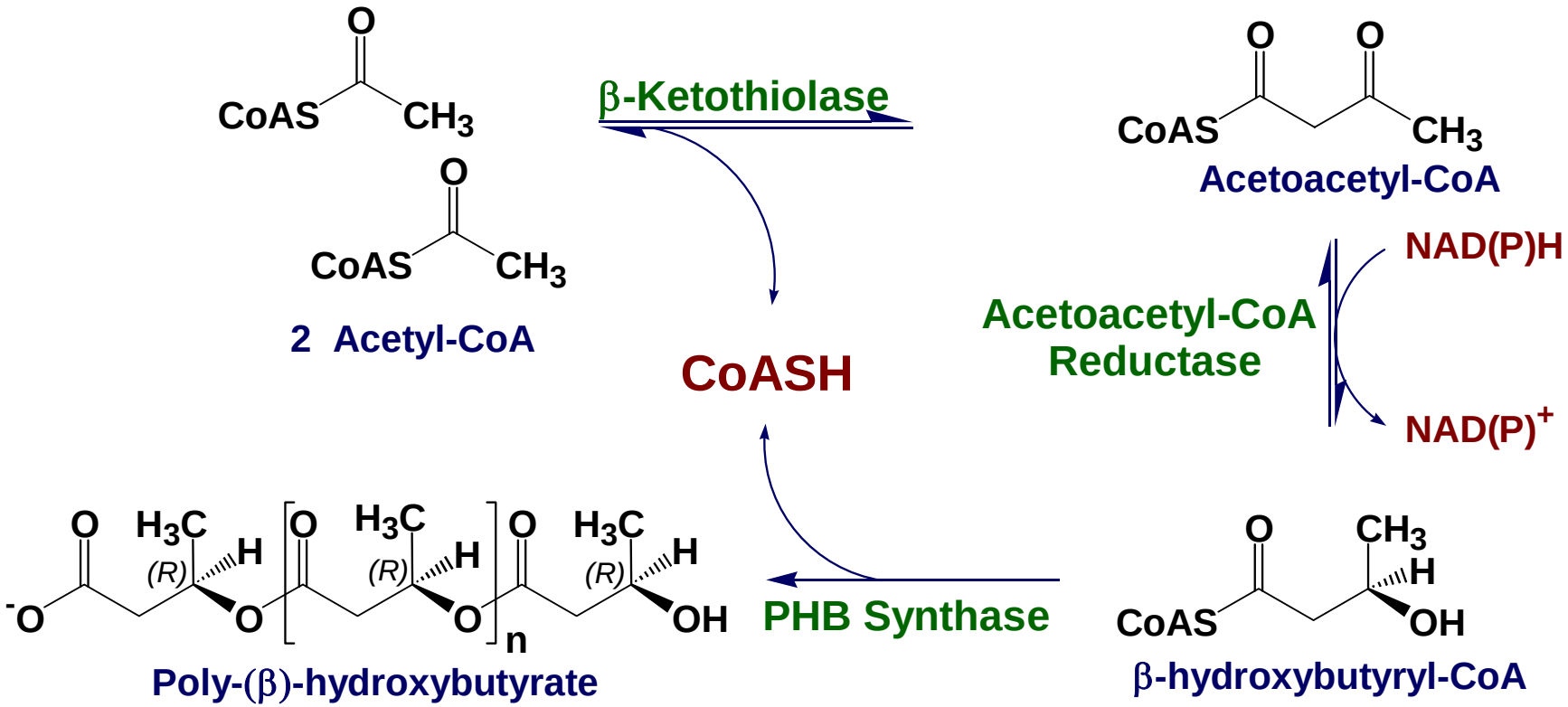

Figure 7. Enzymatic Biosynthesis of PHB in *C. necator*.

PHA Depolymerases. Several additional proteins are involved in the biosynthesis and biodegradation of PHB *in vivo* (138). Several bacteria employ PHA depolymerases to degrade PHAs. *C. necator* has been shown to exhibit five different PHA depolymerases designated as PhaZ1 (139), PhaZ2 (140), PhaZ3 (140), PhaZ4 (141), and PhaZ5 (142). The best studied PHA depolymerase, PhaZ1, has been shown by western blot to be expressed in nitrogen-limited, carbon-rich environments, but not in complete nutrient rich environments (138). We note that a granule associated D-(-)-β-hydroxybutyrate oligomer hydrolase has also been detected in *C. necator* and to avoid confusion with the depolymerases, this enzyme is designated as PhaY (138).

Studies of the PHA depolymerase enzymes are integral to understand the rate and mechanism of PHA biodegradation in the different microenvironments, such as in landfills or compost facilities. Several groups have investigated relationships between PHA chemical structure, crystallinity, and even various environmental situations on PHA depolymerase function and degradation rate (143-146). The presence of PHA depolymerase enzymes are obviously not desirable if the objective is to produce large quantities of PHA. Consequently, researchers have genetically modified bacteria that do not have depolymerase enzymes to contain the genes for PHA production (125). Metabolix now report a genetically engineered *E. coli* Strain K-12, which lacks PHA depolymerase enzymes, and can generate up to 90% of its dry cell weight as PHB (147).

The Phasins. First discovered in 1995 by Steinbuchel and Coworkers (148,149), the phasins, PhaP, are a fascinating class of proteins, which appear to be integral to production of PHA *in vivo*. The phasins are a non-catalytic class of proteins that represent up to 5% of the total cell protein of PHA laden cells; these proteins tightly associate with both native and synthetic PHB granules by binding the hydrophobic domain of the polymer while exposing their hydrophilic/amphiphilic domain to the cell cytoplasm (138). Four PhaP gene homologues, which generate the Phasin proteins, have been identified and are reported to be expressed in *C. necator* (138,142). The individual role of each phasin, designated PhaP1-4, is not yet known but PhaP1 and PhaP2 have been shown to bind PHB granules *in vitro* (142).

The high binding affinity and the large quantity of phasins is believed to prevent aggregation of the PHB and therefore stabilize the formation of PHA granules (138). Phasins also dramatically affect the rate of the PHA synthase enzyme, presumably by shifting the reaction equilibrium toward the direction of PHA synthesis by effectively removing the polymer product from solution by stabilizing the granule formation (138). Insertion of the PhaP gene from *C. necator* into the *P. aeruginosa* genome increases the activity the PHA synthase enzyme by approximately 50% (138,150). Additionally, *C. necator* mutants that lacked the ability to produce Phasins could generate PHB but did so at a much slower rate and nearly all the PHB was in a single granule instead of many small granules as is typical

(138,148). Also, experiments in which the PhaP genes were deleted from bacteria, showed production of 50% less PHA with respect to non-modified controls grown under identical conditions (138,151). Finally, experiments which overexpressed Phasins showed multiple small PHA granules (138,152).

Phasin Regulation. Phasins are regulated via an exquisitely sensitive and elegant mechanism, which was proposed by Potter and Steinbuchel (138), and is illustrated in Figure 8. The transcriptional repressor, PhaR, from *C. necator* binds at the PhaR promoter, the PhaP promoter region, and the PHA granule surface. As shown in Figure 8, Situation A, under conditions of normal growth, in which no PHA exists, PhaR is bound to the promoter regions of PhaP1 (a phasin gene) and PhaR; this serves to repress transcription of PhaP and prevent overexpression of the PhaR repressor protein. In the initial stages of PHA production, shown in Situation B, PhaR begins to associate with the areas of the PHA granule that are not in direct contact with the constitutively expressed PHA synthase enzyme. The association between PhaR and the PHA granule effectively lowers the cytoplasmic concentrations of PhaR until the levels of PhaR are no longer high enough to repress PhaP transcription, as shown in Situation C. At this point, illustrated by Situation D, PhaP transcription continues to generate the Phasin protein until the PHB granule is nearly covered with Phasins. The PHB granule has a higher affinity for phasins than PhaR so, as Situation E indicates, the PhaR transcriptional repressor is eventually

displaced from the granule surface. This results in higher cytoplasmic concentrations of cytoplasmic PhaR which favor the binding of PhaR to the PhaP promoter leading to eventual shut down of phasin production and consequently of further PHB synthesis (138).

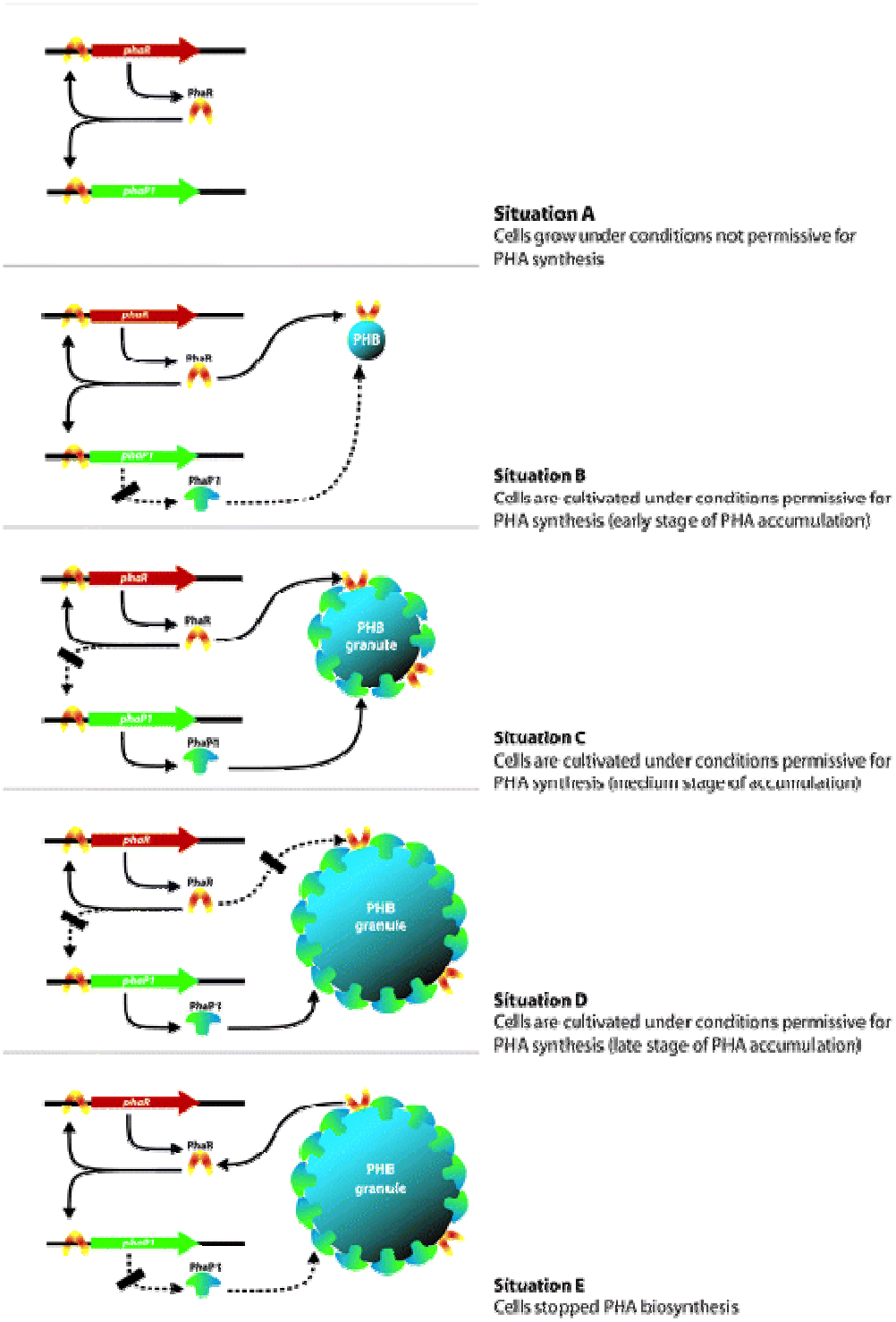

Figure 8. Model of Regulation of PHA Granule Formation by the Transcriptional Regular Protein, PhaR. Reproduced from Potter *et al* (138).

Several lines of evidence support the proposed mechanism for Phasin regulation of PHA production (138). Deletion mutants of PhaR constitutively express high levels of PhaP1. PhaC (PHB synthase) deletion mutants, which obviously generate no PHB, produce no PhaP gene products (153). PhaR and PhaC double deletion mutants express high levels of PhaP (154). This evidence suggests that PhaR binds to the promoter region and represses transcription of PhaP (138). Western blots using antibodies for PhaR and other proteins that copurify with the PHA granule indicate that PhaR does indeed bind the PHA granule (155). Additionally, the gel shift between PhaR and a known DNA binding sequence is reversed by the presence of PHA suggesting that PhaR does indeed bind to PHA and with a higher affinity than to the DNA sequence (138,155).

A History of In Vitro Syntheses of PHB. *In vitro* or cell free enzymatic syntheses have been reported in the literature since the early 20th century (156). Indeed, cell free syntheses were integral to elucidating most of the biochemical pathways that are so familiar today (156,157). Thus, it comes as no surprise that *in vitro* techniques were employed for the elucidation of the biochemical pathways for PHB.

As early as 1961, Merrick and Doudoroff (158) reported in the Journal Nature, an *in vitro* synthesis of radioactive PHB, which used particulate fractions of cell free extracts from *B. megabacterium* and *R. rubrium*, two bacteria that were know at the

time to generate PHB. Merrick and Doudoroff chemically synthesized the radioactive β-hydroxybutyryl-CoA substrate for the *in vitro* radioactive PHB synthesis (158) from radioactive β-hydroxybutyric acid, which was produced via alkaline hydrolysis of radioactive PHB, that had been synthesized *in vivo* by feeding the bacteria *R. rubrium* radioactive acetate (158). The enzyme for Merrick and Doudoroff's synthesis was isolated from bacterial cells by osmotic lysis using lysozyme followed by sonic oscillation and centrifugation to separate the polymer granules from the cell membrane. The enzyme isolation technique and *in vitro* reaction results suggest that Merrick and Doudoroff did indeed successfully isolate the enzyme PHB synthase; however, the extract was quite crude and the authors mention that enzyme kinetics were complicated by the presence of a depolymerase (158).

First Multi-Step In Vitro Enzymatic PHB Syntheses. In 1977, Saito *et al*. (159) reported the first multi-step *in vitro* enzymatic synthesis of PHB. The authors used the radioactive acetyl-CoA substrate, the NADPH cofactor, and three enzymes, β-ketothiolase, acetoacetyl-CoA reductase and PHB synthase, which were crudely purified from Z. ramigeria for the *in vitro* PHB synthesis (159). The authors also identified two distinct acetoacetyl-CoA reductase enzymes, which were specific for either NAD(H) or NADP(H) and determined that only the NADPH-dependent enzyme was involved in PHB synthesis. The NADPH-dependent acetoacetyl-CoA reductase enzyme stereoselectively produces the

D-(-)-isomer of β-hydroxybutyric acid, which is the only isomer that the PHB synthase enzyme is capable of polymerizing into PHB. As discussed previously, the isotactic property of PHB is essential to its mechanical properties and it is the enantioselectivity of the NADPH-dependent acetoacetyl-CoA reductase and PHB synthase enzymes which ensure that PHB is indeed isotactic (159).

In 1988, Haywood *et al*. (160) reported the multi-step *in vitro* synthesis of radiolabeled PHB using enzymes from *C. necator*. Consistent with Saito's (159) previous study, Haywood *et al*. (160) identified and kinetically analyzed the NADH- and NADPH-dependent acetoacetyl-CoA reductase enzymes and found that, like the enzyme from Z ramigeria, the NADPH-dependent enzyme exclusively generated the D-(-)-isomer of β-hydroxybutyryl-CoA. By reconstituting the complete three enzyme system, the authors established that the NADPH-dependent acetoacetyl-CoA reductase enzyme is involved in the synthesis of PHB in *C. necator* since the NADH-dependent acetoacetyl-CoA reductase did not produce appreciable quantities of PHB activity (160).

Other In Vitro Syntheses of PHB. Several other *in vitro* enzymatic syntheses, diagrammed in Figure 9 (44), have been reported in the literature with varying degrees of complexity and success. The simplest '*in vitro*' synthesis system involves a single enzyme, typically PHB synthase, which polymerizes PHB from β-hydroxybutyryl-CoA. Considering, that this one-enzyme *in vitro*

synthesis is nothing more than the native reaction for the PHB synthase enzyme it is not surprising that there have been multiple literature reports describing this system since Merrick and Doudoroff's (158) initial 1961 report. Additionally, Haywood, Anderson and Dawes reported this one-enzyme *in vitro* synthesis in a 1989 report on the *C. necator* PHB synthase reaction stoichiometries, enzyme kinetics, and C_4-C_5 chain length specificity (161).

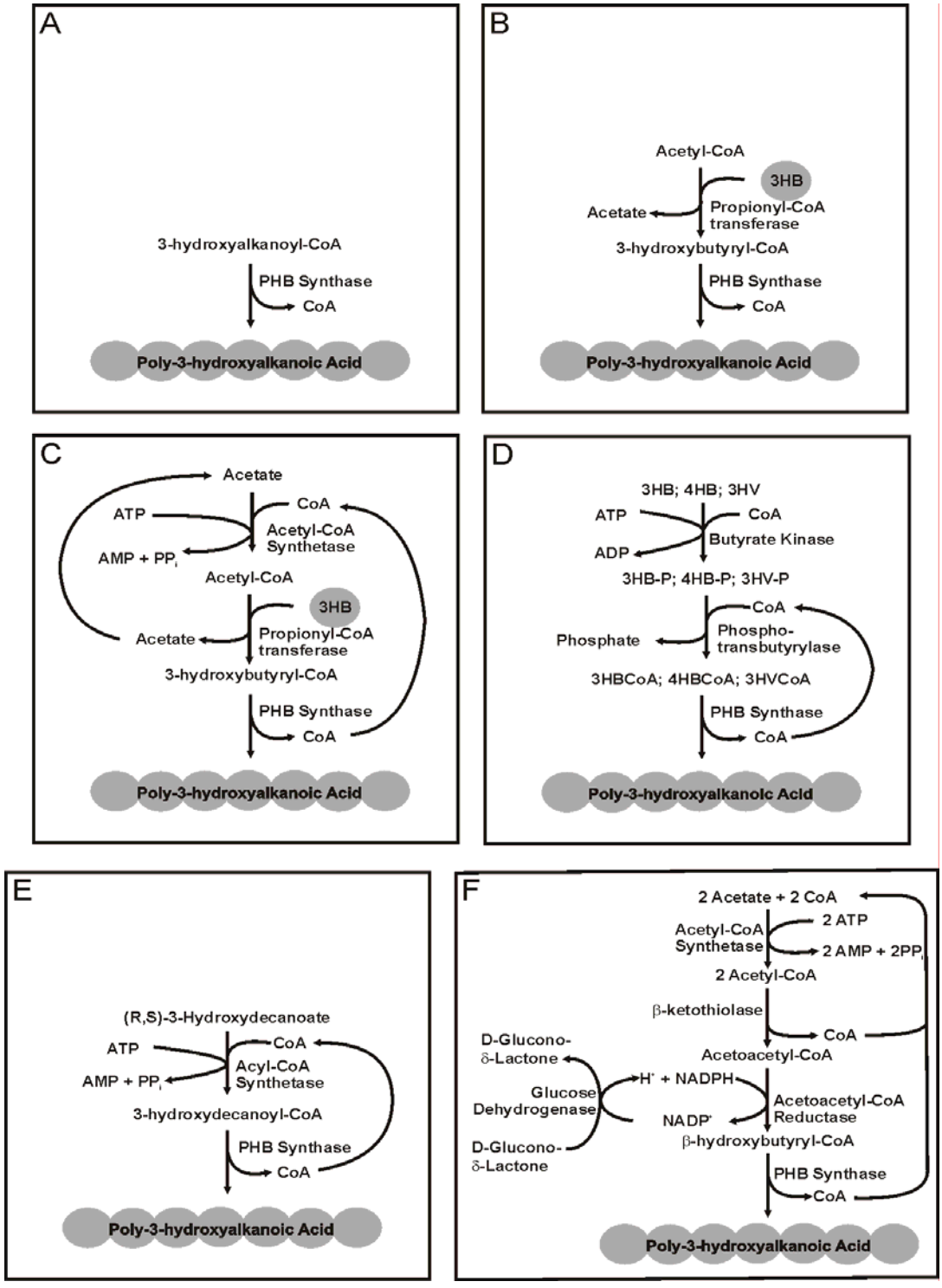

Figure 9. Systems for the I*n Vitro* Synthesis of PHA. Modified from Steinbuchel (44).

One Enzyme In Vitro Syntheses.

First Complete Isolation of PHB Synthase for the One Enzyme In Vitro Synthesis. The 1994 report by Gerngross *et al.* (162) is probably considered the seminal modern report on the PHB synthase reaction, in large part because this paper details the procedure for overexpressing and obtaining highly pure PHB synthase from *E. coli*. The key developments of the Gerngross *et al.* (162) paper include reengineering the 5'-end of the wild type gene to increase expression of the soluble form of the PHB synthase enzyme and transforming the gene into an *E. coli* strain that was deficient in the protease, ompT, which helps to avoid substantial proteolysis during isolation. Additionally, the nonionic detergent Hecameg was added to all buffers to increase enzyme stability (162).

With quantities of overexpressed and highly purified enzyme in hand, Gerngross and Martin (135) reported an *in vitro* PHB polymerization system in 1995 that was capable of generating PHB granules with molecular weights in excess of 10×10^6 Da. The molecular weight of PHB produced *in vitro* in this study exceeds that of the PHB generated *in vivo* by an order of magnitude possibly suggesting that the polymer size restrictions that are present *in vivo* do not affect *in vitro* syntheses. Indeed, the authors suggest that the enzyme in the *in vitro* system may be incapable of transferring to a new chain (135). Gerngross and Martin (135) obtained enantiomerically pure (R)-β-hydroxybutyryl-CoA substrate by using the NADPH-dependent acetoacetyl-CoA

reductase enzyme to catalyze the enantioselective reduction of acetoacetyl-CoA followed by HPLC purification of the β-hydroxybutyryl-CoA enantiomer. The PHB synthesized by the PHB synthase one-enzyme system formed granules within minutes, which reached 3μM. Moreover, granule mass and polymer molecular weight depended on PHB synthase concentrations, with higher synthase concentrations favoring lower polymer molecular weights and greater numbers of small granules (135).

One Enzyme In Vitro Synthesis in C. vinosum. Steinbuchel and coworkers published an extensive study of the PHB synthase reaction from *Chromatium vinosum.* This study of a class III (163) synthase was complete with UV reaction time courses, phase-contrast microscopy, and attractive secondary electron micrographs of gold-coated PHB granules. Reactions were carried out using purified (R)-β-hydroxybutyrl-CoA that was obtained by transesterification of CoA and (R)-β-hydroxybutyric acid catalyzed by propionyl-CoA transferase. In contrast to the enzymes from *C. necator*, NAD^+ and $NADP^+$, but not the respective reduced forms, inhibited the synthase from *C. vinosum*. Stubbe also published an examination of the kinetics of His_6-tagged PHB synthase from *C. vinosum* (163,164).

One Enzyme In Vitro Synthesis in C. necator. The *C. necator* PHB synthase enzyme, overexpressed in and purified from *E. coli*, was employed by Lenz *et al*. in a 1999 (118) study of the enzyme's kinetics with β-hydroxybutyryl-CoA and β-hydroxyvaleryl-CoA as substrates for the one-enzyme *in vitro* polymerization

reaction. This study closely examines the enzyme lag phase, which had previously been reported by Gerngross and Martin (135). The report demonstrates that the lag phase phenomena is dependent on detergent (Hecameg) and BSA concentrations, and could be eliminated by adding either 50% glycerol to the crude enzyme extract or by priming the reaction with the β-hydroxybutyryl-CoA substrate (118). In the absence of the lag phase, PHB synthase showed straight-forward Michaelis-Menten kinetics, with K_M values determined for β-hydroxybutyryl-CoA and β-hydroxyvaleryl-CoA, and a K_I of 370 •M found for CoA (118).

In a 2000 study, Lenz (165) and coworkers expanded upon their previous work (118) by demonstrating that the addition of multihydroxyl compounds could eliminate the lag phase of PHB synthase. Additionally, the K_M values for β-hydroxybutyryl-CoA and β-hydroxyvaleryl-CoA were revised, the K_M for γ-hydroxybutyryl-CoA was determined, K_{cat} values for all substrates were obtained, and CoA was found to be a competitive inhibitor with a revised K_I of 108 μM with respect to β-hydroxybutyryl-CoA. Furthermore, the authors showed that the active form of the PHB synthase enzyme was the dimer, not the monomer form, by using equilibrium experiments and size exclusion chromatography in the presence and absence of 20% fructose (165).

In the same year, Su *et al.* (166) used the one-enzyme PHB synthase *in vitro* system to produce homopolymers, random and block copolymers containing the β-hydroxybutyric acid and β-hydroxyvaleric acid monomers. The results of this study were

consistent with previous kinetic analyses, which indicate that PHB synthase prefers β-hydroxybutyryl-CoA to β-hydroxyvaleryl-CoA. In contrast to synthesis of the PHB homopolymer, which goes to completion, synthesis of the PHV homopolymer (V = valerate) was terminated at approximately 90% conversion. Likewise, PHB(V) copolymer synthesis required four times longer to reach 100% completion than did synthesis of the PHB homopolymer. In contrast to the *in vivo* syntheses in *C. necator*, PHB(V) copolymers synthesized *in vitro* were not essentially random, instead they exhibited characteristics consistent for a more blocky copolymer, which would be expected for this sort of *in vitro* batch copolymerization.

The experiments by Su *et al.* (166) established that the synthesis of PHB *in vitro* meets the criteria for a living polymerization reaction, in which each PHB synthase enzyme initiates the polymerization reaction for a single polymer chain and continues chain propagation with no branching, chain transfer, or termination until the substrate is exhausted or the reaction quenched. This *in vitro* PHB synthesis exhibits a classic diagnostic characteristic for living polymers, specifically that higher monomer to enzyme (initiator) ratios result in a higher molecular weight polymer. Living polymers typically have molecular weight distributions approaching unity, which describes the uniformity of polymer molecular weights. However, this *in vitro* system exhibits somewhat broad molecular weight distributions but *Su et al.* (166) report that the

polydispersity is within a reasonable range for living polymers, and suggest that this variance could occur if the rate of polymer initiation is slower than chain propagation

In subsequent reports, Lenz and Coworkers (167,168) successfully developed a one-step purification procedure for the PHB synthase from *E. coli* that harbored the plasmid containing the PhbC gene from *C. necator*. The isolated PHB synthase enzyme was then used in the *in vitro* one-enzyme synthesis of PHA copolymers that contained the β-hydroxybutyric acid and β-hydroxypropionic acid monomers. Kinetic analyses indicated that CoA was a competitive inhibitor of β-hydroxypropionyl-CoA with a K_I of 85 μM; this level of inhibition could explain the low degree of β-hydroxypropionyl-CoA polymerization, which was reported at less than 40%. Lenz and coworkers also established that, in solution, the PHB synthase enzyme exists in both monomeric and dimeric forms. Mutagenesis analyses indicated that a cystine thiol, C319, is present on each monomer subunit and forms a single catalytic active site at the dimmer interface for polymer initiation and propagation.

One Enzyme In Vitro Synthesis with the PHB Synthase from E. shaposhnikovii. Lenz, Goodwin, and Coworkers (169) studied the enzyme kinetics and substrate specificities of the PHB synthase from *Ectothiorhodospira shaposhnikovii*. In a follow up study (170), the authors use PHB synthase to synthesize the novel homopolymers poly-β-hydroxy-3-cyclopropylpropionic acid and poly-β-hydroxy-4-chlorobutyric acid using the PHB synthase from *E.*

shaposhnikovii. It is highly unlikely that these unusual homopolymers could be synthesized *in vivo*. Thus, this work highlights the promise of *in vitro* syntheses for creating novel polymers that would likely not be generated *in vivo* due to constraints in cellular uptake, potential cell toxicity, or the absence of *in vivo* pathways for monomer generation (171).

In solution the *C. necator* PHA synthase enzyme exists either as the non-active monomer or the active dimer; this is typical of Class I PHA synthase enzymes (168). Class III synthases, of which the enzyme *E. Shapshnikovii* is classified, differ significantly in structure; specifically, the enzyme from *E. shaposhnikovii* is comprised of two protein subunits designated PhaE and PhaC which interact to form either a dodecamer containing 12 PhaE and 12 PhaC subunits, or a hexamer of 6 PhaE and 6 PhaC subunits (171). The dodecameric form of the PHB synthase enzyme exhibits a higher specific activity for PHB polymerization than the hexameric form. Akin to the *C. necator* enzyme, results suggest that the E. shaposhnikovii PHB synthase enzyme may catalyze a living polymerization with each catalytic site consisting of two PhaE and two PhaC subunits (171).

In Vitro One Enzyme Synthesis with A. vinosum. *In vitro* one-enzyme polymerization systems have been developed with PHB synthase enzymes from several other organisms. The His_6-tagged PHA synthase derived from *Allochromatium vinosum* was used for the *in vitro* one-enzyme synthesis of several PHA compounds by Stubbe, Sinskey and Coworkers (172). A thorough analysis of this

enzyme's kinetics and substrate preferences demonstrated that, like the Class III enzyme from *E. Shaposhnikovii*, the *A. vinosum* enzyme has broad substrate specificity and a relatively non-specific binding pocket. In contrast to the Class I *C. necator* enzyme, the enzyme from *A vinosum* accepts moieties that lack large portions of the substrate's CoA moiety such as (R)-β-hydroxybutyryl N-acetylcysteamine thioester and (R)-β-hydroxybutyryl-D-pantetheine thioester (172). A loose binding pocket and relatively broad substrate specificity is somewhat characteristic of the Class III PHA synthases (172).

In Vitro One Enzyme Synthesis with T. thermophilus.

Pantazaki *et al.* (173) used the PHB synthase enzyme from the thermophilic bacterium *Thermus thermophilus* in the one-enzyme *in vitro* synthesis of PHB. The authors also analyzed the *in vitro* activities of the β-ketothiolase and acetoacetyl-CoA reductase enzyme from *T. thermophilus* and established that this bacterium utilizes a similar pathway for PHB biosynthesis as *C. necator* and several other PHA generating bacteria. The reported K_M for (D,L)-β-hydroxybutyryl-CoA is 250 μM and the molecular weight of the enzyme does not permit classification of this PHB synthase as either type I , II or III; thus, this may represent a fourth class of PHB synthases. The authors (173) also suggest that this enzyme may be modified by phosphorylation since dephosphorylation in alkaline phosphatase assays inactivate the enzyme. In contrast to all other PHB synthase enzymes that have been reported in the literature the *T. thermophilus* enzyme did not

exhibit a lag phase (173); however, this may be due to problems with sample purity.

Granule Morphology for the In Vitro Synthesis of PHB. Recently, Doi and Coworkers (174) reported an AFM study of granule morphology for the one-enzyme *in vitro* synthesis of PHA. While AFM has been used to study *in vivo* granule formation (175-177), this is the first report to examine *in vitro* granule formation with AFM (174). Previously, Nobes *et al* (178) examined the morphology of PHA granules produced via one-enzyme *in vitro* syntheses with transmission electron microscopy (TEM) and cryo-TEM. Doi and coworkers (174) note that AFM directly images the surface of bio-based materials without the sample preparations needed for TEM, which can result in artifacts. The authors used AFM to show the time dependent reaction time course of *in vitro* PHA synthesis. Initially, AFM detected spherical 2.7 ± 0.6 nm particles, which were the PHA synthase enzymes that had been isolated from *C. necator* and deposited on highly oriented pyrolytic graphite (HOPG). Within five minutes of initiating the reaction with the substrate β-hydroxybutyryl-CoA, AFM showed fibrillar strands of 0.3 nm thickness extending approximately 25 nm from the PHA synthase enzymes. This suggests that in the initial reaction stages a PHB-enzyme conjugate is formed (174).

Doi and Coworkers (174) reported a second set of AFM experiments in which the β-hydroxybutyryl-CoA substrate was consumed within four minutes. In these experiments, AFM showed

rapid formation of PHB-enzyme conjugates and granule formation from individual micelles within one minute. In the initial stage, granules formed varying in size from 50 to 200 nm, with the larger granules appearing to be aggregates containing between two and five of the smaller 50 nm granules. After 3 minutes, nearly all the β-hydroxybutyryl-CoA had been consumed and the AFM image showed fewer but substantially larger PHB structures, which appeared to be comprised of several smaller, 150-400 nm, spherical granules. At ten minutes, fully six minutes after the reaction reached completion, the AFM images showed massive PHB clusters with lengths in excess of 10 μm. Additionally, multiple smaller 100-250 nm particles now extended from the surface of the massive 10 •M PHB clusters.

The authors speculate that the morphological change from a smooth surface at three minutes to a 'pincushioned' appearance at ten minutes might result from the ejection of water from the granule (174). This conjecture is supported by the AFM images in which the surface spheres physically appeared similar to water (they were clear), and by the previous results of the TEM study by Nobes *et al* (174). Moreover, an examination of these 100-250 nm protrusions revealed a periodical phase shift over the surface, which measured 20-30 nm; this corresponds to the size of the PhaC enzyme from *C. necator*. Treatment of the massive granules with Proteinase K, a general protease, resulted in morphological changes.

Model of Granule Morphology. Doi and Coworkers (174) used the results from the AFM studies to develop a model of PHB granule formation. The authors suggest that granule coalescence continues after completion of PHB synthesis, which leads to the formation of granule clusters exceeding 10 µM in size. The ejection of water from granule clusters eventually changes the surface morphology so that 100-250 nm PHB granules, which are densely covered with PHA synthase enzymes, cover the surface of the large 10µM granules. The 'pincushioned' appearance of PHB granules does not occur *in vivo*, and the authors suggest this morphology may occur *in vitro* because granules are able to interact more freely with one another (174). We note that the authors fail to suggest that the morphological discrepancy between granules formed *in vitro* and *in vivo* could very likely be due to the presence of phasin proteins *in vivo*, which cover and stabilize granules *in vivo*.

Limitations of One-Enzyme In Vitro Systems for PHA Synthesis. One-enzyme *in vitro* PHB syntheses are ideal for dissecting enzyme mechanism, kinetics and substrate specificity. However, these systems suffer from two major drawbacks: 1.) the costs of the acyl-CoA substrate make PHB production prohibitively expensive, in excess of $500.00 U.S. per pound of PHB produced (44), 2.) CoA generates significant product inhibition that substantially retards the PHB synthase enzyme and lowers final

PHB yields (44). These limitations have prompted the development of several multi-enzyme systems for PHA synthesis (44).

In Vitro Multi-Enzyme Systems for PHB Synthesis. Jossek and Steinbuchel (179) used three enzymes, acetyl-CoA synthetase, propionyl-CoA transferase and PHB synthase in an *in vitro* synthesis of PHB from acetate, as shown in Figure 9, Panel C. In this system, acetyl-CoA was generated from acetate by the commercially available ATP-dependent enzyme, acetyl-CoA synthetase, which was from *Sachromyces cerevisiae*. Acetyl-CoA and D-(-)-β-hydroxybutyric acid are then used to synthesize D-(-)-β-hydroxybutyryl-CoA by the action of purified propionyl-CoA transferase from *Clostridium propionicum*. PHB synthase then polymerizes the D-(-)-β-hydroxybutyryl-CoA to PHB (179), and the byproduct of this reaction, CoA, is recycled to generate further acetyl-CoA by the above mentioned acetyl-CoA synthetase. The authors (179) also reported an abbreviated two-enzyme system, illustrated in Figure 9, Panel B, which used only propionyl-CoA transferase and PHB synthase. Unfortunately, this abbreviated two-enzyme system suffered from significant CoA product inhibition, and the cost of acetyl-CoA was prohibitively high.

This study highlights the importance of the addition of the acetyl-CoA synthetase enzyme, which recycles CoA and generates acetyl-CoA, *de novo*. Recycling the CoA will alleviate CoA-product inhibition of the PHB synthase reaction thus allowing polymer synthesis to proceed. Moreover, the three-enzyme system

utilizes the inexpensive substrate, acetate, as a feedstock and hydrolysis of ATP to AMP and Pi drives the reaction forward. Since AMP and acetate are the only inputs into this system, the cost for PHB production is limited by the price of the more expensive substrate, ATP; this reduces polymer costs to approximately $15 per pound (179). Although this cost reduction makes polymer production feasible on a semi-preparative scale , this price is obviously still too high for commercial viability. Another disadvantage of this system is that propionyl-CoA transferase generates both isomers of β-hydroxybutyryl-CoA; thus, either enantiomerically pure starting materials must be used or half of the β-hydroxybutyryl-CoA that is generated by the propionyl-CoA transferase reaction will remain unreacted during polymer synthesis (179).

In 2002, Liu and Steinbuchel (180) introduced another system, diagrammed in Figure 9, Panel D, for the *in vitro* biosynthesis of PHB from β-hydroxybutyric acid. This system used the enzymes butyrate kinase and phosphotransbutyrylase that were derived from *Clostridium acetobutylicum*, and a class III PHB synthase that was derived from *E. coli*, which harbored a plasmid containing the gene from *Chromatium vinosum*. In this system, the enzyme butyrate kinase catalyses the ATP-dependent activation of β-hydroxybutyric acid; this forms β-hydroxybutyryl phosphate, with the liberation of ADP. The high energy phosphodiester bond of β-hydroxybutyryl phosphate is then converted to a high energy thioester linkage by the enzyme phosphotransbutyrylase with

inorganic phosphate released. Finally, the β-hydroxybutyryl-CoA undergoes polymerization by the PHA synthase enzyme (180), liberating CoA in the process.

Liu and Steinbuchel (180) developed this system to overcome a design flaw of the previous Jossek and Steinbuchel system (179). In the Jossek and Steinbuchel system (179), the acetoacetyl-CoA synthetase enzyme converts ATP to AMP with release of pyrophosphate, as shown in Figure 9, Panel C. As discussed above, the cost of ATP sets the price for producing PHB in these types of *in vitro* systems (44). Since converting ATP to AMP consumes two ATP equivalents, recycling AMP back to ATP requires two enzymatic reactions; this is metabolically expensive. Liu and Steinbuchel's (180) three-enzyme system, which uses butyrate kinase, consumes only one ATP equivalent; thus, future implementation of ATP recycling would require only one enzyme and less cost. We do note that recycling of ATP was not actually implemented in this system (180).

The three-enzyme system developed by Liu and Steinbuchel (180), shown in Figure 9, Panel D, elegantly recycles CoA by using the enzyme phosphotransbutyrylase to catalyze the thioesterification of CoA and β-hydroxybutyryl-phosphate to β-hydroxybutyryl-CoA. The phosphotransbutyrylase enzyme acts to effectively decrease CoA-product inhibition of the PHB synthase enzyme, which facilitates polymer synthesis. Moreover, the authors (180) suggest that the phosphotransbutyrylase reaction rapidly converts CoA to β-hydroxybutyryl-CoA, thus effectively

sequestering CoA in the form of β-hydroxybutyryl-CoA, which further diminishes any inhibition of PHB synthase by CoA.

One of the disadvantages of this three-enzyme system, which Liu and Steinbuchel (180) specifically address, is the lack of substrate flexibility of the phosphotransbutyrylase enzyme. Indeed, homopolymers containing the poly-γ-hydroxybutyric acid and poly-γ-hydroxyvaleric acid monomers could not be synthesized *in vitro*. However, this system could synthesize copolymers containing β-hydroxybutyric acid and γ-hydroxybutyric acid monomers that contained from 1 to 46 mole percent of the γ-hydroxybutyric acid monomer (180). This system's poor substrate flexibility stems from the specificity of the phosphotransbutyrylase enzyme and is particularly regrettable because the class III PHA synthase from *Chromatium vinosum* is known to have broad substrate flexibility (180). Another drawback of this system is the inability to produce the D-(-)-β-hydroxybutyryl-CoA isomer exclusively (181). This situation is likened to the previous system developed by Jossek and Steinbuchel (179) in which synthesis of PHB will waste half of the enzymatically synthesized β-hydroxybutyryl-CoA, or enantiomerically pure D-(-)-β-hydroxybutyric acid must be used as a feedstock for this reaction (181).

Qi, Steinbuchel and Rehm (150) developed an interesting *in vitro* PHA synthesis, which used the class II PHB synthase from *Pseudomonas aeruginosa*, as shown in Figure 9, Panel E. This was also the first literature account to successfully purify a class

II PHA synthase; the authors used convenient His_6-tagged technology to facilitate isolation of this notoriously difficult to purify enzyme (150). Class II PHA synthases are similar to the Class I in that they consist of a single subunit, which exists in solution as monomers or dimers (150,173). Typically, the molecular weight of Class I and Class II synthases vary somewhat. Class II PHA synthases, mainly found in the Pseudomonias genome, prefer medium chain length β-hydroxy fatty acids (C_6-C_{14}), which are typically derived *in vivo* from *de novo* fatty acid biosynthesis and fatty acid β-oxidation. PHAs formed from medium chain length monomers tend to be latex-like polymers (150,173).

As depicted in Figure 9, Panel E, Qi, Steinbuchel and Rehm's (150) two-enzyme *in vitro* synthesis used commercially available acetyl-CoA synthetase, which was derived from a Pseudomonias species [E.C. 6.2.1.3], to catalyze the ATP-dependent thioesterification of (R,S)-β-hydroxydecanoate and CoA to form (R,S)-β-hydroxydecanoyl-CoA with liberation of AMP and pyrophosphate. The class II PHA synthase from *P. aeruginosa* then polymerized the (R,S)-β-hydroxydecanoyl-CoA to poly-β-hydroxydecanoic acid (150). This two-enzyme system (150) took advantage of the broad substrate flexibility of the Pseudomonias-derived acetyl-CoA synthetase, which could synthesize β-hydroxydecanoyl-CoA. Furthermore, the acetyl-CoA synthase reaction effectively recycled CoA, which prevented any CoA product inhibition and favored PHA synthesis.

The authors (150) note that the weight average molar mass for PHB synthesis with the Class II PHB synthase from *P. aeruginosa* was 9.8 x 10^4 g/mol. This value is substantially lower than the average molar masses observed for the *in vitro* PHB syntheses that used the class I, *C. necator*, and class III, *C. vinosum*, PHB synthases, which were approximately >12 x 10^6 g/mol (135) and 1.6 x 10^6 g/mol (179), respectively. The study reports that each PHA synthase enzyme synthesizes only about 0.6 polymer chains, which indicates that this should be classified as a living polymerization. The same drawbacks occur with this system as discussed for the previous systems; specifically, that the enantioselectivity of the PHB synthase enzyme results in a desirable isotactic polymer by either wasting half of the β-hydroxydecanoyl-CoA synthesized enzymatically in this system or requires costly, enantiomerically pure β-hydroxydecanoic acid be provided as a substrate (150).

Recently, Satoh *et al*. (182) published a system that was nearly identical to the system developed by Qi *et al* (150). Satoh *et al*. (182) reported the *in vitro* synthesis of the copolymer poly-(β)-hydroxybutyrate-co-(γ)-hydroxybutyrate [P(βHB-*co*-γHB)] which used His_6-tagged PHA synthase isolated from *E. coli*, which harbored the plasmid containing the *C. necator* PhaC gene, and an acyl-CoA synthase from *Pseudomonias oleovorans*. In this system, the acyl-CoA synthetase enzyme catalyzed the ATP-dependent thioesterification of CoA and the hydroxyalkanoic acid to the respective hydroxyalkanoyl-CoA, which was then polymerized

via the PHA synthase. The enzyme pyrophosphatase, which hydrolyzes pyrophosphate to inorganic phosphate, was also added to the reaction mixture presumably to drive the reaction forward by removing the pyrophosphate product, although the authors do not discuss this decision. Despite striking similarities between this system and the one developed by Qi *et al*. (150) to synthesize poly-β-hydroxydecanoic acid with enzymes from *P. aeruginosa*, Satoh *et al*. (182) does not mention the previous work and the authors (182) are apparently ignorant of the previously published system.

The system developed by Qi *et al.* (150) (Figure 9, Panel E) efficiently recycled CoA; likewise, the Satoh *et al*. system was reported to recycle CoA 4.2 times during the synthesis of 1.5 mg of the poly-γ-hydroxybutyric acid homopolymer (182). Perhaps the largest contribution of the Satoh (182) publication is the reported ability to produce copolymers with strict control over monomer composition (182). The authors also reported the *in vitro* production of the poly-(γ)-hydroxybutyric acid homopolymers with a polydispersity and number average molecular weight of 1.5 and 9.3 x 10^5, respectively (182).

In 2003, Satoh *et al*. (181) reported the enzymatic synthesis of PHB from acetate with cofactor recycling. As shown in Figure 9, Panel F, this system uses three His_6-tagged enzymes that were isolated from *E. coli*, which harbored plasmids containing the genes for PHB synthesis from *C. necator*. In addition, His_6-tagged acetyl-CoA synthetase enzyme and the

commercially available glucose dehydrogenase were used in this system for cofactor recycling. His_6-tagged acetyl-CoA synthetase catalyzed the ATP-dependent thioesterification of acetate and CoA to produce acetyl-CoA, AMP, and P_i. Condensation of acetyl-CoA to acetoacetyl-CoA with CoA liberation was catalyzed by the enzyme β-ketothiolase. Acetoacetyl-CoA was dehydrated to β-hydroxybutyryl-CoA by the action of the NADPH-dependent acetoacetyl-CoA reductase, which consumed one NADPH producing $NADP^+$. $NADP^+$ was recycled to NADPH by glucose dehydrogenase, with consumption of the relatively inexpensive substrate glucose. PHB synthase polymerized the β-hydroxybutyryl-CoA to PHB with CoA liberation. The acetyl-CoA synthetase reaction serves to recycle the CoA liberated by the β-ketothiolase and PHB synthase reactions; this effectively closes the loop (181).

Acetate, D-glucose, and ATP are the feed stocks for this five-enzyme system developed by Satoh *et al*. (181), and because ATP is the most expensive of the substrate it essentially sets the cost for this *in vitro* synthesis of PHB. Recycling of CoA by the acetyl-CoA synthetase reaction effectively reduces CoA concentrations, which decrease inhibition of the PHB synthase and the β-ketothiolase reaction; this facilitates the forward polymerization reaction. An attempt by Satoh *et al.* (181) to employ a truncated two-enzyme system, which used only β-ketothiolase and acetoacetyl-CoA reductase, resulted in prohibitively low substrate conversions, which were less than 6%; this emphasizes the critical importance of cofactor recycling.

The authors suggest that recycling the CoA produced by the condensation of acetyl-CoA prevented CoA-mediated product inhibition of the β-ketothiolase enzyme and therefore facilitated the overall reaction progress (181). This certainly seems a reasonable contention considering that CoA is reported to be a competitive inhibitor of the β-ketothiolase and PHB synthase enzymes (181).

Using this system, Satoh *et al*. (181) produced 5.6 mg of PHB in a 5 mL reaction mixture, which had a low polydispersity of 1.36 and a weight average molecular weight of 6.64×10^6. The reaction was monitored for CoA, acetyl-CoA, acetoacetyl-CoA and β-hydroxybutyryl-CoA using a novel HPLC system; this was the first report to actually monitor all CoA-containing metabolites. However, this methodology required over 55 minutes to analyze each reaction time point. During the course of the complete five-enzyme reaction, CoA and NADPH were reported to be recycled at least 26 times in a 24-hour period. Like all systems that use acetyl-CoA synthetase, the AMP produced is difficult to recycle; consequently, this system is limited by the cost of consuming two ATP equivalents for each reaction. This system is the first system to recycle both CoA and $NADP^+$. Furthermore, all of the β-hydroxybutyryl-CoA generated is of the correct enantiomeric form so 100 % of it can be polymerized by the PHB synthase enzyme.

Satoh *et al*. (181) does mention a potential system for recycling AMP to ATP, which uses the enzymes polyphosphate-AMP phosphotransferase from *Myxococcus xanthus* and polyphosphate

kinase from *E. coli*. While this ATP regeneration system, developed by Satoh and coworkers (183), appears to be a feasible solution for recycling ATP in the *in vitro* PHB system, to date the authors have not reported this or any other AMP recycling system (181).

Immobilized In Vitro PHB Syntheses. Immobilized *in vitro* PHB syntheses have been successfully developed by Kim *et al*. (184) using a His_{10}-tagged *C. necator* PHA synthase enzyme, which was immobilized via a tether to a Ni-NTA derivatized surface. PHA synthase catalyzed the polymerization of β-(R)-hydroxybutyryl-CoA to PHB while immobilized on Ni-NTA derivatized agarose beads and/or silicon wafers. Lithographic techniques were used to control the location of the Ni-NTA derivatized surface; this defined the location of the bound PHA synthase and subsequent polymer formation. This novel fusion of surface initiated polymerization and *in vitro* PHA synthesis may have applications in thin films, controlled adhesion, protective coatings, and improved material biocompatibility (184).

In a nearly identical study, Paik *et al*. (185) reported an approach to end-functionalization of PHB. First, $His_{(10)}$-tagged PHB synthase catalyze the *in vitro* synthesis of PHB; this creates PHB-enzyme conjugates. Then, the PHB-enzyme conjugates, were collected by centrifugation, rinsed, and dissolved in chloroform. Finally, the PHB-enzyme conjugates were placed in a chloroform solution containing a Ni-NTA substrate, which was composed of

agarose beads or silicon; this coupled the $(His)_{10}$-tagged enzyme-PHB complex to the surface of the substrate. Nile red dye confirmed the presence of PHB on the substrate surface. AFM studies showed that the Ni-NTA silicon surface was coated with enzyme-PHB complex with an average thickness of 15 nm and evenly distributed grain structures with diameters between 30 and 50 nm (185). These results substantially differed from samples created with the Kim *et al.* (184) surface initiated polymerization method, which had a polymer film thickness of 200 nm and a grain diameter of 600 nm. Paik *et al.* (185) suggest that the considerable morphological discrepancies between the two methodologies results from increased steric constraints in the system developed by Paik *et al (185)*. The Paik *et al. (185)* system requires that the large enzyme-PHB conjugates compete with one another for access to the activated substrate surface. In contrast, less steric hindrance exists with the surface initiated polymerization system developed by Kim *et al.* (184) in which the small molecule substrate, β-hydroxybutyryl-CoA, diffuses to the enzyme-laden substrate surface where polymer accumulation commences.

An interesting variation of the technique of using immobilized PHA enzymes was developed recently by Lee *et al* (186). In this system, the genomic DNA containing the substrate binding domain (SBD) from the PHB depolymerase enzyme of *Alcaligenes faecalis* T1 was used to generate novel fusion proteins. These SBD-containing fusion proteins were capable of

selectively binding to PHB via the SBD, which effectively acts as a capture ligand; this allowed the fusion-proteins to be immobilized on a PHB microbead. Confocal microscopy and flow cytometry studies indicated that this technique (186) successfully immobilized SBD-fusion proteins of the SARS coronavirus envelope protein, enhanced green fluorescent protein, and red fluorescent protein. Immunoassays were also performed using these SDB-fusion proteins, suggesting that these protein chimeras were stable and could be applied for use in immunoassays.

This system exhibits several significant advancements over today's bead-based systems. For example, non-specific absorption of the non-fusion-enhanced green fluorescent protein was virtually nonexistent, a significant advancement. Additionally, with this system there is no need to chemically modify or alter the micro-beads in any way, because the fusion protein binds directly to the PHA polymer itself. Moreover, generation of the fusion protein is accomplished easily with recombinant bacteria harboring the fusion gene-containing plastid, so this system should be simple to implement and applicable to a wide variety of proteins. Finally, different PHA microbeads could be developed to broaden the potential applications of this system with regard to microbead solubility, size, and solvent system (186).

Chemoenzymatic Synthesis of PHB. Chemoenzymatic syntheses have gained substantial popularity in recent years, as these

systems tend to exploit the advantages of traditional chemical syntheses, while incorporating the advances offered by newer *in vitro* enzymatic syntheses. Tajima *et al*. (187) developed a chemoenzymatic synthesis of PHB with CoA recycling that used a water-solvent two-phase system as shown in Figure 10. In this system, thiophenol-(R)-β-hydroxybutyrate is first dissolved in the organic phase, and the PHA synthase and CoA are in the buffered aqueous phase. Under slightly alkaline conditions at pH 7.5, ester exchange will occur between the CoA and thiophenol moieties generating β-hydroxybutyryl-CoA. PHB synthase then polymerizes the β-hydroxybutyryl-CoA to PHB, and the CoA liberated by this process is recycled to convert further β-hydroxybutyryl-thiophenol to β-hydroxybutyryl-CoA. A two-phase hexane-buffered water system was necessary to maintain low levels of thiophenol. The thiophenol was such a significant inhibitor of PHB synthase that it prevented any measurable reaction in a single aqueous phase system. A PHB synthase/PEG complex was also developed by the authors, which stabilized the enzyme and enhanced enzymatic activity by 1.4 fold in the presence of minute quantities of organic solvents (187).

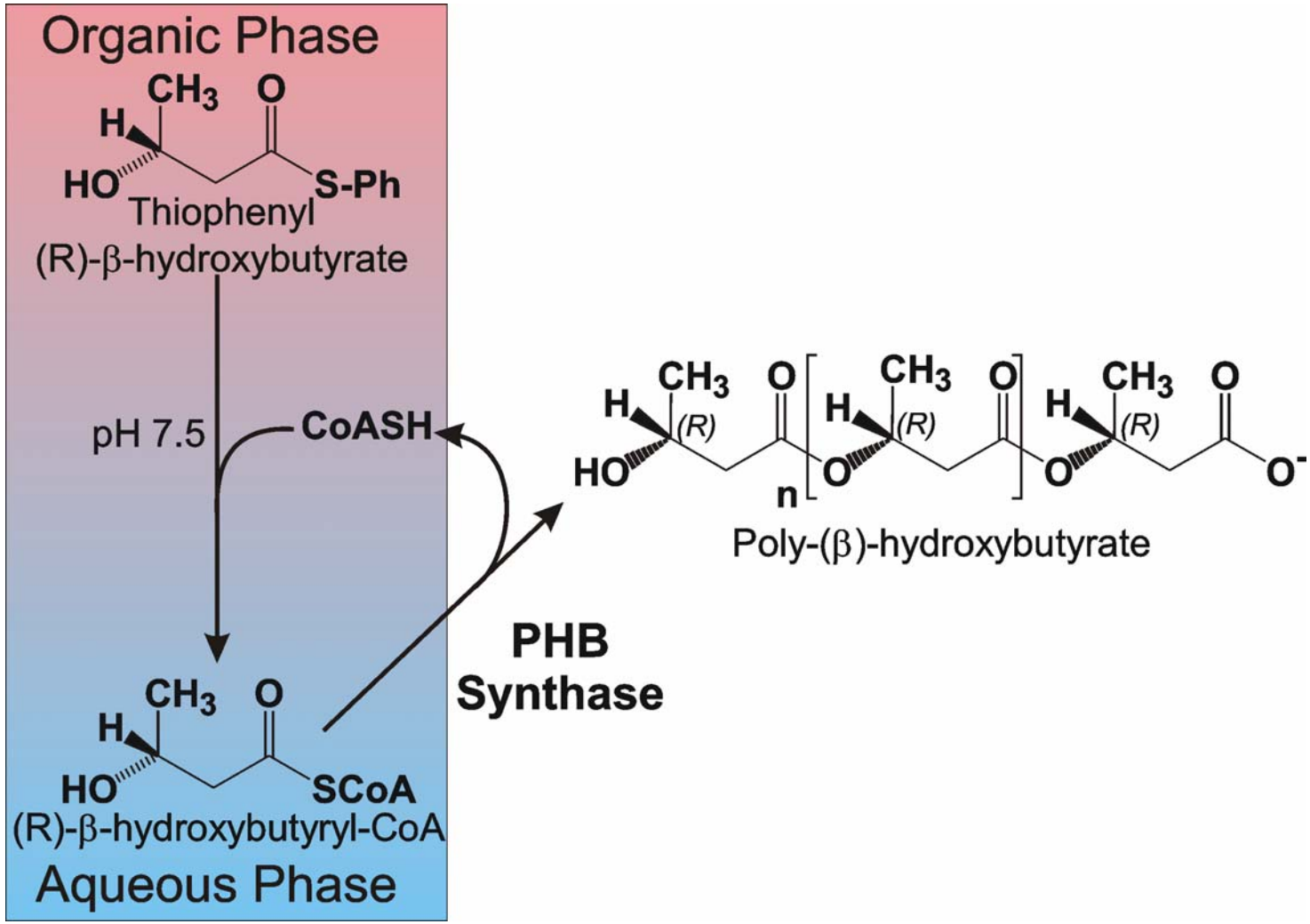

Figure 10. Chemoenzymatic Synthesis of PHB (187).

Recently, Doi and coworkers (188) published a truly novel and innovative *in vitro* enzymatic system for recovering and recycling PHA which is shown in Figure 11. In this system, granulated *Candida Antarctica* lipase B immobilized on silica was used to depolymerize a dilute solution of PHB into cyclic PHA oligomers. These cyclic polymers had molecular weights in the hundreds, and were then concentrated and repolymerized by the same lipase enzyme. Repolymerized oligomers had much lower molecular weights than the parent PHB, approximately 7000 Da; however, repolymerization of cyclic copolymers with ε-caprolactone and β-propiolactone could generate terpolymers with molecular weights of 21,000 and an 84% yield (188). PHA depolymerases from various bacteria were also used to depolymerize PHA into linear monomers, dimers, and trimers. The immobilized lipase did repolymerize these small monomers and oligomers; but molecular weights only ranged in the low thousands (188).

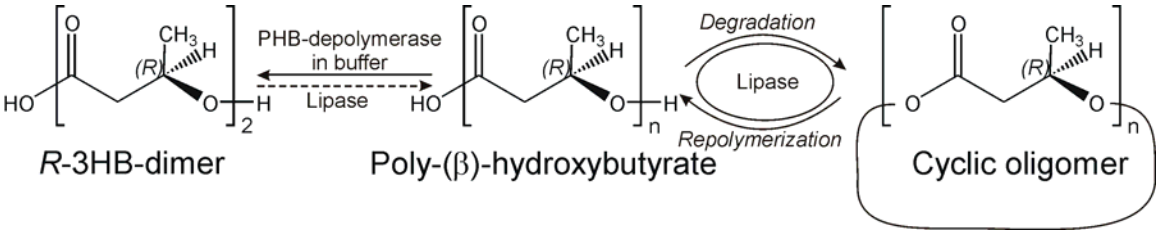

Figure 11. Proposed Chemical Recycling of Biopolyesters using Biocatalysts. (1) Degradation by PHB depolymerase in buffer into hydroxy acid type R-3HB oligomer. (2) Degradation by lipase in organic solvent into cyclic oligomer. Reproduced from Kaihara *et al* (188).

Metabolic Models of PHB Synthesis. Currently, all published metabolic models of PHB synthesis focus on analyzing and predicting the behavior of *in vivo* systems (178,189-211). Such models often focus on parameters including cell growth rate, glucose concentration and percent polymer accumulation. On the other hand, in an *in vitro* enzymatic system substrate concentrations, turnover rates, and enzyme levels are critical to understanding the metabolic flux through the *in vitro* system. Consequently, structured kinetic mathematical models, in which the effects of initial enzyme and metabolite concentrations on the rates of flux PHB synthesis are simulated, are ideal for critically analyzing *in vitro* PHB synthesis. Of the multitude of metabolic models developed to simulate *in vivo* PHB synthesis three publications clearly stand out for their obvious relevance to the field, thorough explanations, and notably in depth analyses (189-191). These publications were used to develop our *in vitro* PHB synthetic model.

In 1998, Leaf and Srienc (190) published what is perhaps the seminal work on structured kinetic models of PHB synthesis. The authors (190) focused on developing a model of *in vivo* PHB synthesis in *C. necator*. By using the reversible complex kinetic equations for each of the three enzymes used in PHB synthesis by *C. necator*, Leaf and Srienc (190) could examine issues including the potential rate limiting steps, regulatory feedback controls, and the outcome of various rate expressions. Individual

metabolite and enzyme concentrations could also be examined with this system.

Leaf and Srienc's (190) simulations indicated that, in actuality no single enzyme could be considered rate limiting because each enzyme substantially contributed to the overall flux of PHB synthesis. Additionally, the reaction byproducts, $NADP^+$ and CoA were both observed to significantly hinder flux through the system; this critically important information would have been overlooked by many less complex models (190). Simplified models often make assumptions regarding the reversibility of rate limiting enzymatic reactions and adjust the rate equations according to these assumptions. Specifically, the inhibition of the β-ketothiolase reaction by CoA, and the inhibition of the acetoacetyl-CoA reductase reaction by $NADP^+$ is a direct consequence of the reversibility of these reactions. The reaction products, CoA and $NADP^+$, compete with substrates for enzyme binding sites, and a model that assumes the reactions are irreversible would be inaccurate.

The following year, Daae and Dunnill (191) from University College, London collaborated with a team at Monsanto company to design a metabolic model of the production of the BioPol copolymer, [PHB(V)], in plants. When this model was being developed, Monsanto was developing genetically modified plants that could produce PHB. Consequently, the Leaf and Srienc (190) model was modified to account for copolymer production in plants.

The Daae and Dunnill (191) model modified the mathematical models to include parameters that describe the cycles of light and dark that affect enzyme activity, expression, and the varying pH levels in plants. Additionally, simulating the desirable product, BioPol--the PHB(V) copolymer, required that different pathways be calculated for the two different β-hydroxyalkanoic acid monomers, and that the enzyme inhibition that resulted from monomers competition for enzyme active sites be taken into account. In plants, the major enzyme that catalyzes the condensation of acetyl-CoA and propionyl-CoA to ketovaleryl-CoA is the BktB β-ketothiolase, instead of the PhbA β-ketothiolase that generates acetoacetyl-CoA from acetyl-CoA. Consequently, the kinetic equation and parameters for the BktB β-ketothiolase reaction were used in the Daae and Dunnill simulation (191).

The simulations performed by Daae and Dunnill (191) indicated that the light/dark cycles have a profound effect on the flux of the PHB system. The authors (191) also incorporated metabolic control analysis and the results suggested that, in contrast to the results by Leaf and Srienc (190), the β-ketothiolase step substantially affects the rate of copolymer production; however, all enzymes affect the copolymer-monomer ratio. Finally, simulation results showed that variations in substrate and cofactor levels can considerably impact copolymer ratio and production (191).

van Wegen, Lee, and Middelberg (189) published a third metabolic model featuring metabolic control analysis and

metabolic flux analysis. This model investigated *in vivo* PHB production in recombinant *E. coli*, which harbored the genes encoding β-ketothiolase, NADPH-dependent acetoacetyl-CoA reductase, and PHB synthase from *C. necator*. The simulation results (189) indicated that pathway flux was highly dependent on the acetyl-CoA/CoA ratio, and the acetyl-CoA and CoA concentrations. Additionally, it was observed that the $NADPH/NADP^+$ ratio exerts to a lesser extent and that the contribution of the NADPH concentration is negligible to pathway flux. Consistent with the results of the simulation developed by Leaf and Srienc (190), no single enzyme was apparently responsible for system flux.

The van Wegen, Lee, and Middelberg (189) study did consider the quantitative effects of the metabolites acetyl-CoA and β-hydroxybutyryl-CoA using laboratory derived HPLC measurements. The concentration of acetoacetyl-CoA was estimated at 0.11 µg. g/RCM which is around 300 fold less than the β-hydroxybutyryl-CoA concentrations; this explains why no acetoacetyl-CoA was detected in this study by HPLC (136,190). The enzyme activities obtained in the simulation were comparable to previous literature values. Interestingly, simulations of this system indicated that oxygen limitation triggered PHA production. Finally, the simulation and laboratory results indicate that during the first two hours of PHB synthesis, control of polymer production is similar to that observed in *C. necator*; specifically, that TCA cycle flux is quelled causing a rise in acetyl-CoA levels and concomitant drop

in CoA concentrations. However, after two hours the acetyl-CoA levels return to normal in the recombinant *E. coli* system and continued PHB production likely results from increased enzyme expression; this contrasts the situation in *C. necator* where polymerization is apparently driven by metabolite concentrations (190).

Our In Vitro Synthesis of PHB. In this study, we report a detailed analysis of the *in vitro* synthesis of PHB via the three-enzyme pathway that is utilized by *C. necator*. We have developed an HPLC method that permits baseline separation of CoA, acetyl-CoA, acetoacetyl-CoA, and β-hydroxybutyryl-CoA within 30 min. By sequentially adding each enzyme in the PHB synthetic pathway, and utilizing our HPLC system to, simultaneously, determine the concentrations of each CoA-containing compound, we are able to examine the effects of each of the enzymes as they are successively coupled for PHB synthesis. Detailed stoichiometric analyses of each step in the PHB pathway demonstrate good agreement with the putative synthetic mechanism. The concentrations of acetoacetyl-CoA in our enzymatic PHB synthesis system were well below the limit of detection by HPLC. This phenomena was investigated via two separate metabolite spiking experiments. Finally, a metabolic model, based on the work of Leaf and Srienc (190), was utilized to examine the kinetic and thermodynamic parameters of each reaction defining the PHB synthesis pathway.

CHAPTER 2

PHB: EXPERIMENTAL

Materials. The sterile filtered antibiotics kanamycin, ampicillin, and spectinomycin, the DEAE Sepharose and Blue Matrex chromatographic supports, the lithium salts of CoA, acetyl-CoA, and β-hydroxybutyryl-CoA, and the sodium salt of acetoacetyl-CoA were purchased from Sigma. Solutions of all CoA-containing compounds were prepared in 25 mM potassium phosphate buffer at pH 4.0, and stored at -70 C. The *E. coli* clones harboring plasmids for the *Cupriavidus necator* [*Cupriavidus necator* has previously been called *Wautersia eutropha, Ralstonia eutropha*, *Alcaligenes eutropha*, and *Hydromonias eutropha*] renamed β-ketothiolase, acetoacetyl-CoA reductase, and PHB synthase used in this work were a generous gift from the Monsanto Co. and have been described elsewhere (212,213). The Methyl-HIC chromatography support was purchased from Bio-Rad (Hercules, CA). Anameg was purchased from Anatrace (Maumee, OH) and triscarboxyethyl phosphine (TCEP) was from Molecular Probes (Eugene, OR). All solvents were of HPLC or Optima Grade. Coomassie Plus Protein Assay Reagent was purchased from Pierce Biotechnology. All other compounds were obtained from Fisher Scientific.

PHB Clones. Three separate *E. coli* clones hosting plasmids (Table 5) which harbored the genes for *phbA*, *phbB*, and *phbC*, respectively, were graciously donated by the Monsanto Co.

Table 5. PHB Clones used in Enzyme Isolations.

Bacteria	*Strain*	*Plasmid*	*Cloned Gene*	*Enzyme Expressed*	*Common Name* *Enzyme*
E. coli	DH5α	pMON25636	*phbA*	PhbA	β-ketothiolase
E. coli	JM101	pMON25628	*phbB*	PhbB	acetoacetyl-CoA reductase
E. coli	UT10	pMON25629	*phbC*	PhbC	PHB synthase

Bacterial Cell Culture. Bacteria were cultivated as described in Slater *et al*. (213) except that bacteria producing acetoacetyl-CoA reductase and PHB synthase were grown in the presence of 50 ppm spectinomycin or kanamycin, and were induced with 1 mM isopropyl-β-D-thiogalactopyranoside or nalidic acid, respectively. The bacteria used to generate the β-ketothiolase enzyme were cultivated in the presence of 75 ppm of ampicillin and induced with 1 mM of isopropyl-β-D-thiogalactopyranoside. Briefly, a frozen suspension of bacterial cells was rapidly thawed in a water bath at 37 C. The bacterial suspension, 1 mL, was then used to inoculate a 250 mL shake flask containing 150 mL of antibiotic-laden LB media, which was cultivated aerobically at 37 C and 250 rpm. When the culture reached an OD_{600} of 0.6 absorbance units, it was transferred to a 1.8 L shake flasks

containing 1.3 L of fresh media and antibiotic. Upon reaching an O.D.$_{600}$ of 0.6 absorbance units, 1 mM of the appropriate inducing agent was added to the large shake flask in order to initiate enzyme expression. Three hours post induction the cells were harvested by centrifugation at 13,800 x g for 10 min. The harvested cell paste was stored at -70 C. Nalidic Acid was used to induce PhbB enzyme expression whereas PhbA and PhbC were induced with isopropyl-β-D-thiogalactopyranoside.

Amplification and Storage of Bacterial Strains. The original *E. coli* clones obtained from Monsanto Co. were amplified and stored for future use in the following manner. A shake flask containing 150 mL of sterile antibiotic-laden Luria-Bertani (LB) media was inoculated with 10 μL of the desired clone and the flask shaken at 250 rpm. and 37 C. When an OD_{600} of 0.6 absorbance units was obtained, signaling the mid-log growth phase ,the cells were aseptically harvested by centrifugation for 10 min at 13,800 x g. The bacterial cell pellet was resuspended into 10 mL of fresh media, which contained 50% LB media and 50% ethylene glycol. The solution was transferred to 15 mL polypropylene centrifuge tubes and stored at -70 C.

Acyl-CoA Compound Storage. CoA, acetyl-CoA, acetoacetyl-CoA, and β-hydroxybutyryl-CoA solutions were prepared at a concentration of 2.5 mM in 25 mM potassium phosphate buffer at pH 4.0. Solutions were stored in 100 μL aliquots at -70 C.

Aliquots were thawed, used once, and discarded. No sample degradation was observed by HPLC over a one-month period.

Enzyme Isolations. Unless stated otherwise, all enzyme isolation steps were performed at 4°C utilizing a Pharmacea ACTA Explorer FPLC system. Spectroscopic measurements were obtained with a Hewlett Packard 8453 UV-Vis Spectrophotometer with UV-Visible Chemstation Software. One unit of enzyme (U) corresponds to 1 μmol of product produced per min.

Protein Concentration Determination. Protein concentrations were determined using the Bradford (214) Coomassie Plus Protein Assay Reagent, purchased from Pierce Biotechnology, and was used as per the manufactures instructions.

β-ketothiolase. β-ketothiolase was isolated using a procedure adapted from Davis *et al* (215). Bacterial cell paste, approximately 3.1 g, was resuspended in 10 mL of buffer A (20 mM Tris pH 7.8, 1 mM EDTA, 5% glycerol, 1% β-mercaptoethanol, and 0.2 mM PMSF) and lysed with a Branson Sonifier 250 on an ice salt bath, using three consecutive rounds of 45 seconds of sonication, 0.4 s exposure per 1 second and 60% amplitude, followed by cooling. Cellular debris was cleared by centrifugation at 35,300 x g for 30 min and the protein was precipitated with 20% (w/v) polyethylene glycol 8000. The precipitated protein was pelleted by centrifugation at 33,300 x g for 45 minutes, re-dissolved in buffer A, and applied to a DEAE-Sepharose CL6B column that was pre-equilibrated in buffer A. A step-gradient was employed with

increasing concentrations of buffer B (buffer A + 1M NaCl) and 3-min fractions were collected as follows: 0-60 min, 0% B; 60-120 min, 0-60% B; 120-180 min, 60% B; 180-200 min, 60-100% B. The pool of active fractions was concentrated and the buffer exchanged to buffer A by ultrafiltration with an Amicon Stirred Cell (Millipore Co.) containing an YM10 membrane. The sample was then loaded onto a 60 mL Blue Matrex column that was pre-equilibrated with buffer A. A 300 min linear gradient was employed with 0-100% buffer C (buffer A + 3M NaCl) and 6 mL fractions. After the active fractions were pooled, concentrated, and the buffer exchanged to buffer A, the enzyme was diluted 50% with ethylene glycol and stored at -20°C.

The specific activity was determined using a continuous spectrophotometric assay, which followed consumption of the magnesium chelated enolate of acetoacetyl-CoA monitored at λ = 303 nm (213). In these assays, 750 μL of the assay solution containing 150 mM EPPS pH 8.0, 66 μM acetoacetyl-CoA, 66 μM CoA, and 50 mM $MgCl_2$ was initiated by enzyme addition. The decrease in absorbance at λ = 303 nm was followed for 120 s and the initial rates determined from the linear portion of the plot for conversion to specific activity. β-ketothiolase was typically purified 3.8 fold with a specific activity of 58 U/mg. One unit of enzyme (U) corresponds to one μmol of product produced per minute.

Enzyme activities for individual fractions obtained during the isolation were determined by end-point analysis. Briefly, the assay solution, 750 μL, was initiated with 50 •L of the isolation fractions, incubated 10 min, and the absorbance at λ = 303 nm determined. Active fractions exhibited lower relative absorbance values.

Acetoacetyl-CoA reductase. Acetoacetyl-CoA reductase was isolated in a procedure modified from Haywood *et al* (160). Bacterial cell paste, typically 5 g, was dissolved in 10 mL of buffer A (12 mM Tris pH 8.3, 9.8 mM β-mercaptoethanol, 1 mM EDTA, 0.2 mM PMSF, and 1% glycerol) and cooled on an ice salt bath. The bacterial cells were lysed with a Branson Sonifier using four consecutive rounds of 30 seconds of sonication, 0.4 s exposure per 1 second and 60% amplitude, followed by cooling. After centrifugation at 31,000 x g for 20 min to remove the cellular debris, the supernatant was loaded onto a 50 mL Sepharose-CL6B column that was pre-equilibrated with buffer A. A step gradient elution profile with a 1.0 mL/min flow rate and collection of 7 mL fractions was performed as follows: 0-120 min, 100% buffer A; 120-150 min, 0-10% buffer B (buffer A +1M NaCl); 150-210 min, 10-100% buffer B; 210-370 min, 100% buffer B. After concentration with an Amicon Stirred Cell containing an YM10 membrane and exchange to buffer A, the pool of active fractions was applied to a 40 mL Blue Matrex column that was pre-equilibrated with buffer A. A 300 min linear gradient from 0-100% buffer C (buffer A + 2M NaCl) was performed with 6 min sample collection. The final pool

of enzyme was concentrated and desalted via ultrafiltration followed by further concentration to a volume of 1 mL with a Millipore Centricon. The final enzyme concentrate was diluted 50% with ethylene glycol and was stored at -20°C.

Specific activities were determined in the forward enzymatic direction using a spectrophotometric method which followed the decrease in absorbance at λ = 340 nm, which results from NADPH consumption (160). The reaction was initiated by addition of 2 µL of enzyme to 750 µL of the assay solution containing 100 mM Tris pH 8.0, 66µM NADPH, 66µM acetoacetyl-CoA. The reaction was followed for 120 s at λ = 340 nm and the linear portion of the plot used to determine the initial rates for calculating the specific activity. Acetoacetyl-CoA isolations typically provided enzyme that was purified 7.2 fold with a specific activity of 41.9 U/mg.

Enzyme activities for individual fractions obtained during the isolation were determined by end-point analysis. The reaction was initiated by addition of 50 µL of the isolation fraction to 750 µL of the assay solution. After incubating for 10 min, the absorbance at λ = 340 nm was determined and active fractions identified by finding the largest relative decrease in UV absorbance.

PHB Synthase. PHB synthase was isolated based on a procedure outlined in Song *et al*. (167) except that the protease inhibitor benzamidine was added to the lysis buffer.

Bacterial cells, approximately 3 g, which harbored a plasmid containing the PHB synthase gene enzyme, were dissolved in 20 mL of lysis buffer, (50 mM potassium phosphate pH 7.0, 5% glycerol, and 5 mM benzamidine) and cooled on an ice-salt bath. The bacterial cells were lysed with a Branson Sonifier using four consecutive rounds of 30 seconds of sonication, 0.4 s exposure per 1 second and 60% amplitude, followed by cooling. After cellular debris was removed by centrifugation at 31,000 x g for 20 min, 15% ammonium sulfate was added slowly to the supernatant on ice. After equilibrating for 20 minutes to ensure adequate protein precipitation, the solution was centrifuged at 31,000 x g for 40 minutes. The supernatant was collected and ammonium sulfate was added to reach a final concentration of 50%. After adequate time for protein precipitation on ice, the protein pellet was collected by centrifugation at 31,000 x g for up to 2 hours. The 50% ammonium sulfate pellet was resuspended in buffer A (50 mM potassium phosphate pH 7.0, 5% glycerol, 0.05% Anameg™, 1.0 M ammonium sulfate) and applied to a 5 mL methyl-HIC column that was equilibrated with the same buffer. After an initial six-column volume wash, the enzyme was eluted with a 12 column-volume linear gradient from 0-100% buffer B (buffer A with no ammonium sulfate) at 2 mL/min with 1 mL fraction collection. Active fractions were pooled and concentrated with an Amicon Stirred Cell using an YM10 membrane followed by further concentration with a Millipore Centricon™ to reach a final volume

of approximately 0.5 mL. The isolated PHB synthase was separated into 55 μL aliquots, snap frozen in liquid nitrogen, and stored at -70 C. PHB synthase was purified 22 fold with a specific activity of 1.42 x 10^{-02} U/mg.

The specific activity was determined using a continuous spectrophotometric assay modified from Fukui *et al*. (216), which detected production of the CoA free thiol via Ellmann's reagent. Initially a continuous assay based on the work by Fukui *et al*. (216) was employed. Unfortunately, the characteristic yellow color, which indicates that Ellmann's reagent is reacting with free thiols, was observed in solutions containing the PHB synthase enzyme even in the absence of CoA. Consequently, this method was modified by adding 50μL of the enzyme to 750μL of the assay solution (76 μM DTNB in 20 mM potassium phosphate at pH 7.0), obtaining an initial background absorbance at λ = 412 nm, and then initiating the reaction with 10 μL of the β-hydroxybutyryl-CoA (133μM, final volume 810 μL) substrate. Simple subtraction of the background rate from the total provided the initial enzyme reaction rate, which could be converted to specific activity.

The relative enzyme activities for individual column fractions eluted during the isolation were often determined using a related end point analysis. In this situation the U.V. absorbance at λ = 412 nm was monitored for the entire set of

column fractions at discrete time intervals so that the difference in the absorbance between time steps indicated the relative enzyme activity in each fraction. Time intervals were necessarily long enough to minimize the time required to hand initiate roughly 40 reaction test tubes while brief enough that the enzyme reaction in the most active test tubes had not reached completion.

Alternatively, an end point analysis using HPLC detection was employed. This assay simultaneously measured the consumption of β-hydroxybutyryl-CoA and the liberation of CoA by the PHB synthase enzyme, and the consumption of acetyl-CoA from an unknown origin. The reaction was initiated by addition of 50 μL of each isolation fraction to 750 μL of a solution containing 150 mM EPPS pH 8.0, 65 μM of β-hydroxybutyryl-CoA, 80 μM of acetyl-CoA, and 5 mM TCEP. After a brief incubation period, the reaction was quenched with perchloric acid at a final concentration of 0.57 M and the samples centrifuged in preparation for HPLC analysis.

High Performance Liquid Chromatography (HPLC). HPLC analyses were performed on a Waters LC Module I Plus HPLC system with auto-injection of samples using the Millennium Chromatography Manager Software (Waters, Milford, MA, USA). A Waters NovaPak C18 Reverse Phase column, 4 μm particle size, 150

mm x 4.6 mm I.D. was used with a Phenomenex SecurityGuard™ containing a C18, 4 mm length x 3.0 mm I.D., guard cartridge. Isocratic analysis was performed at a wavelength of 261 nm with a mobile phase containing 96% 150 mM citrate buffer pH 5.0: 4% acetonitrile and a flow rate of 1.0 mL/min. All buffers were double filtered through a 0.45 µm and a 0.22 um HVLP filter from Millipore. The mobile phase was premixed prior to sparging with H_2 gas and the column pre-equilibrated with mobile phase for at least 1 hour prior to sample analysis. Concentrations of CoA-containing compounds were calculated from the individual HPLC standard curves.

Standard curves, shown in Figure 17, were obtained under conditions equivalent to the *in vitro* enzymatic experiments and *showed excellent linearity with R^2 coefficients of 0.9999*. Under these conditions, the retention times were as follows: CoA, 5.8 min; acetyl-CoA, 18.5 min; acetoacetyl-CoA, 21.1 min; β-hydroxybutyryl-CoA, 26.2 min. The smaller peaks that elute after each CoA-containing compound are the 2'-phospho isomers and exhibit the following retention times: iso-CoA, 7.1; acetyl-iso-CoA, 25.5; acetoacetyl-iso-CoA, 26.9; β-hydroxybutyryl-iso-CoA, 33.6 min. The co-elution of acetoacetyl-iso-CoA and β-hydroxybutyryl-CoA did not pose a problem in our experiments, because acetoacetyl-iso-CoA concentrations were always below the limit of detection by HPLC.

In Vitro Enzymatic Syntheses. All experiments were performed in a shaking water bath at 37°C and enzymes were kept on ice. In a typical experiment, 5 mM TCEP, 1.0 mM NADPH, and 16 μM acetyl-CoA in a solution of 150 mM EPPS at a final of pH 7.8 was pre-equilibrated at 37°C for approximately 10 min. The enzymatic reaction was initiated by the addition of β-ketothiolase at time zero. Subsequently, 80 μL of acetoacetyl-CoA reductase was added at 3 min 30 s followed by the addition of 175 μL of PHB synthase at 10 min 30 s. At set time points, 90 •L aliquots were quenched by addition to 10 μL of ice-cold perchloric acid ([HClO4] final = 0.27 M). Quenched samples were centrifuged to remove the precipitated protein, and the supernatant was transferred to the appropriate vials for autoinjection of 50 μL onto the HPLC column. Quantitation of metabolite concentrations for stoichiometric analysis was determined by integrating the areas of the HPLC peaks and converting to concentration by using the appropriate standard curves.

In experiments that entailed spiking, 40 μL acetoacetyl-CoA reductase and 100 μL of NADPH, which increased the NADPH concentration by 0.5 mM, were added sequentially at 40 min 30 s and 40 min 38 s; and then acetoacetyl-CoA was added at a final concentration of 7.8 μM at 50 min 30 s. Quenched samples were centrifuged for 10 minutes to pellet the protein, and the

supernatant was transferred to the appropriate vials for autoinjection of 50 μL onto the HPLC column.

Enzymatic Rate Simulations. Simulations were performed by coupling the integrated rate equations for each of the three-enzymes in the PHB pathway. The GEPASI (217-219) software package was used for kinetic simulations, fitting, and optimization. Changes in enzyme activities were simulated by proportionally altering the enzyme maximal rates. Excel was used for calculating kinetic constants, Haldane relationships, and for displaying the GEPASI output data. This simulation was developed using literature derived kinetic constants, and the equilibrium constants and maximal rates were determined by fitting the model to the *in vitro* HPLC data.

CHAPTER 3

PHB: RESULTS

In Vitro Biosynthesis of PHB. The enzyme system used in this work for *in vitro* PHB synthesis consists of (Figure 7) β-ketothiolase, acetoacetyl-CoA reductase, and PHB synthase. As depicted in the HPLC chromatograms in Figure 12, PHB synthesis was accomplished by individually adding each enzyme to an acetyl-CoA solution and allowing the reaction to reach equilibrium briefly before adding the next enzyme. With this approach, the reaction progress could be monitored in a sequential manner to elucidate the fluctuations in metabolite concentrations and the effect of each individual enzyme on the overall three-enzyme system for synthesizing PHB.

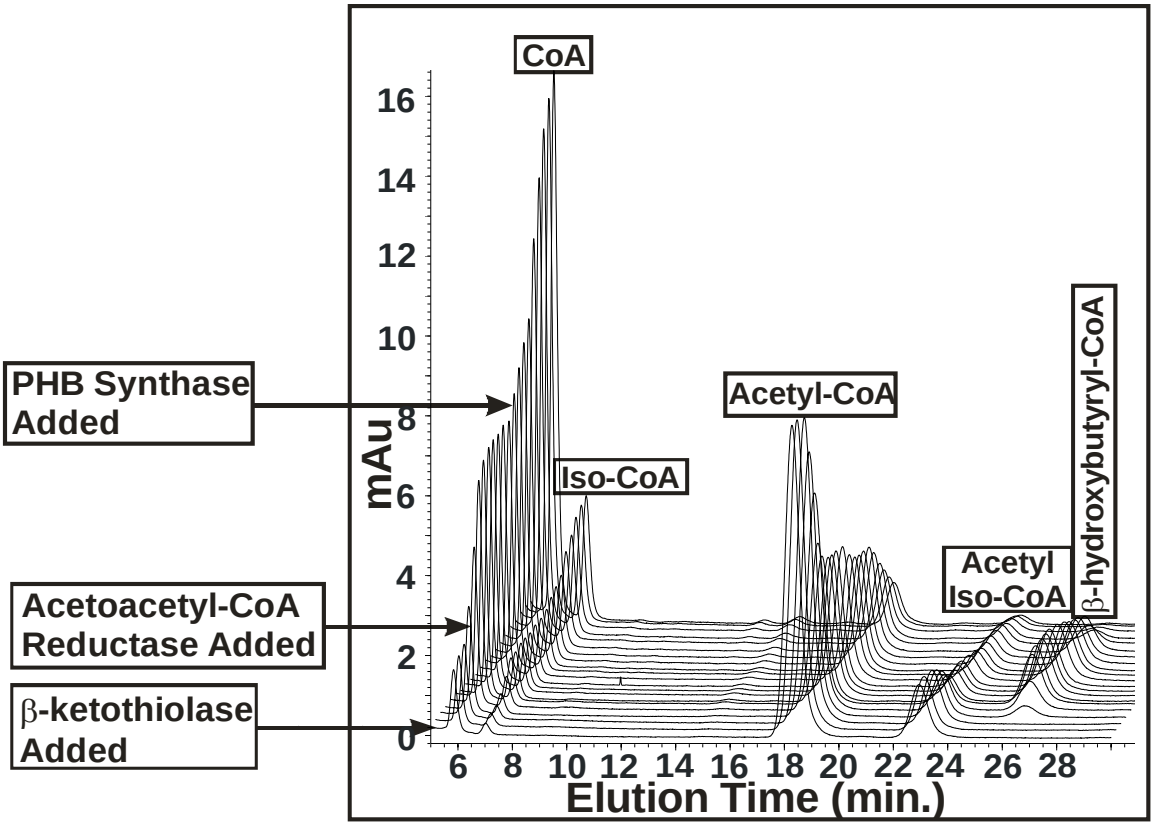

Figure 12. Overlaid HPLC Chromatograms for the Step-wise I*n Vitro* Synthesis of PHB. Overlaid HPLC chromatograms depict the changes in metabolite concentrations upon sequential additions of enzyme during the *in vitro* synthesis of PHB. The reaction was initiated by addition of β-ketothiolase at time 0, followed by acetoacetyl-CoA reductase at 3.5 min, and PHB synthase at 10.5 min. The chromatograms are overlaid to depict the changes in metabolite concentrations over the time course of the reaction from initiation at time zero to the reaction conclusion, as shown from front to back, respectively.

β-ketothiolase. The *in vitro* synthesis of PHB was initiated by the addition of β-ketothiolase to a solution of acetyl-CoA, as shown in the HPLC time course in Figure 13, Panel A. This single enzyme reaction resulted in only negligible changes in the concentrations of acetyl-CoA, and CoA and no acetoacetyl-CoA formation was detected. These results are consistent with the known equilibrium constant for the β-ketothiolase reaction which strongly favors thiolysis of acetoacetyl-CoA (220).

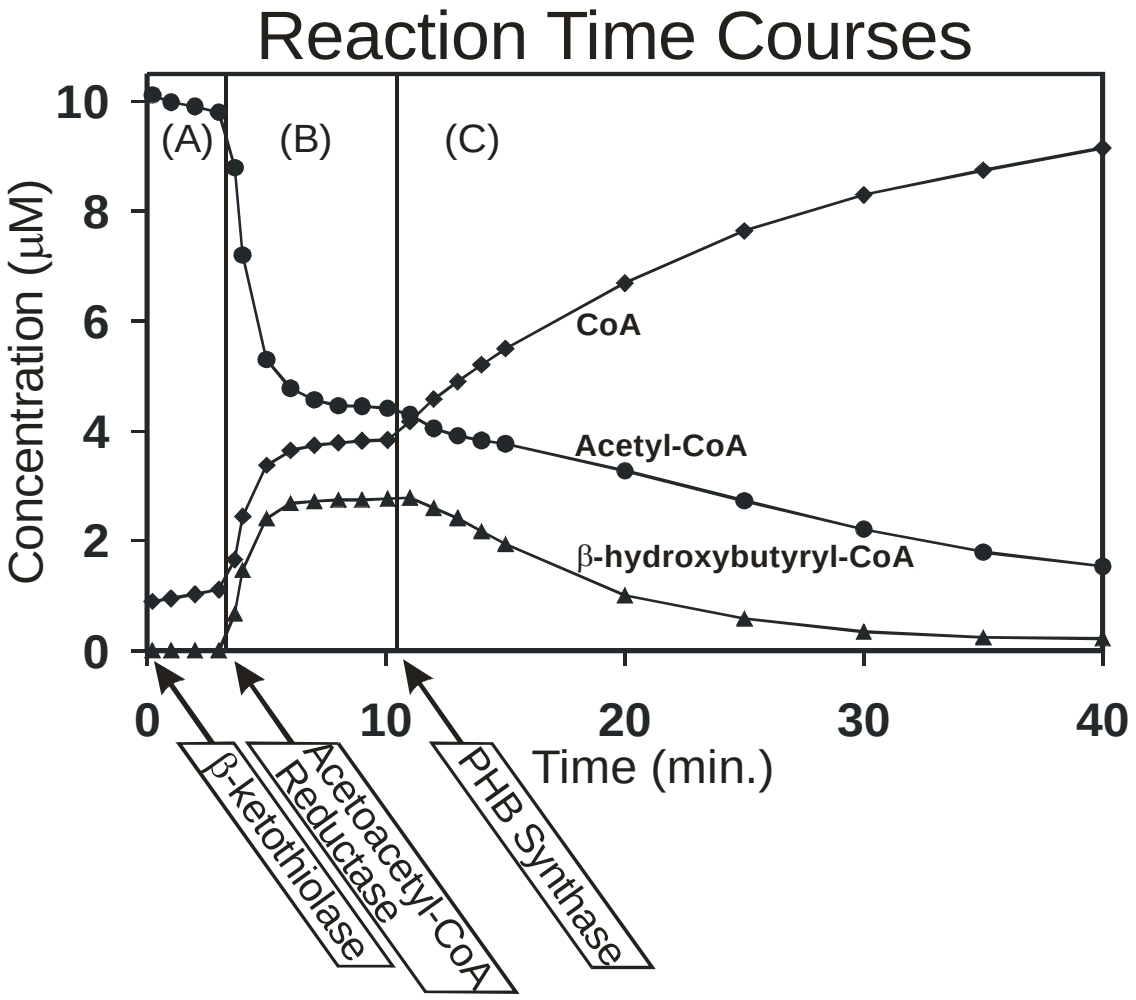

Figure 13. Quantitative Time Courses of Metabolite Concentrations for the I*n Vitro* Synthesis of PHB. Time courses for CoA, acetyl-CoA, and β-hydroxybutyryl-CoA. Panel A: The reaction is initiated upon addition of β-ketothiolase at 0 min to a solution containing 16 μM acetyl-CoA, 1.0 mM NADPH, and 5 mM TCEP in 150 mM EPPS buffered at a final pH of 7.8. Negligible changes in the concentrations of CoA, acetyl-CoA, and β-hydroxybutyryl-CoA are evident (see text). Panel B: Acetoacetyl-CoA reductase is added at 3.5 min and the reaction allowed to reach equilibrium. Stoichiometric changes in metabolite concentrations occur, corresponding to consumption of 5.35 μM of acetyl-CoA, formation of 2.74 μM of β-hydroxybutyryl-CoA, and liberation of 2.71 μM of CoA. Panel C: PHB synthase is added and the reaction allowed to proceed. 5.32 μM of CoA is liberated during the consumption of 2.88 μM of acetyl-CoA and 2.55 μM of β-hydroxybutyryl-CoA.

β-ketothiolase & Acetoacetyl-CoA Reductase. As shown in Figure 13, Panel B, the addition of acetoacetyl-CoA reductase immediately results in a substantial decrease in acetyl-CoA and simultaneous increases in β-hydroxybutyryl-CoA and CoA concentrations. As expected these changes occur with a stoichiometry of 2 acetyl-CoA consumed: 1 CoA formed : 1 β-hydroxybutyryl-CoA formed. This is confirmed by the quantitative HPLC results shown in Table 6, which show that 2.74 •M of β-hydroxybutyryl-CoA and 2.71 •M of CoA are generated in the enzymatic consumption of 5.35 •M of acetyl-CoA. Since the concentration of β-hydroxybutyryl-CoA (2.74 •M) and CoA (2.71 •M) reach a total of 5.45, it is logical that all of the acetyl-CoA (5.35 •M) consumed in the enzymatic reactions was used to generate these species, within a 1.8% margin of error. In this situation, the large forward equilibrium constant for the acetoacetyl-CoA reductase reaction drives the system forward by overcoming the strong reverse equilibrium for the β-ketothiolase reaction (221). After approximately 55% of the initial acetyl-CoA is consumed, the reaction reaches equilibrium (see below). Consistent with literature reports on PHB synthesis both *in vivo* (189) and *in vitro* (181), we detect no buildup of acetoacetyl-CoA (Figure 12).

Table 6. Stoichiometric Relationships for In Vitro Enzymatic Reactions.

	Δ AcCoA[a] *•M* *(% Error*[d]*)*	*Δ CoA* *•M* *(% Error*[d]*)*	*Δ HBCoA*[b] *•M* *(% Error*[d]*)*	*Δ HBCoA + Δ AcCoA*
β-ketothiolase & Acetoacetyl-CoA Reductase *Figure 13, Panel B* Δ 2 AcCoA = Δ CoA + Δ HBCoA 5.35 ≈ 2.74 + 2.71 = 5.45	-5.35 (+1.8%)	+2.71	+2.74	---
β-ketothiolase, Acetoacetyl-CoA Reductase & PHB Synthase *Figure 13, Panel C* Δ CoA = Δ AcCoA + Δ HBCoA 5.32 ≈ 2.88 + 2.55 = 5.43	-2.88	+5.32 (+2.1%)	-2.55	---
β-ketothiolase, Acetoacetyl-CoA Reductase & PHB Synthase *Concatenated from 0-40 min; Figure 13, Panel A-C* AcCoA = CoA + Residual HBCoA 8.27 ≈ 8.04 + 0.22 = 8.26	-8.27 (-0.1%)	8.04	0.22 Remaining	---
β-ketothiolase, Acetoacetyl-CoA Reductase & PHB Synthase *Spiked with 7.84 µM of acetoacetyl-CoA* 7.84 µM AcAcCoA[c] spike = HBCoA + ½ AcCoA 7.84 ≈ 2.81 + 5.03 = 7.84	5.63 [1/2 = 2.81]	1.81[e]	5.03	7.84 (0%)

[a] *acetyl-CoA*
[b] β-hydroxybutyryl-CoA
[c] acetoacetyl-CoA
* % Error shown in parenthesis was determined with % error = |((actual-calculated)/actual)| x 100.
[e] While the stoichiometric relationship for the quantity of CoA consumed to the acetyl-CoA generated should be 1 CoA : 2 AcCoA. The experimentally measured quantity of CoA consumed, 1.81 µM does not equal ½ of the acetyl-CoA 2.81; this is believed to result from additional CoA, which was present as a contaminant in the acetoacetyl-CoA spike. Alternatively, some CoA could have been produced in the polymerization if HBCoA to PHB but this latter case is not believed to be a major factor in such a short (8 s) time span.

β-ketothiolase, Acetoacetyl-CoA Reductase & PHB Synthase.

The *in vitro* time courses, shown in Figure 13, Panel C, illustrate how the addition of the PHB synthase enzyme shifts the equilibrium of the three-enzyme system toward PHB polymer production. The PHB synthase reaction is irreversible and thus polymerization of β-hydroxybutyryl-CoA, by PHB synthase, stimulates the condensation of additional acetyl-CoA molecules, and CoA is liberated by both the β-ketothiolase and PHB synthase reactions. Under these circumstances, the reaction proceeds with stoichiometries that reflect that the total consumption of acetyl-CoA, 2.88 μM, and β-hydroxybutyryl-CoA, 2.55 μM, which equals a sum of 5.43 μM, is equivalent to the total quantity of CoA released, 5.32 μM with a 2% margin of error.

Stoichiometries of the Concatenated Biosynthetic Pathway.

Overall, we observe a stoichiometric conservation of CoA-moieties for the time courses of the concatenated enzymatic system of β-ketothiolase, acetoacetyl-CoA reductase & PHB synthase over the entire time course from 0 to 40 min. Thus, under the conditions of Figure 13, 8.27 μM of CoA-moieties are consumed, as acetyl-CoA, and 8.26 μM CoA-moieties are present in the form of CoA (8.04 μM) and β-hydroxybutyryl-CoA (0.22 μM).

High Performance Liquid Chromatography.

HPLC Peak Determination. It is evident from Figure 14 that two peaks are visible in each commercial sample of CoA, acetyl-CoA, acetoacetyl-CoA, and β-hydroxybutyryl-CoA, respectively. Detailed mass spectrometric and NMR structural analyses carried out in this laboratory established that the earlier-eluting peaks represent the authentic CoA or acyl-CoA compounds, whereas the later-eluting peaks correspond to the 2′-phophate isomers (or iso-CoA-forms) of each compound; these experiments are described elsewhere (222). In addition, it is evident from Figure 12 that over the time course of the enzymatic reactions that both the CoA and the iso-CoA-forms of these compounds are enzymatically metabolized.

HPLC Optimization. We developed an optimized HPLC methodology, based on several previous separations of similar CoA-containing compounds (223-225), which separates CoA, acetyl-CoA, acetoacetyl-CoA and β-hydroxybutyryl-CoA with baseline resolution (Figure 14). Our methodology allows for convenient isocratic elution, which provides baseline separation in about 30 min. The mobile phase developed for this separation provides the strong buffering capacity necessary for excellent resolution, good peak shape, and reproducible retention times but does not employ harsh ion-pairing agents (226) or high phosphate concentrations which damage silica columns (227).

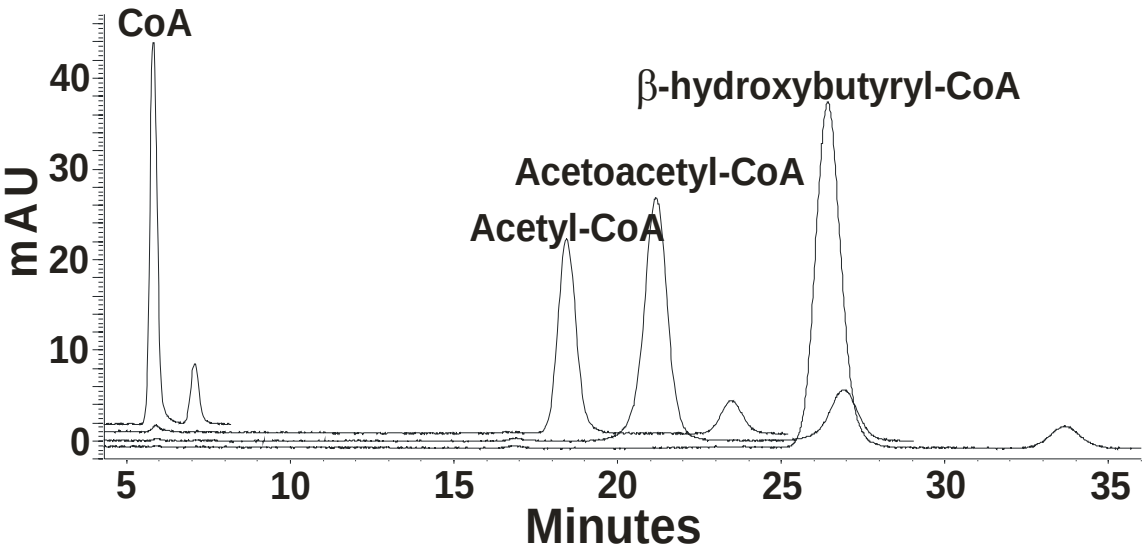

Figure 14. Overlaid HPLC Chromatograms of Commercial CoA and Acyl-CoA samples. Representative HPLC C_{18} chromatograms of CoA, acetyl-CoA, acetoacetyl-CoA, and β-hydroxybutyryl-CoA are shown. Elution conditions are described in the text. For each CoA containing compound the iso-CoA-form appears as a small later-eluting peak with the following retention times: iso-CoA, 7.1; acetyl-iso-CoA, 25.5; acetoacetyl-iso-CoA, 26.9; β-hydroxybutyryl-iso-CoA, 33.6 min.

Ion Pairing Agents in the Mobile Phase. Several groups have reported methodology for separating acyl-CoA compounds via HPLC (223,226,228-238). Two strategies have been reported in the literature to suppress the charges on the phosphate moiety; this facilitates interaction between the compound and the stationary phase, which is crucial for separation by reverse phase chromatography. The ion-pairing technique, developed by Baker and Schooley in 1979 (229), utilizes a mobile phase containing an ion-pairing reagent, such as tetrabutyl ammonium hydrogen sulfate. This method was attempted in our laboratory and successfully separated CoA, β-hydroxybutyryl-CoA, and NADPH, however; acetyl-CoA and acetoacetyl-CoA coeluted.

Strong Buffer in the Mobile Phase. The alternate strategy of using a strong buffering agent, typically 100-200 mM phosphate, in the mobile phase was developed by Ingebretsen and Farstad (239), modified by DeBuysere and Olson (226), and adapted for used in this investigation. While, this strategy does avoid the use of corrosive ion pairing agents, the historic use of phosphate buffer at high concentrations has been reported to be highly damaging to silica-based columns (227); the use of phosphate buffers significantly shortened column lifetimes in our laboratory. Consequently, sodium citrate was used in the mobile phase in this laboratory because of its strong ionic strength, which suppresses sample ionization and provides buffering capacity for acidic samples without extensive column degradation.

Ammonium Acetate Mobile Phase for MS Experiments. A second mobile phase, described in Chapter 7 (Iso-CoA: Experimental) was used for the HPLC-MS analysis of the iso-CoA compounds (222), which required the use of a volatile buffer. This mobile phase, which was based on the report of Norwood *et al*. (235), used the volatile buffer ammonium acetate in the mobile phase to achieve resolution of all CoA-containing compounds as shown in Figure 15. The ammonium acetate mobile phase was not used for any of the time course or quantitative stoichiometric analyses because, as Figure 15 illustrates, high sample acidity resulted in significant tailing. Additionally, column retention times with the ammonium acetate mobile phase tended to be highly variable. These relatively large shifts in retention times are believed to result from minor variations in mobile phase preparations, sample pH, air temperatures around the column, and the extent of column equilibration.

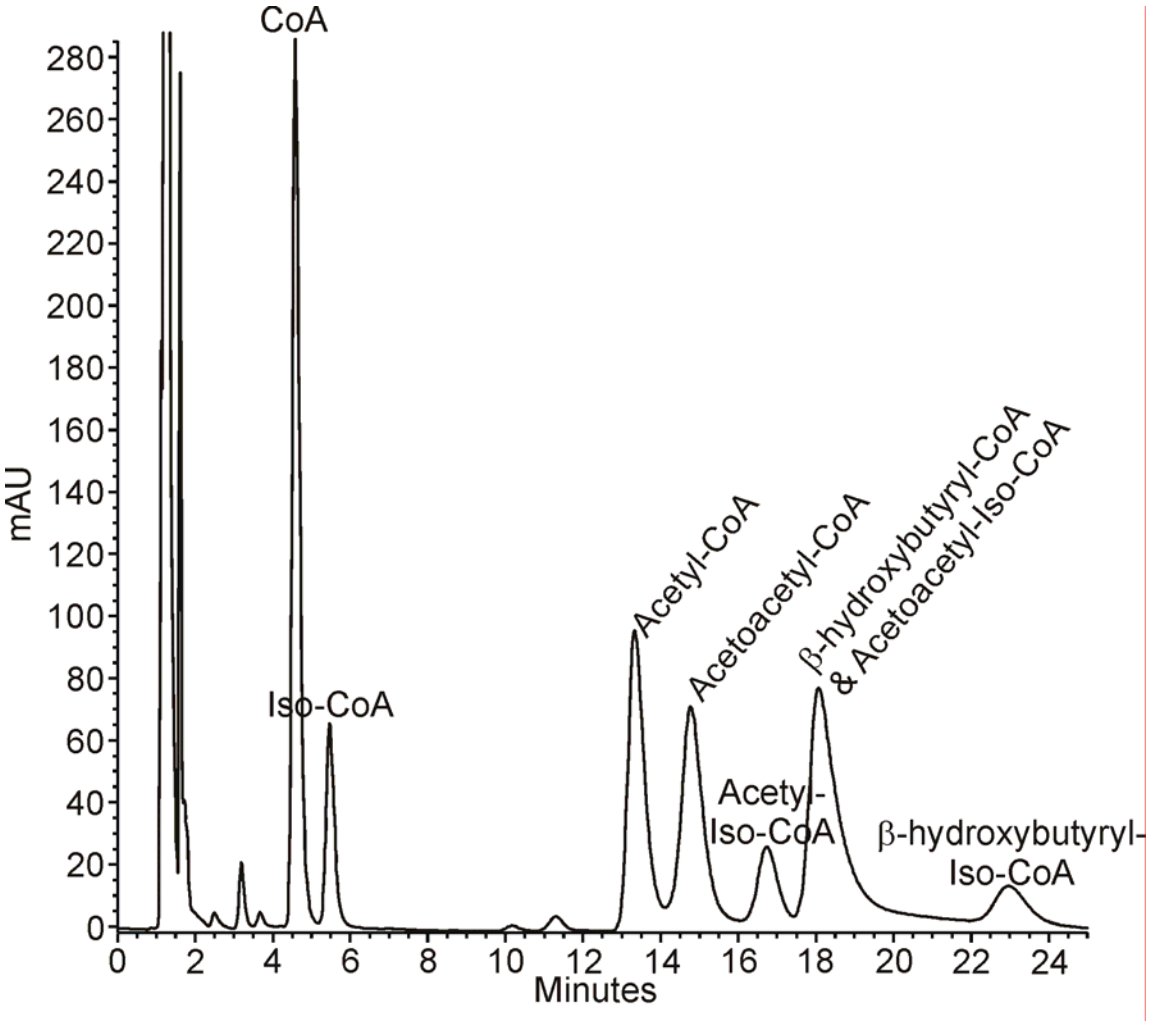

Figure 15. Representative Chromatograms of CoA, Acetyl-CoA, Acetoacetyl-CoA, and β-hydroxybutyryl-CoA. Sample was treated with perchloric acid at a final concentration of 0.57 M with a mobile phase of 96% of 200 mM ammonium acetate: 4% acetonitrile.

Reducing Agents for CoA and Enzyme Activity. Reducing agents are essential for accurate quantitation of free CoA because they prevent oxidation of CoA to the CoASSCoA disulfide dimer. Under the conditions used in these investigations, at pH 7.8, approximately 50% of CoA was oxidized after two hours in the absence of reducing agents (data not shown). The traditional thiol-containing reducing agent, β-mercaptoethanol, generated an unidentified peak, labeled in red in Figure 16 Panel A, which likely results from formation of a mixed disulfide between β-mercaptoethanol and CoA (223). The location of the unknown peak is extremely close to the expected location for acetoacetyl-CoA; however, as Figure 16 Panel B illustrates acetoacetyl-CoA elutes separately from the peak for the unknown compound. We note that this phenomena was only observed in experiments with very low substrate concentrations.

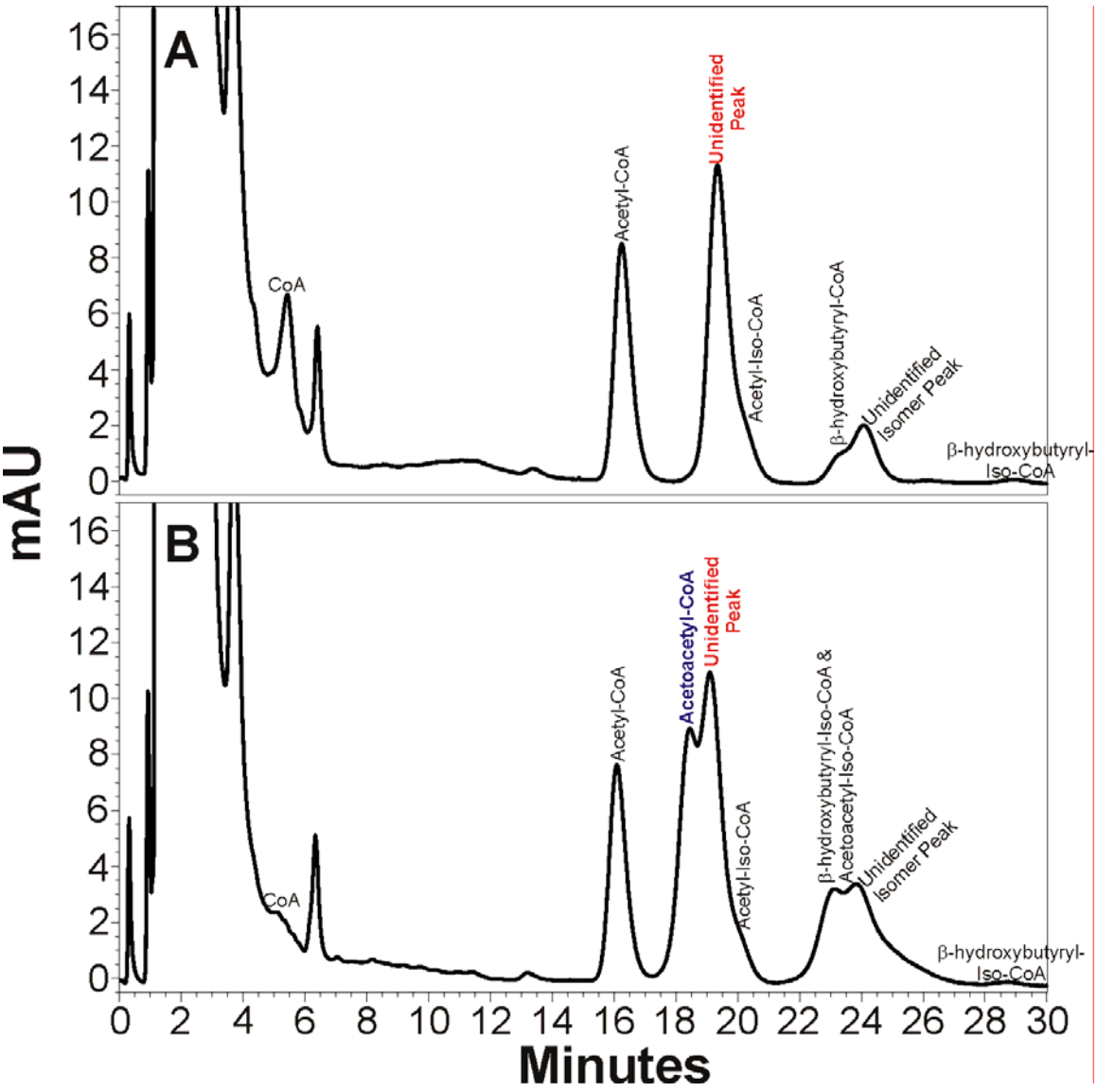

Figure 16. Stacked Chromatograms of an Unidentified Substance. A.) Chromatogram showing the unidentified peak, which is purportedly the mixed disulfide of CoA and β-mercaptoethanol via HPLC at 19 min. B.) Solution in Panel A is spiked with acetoacetyl-CoA to illustrate that the unknown peak is not acetoacetyl-CoA but rather some unique compound.

Since the unknown substance nearly coelutes with acetoacetyl-CoA, we chose the alternative reducing agent triscarboxyethyl phosphine (TCEP) to avoid difficulties with quantitation of acetoacetyl- and β-hydroxybutyryl-CoA. TCEP is a somewhat newly available reducing agent, which is a water soluble, odorless, trialkylphosphine that reacts with disulfides to form two free thiols and the phosphine oxide (240). TCEP does not interact with any of the acyl-CoA compounds tested in this study (Data not shown). TCEP was also substituted for β-mercaptoethanol, to maintain the activity of the β-ketothiolase and acetoacetyl-CoA reductase enzymes during storage. Comparisons of the activities for enzymes stored in β-mercaptoethanol and those rinsed and then stored with TCEP were nearly identical, and were also higher than enzymes stored without reducing agents.

Selection of Organic Eluent and Isocratic Elution.

Acetonitrile and methanol have been reported in the literature for separations of acyl-CoA compounds, but only acetonitrile provided adequate resolution for the acyl-CoA compounds used in this study. Methanol did not resolve acetoacetyl-CoA and β-hydroxybutyryl-CoA without increasing run times in excess of 60 minutes, which resulted in band broadening. We note that this system is extremely sensitive to minor changes in acetonitrile concentration such that retention times would shift by ten minute from a 0.5% increase in acetonitrile. Consequently, isocratic elution was more convenient because it avoided the extensive re-

equilibrations that would be necessary after each gradient. We confirm the report by Hermans-Lokkerbol *et al*. (237), that the elution order of acetoacetyl-CoA and acetyl-CoA are reversed when acetonitrile rather than methanol is used in the mobile phase.

Column Selection. The columns attempted for this separation were the Alltech Platinum EPS C_8, the Waters Spheresorb C_8 and C_{18}, the Phenomenex Luna HexylPhenyl, the Phenomenex Hydro-RP Synergy C_{18} column, and the NovaPak C_{18} Reverse Phase column. Most full size, 250 mm. length, columns were capable of resolving all CoA compounds; however, the run times were often in excess of 70 min to achieve baseline separation. Consequently, the NovaPak C_{18} reverse phase column was used because the increase in resolution provided by its small, 4 Å particles, permitted the use of a shorter column length, 150 mm, which ultimately reduced run times and allowed baseline separation within 33 min.

Standard Curves and Limits of Detection. As shown in Figure 17, standard curves prepared from the areas under the peaks, which were adjusted for the presence of the iso-CoA isomers, showed excellent linearity with R^2 coefficients of 0.9999. Baseline separation was achieved for all CoA-containing compounds including acetoacetyl-CoA, as indicated in Figure 14. However, no acetoacetyl-CoA was detected during any of the *in vitro* experiments; therefore, no standard curve was determined for this compound. The HPLC limits of detection for CoA, acetyl-CoA and β-hydroxybutyryl-CoA listed in Table 7 were determined

with both the acetate and the citrate mobile phases. Sodium citrate has a greater UV absorbance than sodium acetate at 260 nm so the baseline for the sodium citrate mobile phase has slightly higher noise levels; this resulted in marginally higher limits of detection.

Table 7. HPLC Limits of Detection for CoA, Acetyl-CoA and β-hydroxybutyryl-CoA. A C18 Reverse Phase HPLC column run with mobile phases containing sodium acetate or sodium citrate as described in the text.

	Acetate buffer	*Citrate buffer*
CoA	1.7 pmol	3.1 pmol
acetyl-CoA	3.3 pmol	6.5 pmol
β-hydroxybutyryl-CoA	3.1 pmol	12.6 pmol

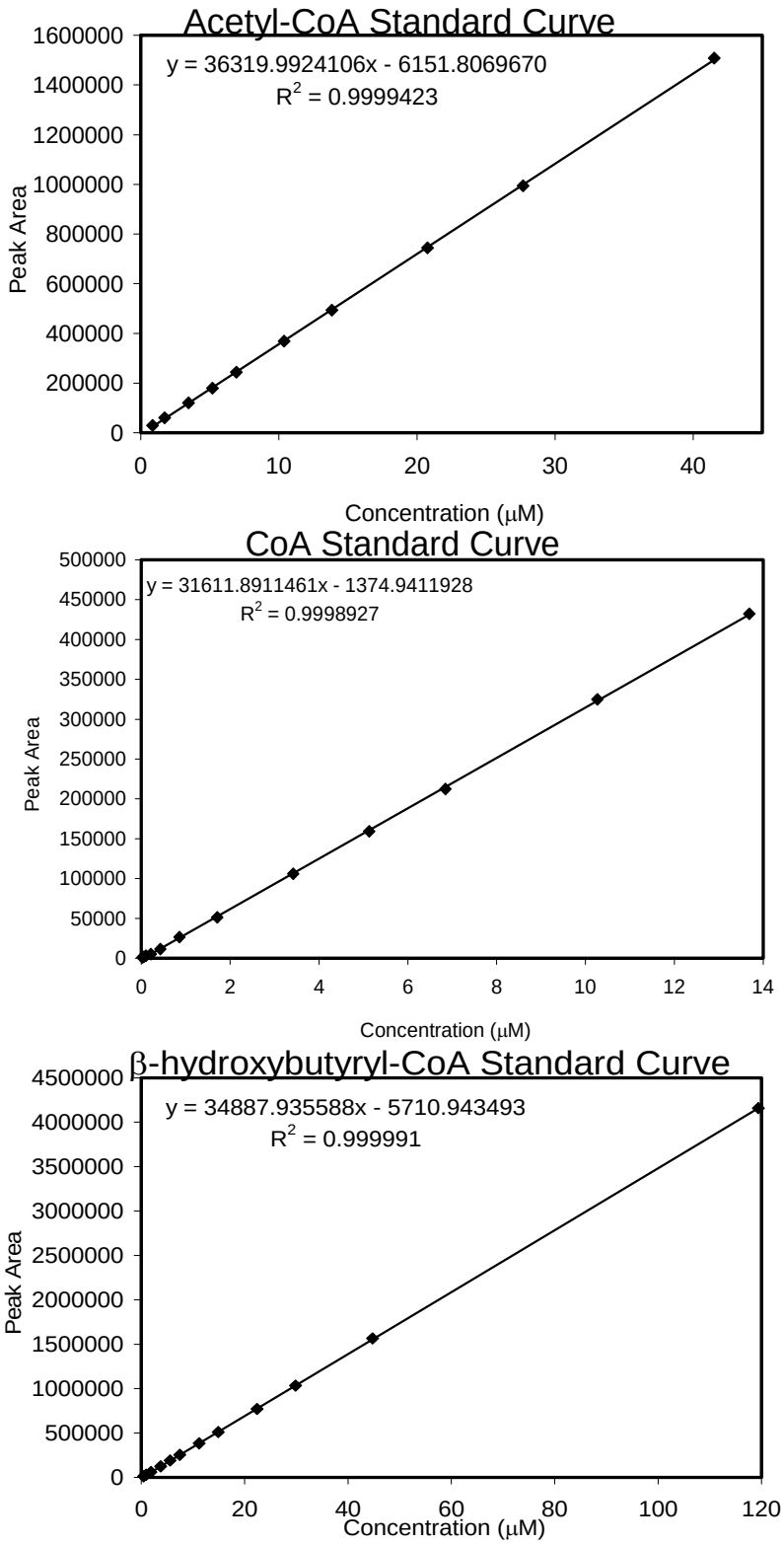

Figure 17. HPLC Standard Curves for Acetyl-CoA, CoA, and β-hydroxybutyryl-CoA.

PHB Metabolic Model. We have developed a structured kinetic model to simulate the *in vitro* synthesis of PHB using the HPLC data gathered in this study. This model is based on the work of Leaf and Srienc (190), van Wegen *et al*. (189), and Daae *et al*. (191), who modeled the *in vivo* synthesis of PHB in *C. necator*, recombinant *E. coli*, and the A*rabidopsis thaliana* plant, respectively. This is the first report of a metabolic model that simulates the *in vitro* biosynthesis of PHB. The model was developed with the BioPathway Explorer and GEPASI (217-219) modeling software packages. Kinetic parameters were gathered either from the literature, from laboratory analysis, or were determined by fitting the simulation to the time course data. Excel was used for calculating kinetic constants, Haldane relationships, and for displaying the GEPASI output data. Figure 18 shows the simulation depicted with solid lines, in comparison to the laboratory data gathered by HPLC indicated by data points. The simulation was performed by coupling the integrated rate equations for each of the three-enzymes in the PHB pathway.

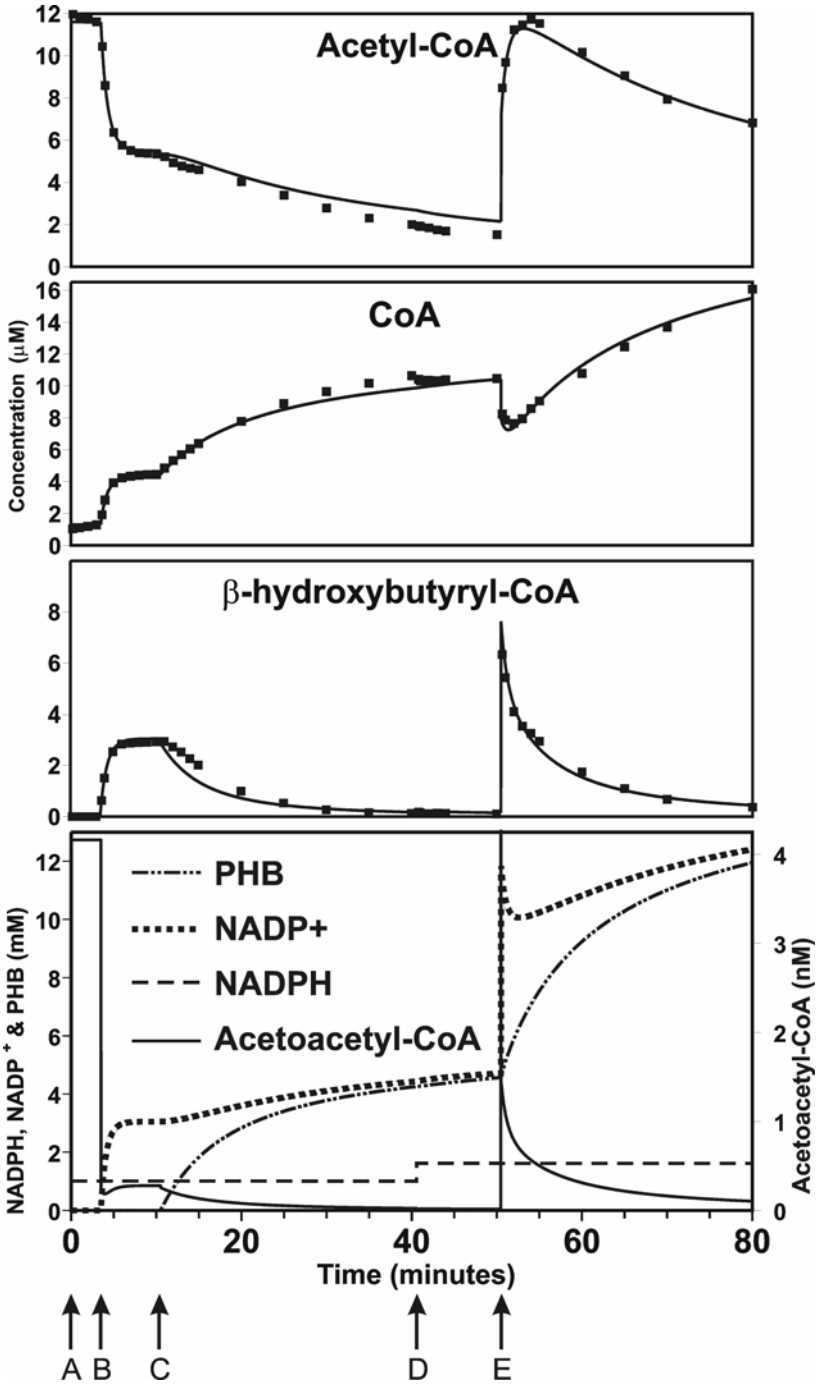

Figure 18. Metabolic Modeling of PHB Synthesis and Spiking Experiments. The HPLC data for the *in vitro* synthesis of PHB is displayed with the data points. Lines show the results of the metabolic model. The labeled arrows indicate enzyme or substrate additions as follows: A. 0 min, β-ketothiolase; B. 3.5 min, acetoacetyl-CoA reductase; C. 10.5 min, PHB synthase; D. 40.5 min, NADPH and acetoacetyl-CoA reductase; E. 50.5 min, acetoacetyl-CoA.

Stepwise Simulation of In Vitro PHB Synthesis. Initially, when only the β-ketothiolase enzyme is added (Point A), both the simulation and the experimental data show no consumption of acetyl-CoA and no production of products. Addition of acetoacetyl-CoA reductase (Point B) results in catabolism of acetyl-CoA with production of CoA and β-hydroxybutyryl-CoA, with excellent agreement between the experimental data and the model. PHB synthase addition (Point C) drives the entire biosynthesis forward resulting in further consumption of acetyl-CoA and liberation of CoA as seen in both the experimental data and in the simulation. The simulation predicts acetoacetyl-CoA concentrations in the very low nanomolar range, reaching 1.3 nM within 1 s, 0.05 nM in 25 min, and 0.01 nM after 40 min (Figure 18). Since concentrations this low would be well below the limit of detection by HPLC, the metabolic model is consistent with the observed lack of acetoacetyl-CoA accumulation in the *in vitro* biosynthesis system (Figure 12).

HPLC Spiking Experiments. HPLC spiking experiments were undertaken to further clarify the lack of acetoacetyl-CoA accumulation throughout the time course of the reaction. The overlaid HPLC chromatograms in Figure 14 clearly show that under our elution conditions acetoacetyl-CoA is well resolved from the other CoA compounds, and its buildup would be easily detectable. In Figure 18, Point E, the reaction mixture was spiked with acetoacetyl-CoA, and the HPLC chromatograms of the reaction mixture immediately before and immediately after spiking are shown in Figure 19. It is evident that even as early as eight seconds after spiking no acetoacetyl-CoA is detectable, whereas large changes in CoA, acetyl-CoA, and β-hydroxybutyryl-CoA are clearly evident. This suggests that the added acetoacetyl-CoA was rapidly consumed both by the β-ketothiolase enzyme, producing two equivalents of acetyl-CoA, and also by the acetoacetyl-CoA reductase enzyme, generating one equivalent of β-hydroxybutyryl-CoA. The stoichiometric correlations, listed in Table 6, support this contention since adding all of the 5.03 µM of β-hydroxybutyryl-CoA to one-half of the 5.63 µM of acetyl-CoA (1/2 equals 2.81 µM) exactly equals the quantity of acetoacetyl-CoA that was added to spike the reaction, 7.84 •M.

A second spiking experiment (Figure 18, Point D) was also carried out in which additional acetoacetyl-CoA reductase and NADPH were added, and it is clear from Figure 18, Point D, and Figure 20 that this does not substantially affect the concentration of any of the CoA-containing compounds. It is also

evident from Figure 18 that the experimental data and simulation are in good agreement for the entire time course of the experiment and for both spiking experiments, including the return to low nanomolar concentrations of the acetoacetyl-CoA levels as early as one second after spiking.

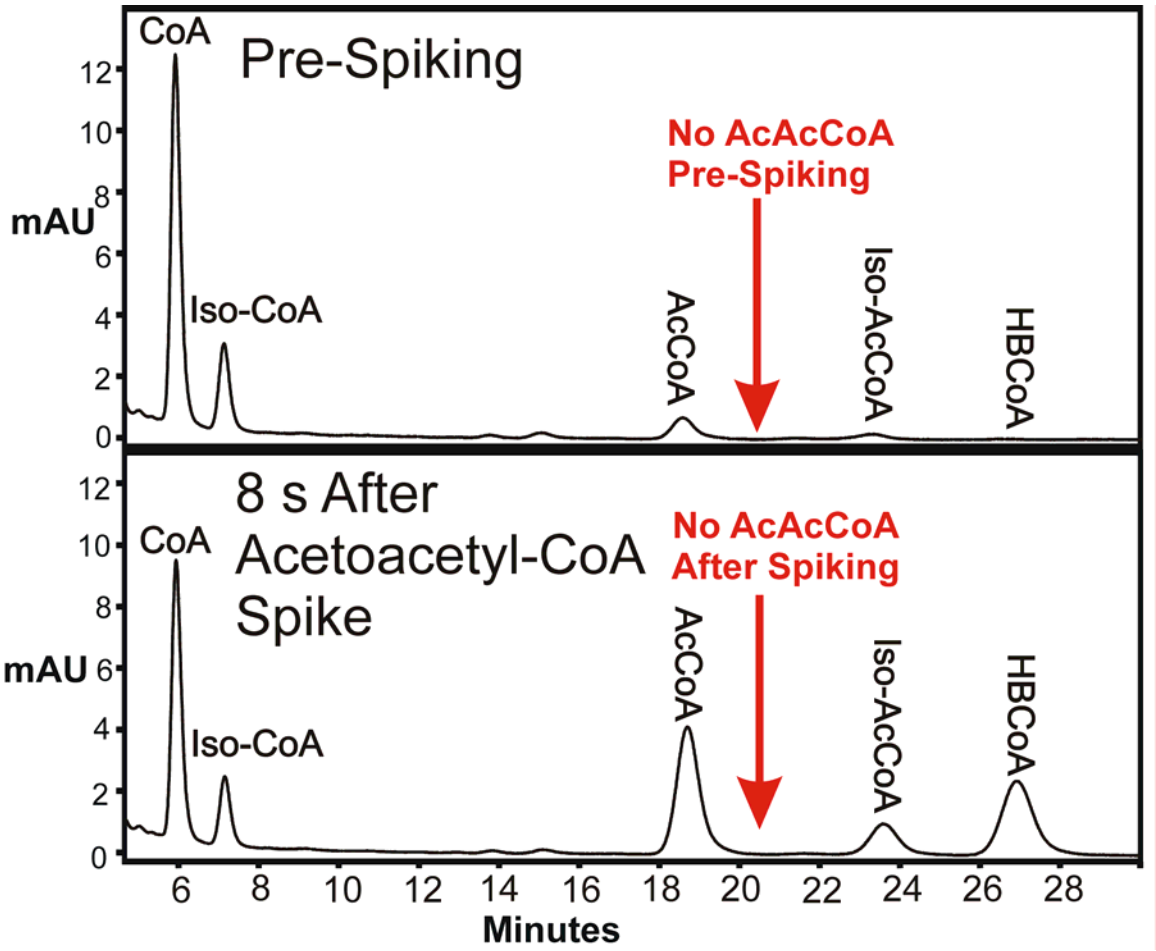

Figure 19. Stacked Chromatograms of the Acetoacetyl-CoA Spiking Experiment. In this experiment 7.8 µM of acetoacetyl-CoA was added to a reaction mixture containing the substrates and the enzymes β-ketothiolase, acetoacetyl-CoA reductase, PHB synthase.

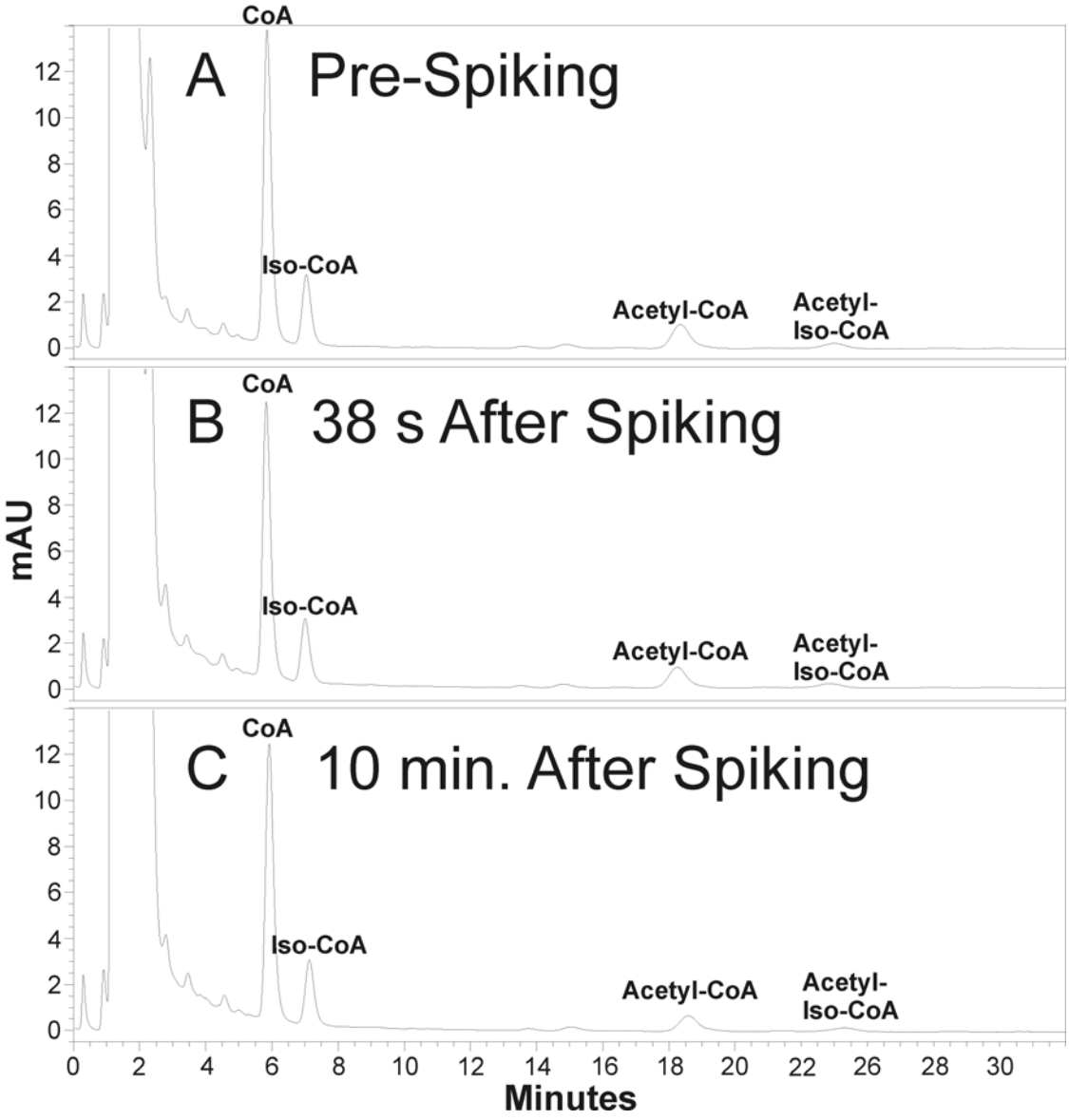

Figure 20. Stacked Chromatograms of the NADPH and Acetoacetyl-CoA Reductase Spiking Experiment. In this experiment, 0.5 mM NADPH and 40 •M of acetoacetyl-CoA reductase were added to the reaction mixture, which contained the substrates and the enzymes β-ketothiolase, acetoacetyl-CoA reductase and PHB synthase. Panel A is before spiking, and Panel B and Panel C are 38 s and 10 min post spiking, respectively.

The goodness of fit for the metabolic model was explored by varying the reaction parameters. The step in which the PHB reaction was spiked with acetoacetyl-CoA was chosen for this analysis because all three enzymes were present and the goodness of fit was high in this section. To perform this analysis each reaction parameter was varied by plus or minus 10 fold and the simulation was run to determine the sum of squares, standard deviation, and RMS error for each parameter variation. As shown in Table 8, the reaction with no parameters changed exhibited a sum of squares of 1.019 and the goodness of fit upon varying each of the reaction parameters are listed in Tables 9-11.

Table 8. Goodness of Fit for the PHB Synthetic Model.

Sum of squares	Standard deviation	RMS error
1.019	0.319	0.304

Table 9. Goodness of Fit for the β-ketothiolase Parameters.

	Normal Values	Sum of squares		Standard deviation		RMS error	
		x 10 fold	÷ 10 fold	x 10 fold	÷ 10 fold	x 10 fold	÷ 10 fold
K_{eq}	4.00×10^{-5}	58.164	41.508	2.412	2.037	2.299	1.943
V_r (µM/s)	2924.00	1.019	1.019	0.319	0.319	0.304	0.304
V_f (µM/s)	9.75	0.801	4.474	0.283	0.669	0.270	0.638
K_{sum} •M	1238.00	13.865	0.476	1.178	0.218	1.123	0.208
K_a •M	0.158	---					
K_b •M	1237.84	---					
K_p •M	16.00	3.605	0.746	0.600	0.273	0.572	0.260
K_q •M	44.00	48.013	1.497	2.191	0.387	2.089	0.369
K_{ia} •M	46.74	---					
K_{ib} •M	1237.84	1.019	1.019	0.319	0.319	0.304	0.304
K_{ip} •M	15.78	0.802	4.473	0.283	0.669	0.270	0.638
K_{iq} •M	0.147	1.019	1.019	0.319	0.319	0.304	0.304

Table 10. Goodness of Fit for the Acetoacetyl-CoA Reductase Parameters.

	Normal Values	Sum of squares		Standard deviation		RMS error	
		x 10 fold	÷ 10 fold	x 10 fold	÷ 10 fold	x 10 fold	÷ 10 fold
K_{eq} •M	2.16 x 10^9	44.063	64.498	2.099	2.540	2.001	2.421
V_r (µM/s)	135.09	27.692	248.368	1.664	4.984	1.587	4.752
V_f (µM/s)	1486.00	7.513	20.284	0.867	1.424	0.826	1.358
K_a •M	19.00	0.900	1.032	0.300	0.321	0.286	0.306
K_b •M	5.00	10.356	2.440	1.018	0.494	0.970	0.471
K_p •M	16.50	0.960	1.025	0.310	0.320	0.295	0.305
K_q •M	31.00	0.513	1.135	0.227	0.337	0.216	0.321
K_{ia} •M	50.00	0.799	0.518	0.283	0.228	0.269	0.217
K_{ib} •M	28.83	---					
K_{ip} •M	5.00	1.429	0.918	0.378	0.303	0.360	0.289
K_{iq} •M	47.15	1.019	1.006	0.319	0.317	0.304	0.302

Table 11. Goodness of Fit for the Parameters for the PHB Synthase Reaction.

	Normal Values	Sum of squares		Standard deviation		RMS error	
		x 10 fold	÷ 10 fold	x 10 fold	÷ 10 fold	x 10 fold	÷ 10 fold
V_f	0.309	55.203	40.068	2.350	2.002	2.240	1.909
K_M •M	103.00	39.442	50.159	1.986	2.240	1.894	2.135
K_I •M	108.00	1.111	2.850	0.333	0.534	0.318	0.509

CHAPTER 4

PHB: DISCUSSION

In 1977 Saito *et al.* (159) reported the first multi-enzyme *in vitro* enzymatic synthesis of PHB using crudely purified enzymes from *Z. ramigeria*, then later Haywood *et al.* (160) used enzymes isolated from *C. necator*; both monitored PHB production via incorporation of radiolabeled [1-^{14}C]acetyl-CoA. Recently, Satoh *et al.* (181) reported the enzymatic synthesis of PHB from acetate with cofactor recycling using the three *C. necator* enzymes plus the enzymes acetyl-CoA synthetase and glucose dehydrogenase. Satoh *et al.* (181) implemented cofactor recycling because prohibitively low substrate conversion (<6%) was encountered with the two-enzyme system, which contained only β-ketothiolase and acetoacetyl-CoA reductase. These authors suggested that recycling the CoA produced by the condensation of acetyl-CoA prevented CoA-mediated product inhibition of the β-ketothiolase enzyme and therefore facilitated overall reaction progress (181). While cofactor recycling does effectively increase overall reaction yields, it also entails inclusion of additional enzymes, which alter metabolite flux and create an enzyme system that is more complex than the three-enzyme *C. necator* biosynthetic system.

The results presented here provide a clear illustration of the individual effect of each of the three key enzymes from *C. necator* on the *in vitro* progress of PHB biosynthesis. We have circumvented the problem of cofactor inhibition by dramatically reducing initial substrate concentrations such that cofactors do not accumulate to levels capable of significant enzyme inhibition. Each enzymatic reaction was performed in a step-wise manner and monitored by HPLC in order to elucidate the fluctuations in metabolite concentrations and the effect of each individual enzyme on the overall system. Our strategy of using low substrate concentrations to overcome product inhibition proved to be successful since the two-enzyme system sans cofactor recycling, which consists of β-ketothiolase and acetoacetyl-CoA reductase, achieved 55% conversion of the acetyl-CoA substrate in our experiments, as compared to the less than 6% conversion obtained by Satoh *et al.* (181) After addition of the third enzyme, PHB synthase, approximately 83% of the initial acetyl-CoA was consumed within 40 min. These results validate our strategy of lowering initial enzyme substrate concentrations to achieve a well-behaved model system.

We report here the development of optimized HPLC methodology which separates CoA, acetyl-CoA, acetoacetyl-CoA, and β-hydroxybutyryl-CoA with baseline resolution in approximately 30 min, which is approximately half of the time required by the only procedure (181) reported in the literature to separate this

series of CoA compounds. Convenient isocratic elution and selection of an efficient column facilitated shorter run times. It is significant that this method gives baseline resolution of acetoacetyl-CoA so that we were able to unequivocally demonstrate that this compound does not accumulate to detectable levels in the enzymatic system. Baseline separation was also essential to accomplish accurate quantitation, which was necessary to obtain the excellent stoichiometric mass balances reported in this study. Our mobile phase does not employ harsh ion-pairing agents (226) or high phosphate concentrations which damage silica columns (227), yet still provides the strong buffering capacity necessary for excellent resolution, good peak shape, and reproducible retention times.

Three Enzyme System.

β-ketothiolase. The series of *in vitro* enzymatic reactions performed in this study were designed specifically to delineate the mechanisms by which the enzymes and metabolites affect overall pathway flux for PHB synthesis. As Figure 13 indicates initiation of the reaction with β-ketothiolase results in only minor changes in acetyl-CoA and CoA concentrations, and no acetoacetyl-CoA is detected by HPLC. The equilibrium of β-ketothiolase is reported in the literature to range from 1×10^{-4} (190,207) to 6×10^{-6} (221,241,242), which strongly favors thiolysis of acetoacetyl-CoA to acetyl-CoA. Therefore, it seems reasonable that the reaction equilibrium would allow only very

small concentrations of acetoacetyl-CoA concentrations to accumulate and this would be below the limit of detection by HPLC. We note that stoichiometric analysis for the β-ketothiolase reaction was not possible because the acetoacetyl-CoA could not be detected or quantified by HPLC.

β-ketothiolase and acetoacetyl-CoA reductase. Addition of the acetoacetyl-CoA reductase enzyme to the reaction mixture as illustrated in Figure 13 Panel B generates an immediate and substantial decrease in acetyl-CoA concentrations with a corresponding increase in the concentrations of CoA and β-hydroxybutyryl-CoA. In this situation β-hydroxybutyryl-CoA is generated by the acetoacetyl-CoA reductase catalyzed reduction of acetoacetyl-CoA (refer to Figure 7). The depletion of acetyl-CoA and generation of CoA suggests that the acetoacetyl-CoA is being consumed by the by acetoacetyl-CoA reductase, which would displace the unfavorable equilibrium of the β-ketothiolase reaction effectively driving the β-ketothiolase reaction toward the forward thiolysis direction. This phenomenon is supported by the equilibrium constants in the literature for the enzymatic reactions. When coupling the two enzymes, the large forward equilibrium constant of the acetoacetyl-CoA reductase reaction, which ranges in the literature from 5×10^{9} (221) to 6.3×10^{11} (243), overcomes the large reverse β-ketothiolase equilibrium constant (between 1×10^{-4} (190,207) and 6×10^{-6} (221,241,242)); this effectively drives the entire reaction system forward. The coupled reaction does not reach completion; instead, equilibrium

is achieved after about 10 min with approximately 55% of the acetyl-CoA starting material consumed (Figure 13). The equilibrium constant, which was calculated from the laboratory derived HPLC data at 10 min is 8.6×10^4; this agrees well with the 5.1×10^4 value for the equilibrium constant which was determined by Gilbert *et al.* (221) for the same reaction catalyzed by pig heart thiolase and β-hydroxybutyryl-CoA dehydrogenase. Furthermore, excellent stoichiometric results were obtained (Table 7) which show that 2 acetyl-CoA molecules generate 1 β-hydroxybutyryl-CoA and one CoA molecule, with a low 1.8% margin of error.

β-ketothiolase, acetoacetyl-CoA reductase, and PHB Synthase. Addition of a third enzyme, PHB synthase, results in the consumption of acetyl-CoA and β-hydroxybutyryl-CoA with liberation of CoA as shown in Figure 13, Panel C. The PHB synthase catalyzed polymerization reaction is regarded as irreversible; therefore, addition of this enzyme will drive the entire reaction toward polymer formation. Indeed, the movement of the system toward PHB production accounts for each of the changes in metabolite concentrations that occur upon addition of the PHB synthase enzyme (Figure 13, Panel C). The concentration of β-hydroxybutyryl-CoA decreases as it is consumed by the PHB synthase enzyme to generate PHB. Likewise, acetyl-CoA concentrations decrease in response to the decrease in β-hydroxybutyryl-CoA. This is a result of the consumption of the product of the β-ketothiolase reaction, acetoacetyl-CoA, by the

acetoacetyl-CoA reductase enzyme, which stimulates the β-ketothiolase reaction to consume further acetyl-CoA and liberate CoA. We note that CoA is liberated in two processes, by both the β-ketothiolase and the PHB synthase reactions; this results in a stoichiometric relationship in which two CoA molecules are released for every acetyl-CoA and β-hydroxybutyryl-CoA molecule consumed. Under these circumstances, the reaction proceeds with stoichiometries that reflect the liberation of 5.32μM of CoA, in the β-ketothiolase and the PHB synthase reactions, corresponding to a cumulative consumption of acetyl-CoA and β-hydroxybutyryl-CoA of 5.42μM, as reported in Table 6.

Overall Analysis. HPLC analysis of the concatenated *in vitro* enzymatic reaction over the entire time course of the reaction from start to finish (T=0 to 40 min) confirms stoichiometric conservation of CoA-moieties. In this investigation (Table 7), the quantity of CoA moieties consumed in the reaction as acetyl-CoA equals the concentration of CoA moieties liberated, in the form of free CoA and β-hydroxybutyryl-CoA, with an excellent experimental error of 0.1%.

Acetoacetyl-CoA Spiking Experiments and Stoichiometry. Acetoacetyl-CoA was not detected by HPLC in any of the enzyme experiments performed in this study. This phenomena has been reported in the literature in both *in vivo* (189) and *in vitro* (181) experiments, but has never been thoroughly explored or

explained. We investigated this lack of acetoacetyl-CoA by performing spiking experiments. The absence of the accumulation of acetoacetyl-CoA during the enzymatic reactions was initially investigated using a spiking experiment which explored the hypothesis that acetoacetyl-CoA was present but potentially invisible to detection by HPLC. As Figure 18, Point D and Figure 20 shows, additional NADPH and acetoacetyl-CoA reductase were added to the three-enzyme *in vitro* system in an attempt to drive the acetoacetyl-CoA reductase reaction forward. Theoretically, if acetoacetyl-CoA were present, but the detection by HPLC was masked, doubling the concentration of acetoacetyl-CoA reductase and adding 0.5 mM NADPH should convert the residual acetoacetyl-CoA to β-hydroxybutyryl-CoA, which would be easily detectable by HPLC. As seen in Figure 18, Point D and Figure 20, no significant change in the concentration of β-hydroxybutyryl-CoA is observed upon spiking the reaction. This experiment provides initial evidence that the steady state concentrations of acetoacetyl-CoA are maintained at extremely low levels, which are below the limit of detection by HPLC.

To further assess the premise that the steady state concentrations of acetoacetyl-CoA were below the limit of HPLC detection, a spiking experiment was performed in which 7.84 μM of acetoacetyl-CoA was added to the *in vitro* three-enzyme system at t = 50 min. As the HPLC elution profiles in Figure 19 illustrate, no acetoacetyl-CoA is visible in the sample acquired only eight seconds after spiking; however, there are significant

increases in acetyl-CoA and β-hydroxybutyryl-CoA. The sharp increase in these two metabolites indicates that upon addition of acetoacetyl-CoA, β-ketothiolase rapidly converts the acetoacetyl-CoA to acetyl-CoA while, simultaneously, acetoacetyl-CoA reductase reduces the acetoacetyl-CoA to β-hydroxybutyryl-CoA. Basically, the system reacts to rapidly decrease the concentration of the spiked acetoacetyl-CoA; it does this through both thiolysis and reduction.

Stoichiometric quantification of the products formed immediately after acetoacetyl-CoA spiking support the assertion that acetoacetyl-CoA is quantitatively converted to acetyl-CoA and β-hydroxybutyryl-CoA in the three-enzyme system. The time point taken immediately (eight seconds) after spiking with acetoacetyl-CoA was used to calculate the resulting concentration changes. This time point was chosen because in this small time span little formation of PHB has occurred; therefore, all carbon units should be accounted for amongst the CoA-containing compounds (acetyl-CoA, β-hydroxybutyryl-CoA, and CoA). In this situation, one molecule of acetoacetyl-CoA is converted to either one molecule of β-hydroxybutyryl-CoA or two molecules of acetyl-CoA with consumption of CoA. Therefore, the sum of the increase in β-hydroxybutyryl-CoA plus one-half of the increase in acetyl-CoA should equal the concentration of acetoacetyl-CoA used to spike the experiment. As listed in Table 6, 7.84 μM of acetoacetyl-CoA was added to the reaction mixture; eight seconds

after spiking an increase of 5.628 μM of acetyl-CoA (½ acetyl-CoA is 2.814) and 5.033 μM of β-hydroxybutyryl-CoA were detected, which result in a calculated sum of 7.84 μM. The stoichiometries clearly demonstrate excellent correlation to the quantity of acetoacetyl-CoA (7.84 μM) used to spike the reaction.

The results of the two previous spiking experiments clearly support the premise that low steady state concentrations of acetoacetyl-CoA are maintained during the *in vitro* enzymatic synthesis of PHB. The absence of acetoacetyl-CoA is not believed to be an artifact or due to a difficulty in detecting acetoacetyl-CoA by HPLC. This phenomenon does agree with the equilibrium constants and apparent Michaelis-Menten constant for acetoacetyl-CoA for the β-ketothiolase reaction ($K_{eq} = 10^{-5}$; K_M = 44μM), which lies strongly in the reverse direction, and the acetoacetyl-CoA reductase reaction ($K_{eq} = 10^{10}$; $K_{acetoacetyl\text{-}CoA}$ = 5μM), which drives the reaction forward. This suggests that the acetoacetyl-CoA produced by β-ketothiolase will rapidly react with the acetoacetyl-CoA reductase enzyme thus maintaining very low steady state concentrations of acetoacetyl-CoA. We note that, it is feasible that some acetoacetyl-CoA decomposed during the course of the reaction. Acetoacetyl-CoA is known to be labile at neutral and basic pH; however, the acid quenching step of the procedure should prevent significant decomposition prior to sample analysis.

Metabolic Model of the PHB Pathway. Metabolic modeling is a convenient tool to evaluate complex enzymatic pathways. Multiple literature reports detail the development of PHB metabolic models (189-206,208-211,244); however, all of these models were designed to analyze *in vivo* biosynthesis, typically in bacteria but also in yeast and plants. Furthermore, few if any, of these simulations use laboratory data for the PHB pathway metabolites: acetyl-CoA, CoA, acetoacetyl-CoA, and β-hydroxybutyryl-CoA. Instead, many use parameters, such as glucose concentration, cell growth rate, and product accumulation, which may not be amenable to straightforward kinetic/thermodynamic analyses. The detailed HPLC data of PHB metabolites that was obtained in this study are ideal for the development of a PHB metabolic model.

We report here the development of the first kinetic model of *in vitro* PHB biosynthesis. This is the first structured kinetic metabolic model developed using *in vitro* data of metabolite concentrations, which simulates the *in vitro* biosynthesis of PHB; it is based on the work of Leaf and Srienc (190), van Wegen *et al*. (189), and Daae *et al* (191). This model should serve to elucidate the interplay between the kinetics and thermodynamics, which govern each step in the enzymatic pathway for PHB synthesis. Future optimization of the system flux using metabolic modeling could aid in the optimization and design of this and other enzymatic systems.

Results of the PHB Pathway Simulation. The model accurately shows that addition of the first enzyme, β-ketothiolase, generates only negligible changes in metabolite concentrations. This is consistent with the equilibrium constant for this reaction (1×10^{-4} (190,207) to 6×10^{-6} (221,241,242)), which strongly favors thiolysis of acetoacetyl-CoA. The model does appear to deviate slightly from the experimental HPLC-data by showing some hydrolysis of acetyl-CoA by the β-ketothiolase enzyme (Figure 18, Point A); acetyl-CoA hydrolysis liberates stoichiometric amounts of CoA without generating any acetoacetyl-CoA. The hydrolysis observed in our *in vitro* system occurs with a first order rate constant of approximately 3×10^{-3} s^{-1}, which is not too dissimilar to the first order rate constant for hydrolysis of the Ac-S-enzyme ($k = 2.6 \times 10^{-4}$ s^{-1} at pH 6.8 and 25 C) reported in the literature for the porcine heart thiolase (221). On the other hand, Thompson *et al*. (242) report that the *Z.ramigeria* β-ketothiolase catalyzed rates of condensation (k_{cat} 810 s^{-1} (242)) and thiolysis (k_{cat} 71 s^{-1} (242)) are several magnitudes greater (3×10^6 and 3×10^5 fold, respectively) than the rate of hydrolysis of the Ac-S-enzyme by porcine heart thiolase (221,242,245). The authors suggest that this implies that the β-ketothiolase catalyzed rates of condensation and thiolysis will effectively overwhelm any enzymatic hydrolysis of the Ac-S-enzyme so hydrolysis should not be observed. Nevertheless, some hydrolysis of acetyl-CoA was observed *in vitro* in our system and it is possible that this hydrolysis might occur

because the system is at equilibrium and, unlike the Thompson *et al*. report (242), our ketothiolase-only system does not contain enzymes capable of displacing the unfavorable equilibrium, which permit the reaction to proceed and prevent observable enzymatic hydrolysis.

Addition of the second enzyme (Figure 18, Point B), acetoacetyl-CoA reductase, generates a dramatic decrease in the acetyl-CoA concentration and increases in CoA and β-hydroxybutyryl-CoA levels. In this situation, the model shows excellent correlation to the *in vitro* HPLC-data. These simulation results indicate that the large forward equilibrium constant of the acetoacetyl-CoA reductase reaction (5×10^{9} (221) to 6.3×10^{11} (243)) overcomes the large reverse β-ketothiolase equilibrium constant; thus, effectively driving the simulated system forward. The simulation also reaches equilibrium after approximately 55% of the starting material is consumed, which is consistent with the *in vitro* HPLC data.

In the third step, when the PHB synthase enzyme is added, the simulation shows consumption of the β-hydroxybutyryl-CoA, which had accumulated in the previous step; this effectively displaces the previously established equilibrium and shifts the system toward PHB polymer production. The simulation confirms that the irreversible polymerization of β-hydroxybutyryl-CoA does indeed shift the entire three-enzyme system towards PHB production, and simultaneously stimulates the condensation of

additional acetyl-CoA, with CoA liberated by both the β-ketothiolase and PHB synthase reactions.

While the simulation of the third step (Figure 18, Point C) agrees reasonably well with the experimental data, it is apparent that some deviation from the experimental data occurs. This is likely because a simplified kinetic equation for the PHB synthase reaction is employed in the model. Studies by Goodwin and coworkers (165,167,168) established that the PHB synthase reaction exhibits a substantial lag phase prior to achieving maximal reaction rates. The lag phase is a consequence of the formation of the enzymatically active homodimers from the inactive monomer enzyme form, and also results from an initiation phase in which the enzyme must be primed with either substrate or a multihydroxyl compound in order to achieve maximal rates (165,167,168). The straightforward irreversible Michaelis-Menten kinetic equation with substrate inhibition that was used in this model does not include the priming or lag phase; therefore, the model deviates somewhat from the experimental data in this step (Point C).

One of the more interesting observations from the simulation is that there is no accumulation of acetoacetyl-CoA. In this regard the simulation is consistent with our *in vitro* experiments as well as with the literature reports on PHB synthesis both *in vivo* (189) and *in vitro* (246). Since low acetoacetyl-CoA concentrations are seen in the simulated data it seems reasonable to conclude that it is the physical equilibrium

and apparent Michaelis-Menten constants that govern the β-ketothiolase and reductase enzymatic reactions, which generate in this phenomena. Indeed, the equilibrium for the β-ketothiolase reaction strongly favors thiolysis of the acetoacetyl-CoA; in addition, the k_{cat}/K_M for the acetoacetyl-CoA reductase reaction from *Z. ramigeria* is near diffusion controlled at 1.8×10^8 M^{-1} s^{-1} (220) so establishment of the equilibrium state should be extremely rapid. Thus, the data strongly suggests that it is the action of the β-ketothiolase and acetoacetyl-CoA reductase enzymes, which maintain the vanishingly low levels of acetyl-CoA.

The inherently low levels of acetoacetyl-CoA in this system are particularly evident in the spiking experiments. In the simulation of the experiment in which 7.84 •M of acetoacetyl-CoA is used to spike the reaction mixture, the concentration of acetoacetyl-CoA returns to 1.3 nM within 1 s, reaches 0.05 nM in 25 min and 0.01 nM after 40 min (Figure 18). This rapid reestablishment of extremely low levels of acetoacetyl-CoA with concomitant increases in acetyl-CoA and β-hydroxybutyryl-CoA suggest that the enzymes, acetoacetyl-CoA reductase and β-ketothiolase, act to rapidly metabolize the acetoacetyl-CoA. In effect, the simulation shows that the acetoacetyl-CoA simultaneously undergoes β-ketothiolase mediated thiolysis in addition to reduction by the acetoacetyl-CoA reductase. Likewise, the simulation also matches the *in vitro* data by showing a rebound in which acetyl-CoA and β-hydroxybutyryl-CoA concentrations begin to drop and CoA concentrations rise. This

rebound is no doubt a result of the forward movement of the PHB synthase reaction, which is driving the reaction towards PHB polymer production. Since these behaviors can be simulated, they must result from the kinetic and thermodynamic constants that govern these equations.

The simulation of the NADPH and acetoacetyl-CoA reductase spiking experiment shows good agreement with the *in vitro* data (Figure 18, Point D), which suggests that acetoacetyl-CoA is indeed maintained at low levels (i.e. it is not masked to analysis by HPLC). It is clear that the reaction is currently moving at a velocity that can not be influenced by spiking in this manner. Under these reaction conditions, the acetoacetyl-CoA reductase reaction is not rate limiting, but it seems likely that addition of more of the β-ketothiolase or the PHB synthase enzymes might possibly speed the reaction.

The stringent regulation of acetoacetyl-CoA, which is observed in this and other PHB synthesis systems, might result from the metabolic importance of acetoacetyl-CoA. Acetoacetyl-CoA is critical to several metabolic processes including fatty acid β-oxidation, ketogenesis, mitochondrial fatty acid elongation, and, in certain bacteria, PHB synthesis (247). This metabolic importance could have lead to a tendency for acetoacetyl-CoA to be carefully regulated *in vivo*. Additionally, acetoacetyl-CoA is labile at neutral and basic pH so the tight control of acetoacetyl-CoA concentrations could result from the need to rapidly metabolize this compound before substantial *in*

vivo hydrolysis. Labile reaction intermediates are often carefully regulated *in vivo* through kinetic and thermodynamic mechanisms, which include substrate channeling, to prevent the loss of valuable unstable intermediates (248).

Kinetic and thermodynamic parameters used in this model were gathered from the literature, from laboratory analysis, by fitting the simulation to the time course data, and by calculations based on the kinetic rate and Haldane equations. It is clear that the simulation closely mimics the *in vitro* data (Figure 18). The rate for the PHB synthase reaction, which was determined by simulated fit, is approximately seven fold greater than the literature and laboratory derived values; this correlates reasonably well. However, the rate for the β-ketothiolase and acetoacetyl-CoA reductase reactions which were determined by simulated fit were each 64 fold greater than the laboratory determined maximal rates. This larger discrepancy likely reflects the use of kinetic and thermodynamic constants from the literature, which were gathered under somewhat different experimental conditions, i.e. temperature, buffer type, ionic strength, magnesium concentration.

It is possible that the large deviations in reaction rates for the β-ketothiolase and acetoacetyl-CoA reductase reactions are evidence for substrate channeling. Substrate channeling has been relatively well established for the long chain β-

ketothiolase and acetoacetyl-CoA reductase enzymes which are involved in fatty acid β-oxidation in mitochondria (249). However, substrate channeling has never been reported for PHB production in bacteria. Furthermore, substrate channeling tends to be a very controversial subject and much more evidence would be required to state, definitively, whether substrate channeling is present.

A statistical analysis of how each parameter in the model affects the goodness of fit is shown in Tables 8-11. It is clear that altering the equilibrium constant, the K_{sum} ($K_{sum} = K_a + K_b$), and the K_q of the β-ketothiolase reaction dramatically decrease the goodness of fit. For the acetoacetyl-CoA reductase reaction the goodness of fit is most significantly affected by altering the equilibrium constant, the rate constants, or the K_b. Adjusting any of the parameters in the PHB synthase reaction make the goodness of fit worse with the rate constant and K_M exhibiting the greatest impact. We note that for the parameters in both the acetoacetyl-CoA reductase reaction and β-ketothiolase reaction changing certain parameters can make the goodness of fit better; however, this increased fit is not substantial (i.e. greater than an order of magnitude). Moreover, altering certain of these parameters may make other sections of the simulation worse since the simulation was designed by combining each step in the synthesis of PHB (See Figure 18, Points A-E).

CHAPTER 5

DEVELOPMENT OF A PHB LABORATORY

As part of a multidisciplinary Polymer Science and Engineering laboratory course, which was cross-listed between five departments, we developed a hands-on laboratory for culturing, producing, isolating, and purifying the bacterial biopolyesters PHB. Poly-β-hydroxybutyrate (PHB) is an intracellular polymer that accumulates in the cytoplasm of bacterial cells if a carbon source is provided, and if at least one nutrient, such as nitrogen, is limited. Because it is a biodegradable polyester, there is much interest in its production. In addition to being biodegradable, PHB possesses piezoelectric properties and has characteristics similar to polypropylene, making it suitable for a wide range of applications in surgery, medicine, agriculture, the food industry, and environmental protection.

The Discovery of PHB. Since the discovery of PHB in the early 1800th century, intense interest has been directed toward optimizing bacterial production. In the 1950s, Schlegel and coworkers (116,250,251) first discovered that PHB could be produced by knallgas bacteria (*Hydrogenomonas*). The authors reported methodology for cultivating this Hydrogenomonas

bacteria, which was recently renamed *Cupriavidus necator*, and for generating PHB *in vivo*. *C. necator* is one of many bacterial species that will produce PHB under nitrogen-limiting conditions. It has been reported in the literature that *C. necator* is able to produce up to 60% of its biomass in the form of PHB, when using fructose as the carbon source.

Two Phase Cultivation of PHB. PHB production in *C. necator* requires a two phase cultivation, whereby a given quantity of bacteria are initially grown under optimal growth conditions, and then the bacteria are transferred to a nitrogen-limited minimal media for the bacterial generation of PHB. In this laboratory, all bacterial cultivations were performed via batch fermentation in order to minimize expensive equipment and provide students with an easily accessible methodology. For this laboratory, *C. necator* was initially cultivated with twice concentrated L.B media. As shown in Table 12, supplementing the traditional LB growth media with yeast extract and ammonium sulfate doubled the mass of PHB and the dry cell weight of *C. necator*, and increased the percent yield of PHB.

Table 12. Development of *C. necator* Growth Media.

	Final OD_{600}	*Final DCW[a] g*	*Mass PHB g*	*% PHB*
NB[b]	12.5	o.28	0.15	51.0%
2xNB	24.9	0.46	0.24	51.3 %
2xNB Supp[c]	37.9	0.84	0.45	53.4 %

[a]DCW: Dry Cellular Weight
[b]NB: Nutrient Broth
[c]Supp: Supplemented with ammonium sulfate

Bacterial production of PHB in this laboratory was performed by transferring the *C. necator* bacterial cells into a nutrient-limited minimal media, which was modified from Schlegel's original media (250) using the literature reports of Repaske and Coworkers (252,253) and Meier-Schneiders *et al* (251). Specifically, Co^{2+} & Cr^{3+} were added to increase PHB production as discussed in the literature (251-253). In addition, a chelated form of iron, ferric ammonium citrate, was used because this form of iron remained in solution over a substantially longer period (days instead of hours). The non-chelated iron form, iron (III) chloride, rapidly precipitated out of solution and resulted in orange-colored PHB due, presumably, to contamination of the polymer with iron.

Laboratory Layout. This laboratory is designed in such a way that the students can perform the entire PHB cultivation process in several short sessions over one week. In the first session, the students can make the growth media, autoclave and leave it to cool. A short follow up session will allow students to inoculate their media with the *C. necator* bacteria and begin incubating the bacteria. In a third session the students can pellet, wash and transfer the cultured mass of *C. necator* cells to the minimal media for PHB production. For convenience, this PHB laden cell mixture can be stored in a refrigerator for up to one week before PHB extraction and purification analysis. Finally, the students can perform the PHB extraction and

purification in a single four hour session or two-two hour sessions.

Coagulant Methods Aid Removal of PHB-Laden Cells from the Culture Media. Chang and coworkers have developed methodology, which more efficiently separates the bacterial cells of *C. necator* from the fermentation broth by employing Al- and Fe-based coagulants. Bacterial cells are typically removed from culture broth via centrifugation or filtration; however, the very small particle size of *C. necator* bacterial cultures results in very low sedimentation rates (254). Fe- and Al-based coagulants utilized by Chang and coworkers (254) effectively increase particle sizes thus increasing sedimentation rates and facilitating removal of cellular material from the fermentation broths (254). Indeed, the energy demand decreased by 89-97% when coagulation methodology was employed (255). Further analyses revealed that coagulant based methodology coupled with PHB extraction via chemical digestion with sodium hypochlorite/chloroform generated PHB with 90-94% recoveries and 98-99% purities (255). Chang and coworkers (255) note that Al-based coagulants are more advantageous than the Fe-based counterparts since these were observed to colorize the final product (255). While these methodologies are ideal for implementation in industrial processes, this strategy seemed excessive for a small-scale student laboratory and was not utilized herein.

Extraction of PHB.

Solvent Extraction. Historically, the majority of PHB purifications employ a solvent, such as chloroform, to extract the PHB granules from inside the bacterial cell (255-259). These methods typically require pretreatment of the cell mass via milling or grinding, and spray-, freeze-, or oven-drying of the bacterial mixture, which increases the solvent extractability. Since these methods typically require a lengthy drying processes followed by a long, typically 24 hour, extraction period this methodology is not conducive to being performed in a hands-on student laboratory.

Extraction via Enzymatic Digestion. Zeneca (formerly ICI) developed an enzymatic digestion method for purifying PHB (255-257,260,261). This technique involved the thermal treatment of PHB-laden bacterial cells followed by enzymatic digestion and washing of the cells with an anionic surfactant and possibly EDTA. This solublized the non-PHB cellular material and thereby purified the PHB. Specialty reagents used in this technique (such as proteases) increase extraction costs and require careful treatment of the cells; therefore, this technique was not chosen for the student laboratory.

Hypochlorite Extraction Methods. Other well known techniques involve the use of hypochlorite (261-263) or hypochlorite/chloroform dispersions (257) to purify PHB from the bacterial cell. In the hypochlorite/chloroform dispersion methodology, the hypochlorite serves to digest the non-polymer

cellular material, disrupt the cell, bleach the polymer, and reduce the solution viscosity. Likewise, the chloroform serves to extract and purify the PHB and it protects the PHB molecules from the hypochlorite (257,259). Treatment with hypochlorite can cause severe degradation of the PHB; therefore, hypochlorite concentrations must be carefully controlled to produce PHB of good quality. The hypochlorite techniques were not selected in order to avoid possible PHB degradation during the student laboratory; this ensured that students would have high molecular weight PHB with good polydispersity for future analyses.

Extraction of PHB from E. coli with NaOH. In 1999, Choi and Lee (256) developed and optimized a method for recovering PHB from genetically engineered *E. coli* cells. This technique took advantage of the fragility of the *E. coli* bacterial cell. The authors treated the cells with 0.2 N NaOH at 30° C for one hour and recovered PHB with a purity of 98.5%. PHB recovered with this method cost only US$ 3.66/Kg of PHB, which was approximately 25% cheaper than PHB recovered with the surfactant-hypochlorite digestion method. *E. coli* engineered to express the PHB generating enzymes from *C. necator* is not commercially available and the applicability of this method to *C. necator* bacteria is currently unknown so this method was not further investigated for the student laboratory (256).

Detergent Extraction. Chang and coworkers (264) developed a simple and effective method for recovering PHB from *C. necator* cells, which employed direct addition of a detergent, SDS, to the

culture broth; this dissolved the non-PHB cellular material which allowed recovery of a PHB pellet by centrifugation. Using this method the authors observed purities as high as 97% when SDS/Biomass ratios were greater than 0.4. This technique required addition of SDS to the culture broth, followed by shaking for one hour, heat treatment via autoclave, and washing/centrifugation (264). PHB granules have strong associations with the proteins that physically surround the granule so the authors found that the autoclaving treatment was necessary to facilitate protein removal from the PHB (264). This methodology was adapted for use in the student laboratory.

Techniques Used in This Student Laboratory. The purpose of this student laboratory (detailed in Appendix 2) is to familiarize the student with the production of PHB using *C. necator*, and to provide a biopolymer sample that can be characterized and compared with other types of polymers. The methodology developed by Chang and coworkers (264) was modified for use in this student laboratory. SDS concentrations were adjusted to optimize PHB extraction. EDTA was added to the cellular mixture to aid in cell lysis and because it helped to chelate heavy metals; this generated a product with less coloration. The PHB bacterial cells were pelleted via centrifugation prior to detergent addition in order to optimize extraction of PHB under our laboratory conditions. The autoclaving step was made optional (although autoclaving the

solution generates the highest quality product) and was replaced with a boiling step for student laboratories lacking large-scale autoclave equipment. The detergent shaking step and the autoclaving/boiling steps were shortened to facilitate completion within a single laboratory period. Finally, a chloroform purification and methanol precipitation procedure was developed in order to remove remaining non-PHB cellular material and to provide the students with high quality chloroform soluble PHB for future analyses.

AN EXPLORATION OF BIOCHEMISTRY INCLUDING BIOTECHNOLOGY, STRUCTURAL CHARACTERIZATION, DRUG DESIGN, AND CHROMATOGRAPHIC ANALYSES

VOLUME II

By

Kristi Lee Burns

CHAPTER 6

ISO-COENZYME A: INTRODUCTION

Iso-coenzyme A. Iso-coenzyme A (iso-CoA) is an isomer of coenzyme A (CoA) in which the monophosphate is attached to the 2′-carbon of the ribose ring. Iso-CoA was first reported in 1959 by Khorana and coworkers (265,266) to be a byproduct of the chemical synthesis of CoA. The final step of this synthesis entailed acid-catalyzed hydrolysis of cyclic-coenzyme A (Figure 21), to produce a 50:50 mixture of two products which were separated using ECTEOLA-cellulose ion exchange chromatography (265,266). Direct structural analysis was not readily available in 1959; consequently, the authors deduced the structure of iso-CoA by establishing that, in contrast to CoA, iso-CoA was not a substrate for the enzyme phosphotransacetylase (265,266). Khorana and coworkers also used paper chromatography of phosphodiesterase hydrolysates to show that enzymatic hydrolysis of iso-CoA produces adenosine-2′,5′-diphosphate, exclusively (265,266).

The position of the phosphate on the nucleotide diphosphates, which were used as standards by Khorana and coworkers, was originally determined by Cohn and coworkers (267). These authors used a clever an ion-exchange technique, which exploited borate's ability to complex with cis-α-glycols,

exclusively. Ribose 3′-phosphate, unlike ribose 2′-phosphate, contains a cis-α-glycol moiety; this forms a complex with borate, which generates a different ion-exchange elution profile than does ribose 2′-phosphate.

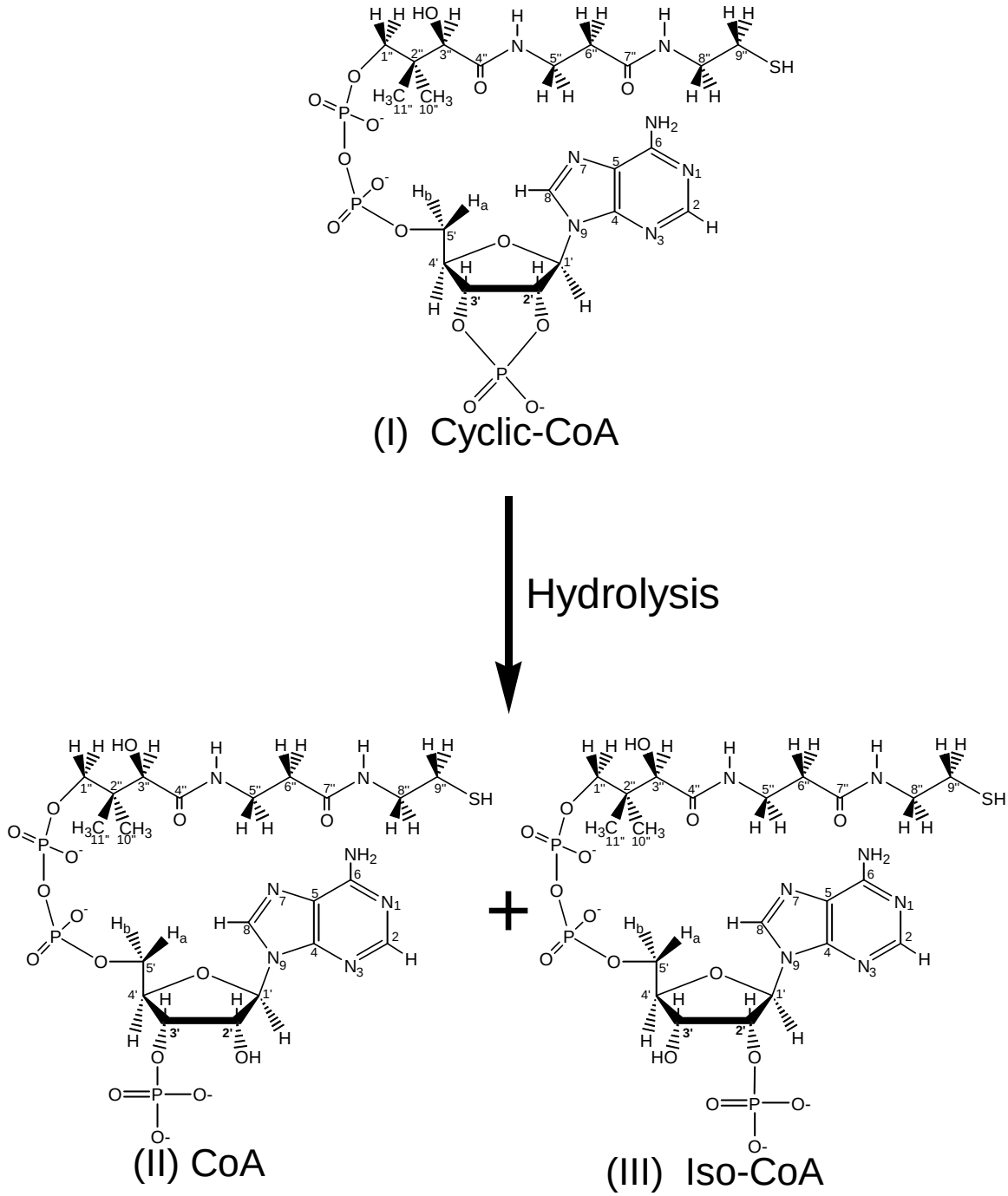

Figure 21. Final Step in the Total Synthesis of Iso-CoA. Chemical hydrolysis of cyclic-CoA (I) produces two products, CoA (II) and Iso-CoA (III). Carbons are labeled according to d'Ordine *et al* (268).

The History of Coenzyme A. In 1963, the Nobel foundation awarded its coveted prize to Fritz Lipmann (269) for 'the discovery of Coenzyme A and its importance for intermediary metabolism'. While Lipmann certainly played a pivotal role in this seminal research, elucidation of the structure of Coenyzme A, shown in Figure 22, was determined through years of methodical research by teams of scientists who painstakingly identified each individual portion of the CoA structure (269-279). Lipmann's discovery of CoA dates back to a 1945 publication (270,271) which was the first mechanistic account demonstrating acetylation of sulfanilamide *in vitro* with pigeon liver extracts; this was in contrast to other studies carried out in perfused organs, on intact animals, or *in vitro* with rabbit liver slices.

Determination of the Structure of CoA. The initial advance towards determining the structure of CoA, shown in Figure 22, was provided in 1947 by Dr. Beverly Guirard of Dr Roger William's laboratory who detected pantothenic acid upon prolonged enzymatic treatment of CoA, and β-alanine after acid hydrolysis of CoA extracts (272). By 1950, Novelli and Kaplan, of Lipmann's laboratory, had reported that CoA preparations contained large quantities of adenylic acid (273)—the A in CoA stands for adenylic acid—and identified the pyrophosphate bridge (274). Additionally, Snell and coworkers (275) determined that the sulfur-containing moiety that was detected in CoA was thioethanolamine linked in a peptide bond to pantothenic acid.

The following year, Baddiley and Thain (276) identified the 5'-adenylic acid moiety though chemical cleavage and further honed in on the CoA structure by determining that the pyrophosphate bridge attached at the 4-position of pantothenic acid. The year 1952 brought an initial account, by Wang, Shuster and Kaplan (277), placing the CoA monophosphate on the 3'-carbon of the adenosine ribose moiety (278,279). Finally, in 1953 Novelli (now at Case Western) completed the structural analysis of CoA by presenting the enzymatic synthesis of CoA (270,280).

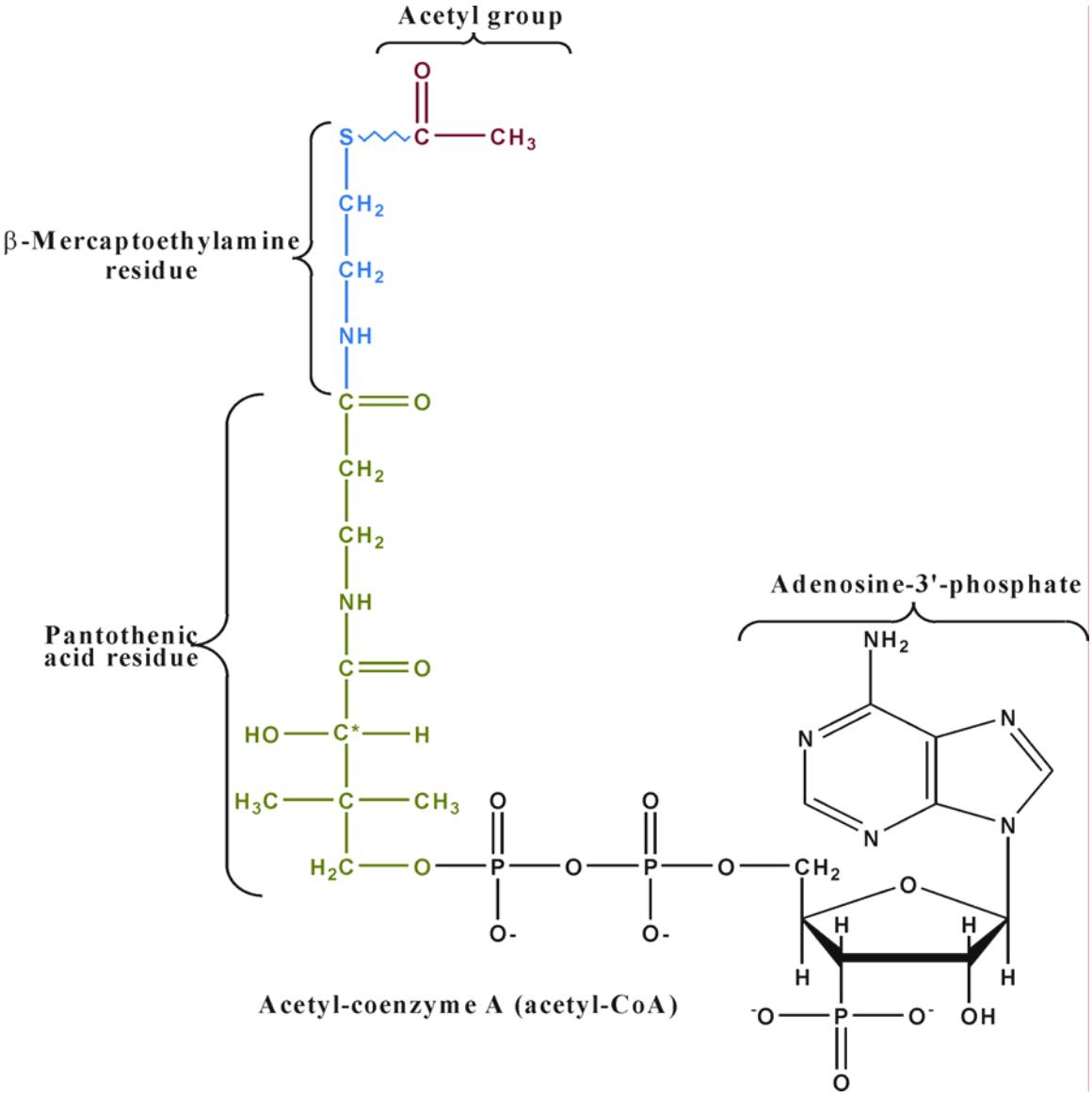

Figure 22. Chemical Structure of Acetyl-Coenzyme A (281).

Chemical Syntheses of CoA. Since Khorana's original work, four additional chemical syntheses of CoA have been reported (282-287), and as summarized in Table 13, in each of these syntheses the free 3'-phosphate group is protected by forming a 2',3'-cyclic moiety. In Khorana's *the Total Synthesis of Coenzyme A* (265,266), 2',3'-cyclic-CoA was produced by the formation of a adenosine-2',3' cyclic phosphate-5'-phosphormorpholidate and D-panetheine-4' phosphate to produce 2',3'-cyclic-CoA. In 1972, Hashimoto and Mukaiyama (286) optimized Khorana's method by utilizing the coupling agents triphenylphosphine and 2,2'-dipyridyl disulfide to produce the key intermediates in high yields. Michelson's (282,283) 1964 synthesis used P^1-adenosine (2', 3'-cyclic phosphate)-5'-P^2-diphenylpyrophosphate and pantethine 4',4'-*bis*-phosphate in pyridine to produce the 2', 3'-cyclic-CoA product. Shimizu *et al.* (284,285) synthesized CoA by generating an intermediate containing a thiazoline moiety on the pantothenate arm; acid catalyzed hydrolysis of the thiazoline moiety then generated CoA. 2',3'-cyclic CoA was produced by Taguchi *et al.* (287), in 1976, by reacting adenosine-5' 2-dimethylamino-4-nitrophenyl phosphate with D-pantethine-4',4"-diphosphate in the presence of acetic acid in pyridine. A key intermediate in each of these syntheses is a 2', 3'-cyclic moiety which is then hydrolyzed either chemically, to produce CoA and iso-CoA (265,266,283-285,287), or enzymatically using the regioselective enzyme ribonuclease T2,

which Michelson (282,283) first used to produce CoA from cyclic CoA (282-286).

Table 13. Chemical Syntheses of CoA and Iso-CoA.

Author and Date	***Acid-Catalyzed Hydrolysis[a]***	***Enzyme-Catalyzed Hydrolysis[b]***
	Comments	
	Key reaction intermediates for forming cyclic-CoA or CoA	
Khorana 1959	Yes	No
1961	Yes	No
(265,266)	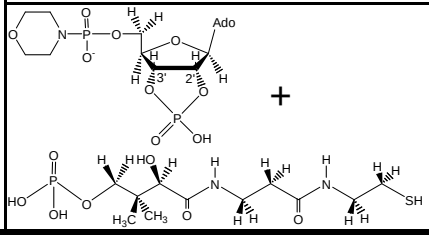	
Hashimoto 1972 (286)	No	Yes
	Optimized Khorana's synthesis using oxidation reduction condensation coupling agents	
Michelson 1961	No	Yes
1964	Yes	Yes
(282,283)	First enzymatic hydrolysis of cyclic-CoA 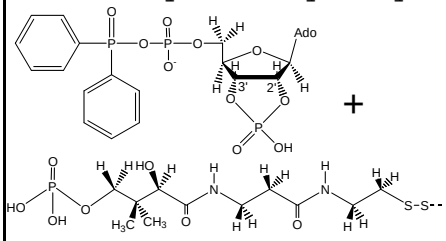	

Table 13 Continued

Shimizu 1965 1967 (284,285)	*Yes* Yes	*Yes* Yes
	adenosine-2′,3′-cyclic phosphate compound is enzymatically hydrolyzed by ribonuclease T_2 prior to reaction with cysteamine to give the thiazoline moiety on the pantothenate arm, which is then hydrolyzed to afford CoA	
	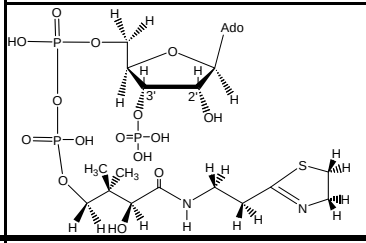	
Taguchi 1976 (284,285)	Yes	No
	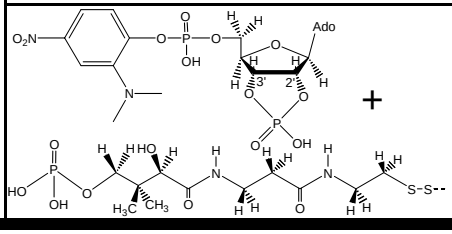	

[a]Acid-catalyzed hydrolysis produces an equilibrium mixture of the 2′- and 3′-phosphate isomers.
[b]Enzyme-catalyzed (Ribonuclease T2) hydrolysis regioselectively generates the 3′- isomer.

Characterizations of Iso-CoA Analogues and Derivatives. No full structural characterization of iso-CoA has ever been reported in the literature. Nevertheless, there exist literature reports of synthetic CoA and iso-CoA analogues, some of which have been characterized using techniques including 1D-NMR and MS. In this regard, Retey and coworkers have synthesized several carba(dethia)-CoA (or CH_2-CoA) analogs (288-295), in which the sulfur of CoA is replaced by a methylene, as mixtures of the 2′- and 3′-phosphate isomers. Retey and coworkers synthesized an isomeric mixture of the 2′- and 3′-isomers of propionyl-CH_2-CoA (288,289,295), partially purified the isomers with DE-32 cellulose chromatography using a LiCl gradient. Their analysis by ^{1}H-NMR and ^{31}P-NMR of the HPLC-purified isomers indicated that approximately 9% of the 2′-isomer remained.

In a subsequent publication, the authors synthesized an isomeric mixture of propionyl-dethia-(dicarba)-CoA (propionyl-CH2CH2-CoA), purified the isomers to approximately 91% and reported ^{1}H-NMR, ^{31}P-NMR, and FAB-MS for the CoA isomer only. In a similar paper, Brendelberger and Retey synthesized an isomeric mixture of isobutyryl-CH_2-CoA (291,292); the ^{1}H-NMR spectra of the ion-exchange-purified 3′-isomer indicated that approximately 15% of the 2′-phospho-CH_2-CoA isomer remained after chromatographic purification. These isobutanoyl-2′- and 3′-isomers were purified to homogeneity in a later publication (293) via repeated DEAE-cellulose chromatography and then the pure isomers were characterized by ^{1}H-NMR and ^{31}P-NMR. Wagner and Retey (294)

synthesized an isomeric mixture of myristoyl-CH_2-CoA and successfully purified each isomer to homogeneity using an extremely lengthy RP-HPLC method; then the HPLC-purified isomers were characterized by ^{1}H-NMR, ^{31}P-NMR, and FAB-MS. Finally, Retey and coworkers (290) synthesized propionyl-CoA and briefly reported that the compound was not contaminated with the 2′-phosphate isomer as demonstrated by the presence of only one anomeric ^{1}H-NMR peak. Stewart, Wieland and coworkers (296-299) also synthesized equilibrium mixtures of the CH_2-CoA analogues, acetonyl-CH_2-CoA and heptadecan-2-onyl-CH_2-CoA; unfortunately, they were unable to separate the 2′- and 3′-phosphate isomers and the NMR spectra for heptadecan-2-onyl-CH_2-CoA could only be obtained with isomeric mixtures (297).

The few remaining synthetic analogs of CoA and iso-CoA reported in the literature were characterized using enzymatic activity assay and paper chromatography of enzyme digests, instead of NMR or MS, because, like iso-CoA, these compounds were synthesized before the ready availability of NMR and MS analyses. An isomeric mixture of benzoyl-seleno-CoA was first reported by Gunther and Mautner (300), who found that these benzoyl isomers could be separated with ECTEOLA Cl^- ion-exchange chromatography and homogenous preparations of seleno-CoA and seleno-iso-CoA were obtained following removal of the benzoyl group. Another derivative, oxy-CoA, which contains a hydroxyl group instead of the free thiol present in CoA, was synthesized by Stewart and

coworkers (301), and the isomers were purified to homogeneity by TEAE-cellulose column chromatography.

Recently, Minkler *et al.* (302) reported the identification of the 2′-phosphate isomer of malonyl-CoA in commercial samples (302). These authors obtained homogeneous samples of two peaks observed in the commercial sample of malonyl-CoA by RP-HPLC and analyzed each HPLC-purified isomer by UV, HPLC/MS/, HPLC-MS/MS and 1D-NMR. MS and MS/MS analyses indicated that both HPLC-purified samples exhibited identical $[M-H]^-$ quasi-molecular ions at m/z 852.2, an observation consistent with the presence of isomers of malonyl-CoA. Finally, the ^{1}H-NMR spectra of 2′,5′-ADP was found to be comparable to the spectra of the unknown HPLC-purified isomer; thus, the authors concluded that the unknown HPLC-purified sample was the 2′-phosphate isomer of malonyl-CoA, or malonyl-iso-CoA. This recent NMR, MS, and MS/MS analysis is the only literature account of a 2′-phosphate isomer of a naturally occurring CoA-containing compound published since Khorana's seminal iso-CoA paper; nevertheless, a complete structural characterization of iso-CoA has heretofore never been achieved.

The Enzymatic Activity of Iso-CoA-containing Compounds and Analogues. The issue of whether or not enzymes, which act upon CoA-containing substrates, discriminate between the 2′- and 3′-phosphate isomers is of obvious relevance to the design of new classes of inhibitors and pseudosubstrates. An extensive review

of the literature, summarized in Table 14, revealed that, prior to this study, only ten of the more than 350 CoA-utilizing enzymes have been assayed with the 2′-phosphate isomers of coenzyme A; moreover, eight of these enzymes were assayed with synthetic, non-natural, derivatives of CoA isomers and in only five of cases were purified isomer substrates used.

Enzymes that Reject Iso-CoA-containing Compounds. As previously discussed, in Khorana's early work the enzyme phosphotransacetylase was reported to be unreactive towards purified iso-CoA (265,266). The historic use of phosphotransacetylase for CoA quantitation has resulted in multiple publications that have provided solid evidence that this enzyme is strictly selective for 3′-phosphate-containing compounds. As Table 14 indicates, phosphotransacetylase is not inhibited by oxy-iso-CoA (301) or any adenosine compound containing a 2′-phosphate moiety (303). The significance of the phosphate moiety is highlighted by the discovery that 3′-pyrophospho-CoA exhibits two times the activity of CoA (304).

Other enzymes that do not accept 2′-phosphate compounds have been reported by Retey and coworkers (288,289). The authors report that methylmalonyl-CoA pyruvate carboxylase distinguishes between the isomers, reacting exclusively with propionyl-CH_2-CoA (288,289), and FAD-dependent isobutanoyl-CoA dehydrogenase is reactive with isobutanoyl-CH_2-CoA but not with the iso-CoA analog (293). We note that, while the publications by Retey and coworker used partially purified isomers, they do not show any

data supporting their contention that the 2'-phosphate isomers are not inhibitors.

Enzymes that Accept Iso-CoA-Containing Compounds. Other enzymes appear to accept the 2'-phosphate isomers as inhibitors or substrates. Wagner *et al.* (294) have reported that both HPLC-purified myristoyl-CH_2-CoA and myristoyl-CH_2-iso-CoA competitively inhibit N-myristoyltransferase, and Rossier (305) reported that choline acetyltransferase is inhibited by ion-exchange-purified samples of both seleno-CoA and seleno-iso-CoA, although in both cases the iso-CoA analogs are somewhat less potent. Thorpe *et al*. (298) reported that substrate mixtures containing both CH_2-iso-CoA and CH_2-CoA derivatives are utilized by the general acyl-CoA dehydrogenate to reduce enzyme bound FAD. No significant difference in FAD reduction was observed when different isomer ratios were assayed (i.e. isomeric ratios of 1:1 vs. 65:45) suggesting that acyl-CoA dehydrogenase does not discriminate between the isomers.

In the cases of citrate synthase and carnitine palmitoyltransferase, Ciardelli *et al.* (297) argue that these enzymes do not discriminate between isomers. Unfortunately, the authors draw this conclusion by kinetically comparing S-heptadecyl-CoA, a thioether analog of CoA, to an isomeric mixture of heptadecanoyl-CH2-CoA; the structure of these inhibitors is simply too disparate to draw a clear conclusion from the data. Nikawa *et al.* (299) examined acetyl-CoA carboxylase and fatty acid synthase with isomeric mixtures of acetonyl-CH_2-CoA and

acetonyl-CH_2-iso-CoA, but these isomers were not purified so no conclusion regarding enzyme specificity for phosphate position is possible. Clearly, this issue needs to be reexamined for many of the CoA-utilizing enzymes using purified and fully characterized iso-CoA substrate analogues.

Table 14. Selectivity of Enzymes Examined for 2′- vs. 3′- Phosphate Activity.

Enzyme/Reaction Compound	***R***	***2′***	***3′***	***Pure Y/N***	***Substrate (K_M)***	***Inhibitor (K_I)***
Accepts 2′-phosphate isomers as substrates						
Accepts 2′-phosphate isomers as inhibitors						
Rejects 2′-phosphate isomers as substrates						
Rejects 2′-phosphate isomers as inhibitors						
Specificity unclear						
[E.C. 1.1.1.36] Acetoacetyl-CoA Reductase (222)						
Acetoacetyl-CoA + NADPH ⇌ β-hydroxybutyryl-CoA + $NADP^+$						
Accepts 2′-isomers as substrates with equal affinity. Isomers were run together in the same assay but were quantitated separately by HPLC.						
Acetoacetyl-CoA	AcAcS	H	P	No†	Yes	---
Acetoacetyl-iso-CoA	AcAcS	P	H	No†	Yes	---
β-hydroxybutyryl-CoA	HBS	H	P	No†	Yes	---
β-hydroxybutyryl-iso-CoA	HBS	H	P	No†	Yes	---
[E.C. 1.3.99.3] AcCoA Dehydrogenase (298,306)						
Acetyl-CoA + FAD ⇌ D2-trans-enoyl-CoA + CoA + $FADH_2$						
Accepts 2′-isomer as an inhibitor (in isomeric mixture). Different isomer ratios exhibited the same K_M′s this enzyme putatively does not discriminate between isomers.						
Heptadecan-2-only-CH_2-CoA	HpCH_2	Mix 1:1		No	Yes(58% of palmitoyl-CoA)†	---
Heptadecan-2-onyl-CH_2-CoA	HpCH_2	Mix 65:45		No	Yes†	---
S-heptadecyl-CoA	-S-	H	P	Yes	No	K_d = 17nM; K_I < 40 nM Competitive
Octanoyl-CoA	OcS	H	P	Yes	2.21 μM	---
Octanoyl-dephospho-CoA	OcS	H	H	Yes	1.09 μM	---
[E.C. 1.3.99.12] FAD-dependent isobutanoyl-CoA Dehydrogenase (293)						
Isobutanoyl-CoA + FAD ⇌ Methacrylyl-CoA + $FADH_2$						
Rejects 2′-phosphate isomer as a substrate						

Table 14 Continued

Isobutanoyl-CH_2-CoA	*IsoCH_2*	*H*	*P*	*Yes*	*Yes*	---
Isobutanoyl-CH_2-iso-CoA	IsoCH_2	P	H	Yes	No	---

[E.C. 2.1.3.1] Methylmalonyl-CoA pyruvate carboxylase (transcarboxylase) (288,289)

Propionyl-CoA + oxaloacetate ⇌ Methylmalonyl-CoA + pyruvate

Rejects 2′-phosphate isomers as a substrate. Good example with fully purified isomers

Propionyl-CH_2-CoA	PrCH_2	H	P	Yes	Yes	---
Propionyl-CH_2-iso-CoA	PrCH_2	P	H	Yes	No	---

[E.C. 2.3.1.5] Arylamine N-acetyltransferase (300)

4-aminoazobenzene + ATP ⇌ 4-acetamidoazobenzene + ADP

Accepts 2′-phosphate isomer as a substrate.*
***Reference does not name this enzyme; thus, this is not considered a valid case.**

CoA	SH	H	P	Yes[a]	Yes[††]	---
Iso-CoA	SH	P	H	Yes[a]	Yes (slight)	---
Se-CoA	SeH	H	P	Yes[b]	Yes	---
Se-Iso-CoA	SeH	P	H	Yes[b]	No	---
Dephospho-CoA	SH	H	H	---	Yes	---
dephospho-Se-CoA	SeH	H	H	---	Yes	---

[E.C. 2.3.1.6] Choline Acetyltransferase (305,307,308)

Choline + Acetyl-CoA ⇌ CoA + Acetyl-Choline

Accepts 2′-phosphate isomer as an inhibitor: Se-CoA has a 3.5 x better K_I than Se-iso-CoA

CoA	SH	H	P	?[d]	0.25 µM (3.8)	1.8 µM w.r.t. to AcCoA Competitive
Se-CoA	SeH	H	P	Yes[b]	---	7 µM Competitive
Se-iso-CoA	SeH	P	H	Yes[b]	---	25 µM Competitive
dephospho-CoA	SH	H	H	?[d]	27 µM (39)	500 µM Competitive
dephospho-Se-CoA	SeH	H	H	Yes	---	700 µM Competitive
Ado-3′-P-5′-P	---	H	P	?[d]	---	415 µM Competitive
Ado-2′-P-5′-P	---	P	H	?[d]	---	2200 µM Competitive
Ado-5′-P	---	H	H	?[d]	---	2500 µM Competitive

Table 14 Continued

Acetyl-CoA	*AcS*	*H*	*P*	*Yes*	*25.7 μM*	*Yes*
Acetyl-dephospho-CoA	AcS	H	H	Yes	54.8 μM	Yes
Acetylcholine	---	-	-	---	400 μM (0.9)	

Rejects 2′-phosphate compounds as substrates

Rejects 2′-phosphate compounds as inhibitors

CoA	SH	H	P	Yes[a]	Yes	No
Iso-CoA	SH	P	H	Yes[a]	No	No
Se-CoA	SeH	H	P	Yes[b]	No	No
Oxy-CoA	OH	H	P	Yes[c]	No	0.35 μM Competitive
Isomeric Mix of Oxy-CoA	OH	Mix		No	No	0.6 μM
Oxy-iso-CoA	OH	P	H	Yes[c]	No	No only 0.5 % of oxy-CoA
Dephospho-CoA	SH	H	H	---	0.5% CoA	---
Dephospho-CoA	SH	H	H	---	10% of CoA	--- *Lactobacillus fermenti* only
3′-pyrophospho-CoA	SH	PP	H	---	2x CoA	--- (also from *C. kluyveri*,
CoA-SS-CoA	SCoA	H	P	---	No	--- *L. mesenteroides*, *E. coli*)

	Inhibition Rate Percent (%)	
	E. coli	*Cl. kluyveri*
Ado-3′-P-5′-PP	62	33
Ado-2′-P-5′-PP	5	5
Ado-3′-P-5′-PP-CH_3	33	22
Ado-2′-P-5′-PP-CH_3	0	2
Ado-5′-P	2	0
Ado-3′-P	0	0
ADP	48	0
ATP	37	0
Ado-3′-P-5′-P	36	2
Ado-3′-P-5′-PP-$CH_2CH(CH_3)_2$	81	43

[E.C. 2.3.1.16] β-ketothiolase (222)

2 Acetyl-CoA ⇌ Acetoacetyl-CoA + CoA

Table 14 Continued

Accepts 2′-phosphate isomers as substrates with equal facility. Isomers were run together in the same assay but were quantitated separately by HPLC.						
CoA	SH	H	P	No†	Yes	---
Iso-CoA	SH	P	H	No†	Yes	---
Acetyl-CoA	AcS	H	P	No†	Yes	---
Acetyl-iso-CoA	AcS	P	H	No†	Yes	---
Acetoacetyl-CoA	AcAcS	H	P	No†	Yes	---
Acetoacetyl-iso-CoA	AcAcS	P	H	No†	Yes	---
[E.C. 2.3.1.21] Carnitine Palmitoyltransferase (297)						
Palmitoyl-CoA + carnitine ⇌ palmitoylcarnitine + CoA						
Specificity is unclear. Isomeric mixture inhibits and authors propose that the enzyme doesn't discriminate but further experiments are warranted.						
Heptadecan-2-onyl-CH_2-CoA	HepCH_2	Mix		No	---	1.35 μM (@ <30 μM P-CoA) competitive
S-heptadecyl-CoA	HepS	H	P	Yes	---	3.34 μM (@ <30 μM P-CoA) competitive
[E.C. 2.3.1.85] Fatty acid Synthase (299,309,310)						
acetyl-CoA + n malonyl-CoA + 2nNADPH + 2nH^+ ⇌ long-chain fatty acid + (n+1)CoA + nCO2 + 2n $NADP^+$						
Specificity is unclear. Isomeric mixture inhibits and authors propose that the enzyme doesn't discriminate but further experiments are warranted.						
Acetonyl-CH_2-CoA + iso	AcCH_2	Mix		No	---	No
Ado-2′-P	---	P	H	Yes	---	Prevents inactivation
Ado-3′-P	---	H	P	Yes	---	No protection
CoA	SH	H	P	---	---	Increase inactivation rate (stops inhibition)
Dephospho-CoA	SH	H	H	---	---	Increase inactivation rate (stops inhibition)
[E.C. 2.3.1.97] N-myristoyltransferase (294,311)						
Octapeptide + myristoyl-CoA ⇌ myristoyl-peptide + CoA						
Accepts 2′-isomers as inhibitors. 3′-phosphate isomer has a 6.7 x better K_I than the 2′-isomer. This is a clear example using fully purified isomers.						

Table 14 Continued

Myristoyl-CH_2-CoA	*MyrCH_2*	*H*	*P*	*Yes*[e]	---		*0.3 μM competitive*
Myristoyl-CH_2-iso-CoA	MyrCH_2	P	H	Yes[e]	---		2 μM competitive
					K_d (nM)	% Act	
Lauryl-CoA	LryS	P	H		62	44%	
Lauryl-dephospho-CoA	LryS	H	H		8380	21%	
Myristoyl-CoA	MyrS	P	H		15	100%	
Myristoyl-dephospho-CoA	MyrS	H	H		124	73%	
Palmitoyl-CoA	PalmS	P	H		26	1.6%	
Palmitoyl-dephopho-CoA	PalmS	H	H		232	4%	

[E.C. 2.3.3.1] Citrate Synthase (296,297,312,313)

Oxaloacetate + Acetyl-CoA ⇌ CoA + Citrate

Specificity is unclear. Isomeric mixture inhibits and the authors propose that the enzyme does not discriminate between isomers based on the results with S-heptadecyl-CoA but further experiments are warranted.

Acetonyl-CH_2-CoA + Iso	AcCH_2	Mix		No	---	13.2 μM Competitive
Heptadecan-2-onyl-CH_2-CoA	HepCH_2	Mix 1:1		No	---	6-7.5 μM; 3.7 μM is ≈ to Palmitoyl-CoA @ 4.1 μM; Noncompetitive
S-heptadecyl-CoA	HepS	H	P	Yes	---	1-1.5 μM; 1.2 μM is ≈ to Palmitoyl-CoA @ 4.1 μM; Noncompetitive
110 μM CoA	SH	H	P	Yes	---	109% activity after 10 min
130 μM dephospho-CoA	SH	H	H	Yes	---	110% activity after 10 min
Acetyl CoA	AcS	H	P	Yes	4×10^{-4}	---
Acetyl-dephospho-CoA	AcS	H	H	Yes	1/3 of Acetyl-CoA	---

[E.C. 6.4.1.2] Acetyl-CoA Carboxylase (299,314)

ATP + Acetyl-CoA + HCO_3^- ⇌ ADP + P_i + Malonyl-CoA

Specificity is unclear. Isomeric mixture inhibits but experiments with purified isomers were not performed.

Acetonyl-CH_2-CoA + iso	AcCH_2	Mix	No	96 μM	---

Table 14 Continued

Acetyl-CoA	*AcS*	*H*	*P*	*Yes*	*Yes*	---
Acetyl-dephospho-CoA	AcS	H	H	Yes	Yes ≈Acetyl-CoA	---

[E.C. Not Currently Classified] PHB Synthase (222)

β-hydroxybutyryl-CoA ⇌ PHB + CoA

Accepts 2′-phosphate isomers as substrates with equal facility. Isomers were run together in the same assay but were quantitated separately by HPLC.

β-hydroxybutyryl- CoA	HBS	H	P	No[†]	Yes	---
β-hydroxybutyryl-iso-CoA	HBS	P	H	No[†]	Yes	---
CoA	SH	P	H	No[†]	Yes (Product)	---
iso-CoA	SH	P	H	No[†]	Yes (Product)	---

[†] These compounds were not purified prior to enzymatic analysis but the reaction was monitored by HPLC and the isomers were well resolved by HPLC; thus, the result of isomer specificity with these enzymes is clear.

Herein we report the first structural characterizations of iso-CoA, acetyl-iso-CoA, acetoacetyl-iso-CoA, and β-hydroxybutyryl-iso-CoA. All previous characterizations of the structure of iso-CoA have been based on chromatographic analyses (265,266), which ultimately rest on comparisons with the degradation products of CoA and NADPH (267,277,315), or have been based on assumptions regarding enzyme specificity (284,285,287). We describe HPLC methodology to separate the isomers of several CoA-containing compounds, and the characterization of iso-CoA structures using MS, MS/MS, and NMR analyses. Our experiments reveal the existence of up to 18% of the 2'-phosphate isomer in commercial preparations of several CoA-containing compounds, which are listed as having purities of 90-99%. We also report here the first examples of iso-CoA-containing compounds acting as substrates in enzymatic acyl-transfer reactions. Finally, we describe a simple synthesis of iso-CoA from CoA, which utilizes β-cyclodextrin to produce iso-CoA with high regioselectivity, and we demonstrate a plausible mechanism, which accounts for the existence of iso-CoA isomers in commercial preparations of CoA-containing compounds.

CHAPTER 7

ISO-COENZYME A: EXPERIMENTAL

Materials. The lithium salts of CoA (93% purity) purified from yeast, acetyl-CoA (93% purity), β-hydroxybutyryl-CoA (99% purity), the sodium salt of acetoacetyl-CoA (90% purity), 1-ethyl-3-(3-dimethylaminopropyl) carbodiimide (EDC), β-cyclodextrin and tetrabutyl ammonium hydrogen sulfate (TBAHS) were purchased from Sigma (St. Louis, MO). Triscarboxyethyl phosphine (TCEP) was from Molecular Probes (Eugene, OR). All HPLC or Optima Grade solvents and all other compounds were obtained from Fisher Scientific.

HPLC Mass Spectrometry. Commercial CoA and acetyl-CoA standards were analyzed with a Micromass Quattro LC triple quadrupole tandem mass spectrometer equipped with an ESI source connected to an Hewlett-Packard series 1100 HPLC system. Resolution of the isomers was achieved with an Agilent Hypersil AA-ODS 2.3 x 200 mm column attached to a Phenomenex SecurityGuard™ (C18, 4 mm length x 3.0 mm I.D.), using an isocratic mobile phase of 96% 200 mM ammonium acetate pH 6.0: 4% acetonitrile at a flow rate of 0.2 mL/min. ESI mass spectra were obtained in the positive ion mode with nitrogen used as the nebulizer and desolvation gas at flow rates of approximately 80

and 580 L/h, respectively. The cone voltage was set to 50 V and the capillary voltage to 3.5 kV. Tandem mass spectrometry (MS/MS) using multiple reaction monitoring (MRM) was performed on the $(M+H)^+$ ions of the isomers of CoA (*m/z* 768), acetyl-coA (*m/z* 810), acetoacetyl-CoA (m/z 852), and β-hydroxybutyryl-CoA (m/z 854) using argon as the collision gas at a collision energy of 20 eV for the collision induced dissociation of the precursor ion. The commercial standards were monitored at the following transitions: CoA at *m/z's* 768→159, 768→261 and 768→428; acetyl-CoA at *m/z* 810→303 and *m/z* 810→428; acetoacetyl-CoA at m/z's 852→135, 852→243, 852→261, 852→345, and 852→428; β-hydroxybutyryl-CoA at m/z's 854→136, 854→245, 854→347 and 854→428.

Semi-Prep HPLC Purification of CoA and the Isomer. A 100 µL aliquot containing, at most, 3 mg of a commercial sample of CoA in 5 mM TCEP was injected onto an Allsphere ODS-2 semi-prep column, 250 mm x 10 mm I.D. with a Phenomenex SecurityGuard™ containing a C18, 4 mm length x 3.0 mm I.D., guard cartridge. Peaks were manually collected using isocratic elution with a mobile phase of 97.5% 200 mM ammonium acetate pH 6.0: 2.5% acetonitrile at a flow rate of 7 mL/min with detection at 261 nm. Lyophilization of the collected effluent provided chromatographically pure samples of CoA and the isomer.

High Resolution ESI MS of HPLC-Purified Samples. Exact Mass and MS/MS analyses were performed using HPLC-purified samples of CoA and the isomer on an Applied Biosystems QSTAR XL hybrid quadrupole-TOF LC/MS/MS mass spectrometer. The QSTAR XL was operated in the positive ion mode using a needle voltage of 5500 V. MS analysis was performed over a mass range of *m/z* 310-1500 and MS/MS spectra of the *m/z* 768 precursor ion were obtained over the mass range of m/z 50-800.

NMR Analysis. NMR spectra of iso-CoA were obtained in D_2O in a 5 mm sample tube on a Bruker DRX 500 spectrometer at 500.13 mHz for ^{1}H and 202.46 mHz for ^{31}P using an inverse triple resonance probe maintained at 298K. The COSY experiment was performed using the standard Bruker program cosyprqf, with presaturation during the 2 s relaxation delay on the HOD signal, 2048 data points in the F2 dimension and 128 increments in F1. The data matrix was processed to give a matrix of 1024 x 1024 points, and a sine-bell apodization function was applied before Fourier transformation.

The parameters for the two-dimensional heteronuclear multiple quantum correlation (^{1}H-^{31}P HMQC) experiment are as follows: hmqcqf standard Bruker program, 1.5 s recycle delay, 1024 data points in F2 and 128 increments in F1, 8 Hz coupling constant, GARP ^{31}P decoupling during acquisition; shifted sine-squared apodization before Fourier transform. The chemical shift assignments for the HPLC-purified CoA and iso-CoA are labeled

above their respective peaks in the proton spectra. The few unlabeled peaks were either due to the iso-CoA disulfide formed during purification and analysis, in the absence of reducing agents, or to an unknown impurity. Coupling constants were obtained through successive decoupling experiments, and the unresolved coupling constants were then obtained by simulating the spectra using the gNMR (316) and MestRe-C (317) software packages. ^{1}H-NMR analysis(500 MHz, 99.99% D_2O, reference to 4.67 ppm water peak) δ8.41 (s, 1, H_8), 8.18 (s, 1, H_2), 6.18 (d, 1, $H_{1'}$, $J_{1',2'}$ = 5.15 Hz), 4.98 (m, 1, $H_{2'}$, $J_{2',3'}$ = 5.09 Hz, $J_{2',P2'}$ = 8.69 Hz), 4.56 (t, 1, $H_{3'}$, $J_{3',4'}$ = 4.56 Hz), 4.32 (m, 1, $H_{4'}$, $J_{4',5a'}$ = 3.92 Hz, $J_{4',5b'}$ = 2.83 Hz, $J_{4',P5'}$ = 2.00 Hz), 4.18 (m, 1, $H_{5b'}$, $J_{5b',P5'}$ = 4.58 Hz), 4.13 (m, 1, $H_{5a'}$, $J_{5a',P5'}$ = 5.08 Hz, $J_{5a',5b'}$ = 11.63 Hz), 3.92 (s, 1, $H_{3''}$), 3.73 (dd, 1, $H_{1''}$, $J_{1'',1''}$ = 9.90 Hz, $J_{1'',P1''}$ = 5.09 Hz), 3.48 (dd, 1, $H_{1''}$, $J_{1'',P1''}$ = 4.83 Hz), 3.38 (t, 2, $H_{5''}$, $J_{5'',6''}$ = 6.53 Hz), 3.24 (t, 2, $H_{8''}$, $J_{8'',9''}$ = 6.59 Hz), 2.54 (t, 2, $H_{9''}$), 2.37 (t, 2, $H_{6''}$), 0.89 (s, 3, $H_{10''}$), 0.67 (s, 3, $H_{11''}$). ^{31}P-NMR analysis (202.46 MHz, 99.99% D20) δ -0.90 (s, 1, $P_{2'}$), -9.63 (d, 1, $P_{1''}$), -10.21 (d, 1, $P_{5'}$).

Analytical HPLC Procedure. HPLC analyses of CoA, acetyl-CoA, acetoacetyl-CoA and β-hydroxybutyryl-CoA and the isomers were performed on a Waters LC Module I Plus HPLC system with auto-injection of samples using the Millennium Chromatography Manager Software (Waters, Milford, MA, USA). A Waters NovaPak C_{18} Reverse Phase column, 4 μm particle size, 150 mm x 3.9 mm I.D.

was used with a Phenomenex SecurityGuard™ containing a C18, 4 mm length x 3.0 mm I.D., guard cartridge. Isocratic analyses were performed at a wavelength of 261 nm with a mobile phase containing 96% of 200 mM ammonium acetate pH 6.0: 4% acetonitrile at a flow rate of 1.0 mL/min. The mobile phase was premixed prior to sparging with helium gas and the column pre-equilibrated with mobile phase for at least one hour prior to sample analysis. Under these HPLC conditions, the retention times and purities are listed as follows: CoA, 4.25 min, 90%; iso-CoA, 5.5 min, 10%; acetyl-CoA, 12.75 min, 85%; acetyl-iso-CoA, 17.1 min, 15%; acetoacetyl-CoA, 14.5 min, 82%; acetoacetyl-iso-CoA, 19.5 min, 18%; β-hydroxybutyryl-CoA, 18.25 min, 97%; β-hydroxybutyryl-iso-CoA, 24.6 min, 3%.

Four different mobile phases adequately resolved the 2′- and 3′-phosphate isomers: 96% 200 mM sodium phosphate pH 5.5: 4% acetonitrile; 96% 150 mM sodium citrate pH 5.5: 4% acetonitrile; 96% 200 mM sodium acetate pH 5.5: 4% acetonitrile; 82% of 10 mM TBAHS in H_20 at pH 5.5: 18% Acetonitrile with 10 mM TBAHS. However, we note that the ion-pairing mobile phase, which contained TBAHS, reversed the isomer elution order such that the 3′-phosphate isomer eluted before the 2′-phosphate isomer. Additionally, isomers were resolved for each CoA-containing sample using four different RP-HPLC columns, and three different HPLC systems using both UV-Vis and MS detection. Freshly opened CoA-containing samples dissolved in water exhibited two peaks by HPLC, and HPLC-purified samples did not interconvert in deionized

water, at pH 3 or pH 11 (data not shown). Therefore, the 2'-phosphate isomer is a stable compound and this suggests that it was not generated accidentally in this laboratory.

Enzymatic analysis of Iso-CoA and Acyl-iso-CoA compounds. The enzymes β-ketothiolase (E.C. 2.3.1.16), acetoacetyl-CoA reductase (E.C. 1.1.1.36), and PHB synthase (E.C. currently not classified) which all utilize CoA-containing substrates were examined for the ability to react with the respective iso-CoA-containing analogs. Sequential enzymatic reactions were carried out in a solution of 16 μM acetyl-CoA isomers, 1.0 mM NADPH and 5 mM TCEP in 150 mM EPPS at a final of pH 7.8 and 37 C. The reaction was initiated by addition of 26.5 μL of β-ketothiolase, followed by 80 μL of acetoacetyl-CoA reductase at 3.5 min and finally 175 μL of PHB synthase at 10.5 min. In this manner β-ketothiolase condensed two molecules of acetyl-CoA liberating CoA and producing acetoacetyl-CoA for consumption by the acetoacetyl-CoA reductase, which formed the β-hydroxybutyryl-CoA for polymerization by the synthase enzyme to PHB, with liberation of CoA. Enzyme reactions were quenched at appropriate times with 0.27 M ice-cold perchloric acid followed by centrifugation prior to analysis with 50 μL injections by HPLC as described above.

Regioselective Synthesis of Iso-CoA (3)

CoA disulfide (CoASSCoA). HPLC-purified CoA (II), 10 mg (13 mM), was dissolved in 1 mL of 20 mM ammonium carbonate pH 8.5, reacted overnight at 37 C, and then lyophilized to produce CoA-disulfide with 100% yield by HPLC. The reaction progress was monitored via HPLC using the HPLC procedure described above except the mobile phase contained 6% acetonitrile.

Cyclic-CoA-disulfide. The CoA-disulfide lyophile was dissolved in 1 mL of 20 mM MES pH 6.0, 10 mg (52 mM) of 1-ethyl-3-(3-dimethylaminopropyl) carbodiimide (EDC) was added and the pH readjusted. Reaction progress was monitored by HPLC after rapidly reducing an aliquot of the disulfide to the free thiol with TCEP at pH 8.0 for 2 min. When the reaction was complete, the entire mixture was lyophilized. The lyophile was dissolved in 200 mM Ammonium Acetate pH 6.0 buffer and the entire solution applied to a 500 mg Supelco C8 solid phase extraction cartridge that was pre-equilibrated with the same buffer. Residual EDC and the urea byproduct were eluted from the cartridge with the equilibration buffer, and the cyclic-CoA-disulfide was eluted in ca. 5 mL with 90% 200 mM ammonium acetate pH 6.0: 10% acetonitrile. The cyclic-CoA-containing fractions were pooled and lyophilized.

Regioselective Synthesis of Iso-CoA (III). The cyclic-CoA-disulfide lyophile was dissolved in 160 mL of 0.05 mM bicarbonate buffer (I=0.01) pH 9.5 containing 3 M KCl and 15 mM β-cyclodextrin and the pH readjusted. The solution was stirred at 30^0C, with the pH maintained at 9.5, for approximately 5 days or

until the reaction was complete by HPLC, at which point the pH was adjusted to pH 3.0 to quench the reaction. This provided a final solution of iso-CoA with 92% regioselectivity by HPLC. Acetone precipitation and filtration served to remove some of the KCl and β-cyclodextrin from the iso-CoA-containing solution and permitted rotary evaporation followed by vacuum evaporation to dryness. Residual β-cyclodextrin was removed by repeated trituration with DMF and the remaining solid dried by washing with ethyl ether. The final solid was then dissolved in 200 mM ammonium acetate pH 6.0, the pH readjusted, and the solution desalted by passing through a 500 mg Supelco C8 solid phase extraction cartridge that was pre-equilibrated with 200 mM ammonium acetate pH 6.0. The desalted isomeric mixture of 92% iso-CoA: 8% CoA was eluted as previously described and the desalted mixture lyophilized. Final purification of iso-CoA was performed by dissolving the desalted lyophile in a minimal quantity of 5 mM TCEP in EPPS pH 8.0, to reduce the CoA-disulfide to the free thiol, subjected to semi-prep HPLC as previously described, and lyophilized.

Acid Catalyzed synthesis of Iso-CoA (III). HPLC-purified CoA (II), 1.6 mg, was dissolved in 0.5 mL of 0.5 M HCl, and the reaction monitored by HPLC at room temperature until equilibrium was reached; this generated a mixture of 60% CoA (II) and 40% iso-CoA (III). The identity of iso-CoA produced in this manner

was confirmed by NMR analysis after HPLC purification and lyophilization, as described previously.

CHAPTER 8

ISO-COENZYME A: RESULTS

Mass Spectrometric Structural Characterization of CoA and acetyl-CoA Samples. The HPLC-MS and HPLC-MS/MS chromatograms obtained for commercial CoA samples are shown in Figure 23. The left portion of panel A shows an HPLC-MS chromatogram of a commercial CoA sample, which exhibits 2 peaks with identical $(M+H)^+$ ions at *m/z* 768; this suggests that commercial CoA samples contain two compounds with identical masses. Therefore, HPLC-MS/MS experiments using multiple reaction monitoring (MRM) were carried out to garner further structural information. It is evident from the right portion of Panel A that the CoA samples exhibit two peaks for the MRM transitions *m/z* 768→159, *m/z* 768→261, and *m/z* 768→428. Thus, these HPLC-MS and HPLC-MS/MS results suggest the presence of isomeric compounds with virtually identical fragmentation patterns. To confirm these analyses, each peak in the commercial CoA sample was purified by preparative HPLC, and high resolution exact masses and MS/MS analyses were performed individually on each isomer. As shown in Figure 24, the two HPLC-purified samples exhibited identical exact masses $(M+H)^+$ of 768.1264 with an error of 5.09 ppm with respect to the calculated molecular mass of CoA. Additionally, the MS/MS (precursor ion *m/z* 768) spectra for the two HPLC-

purified samples depict nearly identical fragmentation patterns, which exhibit only minor variations in the relative populations of ions at *m/z* 136, *m/z* 159, and *m/z* 330.

These results unequivocally confirm the presence of isomeric forms of CoA in the commercial material, and the MS/MS results showing that these isomers exhibit virtually identical fragmentation patterns indicate that these isomers have extremely similar structures. HPLC-MS and HPLC-MS/MS experiments were also carried out with commercial acetyl-CoA, acetoacetyl-CoA, and β-hydroxybutyryl-CoA; likewise, these experiments revealed the presence of two isomeric compounds with identical $(M+H)^+$ ions, which exhibited identical fragments by HPLC-MS/MS using MRM at the observed transitions (Figures 25-27).

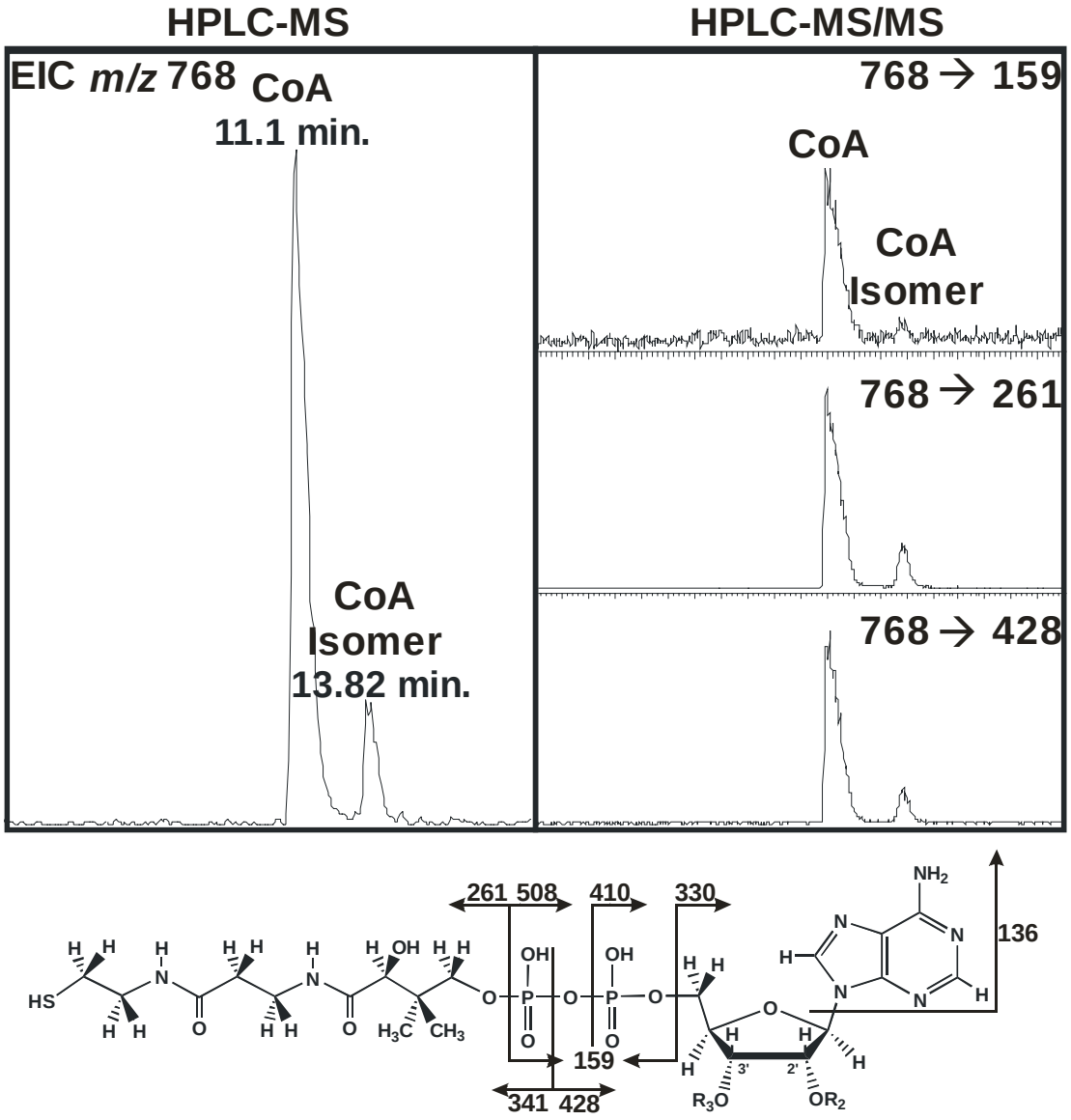

Figure 23. HPLC-MS and HPLC-MS/MS of Commercial CoA Sample. The HPLC-MS extracted ion chromatogram for a commercial CoA sample, shown in the left panel, exhibits two peaks with identical $(M+H)^+$ ions, *m/z* 768. The right panels show the HPLC-MS/MS chromatograms for the transitions *m/z* 768→159, *m/z* 768→261, and *m/z* 768→428. Subsequent NMR analysis established that the earlier-eluting compound, 11.1 min, is authentic CoA and the later-eluting compound, 13.8 min, is iso-CoA. The putative fragmentation patterns are indicated below.

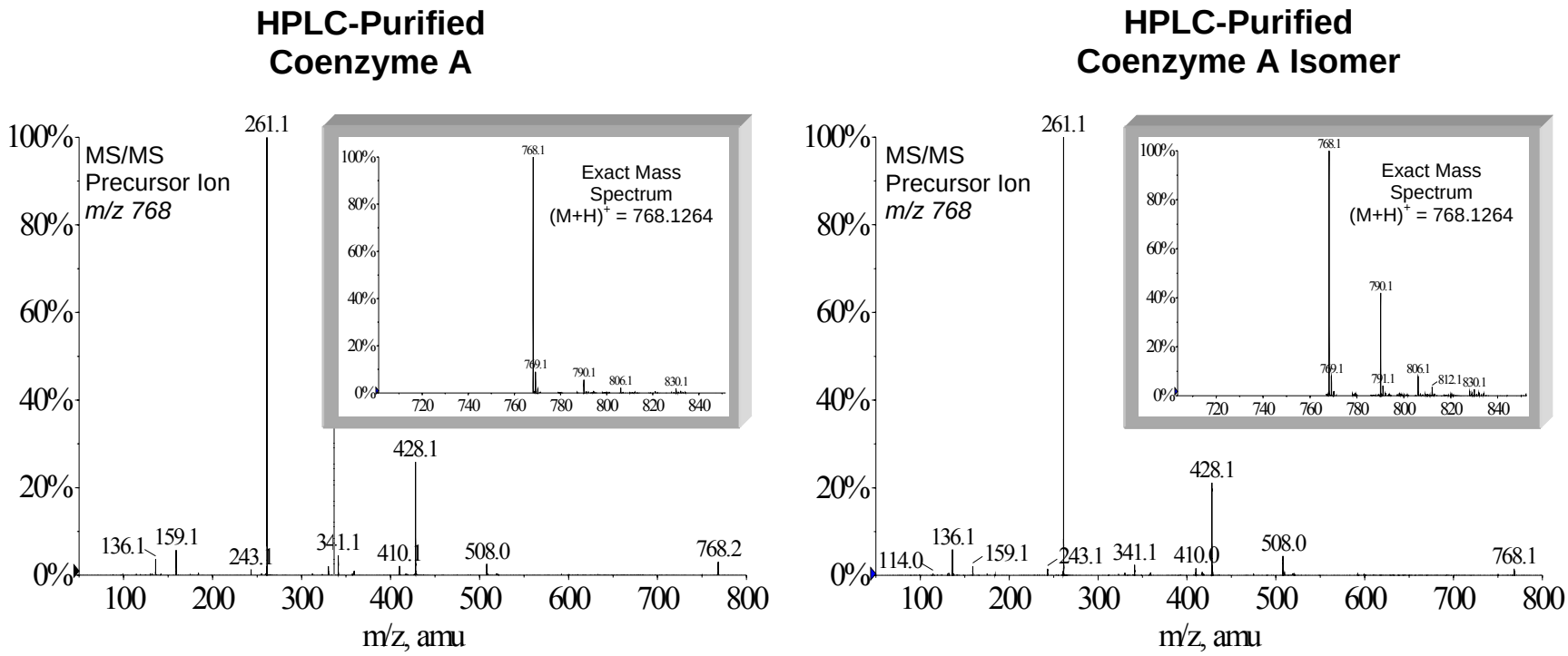

Figure 24. Exact Mass and MS/MS of CoA and Isomer Purified by HPLC from Commercial CoA. The commercial CoA sample was purified by preparative HPLC, and each peak was subjected to high resolution ESI-MS (Inserts) and MS/MS analyses. Authentic CoA is shown on the left and iso-CoA is depicted on the right. The inserts are the exact mass spectra for each HPLC-purified isomer, which exhibited an *m/z* 768.1264 with an error of 5.09 ppm with respect to the calculated molecular mass of CoA.

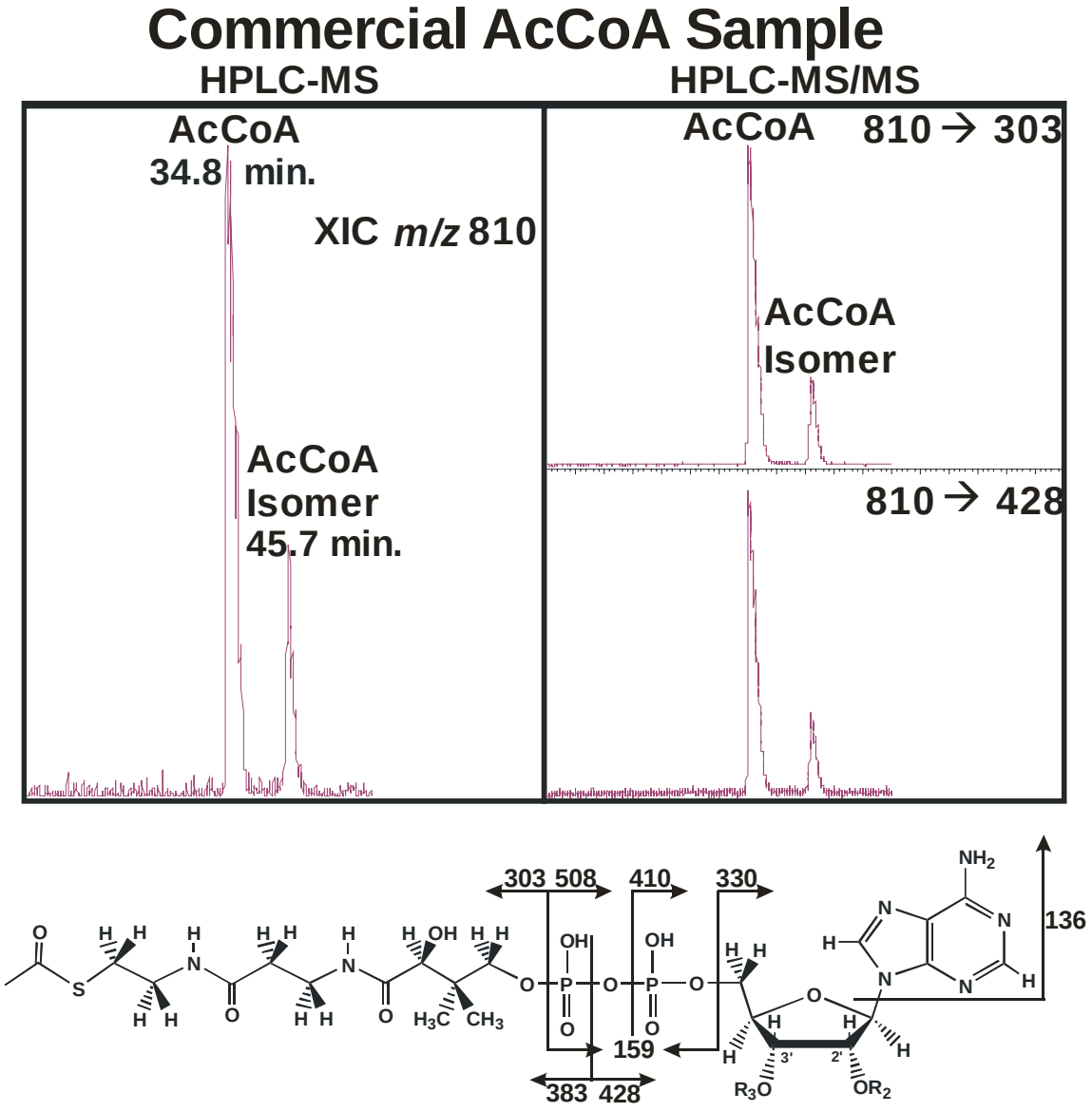

Figure 25. HPLC-MS and HPLC-MS/MS Analyses of Commercial Acetyl-CoA Samples. HPLC-MS of commercial acetyl-CoA exhibited two distinct peaks with identical $(M+H)^+$ ions, *m/z* 810. The earlier-eluting peak is the authentic acetyl-CoA, and the later-eluting peak is acetyl-iso-CoA, which is consistent with the extensive MS and NMR analyses performed on CoA and iso-CoA. HPLC-MS/MS experiments exhibited identical product ions at the *m/z* 810→303 and *m/z* 810→428 transitions. The proposed fragmentation patterns are shown.

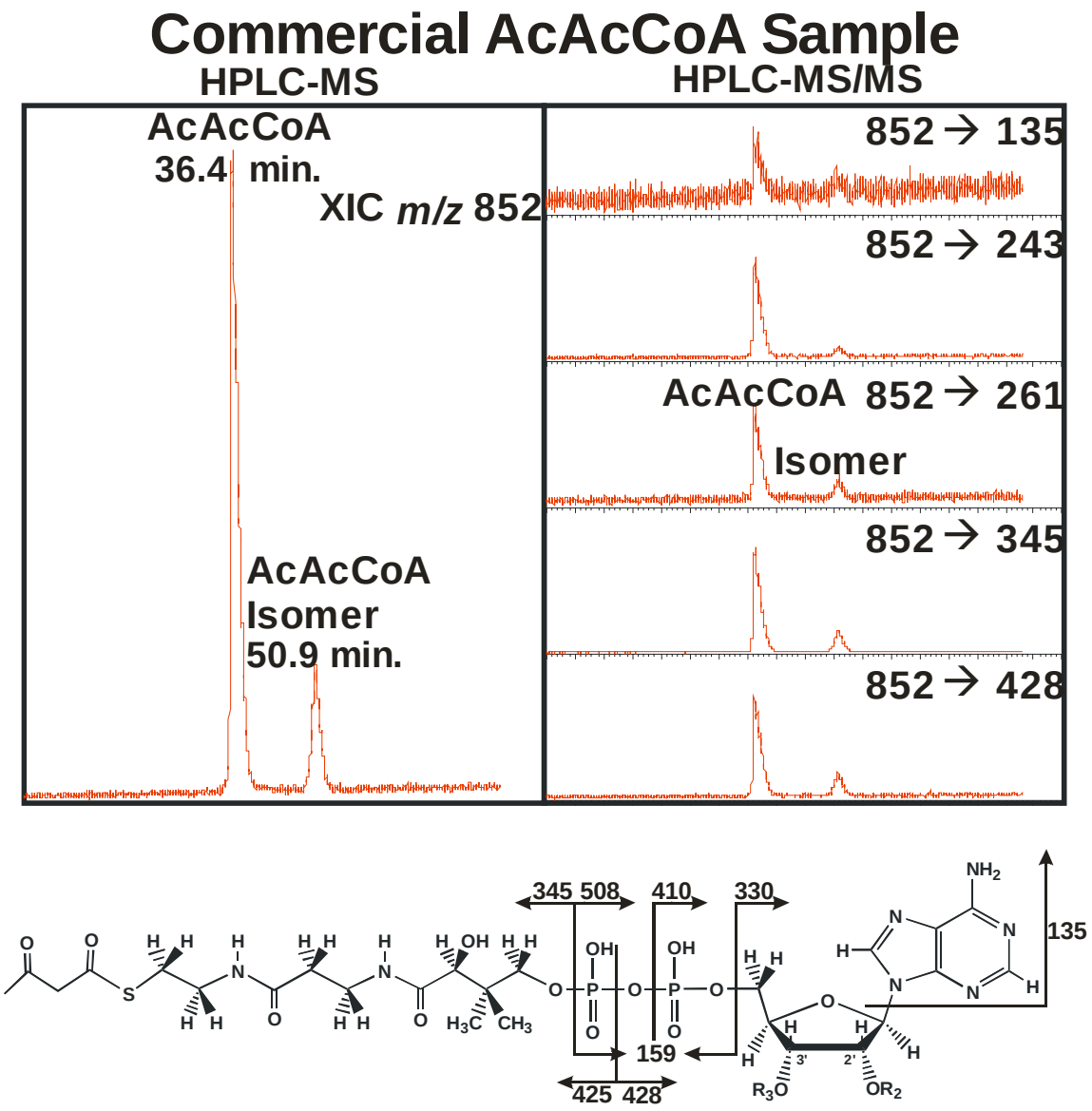

Figure 26. HPLC-MS and HPLC-MS/MS Analyses of Commercial Acetoacetyl-CoA Samples. HPLC-MS of commercial acetoacetyl-CoA exhibited two distinct peaks with identical $(M+H)^+$ ions, *m/z* 852. The earlier-eluting peak is the authentic acetoacetyl-CoA, and the later-eluting peak is acetoacetyl-iso-CoA. HPLC-MS/MS experiments exhibited identical product ions at the *m/z's* 852→135, 852→243, 852→261, 852→345, 852→428 transitions. The proposed fragmentation patterns are shown.

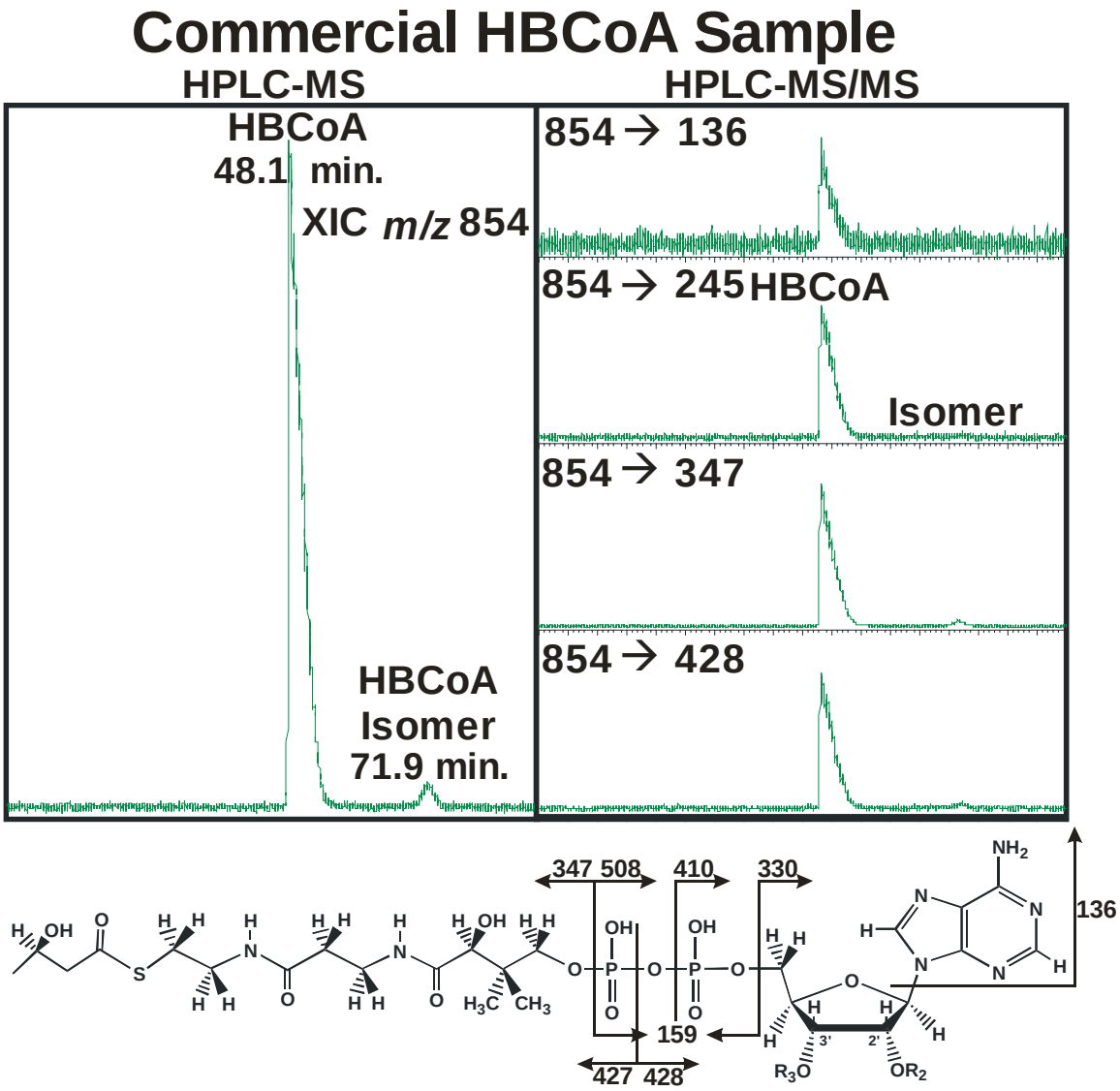

Figure 27. HPLC-MS and HPLC-MS/MS Analyses of Commercial β-hydroxybutyryl-CoA Samples. HPLC-MS of commercial β-hydroxybutyryl-CoA exhibited two distinct peaks with identical $(M+H)^+$ ions, *m/z* 854. The earlier-eluting peak is the authentic β-hydroxybutyryl-CoA, and the later-eluting peak is β-hydroxybutyryl-iso-CoA. HPLC-MS/MS experiments exhibited identical product ions at the *m/z*'s 854→136, 854→245, 854→347, and 854→428 transitions. The proposed fragmentation patterns are shown.

Structural characterization of Iso-CoA by NMR. 1D ^{1}H-NMR spectra for the two HPLC-purified isomers of CoA are shown in Panels A and B of Figure 28, respectively. The spectrum in Panel A, for the earlier-eluting isomer, is very similar to several previously-published CoA spectra (268,318-322), and the chemical shift assignments were made according to d'Ordine *et al* (268). In contrast, the spectrum shown in Panel B, for the later-eluting isomer, is very different in the 4-5 ppm region. Therefore, 2D ^{1}H-^{1}H COSY experiments (Figure 29) were obtained for this isomer in order to assign the chemical shifts. The chemical shift assignments and coupling constants are listed in Table 15. As indicated in Table 16, the chemical shift values for $NADP^{+}$ and NADPH, which are shown in Figure 30 to possess the same 2'-phosphate adenosine diphosphate moiety as iso-CoA, correlate well with the relevant protons of iso-CoA.

It is evident that for the later-eluting isomer the 2'-proton is shifted downfield by approximately 0.20 ppm while the 3'- and 4'-protons are respectively shifted up-field by 0.15 and 0.20 ppm, and the two 5'-protons have significantly different coupling patterns. Since it seemed likely that the position of the phosphate on the ribose ring gives rise to these differences, ^{1}H-^{31}P HMQC experiments were carried out to assign the position of each phosphate, explicitly. The ^{1}H-^{31}P HMQC spectra for iso-CoA, shown in Figure 31, unequivocally establishes that the monophosphate is attached at the 2'-carbon; thus designating this compound as iso-CoA.

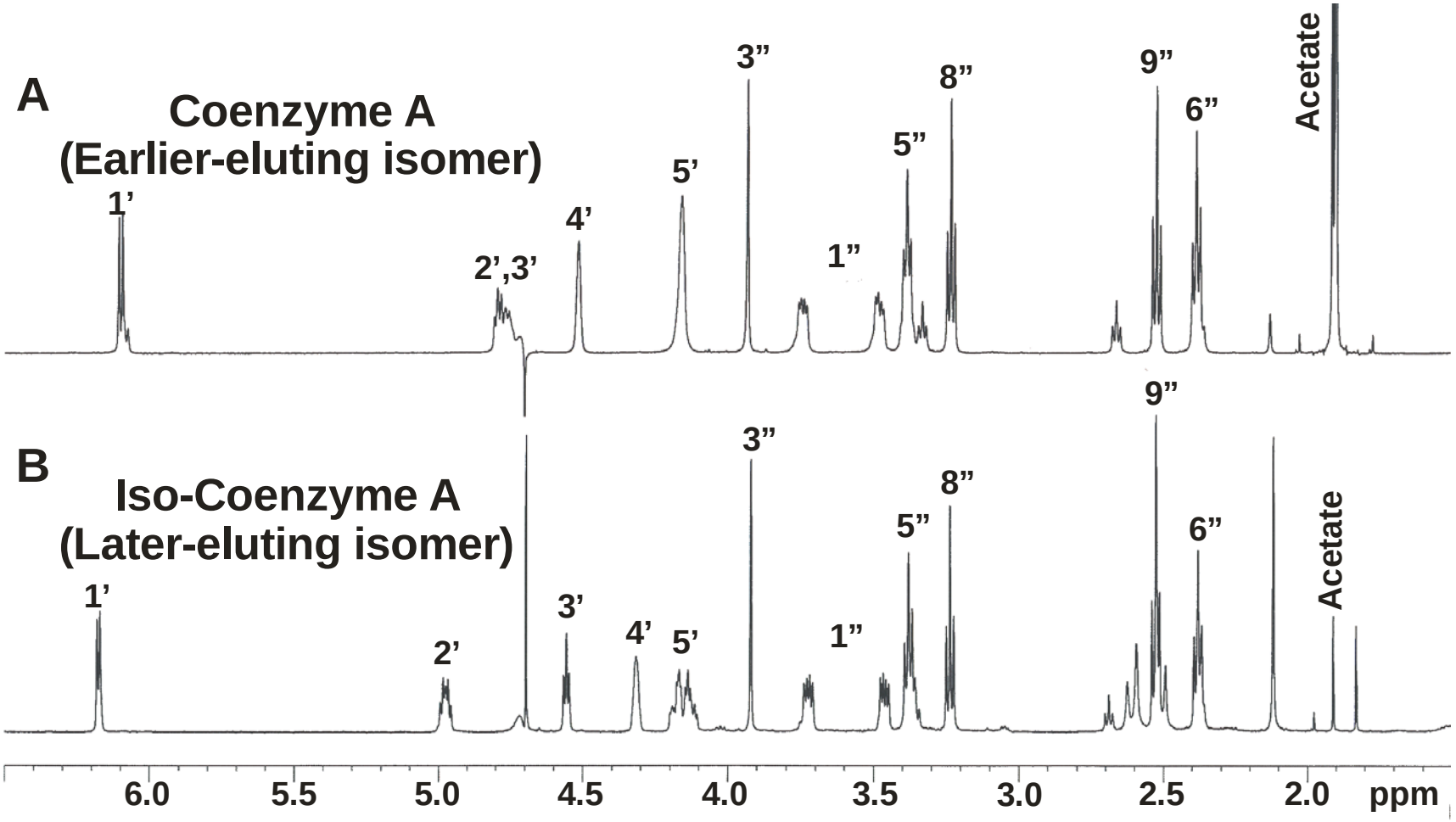

Figure 28. ^{1}H-NMR of HPLC-purified Samples of CoA and Iso-CoA. HPLC-purified samples of CoA and iso-CoA analyzed by ^{1}H-NMR exhibit significant differences in the region between 4-5 ppm, which corresponds to the ribose ring region. Labels corresponding to the numbering scheme shown in Scheme 1,

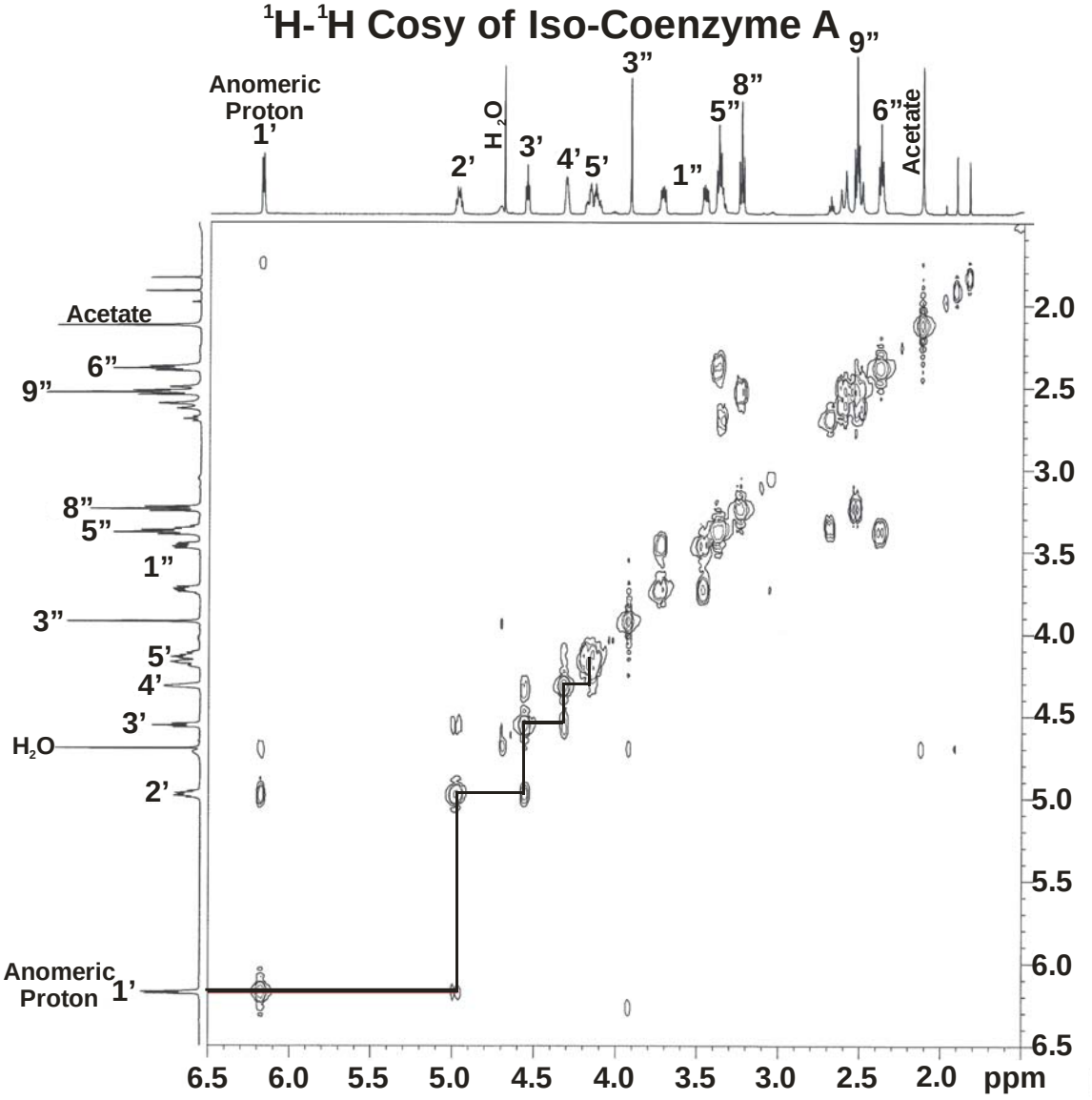

Figure 29. ^{1}H-^{1}H COSY of Iso-CoA. The ^{1}H-^{1}H COSY of HPLC-purified iso-CoA unequivocally assigns the proton chemical shifts of the ribose ring. The inserted marker lines illustrate how the indicative chemical shift of the anomeric proton, labeled at 6.18 ppm, was used to determine the position of each proton on the ribose ring.

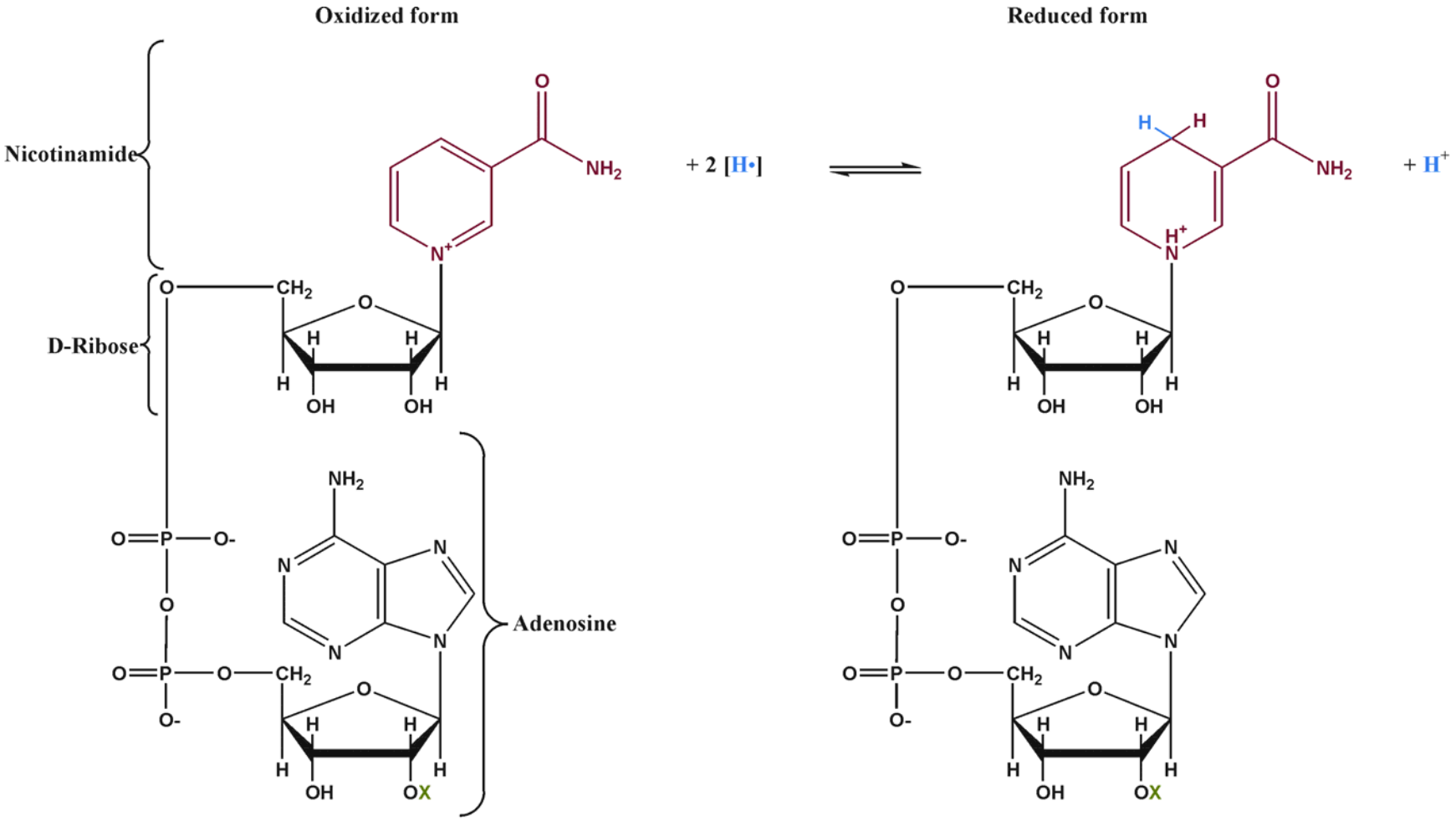

Figure 30. The Chemical Structures and Interconversion of NAD(P)H and NAD(P)$^{+}$. Modified from Voet and Voet (323).

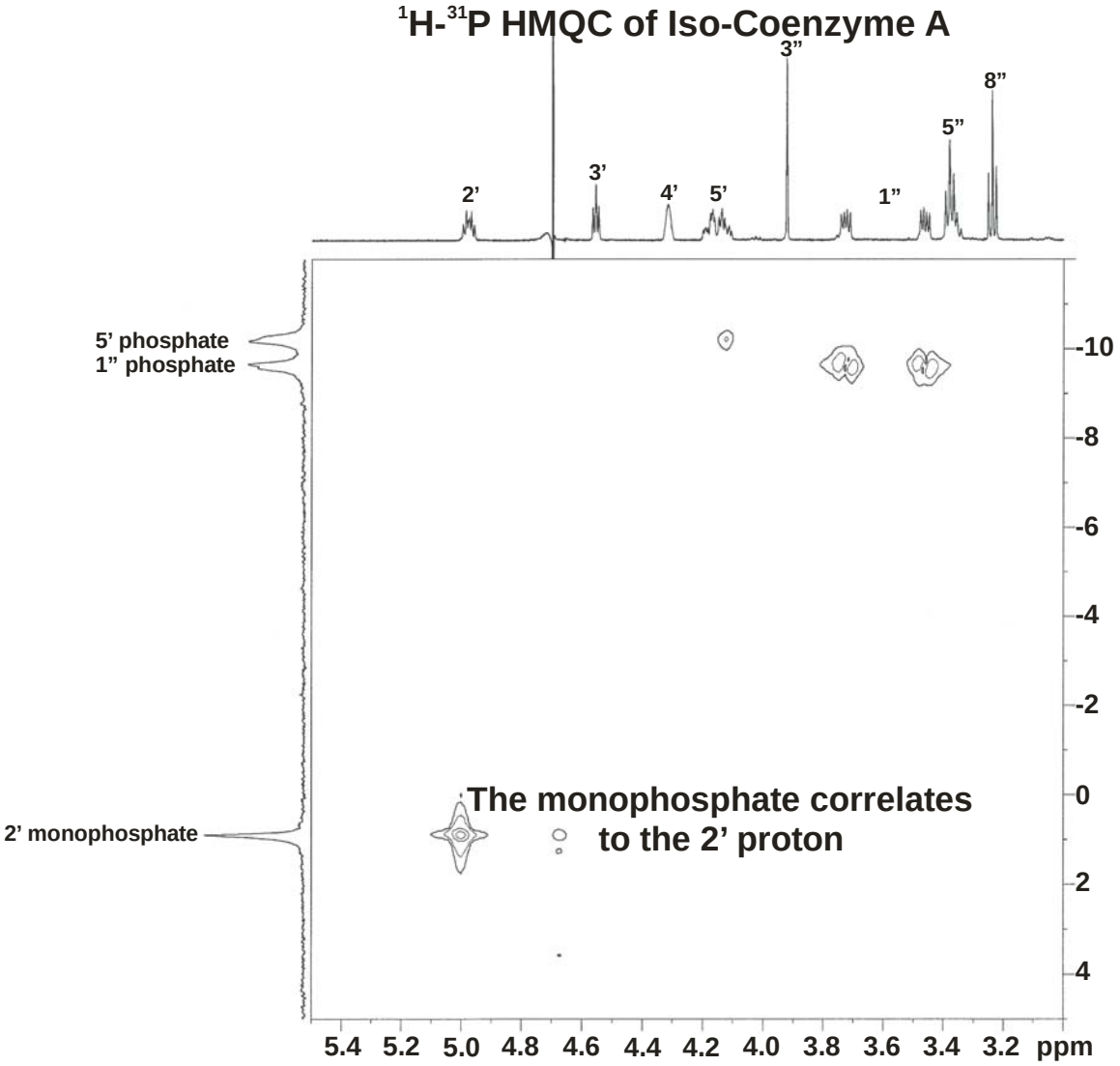

Figure 31. ^{1}H-^{31}P HMQC of Iso-CoA. The ^{1}H-^{31}P HMQC for the HPLC-purified isomer unequivocally demonstrates that the monophosphate, located at 0.9 ppm, clearly corresponds to the 2'-proton of the ribose ring; thus, this isomer is designated as iso-CoA. Additionally, since the two phosphates of the pyrophosphate linkage couple with the protons on the 5' and 1'' carbons, no other phosphate rearrangements are evident.

Table 15. Iso-CoA ^{1}H- and ^{31}P-NMR Chemical Shift Assignments and Coupling Constants.

^{1}H Chemical Shift	Proton Position	Integration	Multiplicity	J (MHz)	
8.41	8	1	s		
8.18	2	1	s		
6.18	1′	1	d	$J_{1'-2'}$	5.15
4.98	2′	1	m	$J_{2'-3'}$	5.09
				$J_{2'-P2'}$	8.69
4.56	3′	1	t	$J_{3'-4'}$	4.56
4.32	4′	1	m	$J_{4'-5'a}$	3.92
				$J_{4'-5'b}$	2.83
				$J_{4'-P5'}$	2.00
4.18	5′b	1	m	$J_{5'b-P5'}$	4.58
4.13	5′a	1	m	$J_{5'a-P5'}$	5.08
				$J_{5'a-5'b}$	11.63
3.92	3″	1	s		
3.73	1″	1	dd	$J_{1''-1''}$	9.90
				$J_{1''-P1''}$	5.09
3.48	1″	1	dd	$J_{1''-P1''}$	4.83
3.38	5″	2	t	$J_{5''-6''}$	6.53
3.24	8″	2	t	$J_{8''-J9''}$	6.59
2.54	9″	2	t		
2.37	6″	2	t		
0.89	10″	3	s		
0.67	11″	3	s		
^{31}P Chemical Shift	**Phosphate Position**				
-0.90	2′	1	s		
-9.63	1″	1	d		
-10.21	5′	1	d		

Table 16: ^{1}H NMR Chemical Shift Parameters for Iso-coenzyme A. A Comparison of iso-CoA with the literature derived coupling constants for $NADP^{+}$ and NADPH.

^{1}H Chemical Shift	***Proton Position***	***J MHz***	***Iso-CoA***	***$NADP^{+}$*** *(324)*	***NADPH*** *(324)*
8.41	8				
8.18	2				
6.18	1′	$J_{1'-2'}$	5.15	5.0	4.7
4.977	2′	$J_{2'-3'}$	5.09	5.3	4.9
		$J_{2'-P2'}$	8.69	7.1	6.8
4.557	3′	$J_{3'-4'}$	4.56	4.6	5.1
4.317	4′	$J_{4'-5'a}$	3.92	4.6	4.4
		$J_{4'-5'b}$	2.83	2.6	2.7
		$J_{4'-P5'}$	2.00	2.0	2.0
4.180	5′b	$J_{5'b-P5'}$	4.58	4.9	4.8
4.129	5′a	$J_{5'a-P5'}$	5.08	5.0	5.2
		$J_{5'a-5'b}$	11.63	11.8	11.8
3.92	3″				
3.73	1″	$J_{1''-1''}$	9.90		
		$J_{1''-P1''}$	5.09		
3.48	1″	$J_{1''-P1''}$	4.83		
3.38	5″ + 8″ ox.	$J_{5''-6''}$	6.53		
3.24	8″	$J_{8''-J9''}$	6.59		
2.54	9″				
2.37	6″				
0.89	10″				
0.67	11″				

HPLC of Commercial Samples of CoA, Acetyl-CoA, Acetoacetyl-CoA, and β-hydroxybutyryl-CoA. The overlaid HPLC chromatograms, presented in Figure 29, established that commercial samples of CoA, acetyl-CoA, acetoacetyl-CoA and β-hydroxybutyryl-CoA, which were designated as 93%, 93%, 90% and 99% pure, also contained approximately 10%, 15%, 18% and 3% of the 2'-monophosphate isomers, respectively.

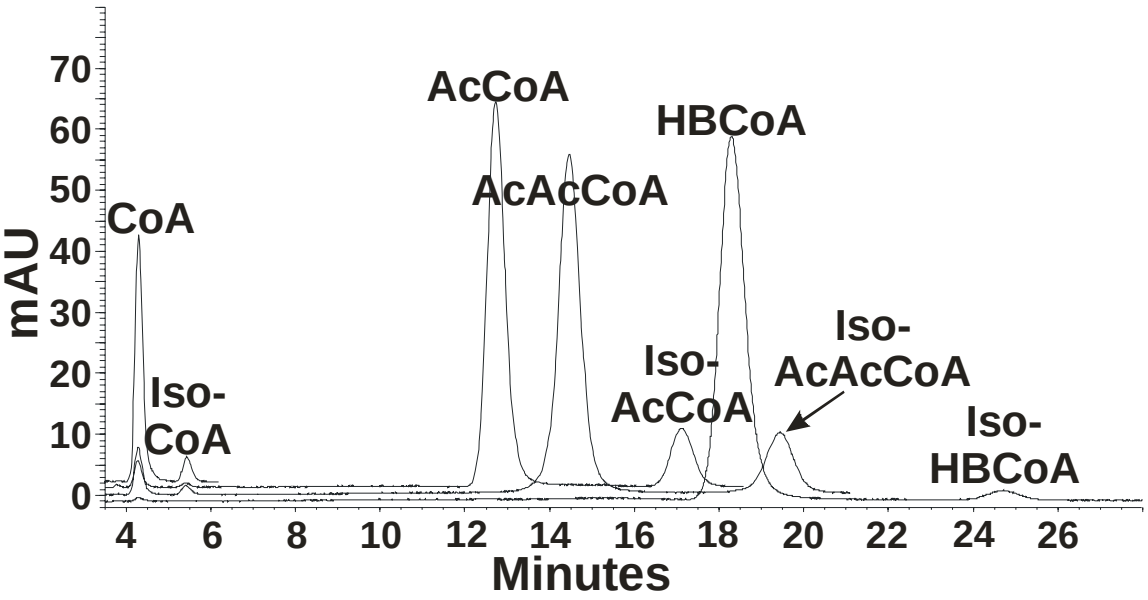

Figure 32. The HPLC Elution Profile of Commercial CoA, Acetyl-CoA, Acetoacetyl-CoA, and β-hydroxybutyryl-CoA. Two peaks are observed for each compound and have the following retention times: 4.25 min, CoA; 5.5 min, iso-CoA; 12.75 min, AcCoA, acetyl-CoA; 14.5 min, AcAcCoA, acetoacetyl-CoA; 17.1 min, Iso-AcCoA, acetyl-iso-CoA; 18.25 min, HBCoA, β-hydroxybutyryl-CoA; 19.5 min, Iso-AcAcCoA, acetoacetyl-iso-CoA; 24.6 min, Iso-HBCoA, β-hydroxybutyryl-iso-CoA

Iso-CoA-containing Compounds are Substrates for the β-ketothiolase, the Acetoacetyl-CoA Reductase, and the PHB Synthase enzymes. The reaction time courses shown in Figure 33 for CoA, acetyl-CoA, and β-hydroxybutyryl-CoA and their respective iso-CoA-isomers demonstrate that the three enzymes, β-ketothiolase, acetoacetyl-CoA reductase, and PHB synthase, can catalyze reactions with either isomer. These data represent the first examples of iso-CoA-containing compounds acting as substrates in enzymatic acyl-transfer reactions. In the coupled two-enzyme system in Panel A, β-ketothiolase converts two molecules of acetyl-CoA to acetoacetyl-CoA, which is immediately reduced to β-hydroxybutyryl-CoA by the second enzyme acetoacetyl-CoA reductase. In Panel B a third enzyme, PHB synthase, has been added which converts the β-hydroxybutyryl-CoA to poly-(β)-hydroxybutyric acid. It is evident from the time courses in both panels that in all cases both the CoA- and iso-CoA-isomers are processed with equal facility. In other experiments, we find that acetoacetyl-CoA and its iso-CoA isomer react with equal facility in the back reaction to produce the acetyl-CoA product (data not shown).

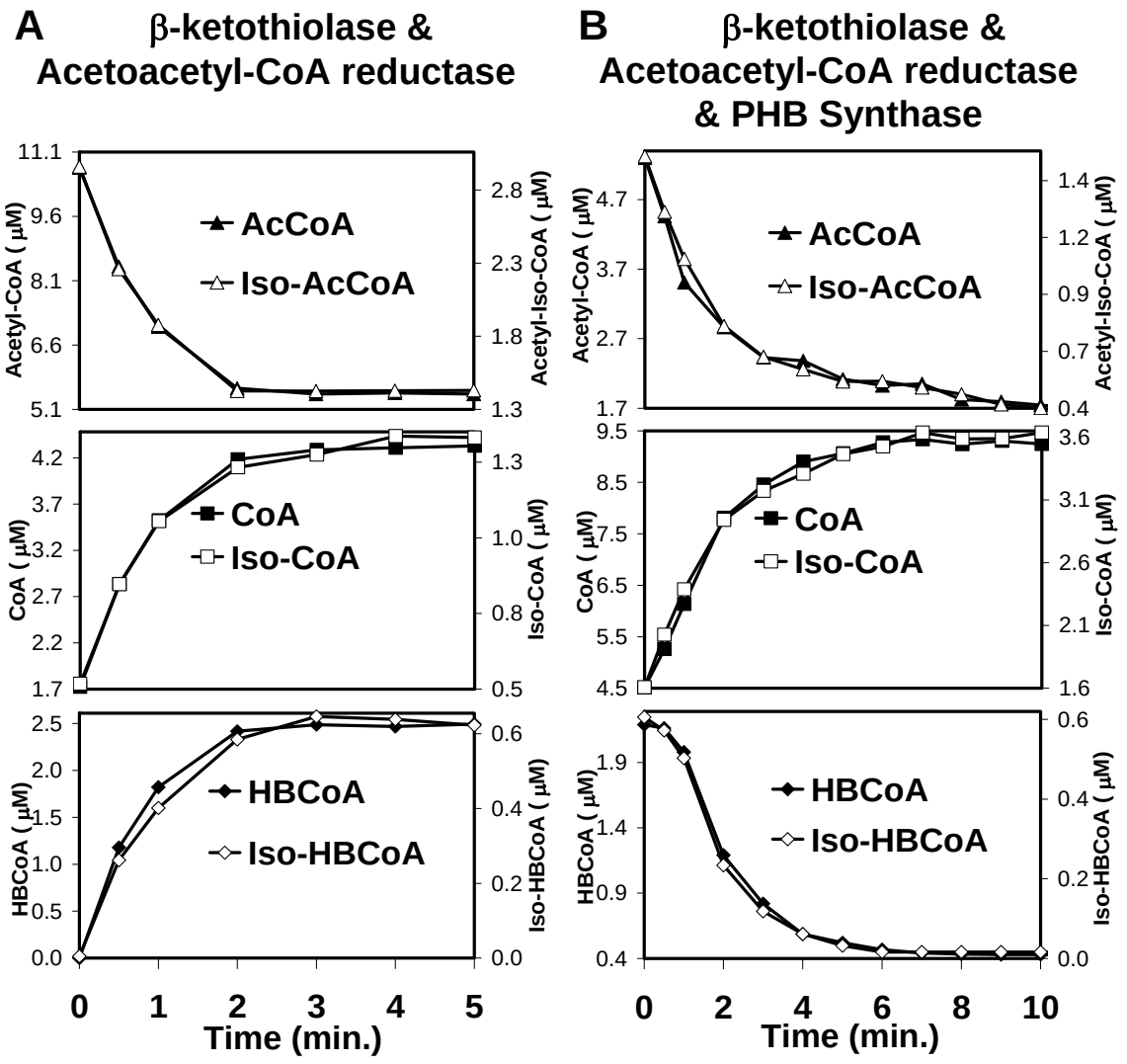

Figure 33. The First Example of Enzymatic Acyl-transfer Reactions occurring with the 2′-isomers of CoA-containing Compounds. Enzymatic reaction time courses for the enzymes β-ketothiolase, acetoacetyl-CoA-reductase, and PHB synthase indicate that these enzymes catalyze identical reactions exhibiting equivalent kinetic rates with both the 2′- and the 3′-isomers of acetyl-CoA, CoA, and β-hydroxybutyryl-CoA. Panel A: β-ketothiolase and acetoacetyl-CoA reductase are added to a 150 mM EPPS solution containing acetyl-CoA and its isomer, NADPH and TCEP at a final pH of 7.8. This coupled-enzyme reaction initiates the consumption of two molecules of acetyl-CoA or acetyl-iso-CoA; thus, generating one molecule of CoA or iso-CoA and one molecule of β-hydroxybutyryl-CoA or the isomer. Panel B: Addition of PHB synthase to the previous coupled-enzyme system (Panel A) results in the conversion of β-hydroxybutyryl-CoA and its isomer to poly-(β)-hydroxybutyric acid; this irreversible polymerization stimulates the consumption of further acetyl-CoA

isomers, with CoA or iso-CoA liberation during both processes. Acetoacetyl-CoA, the product of the β-ketothiolase mediated condensation of 2 acetyl-CoA molecules, is below the limit of detection by HPLC. ▲ AcCoA, acetyl-CoA; Δ Iso-AcCoA, acetyl-iso-CoA; ■ CoA; □ Iso-CoA; ♦ HBCoA, β-hydroxybutyryl-CoA; ◊ Iso-HBCoA, β-hydroxybutyryl-iso-CoA.

Regioselective Synthesis of Iso-CoA. Since iso-CoA and acyl-iso-CoA compounds may be useful as potential inhibitors or pseudosubstrates, a synthesis capable of producing high yields of the 2′-phosphate isomer is desirable; to this end, we report a simple synthesis of iso-CoA from CoA. As shown in Scheme 2, CoA was initially converted to the dimeric disulfide, and the water soluble coupling agent 1-ethyl-3-(3-dimethylaminopropyl) carbodiimide (EDC) was then used to form the 2′,3′-cyclic-CoA intermediate in a reaction analogous to the synthesis of 2′,3′-cyclic-NADP (325). We note that the first steps of the synthesis are carried out using the CoA dimer to avoid possible quenching of the EDC. The dimer is reduced back to the free CoA form in Step 3, in which base-catalyzed hydrolysis is carried out in the presence of β-cyclodextrin and high salt at pH 9.5 to produce iso-CoA with a 92% yield.

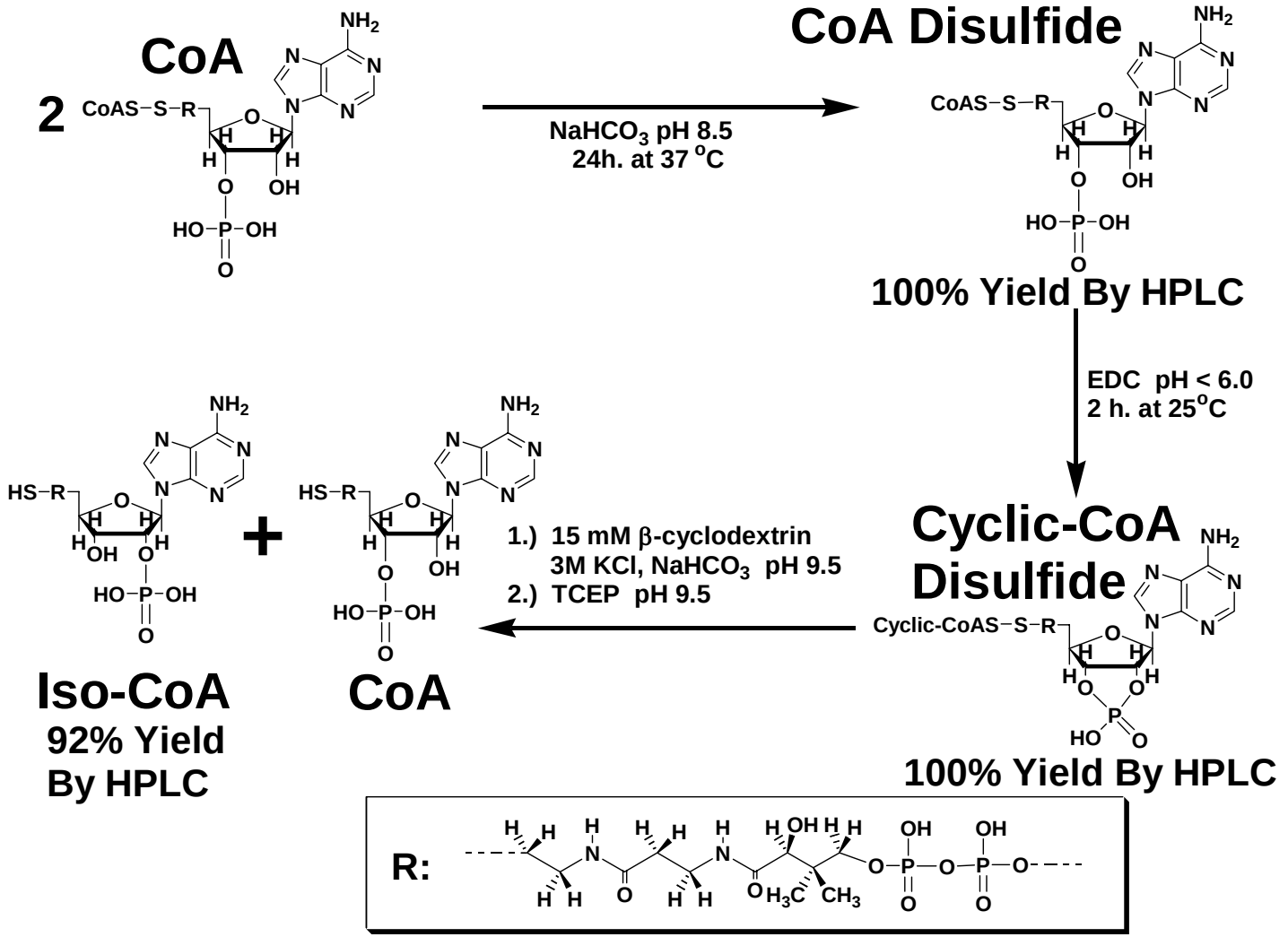

Figure 34. Regioselective Synthesis of Iso-CoA from CoA. This is the first regioselective chemical synthesis of iso-CoA, and utilizes β-cyclodextrin in high salt to confer iso-CoA regioselectively in high yields.

Acid-Catalyzed Phosphate Migration. We investigated the acid-catalyzed migration of the CoA monophosphate group, in an attempt to furnish a plausible mechanism for the existence of the 2′-phosphate isomers in commercial preparations of CoA-containing compounds. In these experiments, HPLC-purified CoA was incubated in the presence of 0.5 M HCl and the relative amounts of CoA and iso-CoA were determined by HPLC as a function of time. As shown in Figure 35, a final equilibrium mixture of 60% CoA and 40% iso-CoA was attained within 60 hours. We note that approximately 10% of iso-CoA is present after only 4 hours, so the iso-CoA content of commercial preparations may indeed be produced in this fashion during the processing of the product.

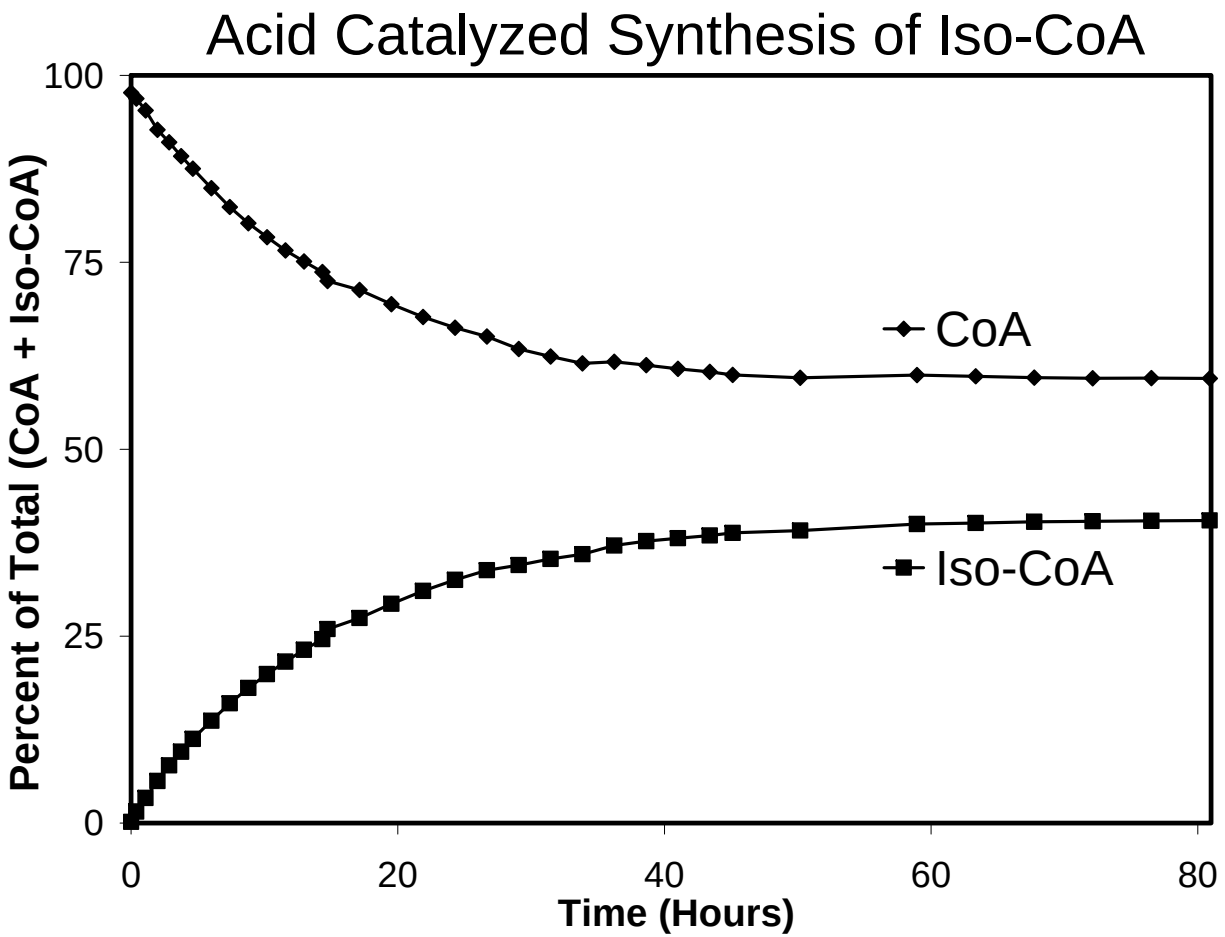

Figure 35. Acid-catalyzed Synthesis of Iso-CoA. HPLC-purified CoA was incubated in the presence of 0.5 M HCl, and the relative quantities of ♦ CoA and ■ iso-CoA were monitored by HPLC as described in the text. Note that this iso-CoA formation occurs in the presence of strong acid and that formation of the CoA : iso-CoA equilibrium does not spontaneously occur in neutral solution to any appreciable rate.

CHAPTER 9

ISO-COENZYME A: DISCUSSION

The vital role of coenzyme A in metabolism is underscored by the sheer quantity of classified enzymes (326) that react with CoA-containing molecules; we count greater than 9% of the total known enzymes to be of this type. The 2′-phosphate isomer of CoA, first named iso-CoA in Khorana's 1959 report (265,266), has traditionally been considered an undesirable synthetic byproduct or has been simply ignored. Indeed, a review of the literature, presented in Table 17, reveals that only eight of the more than 350 CoA-utilizing enzymes (326) have been examined for the ability to discriminate between the 2′- and 3′-phosphate isomers (265,266,288,293,294,297,298,301,305). Additionally, two of these enzymes, N-myristoyl transferase [E.C. 2.3.1.97] and choline acetyltransferase [E.C. 2.3.1.6], have been shown to accept purified 2′-phosphate isomers as inhibitors or substrates, respectively (294,298,305). Moreover, the majority of the compounds examined in these eight cases are synthetic analogs of CoA, such as the dethia- or seleno-derivatives, and not iso-CoA itself. Clearly, these results suggest that other enzymes should be examined for their reactivities towards the 2′-phosphate isomers of their CoA-containing substrates.

Table 17. Eight Literature Accounts that Examine 2'- vs. 3'-phosphate Specificity.

[E.C. Number]	***Enzyme Name***	***Enzyme Reaction***	
Pure Isomer Mixture	**2′-isomer substrates**	**2′-isomer inhibitor**	**Accepts 2′-isomers Rejects 2′-isomers**
[E.C. 2.3.1.97] N-myristoyltransferase (294,311)			
Pure	---	Myristoyl-CH_2-iso-CoA	Accepts 2′-isomers
[E.C. 2.3.1.6] Choline Acetyltransferase (305,307,308)			
Pure	---	Se-iso-CoA	Accepts 2′-isomers
[E.C. 1.3.99.3] AcCoA Dehydrogenase (298,306)			
Mixtures†	Heptadecan-2-only-CH2-iso-CoA	---	Accepts 2′-isomers†
[E.C. 4.1.3.7] Citrate Synthase (296,297,312,313)			
Mixture‡	---	Acetonyl-CH2-iso-CoA; Heptadecan-2-only-CH2-iso-CoA	Accepts 2′-isomers (Unclear‡)
[E.C. 2.3.1.21] Carnitine Palmitoyltransferase (297)			
Mixture‡	---	Heptadecan-2-only-CH2-iso-CoA	Accepts 2′-isomers (Unclear‡)
[E.C. 2.3.1.8] Phosphotransacetylase (265,300,301,303,304,327)			
Pure	No, Rejects Iso-CoA; Oxy-iso-CoA	No, Rejects Iso-CoA	Rejects 2′-isomers
[E.C. 1.3.99.12] FAD-dependent isobutanoyl-CoA Dehydrogenase (293)			
Pure	No, Rejects Isobutanoyl-CH_2-iso-CoA	---	Rejects 2′-isomers
[E.C. 2.1.3.1] Methylmalonyl-CoA pyruvate carboxylase (transcarboxylase) (288,289)			
Pure	No, Rejects Propionyl-CH_2-iso-CoA	--	Rejects 2′-isomers

†Results derived from experiments showing identical reaction rates with 1:1 and 65:45 isomeric mixtures.

‡Specificity is unclear. The authors suggest that since purified S-heptadecyl-CoA inhibits and an isomeric mixture of Heptadecanoyl-dethia-CoA inhibits there must be no difference between the isomers and the enzyme accepts 2′-phosphate; this is a very poor argument proposed by the authors.

The results presented here represent the first complete structural characterization of iso-CoA. CoA and iso-CoA were purified by HPLC, and high resolution exact mass and MS/MS analyses unequivocally established that the compounds are constitutional isomers with extremely similar fragmentation patterns. Direct structural identification of the two HPLC-purified isomers was then performed using ^{1}H-NMR, ^{1}H-^{1}H COSY, and ^{1}H-^{31}P HMQC, and the results unequivocally established that the monophosphate of the iso-CoA isomer is attached to the 2′-carbon of the ribose ring. All previous characterizations of the structure of iso-CoA have been based on chromatographic analyses (265,266), which ultimately rest on comparisons with the degradation products of CoA and NADPH (267,277,315), or have been based on assumptions regarding enzyme specificity (284,285,287).

The HPLC-MS and HPLC-MS/MS experiments on acetyl-CoA samples reported here also reveal the presence of two compounds, both of which exhibited ions (*m/z* 810) corresponding to acetyl-CoA's molecular mass, and showed identical product ion spectra. Similarly, HPLC-MS and HPLC-MS/MS analyses of commercial preparations of acetoacetyl-CoA, and β-hydroxybutyryl-CoA also confirmed the presence of isomeric forms of both of these compounds.

We report here the first example of iso-CoA-containing compounds acting as substrates in acyl-transfer reactions. Three enzymes, β-ketothiolase, acetoacetyl-CoA reductase, and PHB synthase, successfully react with the 2′-isomers of their natural

substrates, and the reaction time courses indicate that all three enzymes react with either isomer with equal facility. Our investigation has provided three additional clear-cut cases of enzymes that accept the 2′-phosphate isomers. A larger population of enzymes needs to be examined to determine how the phosphate position affects ligand binding, catalysis or inhibition.

The Role of the 3′-phosphate of CoA. The role of the 3′-phosphate of CoA in enzyme binding and catalysis has been investigated somewhat more thoroughly by investigations evaluating the ability of an enzyme to interact with dephospho-CoA analogues. Approximately 40 enzymes, detailed in Table 18, have been evaluated, and the vast majority of enzymes reported in the literature do accept the 3′-dephospho-CoA compounds as substrates or inhibitors; though, the enzymes typically exhibit less affinity for the dephospho-derivatives. We have found only three literature examples, highlighted in red in Table 18, of enzymes that reject the dephospho-CoA compounds.

Table 18. Enzymatic Interactions with Dephospho-CoA-containing Compounds.

Enzyme/Compound	R	2′ 3′	Substrate (K_M*)	Inhibitor (K_I*)
Accepts DPCoA as a Substrate: Green				
Accepts Iso-CoA as a Substrate: Bright Green				
Accepts DPCoA as an Inhibitor: Dark Blue				
Accepts Iso-CoA as an Inhibitor: Light Blue				
Rejects DPCoA as a Substrate: Dark Red				
Rejects Iso-CoA as a Substrate: Red				
Rejects DPCoA as a Inhibitor: Violet				
Rejects Iso-CoA as a Inhibitor: Lavender				
Unknown Specificity: Tan				
Accepts DPCoA as an Inhibitor but DPCoA has greater activity than CoA: Turquoise				
CoA-Pyrophosphate analyzed: Yellow				

Enzyme/Compound	R	2′ 3′	Substrate (K_M*)	Inhibitor (K_I*)
[E.C. 1.1.1.36] NADPH-dependent Acetoacetyl-CoA Reductase *C. necator* (160,222), **Rhizobium (Cicer) Sp. Strain CC 1192** (328) ***Methylobacterium extorquens*** (329) **Zoogloea ramigeria** (220)				
Acetoacetyl-CoA + NADPH ⇌ β-hydroxybutyryl-CoA + $NADP^+$				
Accepts 2′-isomers as substrates with equal affinity. Isomers were run together in the same assay but were quantitated separately by HPLC.				
Acetoacetyl-CoA	AcAcS	H P	Yes (222)	---
Acetoacetyl-CoA	AcAcS	H P	5 µM (160)	>32 µM substrate inhibition
Acetoacetyl-CoA	AcAcS	H P	22 ± 10 µM (328)	>100 µM substrate inhibition
Acetoacetyl-CoA	AcAcS	H P	11.6 µM (329)	---
			K_M (M) / K_{cat} (S^{-1}) / K_{cat}/K_M ($M^{-1}S^{-1}$)	
Acetoacetyl-CoA (220)	AcAcS	H P	2×10^{-6} / 300 / 1.8×10^{8}	>10 µM substrate inhibition

Table 18 Continued

Propionylacetyl-CoA (220)	PrAcS	H	P	2 x 10^{-6}	124	6.2 x 10^{7}	
Butyrylacetyl-CoA (220)	BrAcS	H	P	1 x 10^{-5}	9	9.0 x 10^{5}	
2-Methylacetoacetyl-CoA (220)	MeAsS	H	P	7.4 x 10^{-4}	27	3.6 x 10^{4}	
Acetoacetyl-S-(D-pantetheine)11-pivalate (220)	AcAcS	---	---	9.9 x 10^{-4}	267	2.7 x 10^{5}	

Acetoacetyl-iso-CoA	AcAcS	H	H	Yes (222)	---
Acetoacetate	AcAcO	---	---	No (328)	---
NADPH	---	P	H	19 µM (160)	---
NADPH	---	P	H	44 ± 24 µM (328)	---
NADPH	---	P	H	41 µM (329)	---
NADH	---	H	H	400 µM (160)	---
$NADP^+$	---	P	H	31 µM (222)	---
$NADP^+$	---	P	H	135 µM (220)	
$NADP^+$	---	P	H	38 ± 16 µM (328)	% inhibition at given [$NADP^+$] 0.2 mM $NADP^+$ 0.4 mM $NADP^+$ 35% 50%
NAD^+	---	H	H	---	No inhibition (328)
NAD^+	---	H	H	250 µM (222)	---
β-hydroxybutyryl-CoA	HBS	H	P	Yes (222)	---
DL-(β)-hydroxybutyryl-CoA	HBS	H	P	33 µM (222)	---
R-β-hydroxybutyryl-CoA [0.2 mM]	HBS	H	P	120 ± 29 µM (328)	No inhibition (328)
D-β-hydroxybutyryl-CoA	HBS	H	P	26 µM (220) k_{cat} 90 s^{-1}	
β-hydroxybutyryl-iso-CoA	HBS	H	H	Yes (222)	---

[1.1.1.157] 3-hydroxybutyryl-CoA Dehydrogenase (330)

AcAcCoA + NADPH ⇌ L-(+)-HBCoA + CoA

Table 18 Continued

Accepts DPCoA as a Substrate	**2x better % Activity with CoA**				
				% Activity w.r.t. AcAcCoA	
Acetoacetyl-CoA	AcAcS	H	P	100	---
Acetoacetyl-dephospho-CoA	AcAcS	H	H	47	---
Acetoacetylpantetheine	AcAcS	----		10	---
N-acetyl-S-acetoacetyl-cysteamine	AcAcS	----		15	---
[1.2.99.2] Acetyl-CoA decarbonylase/synthase complex (331-333)					
Accepts DPCoA as a Inhibitor	**5 x better K_I with CoA**				
Accepts DPCoA as a Substrate	**1.4 x better K_M with CoA**				
Carbonyl Exchange Assay: [1-^{14}C]-acetyl-CoA + CO ⇌ ^{14}CO + acetyl-CoA (333)					
CoA	SH	H	P	---	7 µM
Dephospho-CoA	SH	H	H	---	35 µM
Desulfo-CoA	CH_3	H	P	---	6000 µM
Pivaloylpantetheine-SH	SH			---	1200 µM
[1-^{14}C]-acetyl-CoA	AcS	H	P	600 µM / V_{Max} 440 min^{-1}	---
Propionyl-CoA	PrS	H	P	---	1300 µM
[1-^{14}C]-propionyl-CoA	PrS	H	P	---	None after 2h
Crotonyl-CoA	CrS	H	P	---	1400 µM
Butyryl-CoA	BuS	H	P	---	1450 µM
CODH-Catalyzed CoA exchange: [3′-^{32}P]-CoA + AcCoA ⇌ CoA +[3′-^{32}P]-AcCoA (332)					
AcCoA	AcS	H	P	1500 µM V_{Max} 2.5 µmol/min	---
CoA	SH	H	P	50 µM	ND
Propionyl-CoA	PrS	H	P	5000 µM V_{Max} 0.15 µmol/min	---
Acetyltransferase: Acetyl-CoA + 3′-dephospho-CoA ⇌ CoA + S-acetyl-3′-dephospho-CoA (331)					

Table 18 Continued

Acetyl-CoA	AcS	H	P	30.8 µM / k_{cat} 3100 min^{-1}	45.4 µM
3'-dephospho-CoA	SH	H	H	42.2 µM	
CoA	SH	H	P	---	6.8µM

[1.3.99.3] Acyl-CoA Dehydrogenase/Acyl-CoA Oxidase (298,306,334,335)

Acyl-CoA + acceptor ⇌ 2,3-dehydroacyl-CoA + reduced acceptor

Accepts DPCoA as a Substrate	**2x better K_M than CoA ; Same V_{Max} as CoA** (306) **9x better K_M; 3.7 x better kcat with CoA** (335) **Study discrepancies purportedly because of sub-saturating concentrations of the electron acceptor or possibly because of different biological origins.**				
Accepts DPCoA as an Inhibitor	**Qualitative: Diminished inhibitor**				
CoA	SH	H	P	---	63µM
Dephospho-CoA	SH	H	H	---	Diminished inhibitor
Heptadecan-2-onyldethia-CoA 1:1	CH_2	Mix		Yes(58% P-CoA)	---
Heptadecan-2-onyldethia-CoA 65:45	CH_2	Mix		Yes	---
S-heptadecyl-CoA	-S-	H	P	No	Competitive K_d = 17nM K_I < 40 nM

				K_M (µM)	V_{Max} (min^{-1})	
Octanoyl-CoA (306)	SH	H	P	2.21±0.28	674.68±40.94	---
Octanoyl-dephospho-CoA (306)	SH	H	H	1.09±0.17	656.63±66.71	---
Octanoyl-pantetheine (306)	---	---	---	106.6±15.5	14.1±1.6	---
Octanoyl-1,N6-etheno-CoA (306)				9.28±1.72	415.95±27.07	---

				K_{Mapp} (µM)	K_{catapp} (S-1)	
Octanoyl-CoA [FPF_6 350 µM]	OcSH	H	P	2.6±0.4	15.6±0.5	---(335)

Table 18 Continued

Octanoyl-dephospho-CoA [FPF_6 1mM]	OcSH	H	H	25.1±2.8	58.3±1.9	---(335)
Butyryl-CoA [FPF_6 300µM]	BuSH	H	P	356±56	8.0±0.6	---(335)
Butyryl-dephospho-CoA[FPF_6 300µM]	BuSH	H	H	1608±134	1.55±0.1	---(335)

[1.3.99.12] FAD-dependent isobutanoyl-CoA dehydrogenase (293)

isobutanoyl-CoA + FAD ⇌ Methacrylyl-CoA + $FADH_2$

Rejects 2′-phosphate isomer as a substrate					
Isobutanoyl-dethia-CoA	CH_2	H	P	Yes	---
Isobutanoyl-dethia-Iso-CoA	CH_2	P	H	No	---

[1.4.3.3] D-amino-acid oxidase *sus scrofa* (336)

D-amino-acid + H_20 + O_2 ⇌ 2-oxo-acid + NH_3 + H_2O_2

Accepts DPCoA as a Inhibitor	**Qualitative: no comparison possible**				
Dephospho-CoA	SH	H	H	---	Inhibitor

[1.6.1.2] NAD(P)$^+$ Transhydrogenase (337-339)

NADPH + NAD^+ ⇌ $NADP^+$ + NADH

Accepts DPCoA as a Inhibitor	**DPCoA K_I is 22 x better than CoA** **Ac-DPCoA is 18 x better than CoA**				
Rejects 3′-NADP(H) isomer as a substrate					
2,4-dinitrophenyl-CoA	DNPS	H	P	---	No inhibition up to 200 µM
2,4-dinitrophenyl-dephospho-CoA	DNPS	H	H	---	3 µM competitive w.r.t. NAD^+ Non-Competitive w.r.t. $NADP^+$
S-7-nitrobenzofurazan-4-yl-CoA	NBFS	H	P	---	2.6 µM Competitive w.r.t. NADPH Non-Competitive vs. NAD^+
S-7-nitrobenzofurazan-4-yl-dephospho-CoA	NBFS	H	H	---	0.3µM Competitive w.r.t. both NADPH & NAD^+ Site-specific inhibitors

Table 18 Continued

					Specificity		K_I	
					NAD(H)	NADP(H)	Nonenergy-linked (µM)	Energy-linked (µM)
CoA	SH	H	P	---	-	+	200	700
Dephospho-CoA	SH	H	H	---	+	-	9	40
Acetyl-CoA	AcS	H	P	---	-	+	200	700
Acetyl-dephospho-CoA	AcS	H	H	---	+	-	11	40
Palmitoyl-CoA	PalmS	H	P	---	-	+	0.15	0.15
ADP	PP	OH	OH	---	+	-	300	400
5′-AMP	P	OH	OH	---	+	-	300	700
2′-AMP		P	OH	---	-	+	700	1200
3′-AMP		OH	P	---	-	+	700	1200
3′,5′-AMP	P	OH	P	---	+	+	400	400
Adenosine		OH	OH	---	+	-	500	500
Ribose		OH	OH	---	---	---	---	---
Adenine				---	---	---	---	---
Nicotinamide				---	---	---	---	---
4′-phosphopantheteine				---	---	---	---	---
Palmitoyl-carnitine				---	---	---	---	---
Nicotinamide mononucleotide				---	---	---	---	---
palmitate				---	---	---	---	---
2′-NADP(H)		P	OH	Yes	---	---	---	---
3′-NADP(H)		OH	P	No	---	---	---	---

[1.8.1.14] Coenzyme A disulfide reductase (340-342)

$CoA\text{-}S\text{-}S\text{-}CoA + NAD(P)H + H^+ \rightleftharpoons 2CoA\text{-}SH + NAD(P)^+$

S. aureus **accepts DPCoA as a Substrate 12x better K_M; 1.4 x better V_{Max} than CoA**

Table 18 Continued

P. horikoshii rejects DPCoA as a substrate

				K_M (µM)	K_{cat} (S^{-1})	K_{cat}/K_M ($M^{-1}S^{-1}x10^{-6}$)	Enzyme Species Origin
CoA disulfide	CoASS	H	P	11±2	1000±200	80±10	*S. aureus* (341)
Dephospho-CoA disulfide	CoASS	H	H	140±40	1400±200	10±2	*S. aureus* (341)
4,4′-diphospho-pantethine	---	---	---	80±10	540±40	3.3±0.4	*S. aureus* (341)
CoASSG	CoASS	H	P	1100±200	800±70	0.72±0.8	*S. aureus* (341)
NADPH	---	P	H	1.6±0.5	1020±60	600±100	*S. aureus* (341)

				K_M (µM)	K_{cat} (S^{-1})	K_{cat}/K_M ($M^{-1}S^{-1}x10^{-6}$)	
CoA disulfide	CoASS	H	P	30	7.1	4.2	*P. horikoshii* (342)
Dephospho-CoA disulfide	CoASS	H	H	No	---	---	*P. horikoshii* (342)
NADPH	---	P	H	<9.0	7.2	0.8	*P. horikoshii* (342)
NADH	---	P	H	73	8.1	0.11	*P. horikoshii* (342)

[1.11.1.9] (Miss)Glutathione peroxidase (343)

2 GSH + H_2O_2 ⇌ GSSG + 2 H_2O

Accepts DPCoA as a Inhibitor	**11-13 x better inhibitor than CoA**				
CoA	SH	H	P	---	Inhibits
Dephospho-CoA	SH	H	H	---	11-13 x less than CoA
ATP	---	OH	OH	---	Inhibition equals CoA

[E.C. 2.1.3.1] Methylmalonyl-CoA pyruvate carboxylase (transcarboxylase) (288,289)

Propionyl-CoA + oxaloacetate ⇌ Methylmalonyl-CoA + pyruvate

Rejects 2′-phosphate isomer as a substrate. Good qualitative example with pure isomers					
Propionyl-CH_2-CoA	PrCH_2	H	P	Yes	---
Propionyl-CH_2-iso-CoA	PRCH_2	H		No	---

Table 18 Continued

[2.3.1.5] Arylamine N-acetyltransferase (300)

AcCoA + an arylamine ⇌ CoA + an N-acetylarylamine

specifically: 4-aminoazobenzene+ ATP ⇌ 4-acetamidoazobenzene

Accepts DPCoA as a Substrate	**Qualitative Results; Bad example, doesn't name the enzyme; not purified**				
Accepts 2′-phosphate isomer as substrate (but not Se-iso-CoA)					
CoA	SH	H	P	Yes	---
Iso-CoA	SH	P	H	Yes [slight]	---
Se-CoA	SeH	H	P	Yes	---
Se-Iso-CoA	SeH	P	H	No	---
Dephospho-CoA	SH	H	H	Yes	---
dephospho-Se-CoA	SeH	H	H	Yes	---

[2.3.1.6] Choline Acetyltransferase (305,307,308,344)

Choline + Acetyl-CoA ⇌ CoA + Acetyl-Choline

[values in brackets were gathered at low anion concentration]

Accepts DPCoA as a Substrate	**10 x better K_M [108 x better K_M with low salt]**				
Accepts DPCoA as a Inhibitor	**100 x better K_I than CoA**				
Accepts 2′-phosphate isomer as an inhibitor: Se-CoA has a 3.5 x better K_I than Se-iso-CoA					
CoA	SH	H	P	3.8±0.1 µM [0.25±0.03 µM] (307)	1.8 µM competitive w.r.t. to AcCoA
Se-CoA	SeH	H	P	---	7 µM competitive
Se-iso-CoA	SeH	P	H	---	25 µM competitive
dephospho-CoA	SH	H	H	39±3 µM [27±2 µM] (307)	500 µM competitive
dephospho-Se-CoA	SH	H	H	---	700 µM competitive
Ado-3′-P-5′-P	---	H	P	---	415 µM competitive

Table 18 Continued

Ado-2′-P-5′-P	---	P	H	---	2200 µM competitive
Ado-5′-P	---	H	H	---	2500 µM competitive
Acetyl-CoA	AcS	H	P	Y 25.7 µM	Yes
Acetyl-dephospho-CoA	AcS	H	H	Y 54.8 µM	Yes Info not in abstract
Acetylcholine	---	-	-	900±100 µM [400±60 µM] (307)	

[2.3.1.8] Phosphotransacetylase (265,300,301,303,304,327,345,346)

Acetylphosphate + CoA ⇌ Acetyl-CoA + Pi

Accepts DPCoA as a Substrate 20 x better K_M; 17 x better k_{cat}; 350 x better k_{cat}/K_M (347)

Rejects 2′-phosphate isomers as substrates

Rejects 2′-phosphate isomers as inhibitors

CoA	SH	H	P	Yes	No
Dephospho-CoA	SH	H	H	0.5% CoA	---
Dephospho-CoA	SH	H	H	10% of CoA	---

				K_M (mM)	K_{cat} (S^{-1})	K_{cat}/K_M ($mM^{-1}s^{-1}$)
CoA (347)	SH	H	P	0.07±0.01	4,880±448	70,000
Dephospho-CoA (347)	SH	H	H	1.4±0.1	272±14	198

Iso-CoA	SH	P	H	No	No
Se-CoA	SeH	H	P	No	No
Oxy-CoA	OH	H	P	No	K_I 0.35 µM Competitive
Isomeric Mix of Oxy-CoA	OH	Mix		No	0.6 µM
Oxy-Iso-CoA	OH	P	H	No	No 0.5 % of oxy-CoA
3′-pyrophospho-CoA	SH	H	PP	Yes 2x CoA	--- (also from *C. kluyveri*,
CoA-SS-CoA	SCoA	H	P	No	--- *L. mesenteroides*, *E. coli*)

Inhibition Rate

Table 18 Continued

					E. coli	*Cl. kluyveri*
Ado-3′-P-5′-PP	---	OH	P	No	62	33
Ado-2′-P-5′-PP	---	P	OH	No	5	5
Ado-3′-P-5′-PP-CH_3	---	OH	P	No	33	22
Ado-2′-P-5′-PP-CH_3	---	P	OH	No	0	2
Ado-5′-P	---	OH	OH	No	2	0
Ado-3′-P	---	OH	P	No	0	0
ADP	---	OH	OH	No	48	0
ATP	---	OH	OH	No	37	0
Ado-3′-P-5′-P	---	OH	P	No	36	2
Ado-3′-P-5′-PP-$CH_2CH(CH_3)_2$	---	OH	P	No	81	43

[E.C. 2.3.1.9] Biosynthetic β-ketothiolase (222)

2 Acetyl-CoA ⇌ Acetoacetyl-CoA + CoA

Accepts 2′-phosphate isomers as substrates with equal facility. Isomers assayed simultaneously but were quantified HPLC which adequately resolved the isomers.

				K_M (μM)	K_{cat} (s^{-1})	K_{cat}/K_M ($M^{-1}s^{-1}$)	K_I (μM)
CoA	SH	H	P	Yes (222)	---	---	---
CoA	SH	H	P	16 (348)	---	---	16 μM
CoA	SH	H	P	9 (242)	---	---	---
Iso-CoA	SH	P	H	Yes (222)	---	---	---
Acetyl-CoA	AcS	H	P	Yes (222)	---	---	---
Acetyl-CoA	AcS	H	P	1100 (348)	---	---	---
Acetyl-CoA	AcS	H	P	1200 (242)	For. 71	For. 60 x 10^3	---
Acetyl-iso-CoA	AcS	P	H	Yes (222)	---	---	---
Acetoacetyl-CoA	AcAcS	H	P	44 (348)	---	---	---
Acetoacetyl-CoA	AcAcS	H	P	Yes (222)	---	---	---

Table 18 Continued

Acetoacetyl-CoA	AcAcS	H	P	15	(242)	Rev. 810		Rev. 53 x 10^6	---
Acetoacetyl-CoA	AcAcS	H	P	24	(215)	K_{cat} 465 s^{-1}		2.0 x 10^7	---
						V_{max} 10.7 mM·s^{-1}/mg			
Acetoacetyl-S-(D)-pantetheine	AcAcS	----		120	(215)	K_{cat} 353 s^{-1}		3.8 x 10^5	---
						V_{max} 8.1 mM·s^{-1}/mg			
Acetoacetyl-S-(D-pantetheine)-11-pivalate	AcAcS	----		73	(215)	K_{cat} 469 s^{-1}		6.9 x 10^6	---
						V_{max} 10.8 mM·s^{-1}/mg			
Acetoacetyl-S-(L-pantetheine)-11-pivalate	AcAcS	----		670	(215)	K_{cat} 256 s^{-1}		3.8 x 10^5	---
						V_{max} 5.9 mM·s^{-1}/mg			
Acetoacetyl-iso-CoA	AcAcS	P	H	Yes	(222)	---		---	---

[2.3.1.21] Carnitine Palmitoyltransferase (297)

Palmitoyl-CoA + carnitine ⇌ palmitoylcarnitine + CoA

Accepts 2′-phosphate isomer compound as an inhibitor (Isomeric Mixture)					
Heptadecan-2-onyldethia-CoA 1:1	CH_2	Mix	---	1.35 µM (@ <30 µM P-CoA)	
S-heptadecyl-CoA	-S-	H	P ---	3.34 µM (@ <30 µM P-CoA)	

[2.3.1.44] AcCoA : Sialate 4-O-acetyltransferase (349)

acetyl-CoA + N-acetylneuraminate ⇌ CoA + N-acetyl-4-O-acetylneuraminate

Accepts DPCoA as a Inhibitor	**1.3 x better K_I than CoA**				
Acetyl-CoA	AcS	H	P	32.1 µM	
				V_{Max} 1.21 pmol/mg	
CoA	SH	H	P		K_I 240 µM
					% Inhibition at 1 mM final concentration
CoA	SH	H	P	---	100%
0.1 mM CoA	SH	H	P	---	40%
Dephospho-CoA	SH	H	H	---	79%

Table 18 Continued

5′-IMP	---	OH	OH	---		---
5′-IDP	---	OH	OH	---		17%
5′-AMP	---	OH	OH	---		---
5′-ADP	---	OH	OH	---		36%
β-NAD	---	H	H	---		25%
β-NADP	---	H	P	---		---
4,4′-diisothiocyanatostilbene	---	H	H	---		95%

[2.3.1.48] Histone Acetyltransferase P300 (350)

Acetyl-CoA + histone ⇌ CoA + acetylhistone

Accepts DPCoA as a Inhibitor	**31.25 x better K_I than CoA**				
Lys-CoA	SH	H	P	No	Y IC_{50} 50 nM
Dephospho-Lys-CoA	SH	H	H	No	Y IC_{50} 1.6 μM

[2.3.1.54] Formate C-acetyltransferase (Pyruvate formate lyase) (351)

Acetyl-CoA + formate ⇌ CoA + pyruvate

Accepts DPCoA as a Substrate	**2.5 x better K_M**				
CoA	SH	H	P	12 μM	Inhibited > 75 μM
Pyruvate	---	---	---	1600 μM	---
Dephospho-CoA	SH	H	H	Yes, replaces CoA up to 40%	---

[2.3.1.57] Spermidine/spermine N-acetyltransferase (352)

Acetyl-CoA + an alkane-alpha, omega-diamine ⇌ CoA + an N-acetyldiamine

Accepts DPCoA as a Inhibitor	**Qualitative; 3′-phosphate considered essential for activity. Importance of 3′-phosphate explains why alkaline phosphatase inactivates the reaction.**			
CoA	S	H	P	---	Prevents Inactivation
Dephospho-CoA	S	H	H	---	< Inactivation than CoA

Table 18 Continued

Acetyl-CoA	AcS	H	P	---	Prevents Inactivation
NAD	---	P	H	---	Did nothing

[2.3.1.71] Glycine N-benzoyltransferase (353)

Benzoyl-CoA + glycine ⇌ CoA + N-benzoylglycine

Accepts DPCoA as a Inhibitor	**Qualitative Results**				
CoA	SH	H	P	---	Yes 0.1 mM CoA inhibits at 40% w/o KCl & 10% w/KCL
Dephospho-CoA	SH	H	H	---	Yes (ions diminishes inhib. ability)

[2.3.1.74] Chloramphenicol Acetyltransferase or Chalcone Synthase (354-356)

3 Malonyl-CoA + 4-coumaryl-CoA ⇌ 4 CoA + naringenin chalcone + 3 CO_2

Accepts DPCoA as a Substrate	**9 x better K_M (Depends on acyl group)**				
Accepts DPCoA as a Inhibitor	**CoA is better than DPCoA (Qualitative-Depends on acyl group)**				
Acetyl-CoA	AcS	H	P	90 μM	---
Acetyl-dephospho-CoA	AcS	H	H	840 μM	---
Malonyl-CoA (355)	MalS	H	P	3 μM	Substrate inhibition above 50μM
Malonyl-dephospho-CoA (355)	MalS	H	H	No	Y 50% inhibition at 3μM
4-coumaryl-CoA (355)	CouS	H	P	0.6 μM (primer)	substrate inhibition > 10μM
4-coumaryl-dephospho-CoA	CouS	H	H	Yes (primer)	---
CoA	SH	H	P	---	Yes
Dephospho-CoA	SH	H	H	---	No

[2.3.1.85] Fatty acid Synthase (299,309,310)

AcCoA + n malonyl-CoA + 2n NADPH + 2n H^+ ⇌ long-chain fatty acid + (n+1) CoA + n CO_2 + 2n $NADP^+$

Accepts DPCoA as a Inhibitor	**Qualitative Results**				

Table 18 Continued

2′-phosphate vs. 3′-phosphate specificity unclear. Isomeric mixture inhibits; authors propose that enzyme doesn't discriminate. Further experiments warranted.					
Acetonyldethia-CoA + isomer	CH_2	Mix	---		N
Ado-2′-P	---	P	H	---	Protects against inactivation
Ado-3′-P	---	H	P	---	No protection
CoA	SH	H	P	---	Increase inactivation Rate (stops inhib.) [17]
Dephospho-CoA	SH	H	H	---	Increase inactivation Rate (stops inhib.) [17]

[2.3.1.87] Serotonin N-acetyltransferase (357)

acetyl-CoA + an arylalkylamine ⇌ CoA + an N-acetylarylalkylamine

CoA is 2x better

Accepts DPCoA as a Inhibitor	**1.25 x better K_I for Acetyltransferase Activity** **2 x better K_I for Alkyltransferase Activity**					
Tryptamine-acetyl-CoA	SH	H	P	---	Inhibition of Stated Activity Acetyltransferase 0.048 µM	Alkyltransferase 33 µM
Tryptamine-acetyl-dephospho-CoA	SH	H	H	---	0.060 µM	60 µM

[2.3.1.97] N-myristoyltransferase (294,311,358)

Octapeptide + myristoyl-CoA ⇌ myristoyl-peptide + CoA

Accepts DPCoA as a Substrate	**Myristoyl-compounds: 8.3 x better K_D; 1.4 x better % Activity** **Palmitoyl-compounds: 8.9 x better K_D; 2.5 x better % Activity** **Lauryl-compounds: 135 x better K_D; 2 x better % Activity**				
Accepts 2′-phosphate isomers as inhibitors: Myristoyl-inhibitors: 6.7 x better K_I					
Myristoyl-carba(dethia)-CoA	CH_2	H	P	---	Competitive K_I 0.3 µM
Myristoyl-carba(dethia)-iso-CoA	CH_2	P	H	---	Competitive K_I 2 µM
				K_d nM	% Act

Table 18 Continued

Lauryl-CoA	S	P	H	62	44
Lauryl-dephospho-CoA	S	H	H	8380	21
Myristoyl-CoA	S	P	H	15	100
Myristoyl-dephospho-CoA	S	H	H	124	73
Palmitoyl-CoA	S	P	H	26	1.6
Palmitoyl-dephopho-CoA	S	H	H	232	4

[2.3.3.1] Citrate Synthase (296,297,312,359)

Oxaloacetate + AcCoA ⇌ CoA + Citrate

Accepts DPCoA as a Inhibitor **Qualitative: Approximately the same inhibition**

2′-phosphate vs. 3′-phosphate specificity is unclear. Isomeric mixture inhibits so authors suggest no discrimination based on the comparison with S-heptadecyl-CoA but further experiments are warranted.

Acetonyldethia-CoA + Iso	CH_2	Mix	---		Competitive 13.2 µM
Heptadecan-2-onyldethia-CoA 1:1	CH_2	Mix	---		Non-Competitive 6-7.5 µM; 3.7 µM is ≈ to P-CoA @ 4.1 µM
S-heptadecyl-CoA	-S-	H	P	---	Non-Competitive 1-1.5 µM; 1.2 µM is ≈ to P-CoA @ 4.1 µM
110 µM CoA	SH	H	P	---	109% activity after 10 min
130 µM dephospho-CoA	SH	H	H	---	110% activity after 10 min
Acetyl CoA				4×10^{-4}	---

[2.3.3.8] ATP : Citrate Lyase (360)

Citrate + CoA + ATP ⇌ AcCoA + oxaloacetate + ADP + Pi

Enzyme is protected from thermal and proteolytic inactivation by 2 classes of compounds that bind at Site 1: the NADPH binding site and Site 2: the CoA binding site

Rejects DPCoA as an Inhibitor **CoA protects against inhibition at 1µM but DPCoA does not at 1mM**

Compounds that provide 50% Protection

Site 1 (NADPH)	Site 2 (CoA)

Table 18 Continued

	R	2′	3′	mM
β-NADPH	---	P	H	0.25
β-$NADP^+$	---	P	H	3
2′,5′-ADP	---	P	OH	2.5
2′-AMP	---	P	OH	20
2′-GMP	---	P	OH	40
α-NADPH	---	H	P	<0.25
α-$NADP^+$	---	H	P	2.5
2′,5′-ADP+NMNH	---	P	H	2.5

	R′	2′	3′	µM
CoA	SH	H	P	1
Acetyl-CoA	AcS	H	P	5
3′-$NADP^+$	---	H	P	25
3′-AMP	---	OH	P	8000
3′,5′-ADP	---	OH	P	100
Etheno-CoA	CH_2	H	P	100
2′-deoxy 3′,5′-ADP	---	H	P	<100

Compounds that do not Protect (Concentration given is the highest tested)

Site 1 (NADPH)

	R′	2′	3′	mM
Nicotinamide	---	--	--	10
NMNH	---	--	--	10
NMN	---	--	--	10
Ribose 5-phosphate	---	OH	OH	10
Nicotinamide hypoxanthine-DPH	---	--	--	10
AMP	---	OH	OH	10
ADP-ribose	---	OH	OH	10
NAD^+	---	P	OH	10
NADH	---	P	OH	10
2′,3′-Cyclic AMP	---			10
2′,3′-Cyclic $NADP^+$	---			10
3′,5′-Cyclic AMP	---			10
Pyrophosphate	---	--	--	10

Site 2 (CoA)

	R′	2′	3′	mM
Dephospho-CoA	SH	H	H	1
Pantothenate	---	--	--	10
Ribose 5-phosphate	---	OH	OH	10
AMP	---	OH	OH	10
ADP-Ribose	---	OH	OH	10
3′-GMP	---	OH	P	40
Guanosine 3′-phosphate 5′-diphosphate	---	OH	P	2
2′,3′-cyclic AMP	---			10
2′,3′-cyclic $NADP^+$	---			10
3′,5′-cyclic AMP	---			10

[2.3.3.9] Malate Synthase (361,362)

Acetyl-CoA + H_2O + glyoxylate ⇌ L-malate + CoA

Table 18 Continued

Rejects DPCoA as a Substrate					
Accepts DPCoA as a Inhibitor	**Qualitative: No comparison available**				
Acetyl-CoA	AcS	H	P	Yes	---
Acetyl-dephospho-CoA	AcS	H	H	No	Inhibitor of *Gossypium hirsutum*

[2.3.3.10] HMG-CoA Synthase (363,364)

Acetyl-CoA + acetoacetyl-CoA + H_2O ⇌ HMG-CoA + CoA

Accepts DPCoA as a Substrate	**Qualitative: No comparison Available**				
CoA	SH	H	P	---	30 µM w.r.t. Acetyl-CoA
CoA	SH	H	P	---	60 µM w.r.t. Acetoacetyl-CoA
				Acetyl transfer from acetyl-CoA to acceptor (µmol/min/unit enzyme)	
Dephospho-CoA	SH	H	H	0.48	
Cysteamine	SH	---		0.24	
Dithiothreitol	SH	---		0.020	
Glutathione	SH	---		0.008	

[2.3.3.13] α-isopropylmalate synthase (312)

Acetyl-CoA + α-ketoisovalerate ⇌ α-isopropylmalate

Accepts DPCoA as a Inhibitor	**Qualitative: Direct comparison not possible but CoA is at least 8x better as an inhibitor than DPCoA**				
					% Inhibition after 10 min
CoA [11 µM]	S	H	P	Salt changes profiles	83±3
CoA [110 µM]	S	H	P	---	>95
Dephospho-CoA [130 µM]	S	H	H	---	12±14
Oxidized-CoA [110 µM]	S-S	H	P	---	7±6
Reduced Glutathione [100µM]	SH	---			6±9

Table 18 Continued

[2.3.3.14] Homocitrate Synthase (312)

Acetyl-CoA + H2O + 2-oxoglutarate ⇌ 2-hydroxybutane-1,2,4-tricarboxylate + CoA

Accepts DPCoA as a Inhibitor	**Qualitative: Direct comparison not possible but CoA is at least 5x better as an inhibitor than DPCoA**	
		% Inhibition after 10 min
CoA [11 µM]	S H P ---	81±4
CoA [110 µM]	S H P ---	>95
Dephospho-CoA [130 µM]	S H H ---	18±14
Oxidized-CoA [110 µM]	S-S H P ---	13±4
Reduced Glutathione [100µM]	SH -------	9±7

[2.7.1.33] Pantothenate Kinase (365-367)

ATP + D-pantothenate ⇌ ADP + D-4′-phosphopantothenate

Accepts DPCoA as a Inhibitor	**At 0.25 µM ATP CoA is 44 x better At 1.00 µM ATP CoA is 2.7 x better At 4.00 µM ATP CoA is 2.8 x better DPCoA 1.3 x better relative activity than CoA (difference is slight and may be due to species differences**			
			% Inhibition at given ATP Concentration (µM) *E. coli* Pantothenate Kinase	
			0.25µM	1.0µM	4.0µM
CoA	SH	H P ---	44	76	94
Dephospho-CoA	SH	H H ---	1	28	51
Acetyl-CoA	AcS	H P ---	49	80	96
Palmitoyl-CoA	PS	H P ---	2	24	80

Table 18 Continued

					Relative Activity at 50 µM of the Stated Inhibitor **(367)** Rat Heart Pantothenate Kinase
CoA	SH	H	P	---	0.77
Dephospho-CoA	SH	H	H	---	0.99
3′,5′-ADP	---	H	P	---	0.98
Acetyl-CoA	AcS	H	P	---	0.94
Succinyl-CoA	SuS	H	P	---	0.84
Malonyl-CoA	MaS	H	P	---	0.91
Acetoacetyl-CoA	AcAcS	H	P	---	0.95

[2.7.8.7] holo-[acyl-carrier-protein] synthase / Surfactin synthetase-activating enzyme (Sfp) (368,369)

CoA + apo-[acyl-carrier protein] ⇌ adenosine 3',5'-bisphosphate + holo-[acyl-carrier protein]

Rejects DPCoA as a Substrate **DPCoA does not react at all**

				Modification of *E. coli* holo-ACP as demonstrated by MS (368)	% Relative Activity from *Streptococcus pneumoniae* (369)
CoA	SH	H	P	Yes	100
dephospho-CoA	SH	H	H	No	0
desulfo-CoA	CH_2	H	P	Yes	76
homocysteamine-CoA	HCSH	H	P	Yes	---
acetonyldethio-CoA	AcylS	H	P	Yes	---
benzoyl-CoA	BnS	H	P	Yes	---
phenylacetyl-CoA	PhAcS	H	P	Yes	---
malonyl-CoA	MaS	H	P	---	12
acetoacetyl-CoA	AcAcS	H	P	---	65
acetyl-CoA	AcS	H	P	Yes	91

Table 18 Continued

[2.8.3.5] Succinyl-CoA:3-oxoacid CoA Transferase (370)

Succinyl-CoA + Acetoacetate ⇌ acetoacetyl-CoA + succinate

3′-P little effect on k_{cat}/K_M for thiol ester intermediate

Accepts DPCoA as a Substrate	**K_S is approximately the same**				
CoA	SH	H	P	---	1.7 ± 0.5 mM
Desulfo-CoA	CH3	H	P	2.7 ± 0.7 mM	---
Acetoacetyl-CoA	AcAcS	H	P	K_S 0.2-1 mM	---
Acetoacetyl-dephospho-CoA	AcAcS	H	H	K_S 0.2-1mM	---
Acetyl-CoA	AcS	H	P	K_S 1.7 mM	---
Succinyl-CoA	SuccS	H	P	K_S 2-7mM	---
5′-ADP	--	OH	OH		45mM

Reactivity of Thiol Esters of CoA Transferase with Carboxylate Substrates

				Succinate		Acetoacetate	
				K_{cat}/K_M ($M^{-1}s^{-1}$)	K_M (M)	K_{cat}/K_M ($M^{-1}s^{-1}$)	K_M (M)
E-CoA	E-S	H	P	8.3×10^4	0.02	5×10^5	9×10^{-5}
E-dephospho-CoA	E-S	H	H	5×10^4	0.007	ND	ND
E-deamino-CoA	E-S	H	P	2×10^3	≥0.05	ND	ND

[2.8.3.10] Citrate-CoA Transferase (371)

Acetyl-CoA + citrate ⇌ Acetate + (3S)-citryl-CoA

Accepts DPCoA as a Substrate	**Same K_M; 28 x better V_{Max} :isolated transferase** **1.8 x better K_M; 2.6 better V_{Max} :transferase + deAc-citrate lyase**	
	Isolated Transferase	Transferase Integrated into deacetyl citrate lyase

Table 18 Continued

				K_M (µM)	V_{Max} µmol/min/mg	K_M (µM)	V_{Max} µmol/min/mg
Acetyl-CoA	AcS	H	P	1300	25 (k_{cat} 1300 min^{-1})	6700	9.1
Acetyl-dephospho-CoA	AcS	H	H	1300	0.9	12500	3.4
Propionyl-CoA	PrS	H	P	1300	25	3300	5500
Butyryl-CoA	BuS	H	P	1300	0.17	n.d.	n.d.
(3S)-citryl-CoA	CitS	H	P	200	(k_{cat} 1600 min^{-1})		

[2.8.3.12] Glutaconate CoA-Transferase (372)

Glutaryl-CoA + Acetate ⇌ AcCoA + Glutaconate

Accepts DPCoA as a Substrate **6.5 x better K_M; 3 x better V_{Max}**

				K_M (µM)	V_{Max} (relative)
Glutaryl-CoA	GS	H	P	15	100

AcCoA + (E)-Glutaconate ⇌ Acetate + glutaconyl-CoA

Acetyl-CoA	AcS	H	P	170	12
Acetyl-dephospho-CoA	AcS	H	H	1100	4

[3.1.3.16] Phosphoprotein Phosphatase (373)

A phosphoprotein + nH_2O ⇌ A protein + n phosphate

Assume does not discriminate, paper doesn't specify the actual values

Accepts DPCoA as a Inhibitor **ND**

Dephospho-CoA	SH	H	H	---	0.1-0.18mM
Acetyl-CoA	AcS	H	P	---	0.1-0.18mM
Isovaleryl-CoA	IVS	H	P	---	0.1-0.18mM
Isobutyryl-CoA	IBS	H	P	---	0.1-0.18mM

[3.4.21.26] Proline endopeptidase [Prolyl oligopeptidase] (374)

hydrolysis of Pro-/-, Ala-/- in oligopeptides

Table 18 Continued

Accepts DPCoA as a Inhibitor		**CoA is better than DPCoA but values are unclear**				
Acyl-CoA	AcS	H	P	---	Y:	Most Inhibition
CoA	SH	H	P	---	Y:	Middle Inhibition
Dephospho-CoA	SH	H	H	---	Y:	Least Inhibition

[4.1.1.31] Phosphoenolpyruvate Carboxylase (375)

phosphate + oxaloacetate ⇌ H_2O + phosphoenolpyruvate + CO_2

CoA-pyrophosphate analyzed in this example: Pyrophospho-derivative 6 x more active					
Acetyl-CoA	AcS	H	P	---	Allosteric effector
Acetyl-pyrophospho-CoA	AcS	H	PP	---	6 x more active

[5.4.99.2] Methylmalonyl-CoA mutase (288)

(R)-methylmalonyl-CoA ⇌ succinyl-CoA; Propionyl-CoA + oxaloacetate □ Methylmalonyl-CoA + pyruvate

Rejects 2′-phosphate isomers as substrates					
Propionylcarba(dethia)-CoA	CH_2	H	P	Y	---
Propionylcarba(dethia)-iso-CoA	CH_2	P	H	N	---

[6.2.1.1] Acetyl-CoA Synthetase (376-378)

ATP + acetate + CoA ⇌ AMP + diphosphate + acetyl-CoA

Accepts DPCoA as a Substrate		**1.24 x better K_M**			
CoA	SH	H	P	247 μM (better at lower ATP)	---
Dephospho-CoA	SH	H	H	307 μM	---
ATP	---	OH	H	235 μM	>36 mM
Acetyl-CoA	AcS	H	P	Yes	---
Acetyl-dephospho-CoA	AcS	H	H	Yes	---

[6.2.1.3] Long Chain Fatty Acid CoA Ligase (379-381)

ATP + long chain carboxylic acid + CoA ⇌ AMP + PPi + Acyl-CoA

Table 18 Continued

Accepts DPCoA as a Substrate	**9 x better K_M; 2.2 x better V_{Max} with *R. norvegicus* 2.75 x better K_M with *C. lipolytica***					
				K_M (µM)	Relative V_{Max} (%)	Species
CoA	SH	H	P	26-28	100	*R. norvegicus*
CoA	SH	H	P	40		*C. lipolytica*
Dephospho-CoA	SH	H	H	230-290	45-46	*R. norvegicus*
Dephospho-CoA	SH	H	H	110		*C. lipolytica*
Pantetheine	---	---	--	1100-1200	26-27	*R. norvegicus*
Pantetheine	---	---	--	2500		*C. lipolytica*
ATP	---	OH	OH	2300-2400		*R. norvegicus*
ATP	---	OH	OH	500		*C. lipolytica*
dATP		H	OH	12500-13000		
4′-phosphopantetheine				410-430	25-26	*R. norvegicus*
4′-phosphopantetheine				3300		*C. lipolytica*

[6.2.1.4] Succinic thiokinase (382,383)

GTP + succinate + CoA ⇌ GDP + phosphate + succinyl-CoA

Accepts DPCoA as a Substrate	**Equal to CoA, values not available**					
CoA	SH	H	P	Yes		---
Dephospho-CoA	SH	H	H	Yes	equal to CoA	---
3′-pyrophospho-CoA			PP	Yes	equal to CoA	---

[6.2.1.5] Pig Heart Mitochondrial succinic thiokinase / Succinyl-CoA Synthetase (304,382,383)

GTP + succinate + CoA ⇌ GDP + phosphate + succinyl-CoA

Accepts DPCoA as a Substrate	**Equal to CoA, values not available**					
CoA	SH	H	P	Yes		---
Dephospho-CoA	SH	H	H	Yes	equal to CoA	---
3′-pyrophospho-CoA			PP	Yes	equal to CoA	---

Table 18 Continued

[6.2.1.26] O-Succinylbenzoate-CoA Ligase (384)

ATP + o-succinylbenzoate + CoA ⇌ AMP + PPi + o-succinylbenzoyl-CoA

Accepts DPCoA as a Substrate	**Equal to CoA, values not available**				
CoA	SH	H	P	10 µM	---
Dephospho-CoA	SH	H	H	Yes	---
ATP	---	OH	OH	400 µM	---

[6.4.1.1] Pyruvate carboxylase (385)

ATP + pyruvate + HCO_3^- ⇌ ADP + phosphate + oxaloacetate

Discriminates 3′-phosphate considered important since acetyldeamino-CoA is a 7x better inhibitor

Accepts DPCoA as a Inhibitor	**DPCoA is an inhibitor no direct comparison possible**					
				K_M µM	% V_{Max}	
CoA	SH	H	P	1070	6	Weak activator
Acetyl-CoA	AcS	H	P	22.7	100	Most Potent activator
Acetyl-3′-dephospho-CoA	AcS	H	H	---	---	$[I]_{0.5}$ 1.1 mM
Acetyldeamino-CoA	AcS	H	P	---	---	$[I]_{0.5}$ 0.15 mM
Adenosine 3′,5′-diphosphate	---	H	P	8000	4	Weak Activator
Adenosine-2′,5′-diphosphate	---	P	H	No	---	inhibitor
3′-AMP	---	OH	P	No	---	---
Propionyl-CoA	PrS	H	P	155	100	Activators

[6.4.1.2] Acetyl-CoA Carboxylase (299,314,386,387)

ATP + acetyl-CoA + HCO^{-3} ⇌ ADP + phosphate + malonyl-CoA

Accepts DPCoA as a Substrate	**Nearly equal**				
Accepts DPCoA derivative as an Inhibitor: CoA is 40 x better 3′-phosphate is considered essential					
Specificity for 2′-phosphate compounds is unclear. Isomeric mixture inhibits but experiments with purified isomers were not performed. Further experiments are warranted.					
Acetonyldethia-CoA + iso	CH_2	Mix		K_M 96 µM, V_{max} 1U	---

Table 18 Continued

Acetyl-CoA				Yes	---
Acetyl-dephospho-CoA				Yes Nearly Same as Acetyl-CoA	---
CoA	SH	H	P	Ka 25 μM; Kd 27 μM	Binding of CoA to AcCoA carboxylase stimulates inactivation of the carboxylase by AcCoA carboxylase kinase
Dephospho-CoA	SH	H	H	Yes	Also Stimulates inactivation by the kinase
Palmitoyl-CoA	PalmS	H	P	---	6.5 nM (387)
Palmitoyl-CoA(L)	PalmS	H	P	---	22 nM
Palmitoyl-keto-CoA	PalmS	H	P	---	21 nM
Palmitoyl-1,N^6-etheno-CoA	PCH_2	H	P		15 nM
Palmitoyl-inosino-CoA	PalmS	H	P		14 nM
Palmitoyl-dephospho-CoA	PalmS	H	H		260 nM
Palmitoyl-4′-phosphopantetheine	PalmS	---			650 nM
S-Cetyl-Coa	-OS-	H	P		10 nM

[E.C. Not Currently Classified] PHB Synthase *C. necator* (222) (A-(172)(B-(135))(D-(118)),(E (166))(F (165)) (G (161)) (H (167))

Ectothiorhodospira shaposhnikovii (I (169))

Bacillus megaterium (Granule bound) (388) , *Chromatium vinosum* (389)(C-Jossek), *Allochromatium vinosum* (A-(172))

β-hydroxybutyryl-CoA ⇌ PHB + CoA

Accepts 2′-phosphate isomers as substrates with equal facility. Isomers were assayed simultaneously but HPLC analysis permitted individual quantification.

iso-CoA	SH	P	H	Yes (Product) (222)	---

Table 18 Continued

CoA	SH	P	H	---			K_I 370 µM (118)	
CoA	SH	P	H	---			K_I 108 µM (165)	
CoA	SH	P	H	Yes (Product) (222)			---	
β-hydroxybutyryl-iso-CoA	HBS	P	H	Yes (222)			---	
β-hydroxybutyryl-CoA	HBS	H	P	Yes (222)			---	
β-hydroxybutyryl-CoA	HBS	H	P	92.5 µM (388)				
β-hydroxybutyryl-CoA	HBS	H	P	63 µM (389)			---	
β-hydroxybutyryl-CoA	HBS	H	P	232 µM (118)			---	
β-hydroxybutyryl-CoA (soluble)	HBS	H	P	680 µM (161)				
β-hydroxybutyryl-CoA (granule)	HBS	H	P	720 µM (161)				
β-hydroxybutyryl-CoA	HBS	H	P	243 µM (166)				
β-hydroxybutyryl-CoA	HBS	H	P	K_M 65 µM K_{cat} 320 s^{-1} (169)				
β-hydroxyvaleryl-CoA	HVS	H	P	1630 µM (161)				
				K_M (M)	K_{cat} (s^{-1})	k_{cat}/K_M ($M^{-1}s^{-1}$)		
β-hydroxybutyryl-CoA (165)	HBS	H	P	103 µM	339	3.3 x 10^6		
β-hydroxyvaleryl-CoA (165)	HVS	H	P	141 µM	253	3.3 x 10^6		
4-hydroxyvaleryl-CoA (165)	4HBS	H	P	301 µM	287	9.5 x 10^6		
3-hydroxypropionyl-CoA (167)	HPS	H	P	119 µM	10			
β-hydroxyvaleryl-CoA	HVS	H	P	202 µM (118)				
				C. necator (172)			A. vinosum (172)	
				% Rel. Activity		% Rel. Activity	k_{cat} (min^{-1})	K_M (mM)
β-hydroxybutyryl-CoA	HBS	H	P	100		100	3920[a]	0.13[a]
							1120[b]	0.45[b]

Table 18 Continued

(R)-3-hydroxypentanoyl-CoA	HPS	H	P	10	43	1680[a]	0.18[a]
						86[b]	0.32[b]
3-hydroxypropionyl-CoA	HPrS	H	P	0.5	1.9	76	0.22
(R)-3-hydroxyhexanoyl-CoA	HHexS	H	P	0.2	1	43	0.25
(2R,3R)—2-Methyl-3-hydroxybutyryl-CoA	MeHBS	H	P	ND	0.2	8.8	0.43
(R)-lactyl-CoA	LacS	H	P	ND	0.04	1.4	0.34
(S)-3-hydroxybutyryl-CoA	S-HBS	H	P	ND	---	---	---
4-hydroxybutyryl-CoA	4HBS	H	P	0.03	---	---	---
(R)-3-hydroxybutyryl-N-acetylcysteamine thioester (172)	HNAcS	---	Yes	0.02	0.09	39	86
(R)-3-hydroxybutyryl-N-acetylcysteamine thioester (135)	HNAcS	---	No		---	---	---
(R)-3-hydroxybutyryl (D)-pantetheine thioester (172)	HPanS	---	Yes	0.002	0.5	19	12
(R)-3-hydroxybutyryl (D)-pantetheine thioester (135)	HPanS	---	No		---	---	---
(R)-3-hydroxybutyryl-N-pantetheinepivalate thioester	HPiS	---	No	(135)			
(R)-3-hydroxybutyryl-N-phosphopantetheine thioester	HPPnS	---	No	(135)			

				% Reactivity	
				C. necator	E. Shaposhnikovii
3-hydroxybutyryl-CoA	HBS	H	P	100	100 (169)
[R]-3-hydroxypropionyl-CoA	HPS	H	P	3.5	0.65 (169)
[R]-3-hydroxyvaleryl-CoA	HVS	H	P	59	40 (169)
[R,S]-3-hydroxy-4,4,4-trichlorobutyryl-CoA	HBS	H	P	14	14 (169)

Table 18 Continued

[R,S]-3-cyclopropane-3-hydroxypropionyl-CoA	HPS	H	P	ND	3.9 (169)
[R]-3-hydroxyhexanoyl-CoA	HHS	H	P	0.94	0.86 (169)
[R,S]-3-hydroxy-4-methyl valeryl-CoA	HVS	H	P	0.45	0.15 (169)
[R,S]-3-hydroxy-4.4-dichlorobutyryl-CoA	HBS	H	P	ND	0.2 (169)
[R]-3-hydroxy-4-chlorobutyryl-CoA	HBS	H	P	ND	ND (169)
[R,S]-3-hydroxy-4-methyl hexanoyl-CoA	HHS	H	P	ND	0.1 (169)
[R]-3-hydroxyoctanoyl-CoA	HOS	H	P	ND	ND (169)
[R,S]-3-hydroxy-4-phenyl butyryl-CoA	HPhS	H	P	ND	ND (169)

*unless noted otherwise
a First Phase of the PHB synthase reaction
b Second Phase of the PHB synthase reaction

Enzymes that Reject Dephospho-CoA Compounds. ATP-citrate lyase, was found by Vogel and Bridger (360) to be protected from thermal or proteolytic inactivation by 1 µM CoA but not by very high (1 mM) concentrations of dephospho-CoA. These authors (360) reported several small molecules which protect ATP-citrate lyase against inactivation by binding to one of two sites. These two sites exhibit remarkable specificity in that a 3'-phosphoryl group on a nucleotide is the most important structural feature for interaction at the CoA-binding site (site 2), and that the NADPH binding site (site 1) is exclusive for 2'-phosphate compounds. Vogel and Bridger (360) further suggest that the existence of this NADPH binding site, which is independent of the catalytic center, may be a regulatory mechanism for lipogenesis.

Holo-[acyl-carrier-protein]-synthase [E.C. 2.7.8.7] from *Streptococcus pneumoniae* and *E. coli* , which catalyze the transfer of the 4'-phosphopantetheinyl moiety of CoA to a serine residue of apo-acyl carrier protein and thereby activates the protein for reactions, including fatty acid biosynthesis, also interacts exclusively with CoA. The impetus for the stringent selectivity of the holo-[acyl-carrier-protein]-synthase is currently unknown; however, this might possibly result from the need for this enzyme to exclude NADP(H), which is present during fatty acid biosynthesis. Considering this unusually stringent enzyme specificity, it seems reasonable that this selectivity may result from evolutionary demands on the enzyme to maintain distinct binding sites for CoA and NADPH.

Reactivity of Enzymes with NADP(H) and CoA Binding Sites with Dephospho-CoA. Remarkably, another enzyme that rejects dephospho-CoA analogues, Coenzyme A disulfide reductase from *P. horikoshii* (340-342), also employs both a NADPH and a CoA-containing compound. Considering that several enzymes that have both NADPH and CoA binding sites exhibit strong specificity for the presence of a 3'-phosphate of CoA, it seems reasonable to conclude that this phenomena may result from the particular evolutionary pressures on this class of enzymes. On the other hand, the Coenzyme A disulfide reductase enzyme from *S. aureus* (341), does react with dephospho-CoA disulfide. Furthermore, 3-hydroxybutyryl-CoA dehydrogenase [E.C. 1.1.1.157] and fatty acid synthase [E.C. 2.3.1.85], enzymes that both employ NADP(H) and a CoA-containing-compound, accept dephospho-CoA substrates. Collectively, these studies appear to suggest that suggest the rejection of dephospho-CoA compounds may be influenced by the enzyme binding to both 2'- and 3'-phosphate; however, other unknown factors are clearly involved. We note that many more enzymes, which reject dephospho-CoA compounds, may exist, but unfortunately, literature accounts are skewed toward reports of compounds that do interact with enzymes rather than those that do not.

Enzymes that Accept or Prefer the Dephospho-CoA Compounds. Most of the enzymes reported in the literature accept the dephospho-CoA derivatives albeit with less affinity than the CoA-containing compound. $NAD(P)^+$ transhydrogenase, highlighted in

purple in Table 18, is the only enzyme we found in the literature that actually showed a preference for the dephospho-CoA-derivatives (337,339). The enzyme, $NAD(P)^+$ transhydrogenase, catalyzes the reversible transfer of a hydride ion between NADPH and NAD^+. Rydstrom (339) reported that the presence of a 2′- or 3′-phosphate on the adenosine moiety determines the site specificity of the inhibitor. Specifically, that 2′- or 3′-phosphate-containing compounds inhibit with respect to NADP(H) whereas only dephospho-adenosine compounds inhibit with respect to NAD(H). Moreover, although Rydstrom (339) found that both 2′-ATP and 3′-ATP inhibit $NAD(P)^+$ transhydrogenase with equal facility, the synthesized 3′-NADP(H) is not a substrate. This indicates that during enzymatic catalysis, in which optimal binding conditions must be met, that this enzyme differentiates between phosphate locations. The author (339) further discusses how inhibition of $NAD(P)^+$ transhydrogenase by CoA-containing compounds might be a regulatory mechanism since palmitoyl-CoA (and other saturated long-chain acyl-CoA compounds) is a highly potent enzyme inhibitor within physiological ranges. Thus, Rydstrom (339) suggests that palmitoyl-CoA inhibition may help regulate between NAD^+ use in fatty acid β Oxidation and $NADP^+$ consumption in biosynthesis.

Mechanisms of 3′-phosphate Enzyme Binding. Our survey of the literature indicates that the 3′-phosphate moiety of CoA is a rigid requirement for only a select few enzymes, and while most

enzymes prefer the presence of the CoA-phosphate moiety, the extent of this preference is dependent on the individual enzyme. To further elucidate the mechanisms behind this enzyme selectivity we undertook a comprehensive PDB databank search and a review of the literature to determine the specific residues involved in enzyme recognition of the 3′-phosphate moiety, and in some cases the ribose and/or the adenosine moieties of CoA, presented in Table 19. The data gathered in Table 19 was cross listed with Table 18 and annotations are inserted (in color) for those enzymes in which information was available in the literature regarding enzyme specificity for the dephospho-CoA or 2′-phosphate isomers, and the residues involved in CoA binding.

The information presented in Table 19, indicates that charged amino acid side chains (highlighted in yellow for arginine; green for lysine; and pink for histidine, and aspartate) comprise the majority of interactions with the negatively charged 3′-phosphate moiety of CoA. Most enzymes utilize arginine and/or lysine to interact with the 3′-phosphate of CoA but histidine and/or aspartate are also often involved. Additionally, several interactions were reported with the residues serine, threonine, asparagine, and tyrosine, which possess uncharged polar side chains and are able to form hydrogen-bonds with the phosphate moiety.

Table 19. Protein Residue Interactions with the 3'-phosphate of CoA.

[E.C.] Enzyme Name Reaction

Accepts DPCoA-Derivatives as Substrates: Green

Accepts DPCoA Derivatives as Inhibitors: Dark Blue

Accepts 2′-phosphate-derivatives as Inhibitors: Light Blue

Rejects DPCoA-derivatives as Substrates: Dark Red

Rejects 2′-phosphate-derivatives as Substrates: Red

Rejects 2′-phosphate-derivatives as inhibitors: Lavender

- Presence and/or Location of specific residues that interact with the 3′-phosphate, ribose, or ADP moiety of CoA and CoA-derivatives
- Coloring Schemes of amino acid residues:
  - Charged Amino Acids: Arginine (R); Lysine (L); Histidine (H); Aspartate (D)
  - Uncharged polar side chains: Serine (S); Threonine (T); Asparagine (N); Tyrosine (Y)
  - Nonpolar side chains: Phenylalanine (F); Tryptophan (W); Isoleucine (I)

[E.C. 1.1.1.34] HMG-CoA reductase (390,391)

(R)-mevalonate + CoA + 2 $NADP^+$ ⇌ (S)-3-hydroxy-3-methylglutaryl-CoA + 2 NADPH + 2 H^+

- Y479 (OH) near (4.0-5.0 Å) 3′-phosphate
- R571 ^{1}H-bonds to 3′-Phosphate.
- N567 (3.0-3.2 Å) ^{1}H-bonds to ribose-2′-hydroxyl.
- CoA is tightly bound in a positively charged pocket near the enzyme surface.
- Pantothenic acid moiety extends deep into protein's interior.

- NADPH binding: S626; R627 ^{1}H-bond to 2′-hydroxyl of NADPH

[E.C. 1.1.1.35] L-3-hydroxyacyl-CoA dehydrogenase (392)

(S)-3-hydroxyacyl-CoA + NAD^+ ⇌ 3-oxoacyl-CoA + NADH + H^+

- K68 (a conserved basic residue) ^{1}H-bonds with 3′-phosphate group
- 3′-phospho-ADP of CoA is poorly defined suggests fairly mobile.

- NAD^+ Binding: S137 OH interacts with 2′-hydroxyl group of the nicotinamide ribose of NAD^+

[E.C. 1.3.99.2] Butyryl-CoA Dehydrogenase (393)

butanoyl-CoA + acceptor ⇌ 2-butenoyl-CoA + reduced acceptor

- N182 weak ^{1}H-bond with 3′-phosphate (393)
- other interactions similar to MCAD (394)

Table 19 Continued

[E.C. 1.3.99.3] medium-chain acyl-CoA dehydrogenase from Pig Liver mitochondria *(395)*

acyl-CoA + acceptor ⇌ 2,3-dehydroacyl-CoA + reduced acceptor

Accepts DPCoA-Derivatives as Substrates: 2x better K_M than CoA ; Same V_{Max} as CoA (306)
9x better K_M; 3.7 x better kcat with CoA (335)

Study discrepancies purportedly because of sub-saturating concentrations of the electron acceptor or possibly because of different biological origins.

Accepts DPCoA-Derivatives as an Inhibitor: Qualitative: Diminished inhibitor

- S19 potentially ^{1}H-bonds with 3′-AMP moiety of octanoyl-CoA
- solvent exposed 3′-AMP moiety of octanoyl-CoA

[E.C. 1.3.99.10] Isovaleryl-CoA dehydrogenase (396)

3-methylbutanoyl-CoA + acceptor ⇌ 3-methylbut-2-enoyl-CoA + reduced acceptor

- R191; S190; Y245 ^{1}H-bonds with 3′-phosphate

[E.C. 2.1.3.1] Methylmalonyl-CoA carboxytransferase (397)

(S)-methylmalonyl-CoA + pyruvate ⇌ propanoyl-CoA + oxaloacetate

Rejects 2′-phosphate-derivatives as Substrates: Good qualitative example with pure isomers

- R35 ^{1}H-bonds with the 3′-phosphate

[E.C. 2.3.1.6] Choline Acetyltransferase (307,344,398)

Choline + Acetyl-CoA ⇌ CoA + Acetyl-Choline

[values in brackets were gathered at low anion concentration]

Accepts DPCoA-Derivatives as Substrates: 10 x better K_M [108 x better K_M with low salt]

Accepts DPCoA Derivatives as Inhibitors: 100 x better K_I than CoA

Accepts 2′-phosphate-derivatives as Inhibitors: Se-CoA has a 3.5 x better K_I than Se-iso-CoA

- K413; K417 interact with the 3′-phosphate (398),
- Previous reports (307,344) that the 3′-phosphate interacts with R452 appear to be incorrect since this residue is too far away (11A) to interact with the 3′-phosphate group of CoA.

[E.C. 2.3.1.7] Carnitine Acetyltransferase (399)

acetyl-CoA + carnitine ⇌ CoA + O-acetylcarnitine

- K419; K423 (conserved residues) recognize the 3′-phosphate group.

[E.C. 2.3.1.8] Phosphotransacetylase (346,347,400)

Acetylphosphate + CoA ⇌ Acetyl-CoA + Pi

Table 19 Continued

Accepts DPCoA-Derivatives as Substrates: 20 x better K_M; 17 x better k_{cat}; 350 x better k_{cat}/K_M *(347)*

Rejects 2′-phosphate-derivatives as Substrates

Rejects 2′-phosphate-derivatives as inhibitors

- R87 salt bridge with the 3′-phosphate.

[E.C. 2.3.1.9] β-ketothiolase bacterial synthetic thiolase from *Z. ramigeria* (215,401-403)

AcCoA + AcCoA ⇌ AcAcCoA + CoA

Accepts DPCoA-Derivatives as Substrates: Biosynthetic thiolase is almost as active towards dephospho-Acetoacetyl-CoA as towards acetoacetyl-CoA (215,402,403)

- no direct contacts and no ^{1}H-bonding of 3′-phosphate and ribose moiety with protein observed for CoA (403) and Acetyl-CoA (402) bound crystal structures (402,403).

[E.C. 2.3.1.9] Human Cytosolic Thiolase (404)

2 acetyl-CoA ⇌ CoA + acetoacetyl-CoA

- K210; K211 point toward the 3′-phosphate.
- R223 side-chain ^{1}H-bonds to the ribose O2 atom
- 2′-*endo* ribose conformation..

[E.C. 2.3.1.18] Galactoside acetyltransferase of *E. coli* (405)

acetyl-CoA + a beta-D-galactoside ⇌ CoA + a 6-acetyl-beta-D-galactoside

- K166; R180 interacts with 3′-phosphate.
- solvent exposed 3′-phosphate group
- anti glycosidic linkage of the adenine base directs it toward the protein.
- T165 ^{1}H-bonds to the ribose 2′-hydroxyl.

[E.C. 2.3.1.48] Histone acetyltransferase (406,407)

acetyl-CoA + histone ⇌ CoA + acetylhistone

Accepts DPCoA Derivatives as Inhibitors: CoA is 31.25 x better K_I

- No residues specifically interact with the 3′-phosphate or the ADP group
- Solvent exposed 3′-phosphate and ADP group.

[E.C. 2.3.1.54] formate c-acetyltransferase/pyruvate formate-lyase (408)

acetyl-CoA + formate ⇌ CoA + pyruvate

Accepts DPCoA-Derivatives as Substrates: CoA's K_M is 2.5 x better than DPCoA

Table 19 Continued

- *K161 salt bridge with the 3′- and 5′-phosphates*
- *R160 (strictly conserved) weak ^{1}H-bonds with ribose ring oxygen.*
- *2′-endo ribose conformation.*

[E.C. 2.3.1.74] Chalcone synthase (354-356,409)

3 Malonyl-CoA + 4-coumaryl-CoA ⇌ 4 CoA + naringenin chalcone + 3 CO_2

Accepts DPCoA-Derivatives as Substrates: CoA is 9 x better K_M

Accepts DPCoA Derivatives as Inhibitors: CoA is CoA is better than DPCoA (Qualitatively)

- R58; K77 ^{1}H-bonds with 3′-phosphate (409)
- R58; K55 interacts with 3′-phosphate (410)
- anti-glycosidic bond torsion angle of ribose
- 2′-endo ribose conformation

[E.C. 2.3.1.81] aminoglycoside N-acetyltransferase (411)

acetyl-CoA + a 2-deoxystreptamine antibiotic ⇌ CoA + N3'-acetyl-2-deoxystreptamine antibiotic

- CoA adopts different positions in the two halves of the asymmetric unit
- In complex 1: R119 (NH1-H_2O = 2.3 Å and H_2O-O32 = 3.0 Å) water-mediated interaction with 3′-phosphate.
- In complex 2, R119 interacts directly (NH1-O32 = 2.8 Å) with the 3′-phosphate oxygen
- solvent-exposed 3′-phosphate
- 2′-*endo* ribose conformation

[E.C. 2.3.1.97] N-myristoyltransferase (294,311,358,412)

Octapeptide + myristoyl-CoA ⇌ myristoyl-peptide + CoA

Accepts DPCoA-Derivatives as Substrates: (294,311,358)

Myristoyl-compounds: 8.3 x better K_D; 1.4 x better % Activity

Palmitoyl-compounds: 8.9 x better K_D; 2.5 x better % Activity

Lauryl-compounds: 135 x better K_D; 2 x better % Activity

Accepts 2′-phosphate-derivatives as Inhibitors: 6.6 x better K_I for CoA-derivatives (294,311)

R181 (guanido) salt bridge with 3′-phosphate (412).

H38 interacts with the 3′-phosphate (412).

K39; F40; W41 backbone amides interact with 3′-phosphate (412).

[E.C. 2.3.1.117] Tetrahydrodipicolinate (THDP) N-Succinyltransferase (413)

tetrahydrodipicolinate + succinyl-CoA ⇌ L-2-(succinylamino)-6-oxopimelate + CoA

Table 19 Continued

- *R217; R213 interact with 3′-phosphate*
- *solvent exposed 3′-phosphate*

[E.C. 2.3.3.1] Citrate Synthase (414,415)

acetyl-CoA + H2O + oxaloacetate ⇌ citrate + CoA

Accepts DPCoA as a Inhibitor: Qualitative: Approximately the same inhibition

2′-phosphate vs. 3′-phosphate specificity is unclear. Isomeric mixture inhibits so authors suggest no discrimination based on the comparison with S-heptadecyl-CoA but further experiments are warranted.

- R164 interacts with 3′-phosphate from Pig
- K254; K305 interacts with 3′-phosphate from *Pyrococcus furiosus*
- K313 interacts with 3′-phosphate from Antarctic bacterial strain DS2-3R overexpressed in *E. coli*; unlike the previous two, all CoA binding residues are on a single monomer (415).

[E.C. 2.3.3.9] Malate Synthase (416)

acetyl-CoA + H2O + glyoxylate ⇌ (S)-malate + CoA

Rejects DPCoA-derivatives as Substrates

Accepts DPCoA Derivatives as Inhibitors: Qualitative: No comparison available

- R125; R312 salt bridge 3′-phosphate
- Specifically, 3′-phosphate salt bridge between R125 (NH2 being 2.6 and 2.7 A away from A07 and A09 phosphate oxygens, respectively) and R312 (NH1 and NH2 are 3.0 and 2.8 A away from the phosphate oxygen A08)
- 2′-endo nucleoside conformation.

[E.C. 2.7.1.33] Pantothenate Kinase (417)

ATP + (R)-pantothenate ⇌ ADP + (R)-4'-phosphopantothenate CoA inhibits competitively w.r.t. ATP

Accepts DPCoA Derivatives as Inhibitors: DPCoA is a less potent inhibitor than CoA (417)

At 0.25 µM ATP CoA is 44 x better
At 1.00 µM ATP CoA is 2.7 x better
At 4.00 µM ATP CoA is 2.8 x better
DPCoA 1.3 x better relative activity than CoA (difference is slight and may be due to species differences

- R106 (guanidinium) salt bridge with the 3′-phosphate
- S102 (OH); I42 (amide) ^{1}H-bonds to 3′-phosphate

Table 19 Continued

[E.C. 2.7.7.3] Phosphopantetheine Adenylyltransferase
ATP + pantetheine 4'-phosphate ⇌ diphosphate + 3'-dephospho-CoA
D95 (Amide); a H_2O molecule ^{1}H-bond to the 3′-phosphate
[E.C. 2.7.7.23] UDP-N-acetylglucosamine diphosphorylase (418)
UTP + N-acetyl-alpha-D-glucosamine 1-phosphate ⇌ diphosphate + UDP-N-acetyl-D-glucosamine
• K446 interacts with 3′-phosphate through a conformationally mobile C-terminal tail that forms a portion of the acyltransferase active site. • R429 ^{1}H-bond with 3′-phosphate • 3′-phosphate may be critical to proper active site formation
[E.C. 2.7.8.7] Surfactin synthetase-activating enzyme (Sfp)/ holo-[acyl-carrier-protein] synthase (419,420)
CoA + apo-[acyl-carrier protein] ⇌ adenosine 3',5'-bisphosphate + holo-[acyl-carrier protein]
Rejects DPCoA-derivatives as Substrates: DPCoA does not react at all (368,369) **"The strong binding of the 3′-phosphate group agrees with other results that this moiety is indispensable for CoA binding** (420)**."**
• K28; K31 (ζ-amino); H90 (imidazole ε-nitrogen) salt bridge with the 3′-phosphate (420) • T44 ^{1}H-bonds to 3′-phosphate (420) (SFP) • 3′-endo ribose conformation with axial 2′-hydroxyl and equatorial 3′-phosphate group. This contrasts all other known protein-bound CoA structures (420) (SFP). • R53; H105 ^{1}H-bond to 3′-phosphate (419) (holo-[acyl-carrier-protein] synthase) • 3′-endo ribose conformation with axially 2′-hydroxyl and an equatorial 3′-phosphate (419) (holo-[acyl-carrier-protein] synthase)
[E.C. 2.8.3.16] Formyl-CoA transferase (421)
formyl-CoA + oxalate ⇌ formate + oxalyl-CoA
• R104 ^{1}H-bonded to 3′-phosphate, • Solvent exposed 3′-phosphate, ribose, and pyrophosphate. • Adenine moiety wedged into a thin cleft and solvent buried
[E.C. 3.1.2.23] 4-Hydroxybenzoyl-CoA Thioesterase (422)
4-Hydroxybenzoyl-CoA + H2O ⇌ 4-hydroxybenzoate + CoA
• R102; R150 interact with 3′-phosphate.

Table 19 Continued

[E.C. 3.8.1.7] 4-Chlorobenzoyl Coenzyme A Dehalogenase *(423)*

4-chlorobenzoyl-CoA + H2O ⇌ 4-hydroxybenzoyl-CoA + chloride

H23; R67 form positively charged pocket possibly interacting with the 3′-phosphate group
No electron density for the 3′-phosphate was observed; suggests study was contaminated by dephospho-CoA or dephosphorylation occurred (423).

[E.C. 4.1.1.41] Methylmalonyl-CoA Decarboxylase (424)

(S)-methylmalonyl-CoA ⇌ propanoyl-CoA + CO_2

Solvent exposed 3′-phosphate

- K253 (N^{ζ}) within ^{1}H-bonding distance of ribose 2′-hydroxyl

[E.C. 5.4.99.2] Methylmalonyl-CoA mutase (288,425)

(R)-methylmalonyl-CoA ⇌ succinyl-CoA

Rejects 2′-phosphate-derivatives as Substrates: Specifically rejects Propionylcarba(dethia)-iso-CoA

5 arginines; 1 lysine
[R45, R321, R283, K321] (425)

[E.C. 6.2.1.1] Acetyl-CoA synthetase (426)

ATP + acetate + CoA ⇌ AMP + diphosphate + acetyl-CoA

Accepts DPCoA-Derivatives as Substrates: 1.24 x better K_M

- R584 (From CT-domain) interact with 3′-phosphate
- R194 (adopts two conformations) may interact with the 3′-phosphate from the CoA bound to a symmetry related Acetyl-CoA Synthetase molecule—purportedly a crystal artifact and not true dimerization.
- Nucleotide portion of CoA is bound on the surface of the protein
- Phosphopantetheine moiety directed into the active site **(426).**

[E.C. 6.2.1.5] Succinyl-CoA Synthetase (427,428)

Succinyl-CoA + NDP + Pi ⇌ Succinate + CoA + NTP

Accepts DPCoA as a Substrate: DPCoA is equal to CoA and 3′-pyrophospho-CoA

- K42; S36; K66; T39 interact with 3′-phosphate.
- Anti glycosidic bond of adenine ring and the ribose moiety.
- 1′-exo ribose conformation (unusual); equatorial ribose OH and 5′-group and axial 3′-phosphate

[6.4.1.2] Acetyl-CoA Carboxylase (299,314,386,387)

ATP + acetyl-CoA + HCO^{-3} ⇌ ADP + phosphate + malonyl-CoA

Table 19 Continued

Accepts DPCoA as a Substrate: Nearly equal

Accepts DPCoA derivative as an Inhibitor: CoA is 40 x better 3′-phosphate is considered essential

Specificity for 2′-phosphate compounds is unclear. Isomeric mixture inhibits but experiments with purified isomers were not performed. Further experiments are warranted.

- K2034′ interacts with the 3′-phosphate

[E.C. Currently Not Classified] ZhuH, the priming β-ketoacyl synthase of the R1128 biosynthetic pathway. (429) Decarboxylative condensation between an acyl group derived from the corresponding acyl-CoA and a malonyl extender unit attached to an acyl carrier protein (ACP), resulting in the formation of a β-ketoacyl-ACP product.

- No interactions with the 3′-phosphate or ribose moieties
- Solvent exposed 3′-phosphate and ribose,.

[E.C. Currently Not Classified] Vat(D) a Streptogramin Acetyltransferase (430)
Inactivates Streptogramin Group A Antibiotics

- Solvent exposed 3′-Phosphate
- Anti glycosidic linkage of adenine and ribose
- Adenine ring points toward the protein.

[E.C. Currently Not Classified] CaiB: a CoA transferase (431)
γ-butyrobetaine-CoA + carnitine ⇌ γ-butyrobetaine + carnityl-CoA

- K97 and R104 coordinated by 3′-phosphate.
- CoA induces a substantial (3 Å) movement of the small domain toward the large domain which somewhat closes the active site.

[E.C. Currently Not Classified] Hexapeptide Xenobiotic Acetyltransferase (432)
Utilizes Acetyl-CoA to acylate a variety of hydroxyl-bearing acceptors

- R159 contacts the 3′-phosphate
- K144 ^{1}H-bonds to ribose 2′-hydroxyl

Salt Bridge Interactions with the 3'-phosphate of CoA.

Salt bridges are reported to occur with the 3'-phosphate moiety of CoA in seven different enzymes. In the case of pyruvate formate-lyase [E.C. 2.3.1.54], Becker and Kabsch (408) observed formation of a salt bridge between Lys-161 and the 3'- and 5'-phosphate of CoA. This is the only literature report in which a single residue generates salt bridges with two separate phosphate groups. Since Lys-161 is already donating a portion of its electron density to the ion pair with the 5'-phosphate, the presence of a 3'-phosphate may not substantially perturb the system. This might explain the why the K_M of CoA is only 2.5 fold better than that of the dephospho-derivative, since the 3'-phosphate may not contribute a great deal to the energy to bind this enzyme.

N-myristoyltransferase [E.C. 2.3.1.97] binds the 3'-phosphate of CoA via a salt bridge to the guanidinium of Arg-181 in addition to interactions with His-38, Lys-39, Phe-40, and Trp-41. Given the large number of interactions between the enzyme residues and the 3'-phosphate of CoA it is somewhat surprising that this enzyme does accept both the dephospho-derivatives and the 2'-phosphate isomers of CoA; however, the K_D for myristoyl-CoA is 8.3 fold better than the dephospho compound, and the K_I for myristoyl-CH2-dethia-CoA is 6.6 fold better than for the 2'-phosphate isomer.

With pantothenate kinase [E.C. 2.7.1.33] the 3'-phosphate of CoA forms a salt bridge with the guanidinium group of Arg-106

and hydrogen bonds to the Ser-102 hydroxyl moiety and to the Ile-42 amide. Yun *et al.* (417) asserts that the interactions of the 3′-phosphate of CoA are critical for CoA inhibition of pantothenate kinase since dephospho-CoA is significantly less potent.

Malate synthase [E.C. 2.3.3.9] presents an interesting example because acetyl-dephospho-CoA is an inhibitor for but not a substrate of this enzyme. The 3′-phosphate of CoA reacts with malate synthase via two salt bridges to separate arginine residues, Arg-125 and Arg-312. It seems reasonable to speculate that the 3′-phosphate moiety is essential for optimal substrate binding with ensuing catalysis whereas less the favorable binding of the acetyl-dephospho-CoA is adequate to the task of inhibiting malate synthase.

Iyer and Ferry (347) utilized mutagenesis studies of phosphotransacetylase [E.C. 2.3.1.8] to identify a specific arginine residue, Arg-87, that they report forms a salt bridge with the 3′-phosphate of CoA. The authors suggest that it is this salt bridge, which imparts the 350-fold preference for CoA over dephospho-CoA. Recently, Iyer and colleagues (400) published the first crystal structure of a phosphotransacetylase, and although this crystal was in its apo state (without CoA bound) the preliminary structure is consistent with formation of a salt bridge to the 3′-phosphate of CoA at Arg-87.

A salt bridge between Arg-452 and the 3′-phosphate moiety of CoA has also been reported for choline acetyltransferase

[2.3.1.6] by Wu and Hersh (307) and Mautner *et al* (344). However, McKenna and coworkers (398) recently refuted the conclusions of these two previous studies in their investigation of the apo crystal structure of choline acetyltransferase with modeled CoA and acetylphosphate substrate binding. McKenna and coworkers (398) state that the distance between Arg-452 and the 3′-phosphate moiety is too great (11 Å) for salt bridge formation and suggest instead that Lys-413 and Lys-417 interact with the 3′-phosphate moiety of CoA. Clearly, this discrepancy underscores the importance of unambiguous data from crystals with the ligand bound in order to determine the minute structural variations, which affect the binding of important substrates.

Perhaps the most intriguing example of salt bridge formation occurs with surfactin synthetase-activating enzyme (SFP) [E.C. 2.7.8.7] (420) which flatly rejects the dephospho-CoA as a substrate and maintains fully three salt bridges between the 3′-phosphate of CoA and Lys-28, Lys-31, and His-90 in addition to a hydrogen bond to Thr-44. Remarkably, the ribose unit of CoA is bound to SFP in a 3′-endo conformation, in which the 3′-phosphate is oriented equatorially, and the 2′-OH is oriented axially. This differs from all other known orientations of CoA bound to proteins, since the 2′-endo conformation is most common and the 1′-endo conformation observed only in the succinyl-CoA synthetase enzyme [E.C. 6.2.1.5] (427,428). Clearly, it is the tight binding of the 3′-phosphate CoA to this molecule in addition to other bonds, such as an additional ion pair between His-90 and

the 5′-phosphate of CoA, which maintain the unusual sugar conformation and results in this enzyme's strict specificity for the 3′-phosphate containing compounds (420).

As previously mentioned, the succinyl-CoA synthetase [6.2.1.5] enzyme (427,428) also binds the ADP-moiety of CoA in an unusual conformation. In this enzyme, the ribose is positioned in the 1′-exo conformation in which the hydroxyl-group of ribose is equatorial and the 3′-phosphate is axial via interactions with two lysines, a serine and a threonine. In contrast to SFP, succinyl-CoA synthetase accepts dephospho-CoA and 3′-pyrophospho-CoA with apparently equal facility as the physiological substrate CoA (304,382,383). In this case, despite the large number of interactions and the unusual conformation of the ribose ring, the 3′-phosphate of CoA is not critical to the functioning of succinyl-CoA synthetase.

Hydrogen Bonding Interactions with the 3′-phosphate of CoA.

Hydrogen bonding interactions are also an important mode of binding the 3′-phosphate of CoA. Hall *et al.* (397) reported the occurrence of a hydrogen bond between the 3′-phosphate of CoA and Arg-35 of methylmalonyl-CoA carboxytransferase [E.C. 2.1.3.1] (397). This enzyme accepts purified propionyl-CH2-CoA as a substrate but rejects the purified 2′-phosphate isomer, propionyl-CH_2-iso-CoA (288,289). In contrast, medium-chain acyl-CoA dehydrogenase [E.C. 1.3.99.3] (298,306,334,335) and chalcone synthase [E.C. 2.3.1.74] (354-356) accept dephospho-CoA derivatives as substrates and inhibitors (the specificity for the

2′-phosphate isomers is currently unknown) with the former enzyme generating a hydrogen bond between the 3′-phosphate and Ser-19, and the latter enzyme hydrogen bonding to an arginine and a lysine.

Enzymes with No Contacts to the 3′-phosphate of CoA. The crystal structures of several enzymes revealed no contacts between residues and the 3′-phosphate moiety of CoA. In the case of histone acetyltransferase [E.C. 2.3.1.48] (406,407) there are no interactions with the 3′-phosphate; this probably accounts for the promiscuity of this enzyme which is reported to accept dephospho-CoA derivates as inhibitors. However, Cebrat *et al.* (350) report that this enzyme exhibits a 31 fold preference for lys-CoA over dephospho-lys-CoA. The mechanism for the specificity with the lys-CoA isomers is not explained by the crystal results and remains to be determined.

Crystal Structure and Substrate Specificity for the Enzymes Involved in PHB Synthesis.

β-ketothiolase. Regarding the enzymes studied in this laboratory, the crystal structure has been reported for the β-ketothiolase enzyme [E.C. 2.3.1.9] from the prokaryote *Z. ramigeria*. Modis and Wierenga (402,403) have reported in two separate investigations that no direct contacts are observed in the crystal structure between the β-ketothiolase protein and either the 3′-phosphate or the ribose moieties of CoA and acetyl-CoA. These structural studies indicate that β-ketothiolase

should not discriminate on the basis of the position or presence of the 3′-phosphate; this is consistent with our own (222) as well as other investigations into the specificity of this enzyme. Davis *et al*. (215) reported that acetoacetyl-S-(L-pantetheine) is a substrate for the β-ketothiolase enzyme from *Z. ramigeria*, although the catalytic efficiency (K_{cat}/K_M) for this substrate (which lacks the adenosine 3′-phosphate, 5′-diphosphate moiety) is 53 fold lower than the native substrate, acetoacetyl-CoA (215). These results corroborate the studies performed in this laboratory that demonstrate clearly that the β-ketothiolase enzyme from *C. necator* accepts both the 3′-phosphate and the 2′-phosphate isomers of CoA with equal facility (222).

Acetoacetyl-CoA Reductase. While no crystal structure has been obtained for the NADPH-dependent acetoacetyl-CoA reductase [E.C. 1.1.1.36] enzyme that was studied in this laboratory, a crystal structure does exist for the closely related L-3-hydroxyacyl-CoA dehydrogenase enzyme [E.C. 1.1.1.35], which catalyses the same reaction, except NADH instead of NADPH is used. Baryckii *et al*. (392) reported that the electron density of the 3′-phospho-ADP moiety of β-hydroxybutyryl-CoA and acetoacetyl-CoA was poorly defined in the crystal structure of L-3-hydroxyacyl-CoA dehydrogenase. The authors (392) suggest that this indicates that the moiety is relatively mobile in the binding pocket. However, the authors further discuss how the current x-ray model supports a hydrogen bonding interaction between a conserved lysine residue, Lys-68, and the 3′-phosphate

group of CoA. The NADH-dependent L-3-hydroxyacyl-CoA dehydrogenase crystal data is in relatively good accord with our own laboratory results, which demonstrate that the closely related NADPH-dependent acetoacetyl-CoA reductase enzyme reacts with both the 2'- and 3'-phosphate isomers with apparently equal affinity (222). Our results are compatible with the kinetic studies performed by Ploux, Masamune and Walsh (220) on the acetoacetyl-CoA reductase from *Z. ramigeria* in which they demonstrated that acetoacetyl-S-(D-pantetheine)11-pivalate (absent the adenosine 3'-phosphate, 5'-diphosphate moiety) is an enzyme substrate, albeit with a catalytic efficiency 667 fold less than the physiological substrate, acetoacetyl-CoA. Further crystal studies of the NADPH-dependent acetoacetyl-CoA reductase enzyme would certainly be of interest.

PHB Synthase. PHB synthase was observed to react with both isomers of CoA-containing compounds in our laboratory (433), and this is the first report of an alteration to the structure of the CoA portion of the moiety which does not destroy or substantially diminish the capacity for enzymatic catalysis. Gerngross and Martin (135) reported that the PHB synthase enzyme from *C. necator* does not catalyze polymerization reactions with the (R)-3-hydroxybutyryl thioesters of pantetheine, pantetheinepivalate, phosphopantetheine, and N-acetylcysteamine, which are all absent the 3',5'-ADP moiety of CoA. In contrast, further studies by Sinskey, Stubbe and coworkers (172) demonstrate that the N-acetylcysteamine and the pantetheine thioesters are substrates

but with rates, respectively, 1/5,000 and 1/50,000 that of the native substrate. Despite this minor disparity, both groups agree that the 3′,5′-ADP moiety of CoA is critical to the polymerization reaction of PHB synthase (135,172). To date, no studies have been performed regarding enzyme specificity for substrates altered in the 3′,5′-ADP moiety of CoA, thus our results are the first to demonstrate that PHB synthase can accept alterations to this portion of the CoA molecule. Unfortunately, this membrane-associated enzyme is difficult to obtain in high yields with good purity; thus, no crystal structure is currently available. However, crystallization studies are currently underway at the USDA.

This careful review of the literature data has revealed that the specificity for the 3′-phosphate of CoA is somewhat of a mixed bag, and while some inferences can be drawn from the crystal data, few sweeping generalities can be made. For many enzymes, it remains to be determined whether salt bridges, hydrogen bonds and other binding interactions would be distorted by the presence of a phosphate in the 2′-position, rather than the 3′-position, of the ribose ring. From the literature, it is clear that each enzyme must be evaluated on a case-by-case basis using purified isomers to determine how the phosphate position would affect the binding of CoA.

High Performance Liquid Chromatography. The traditional method for resolving isomers of CoA-containing compounds, ion

exchange chromatography (265,266,301), is often lengthy and, historically, neither ion exchange nor reversed phase separations have achieved baseline resolution. This limitation may have hampered investigations into isomers of CoA (305). Indeed, Rossier (305) reported using iso-seleno-CoA instead of iso-CoA in investigations of the importance of the CoA 3'-phosphate moiety on the activity of choline acetyltransferase. Wagner and Retey (294) resorted to multiple rounds of a complex 500 min gradient elution profile in order to adequately purify the isomers of myristoyl-carba(dethia)-CoA.

We report here efficient HPLC methodology, which achieves baseline resolution of CoA and acyl-CoA isomers. This technique, improves upon and simplifies the earlier work by Norwood *et al.* (225), and is the first HPLC method to separate a series of iso-CoA compounds, and we are able to separate four iso-CoA isomers within 30 minutes with baseline resolution using convenient isocratic elution. The methodology employed by Norwood *et al.* (225), which resolved short and medium chain (C_2-C_8) acyl-CoA compounds (including acetyl-CoA and β-hydroxybutyryl-CoA), required a two-step linear gradient and a complex mobile phase consisting of Buffer A: 0.2M ammonium acetate: 1.75% acetonitrile:2% glycerol; Buffer B: acetonitrile. We note that inspection of published HPLC elution profiles of CoA-containing compounds reveal several chromatograms which appear to contain iso-CoA-compounds that were not identified as such by the authors (434-438). Furthermore, iso-CoA isoforms may have been

overlooked by previous authors because the isomers will co-elute under stronger HPLC elution conditions.

The First Regioselective Chemical Synthesis of Iso-CoA. We also report here the first regioselective chemical synthesis of iso-CoA from CoA. Previously reported methods which produce iso-CoA as a byproduct of cyclic-CoA (I) hydrolysis yield mixtures containing both the 2′- and 3′-phosphate isomers in ratios of approximately 40%; 60%, respectively (265,266,284,285,287). In our simple synthesis, the cyclic-CoA moiety is efficiently produced from CoA, and then base-catalyzed hydrolysis in the presence of β-cyclodextrin in high salt produces iso-CoA regioselectively in high yields. Our results are in agreement with those of Komiyama and coworkers (439,440), who previously reported that β-cyclodextrin-based hydrolysis of adenosine and guanosine 2′,3′-cyclic phosphates gives reversed regioselectivity (i.e. 3′-clevage) as compared to the enzyme, ribonuclease.

As illustrated in Figure 36, Komiyama and coworkers (439,440) theorize that an adenine moiety will form an inclusion complex with β-cyclodextrin, resulting in steric constraints that direct base-catalyzed hydrolysis toward the 3′-bond; thus, producing the 2′-phosphate species, regioselectively. Selection of the alkali-metal halide is critical to the reaction selectivity. The chloride anion purportedly facilitates penetration of the adenine moiety deep into the β-cyclodextrin cavity, this enhances the steric clash at the 2′-position thus

favoring hydrolysis of the 3′-phosphate bond. Komiyama *et al.* demonstrate that the 2′/3′ selectivity is proportional to the electronegativity and inversely proportional to the size of the metal-halide anion such that the 2′/3′ selectivity follows the F>Cl>Br>I trend. We note that high concentrations of KF salted out some of the β-cyclodextrin and prevented easy rotary evaporation; the slight increase in regioselectivity afforded by KF over KCl did not merit these difficulties.

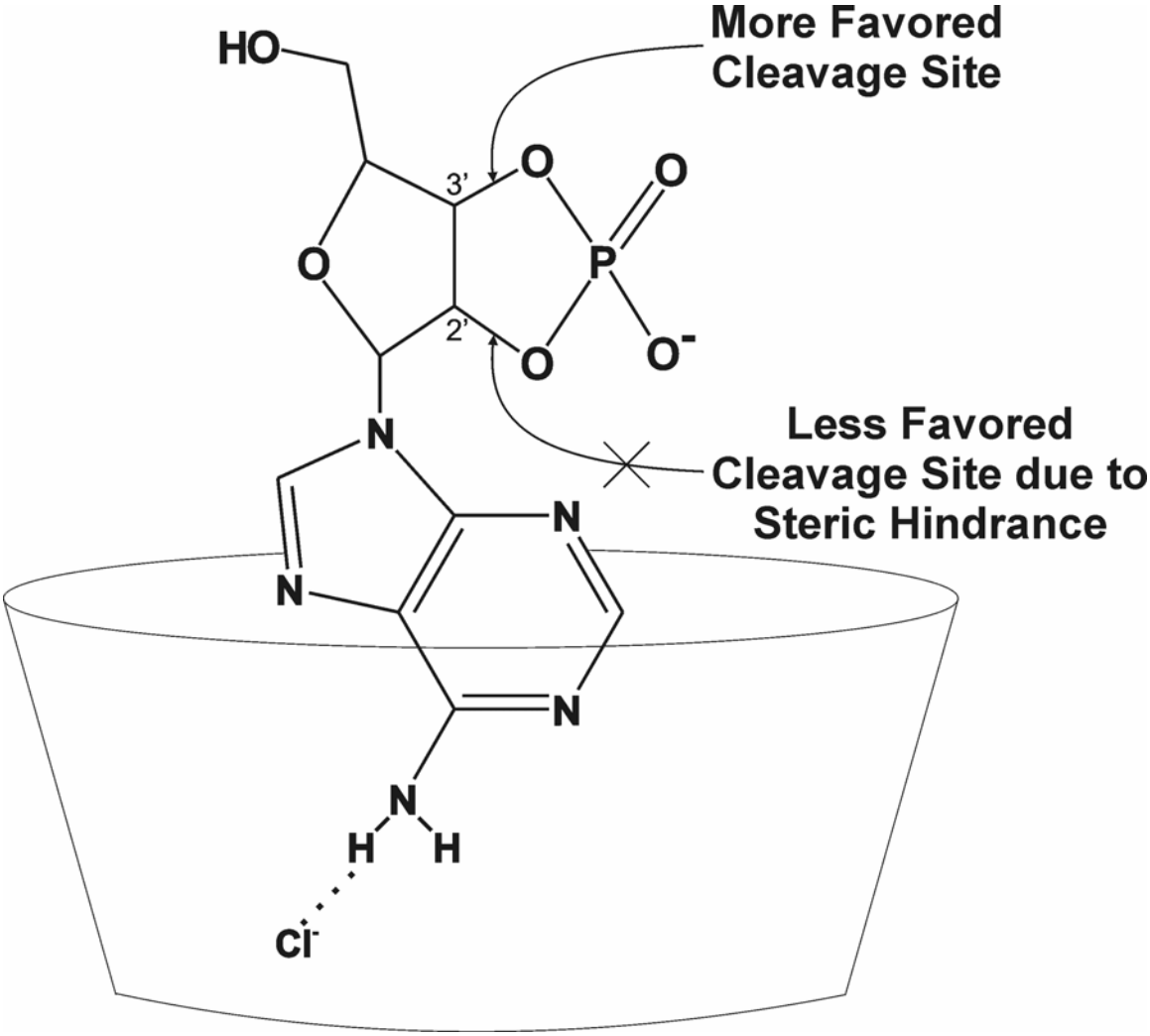

Figure 36. Proposed Structure of the [β-cyclodextrin-CL^{-} adenosine cyclic phosphate] Ternary Complex. Base-catalyzed hydrolysis at the 2′-position is less favorable due to steric hindrance; thus, the 3′-position is hydrolyzed leading to regioselective formation of the 2′-phosphate compound. (reproduced from (440))

Mechanism of Acid Catalysis for Iso-CoA Formation. We propose acid-catalysis as a plausible mechanism to account for the existence of the 2′-phosphate isomers in commercial preparations of CoA-containing compounds. In 1954, Kaplan and coworkers published preliminary reports about the acid-catalyzed synthesis of iso-CoA from CoA (278,315). These authors did not prove iso-CoA formation and only demonstrated that exposing CoA to strong acid decreased specific 3′-nucleotidase activity. Nevertheless, the acid-catalyzed migration of the 2′- and 3′-phosphate groups of NADPH (441) and nucleotides (156,442-444) is well established in the literature. The theoretical mechanism for the acid-catalyzed migration of phosphate compounds is depicted in Figure 37. In our hands, treatment of CoA with 0.5 M HCl produces an equilibrium mixture of 40% iso-CoA and 60% CoA within 60 hours, and 10% of the isomer can be generated within 4 hours. These results indicate that acid catalysis is a viable mechanism for rapidly producing iso-CoA from CoA, especially considering that strong acids are often used in several published CoA isolation procedures (273,445-448).

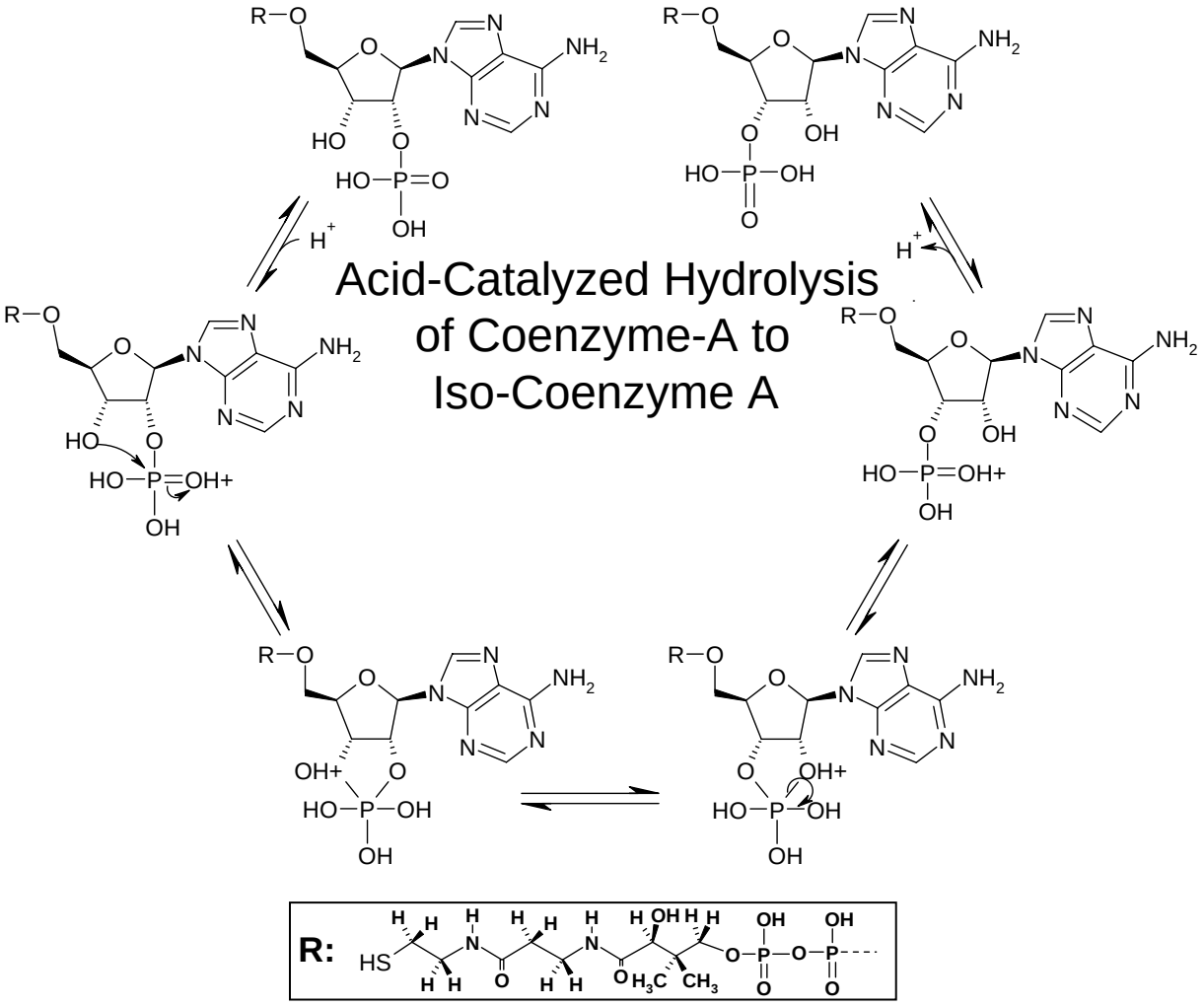

Figure 37. The Theoretical Mechanism for the Acid-catalyzed Hydrolysis of CoA to Iso-CoA. In the presence of strong acid the phosphate group of CoA forms a 2′, 3′-cyclic intermediate, which then is hydrolyzed forming an equilibrium mixture of CoA and iso-CoA.

The Biological Significance of Iso-CoA. The biological significance of iso-CoA-compounds is currently unknown. Khorana's original report (265,266) stating that phosphotransacetylase excludes iso-CoA probably has led to the generally held contention that the 2'-isomers are unnatural compounds. In contrast, Kurooka *et al.* (449) suggested that iso-CoA might be formed from crude cell extracts of *Proteus mirabilis* in the presence of 3'-dephospho-CoA. Kurooka *et al.* (449) reported that in buffered cell extracts containing a phosphotransferase from P. mirabilis, radioactive pNP^{32}P (p-nitrophenyl phosphate) and 3'-dephospho-CoA generated radiolabeled [^{32}P]-CoA. Detection of the radiolabeled [^{32}P]-CoA was accomplished using three separate methodologies: 1.) 0.0134 µmol of [^{32}P]-CoA was found with the phosphotransacetylase-hydroxamic acid assay that used CoA from Sigma as a standard; 2.) 0.016 µmol of [^{32}P]-CoA was detected by UV absorbance (260 nm; ε=14,600); 3.) 0.0175 µmol of [^{32}P]-CoA was detected via a radioactivity assay utilizing pNP^{32}P as the radioactive standard. Of these three detection methodologies, only the phosphotransacetylase-hydroxamic acid assay is specific for CoA, since the enzyme phosphotransacetylase does not accept iso-CoA as a substrate or inhibitor. The UV and radioactivity assay results indicate that more CoA is present than was detected using the stereospecific enzymatic assay. Furthermore, the results of the radioactivity assay suggest that the additional material is generated *de novo* by the phosphotransferase reaction or

radioactivity would not have been detected. These results lead the authors to suggest that the 3′-dephospho-CoA is also enzymatically phosphorylated at 2′-phosphate position giving rise to [^{32}P]-iso-CoA. Further, Kurooka *et al.* (449) cite two studies by Mitsugi *et al*. (450,451) which support Kurooka's contention for *de novo* generation of [^{32}P]-iso-CoA. The Mitsugi *et al*. studies (450,451) demonstrate production of adenosine 2′,5′-diphosphate and adenosine 3′,5′-diphosphate from the treatment of crude cell extracts with 5′-DMP and p-nitrophenyl phosphate (pNPP).

Similarly, Michaelson (282) reported that an unnamed partially-purified enzyme from calf brain selectively generated iso-CoA from cyclic-CoA *in vitro*. Michaelson stated that this enzyme (although unnamed) was known to cleave adenosine 2′,3′-cyclic phosphates to the 2′-phosphate. This enzyme was probably 2′,3′-cyclic 3′-phosphodiesterase [3.1.4.37], which belongs to the 2H phosphodiesterase superfamily of enzymes. This enzyme selectively produces 2′-phosphate nucleosides from their 2′,3′-cyclic species, such as NADP$^+$ generation from cyclic-NADP$^+$ (325). Although this enzyme constitutes approximately 4% of all myelin protein, to date the *in vivo* substrate for the 2′,3′-cyclic 3′-phosphodiesterase's [3.1.4.37] esterase activity has not been established (452-455). Kurooka *et al.* (449) and Michaelson's (282) reports suggest that iso-CoA could possibly be generated enzymatically *in vivo* from dephospho-CoA or 2′, 3′-cyclic-CoA; however, no definitive evidence for this notion exists.

Could Iso-CoA or a derivative be a substrate for the 2′,3′-cyclic-nucleotide 3′-phosphodiesterase (CNP) class of enzymes? Despite the importance of the 2′,3′-cyclic-nucleotide 3′-phosphodiesterase (CNP), which has been implicated in several myelin-related diseases including Alzheimer's and multiple sclerosis (455), the *in vivo* substrate remains an enigma. It is attractive to speculate that this enzyme may be involved in processing CoA, iso-CoA or some derivative of CoA. Indeed, in a 2003 report Kozlov *et al.* (454) postulated a similar hypothesis: that CNP might potentially act on signaling molecules such as nicotinic acid-adenine dinucleotide phosphate and cADP-ribose.

Structure and Specificity of CNP Proteins. The solution NMR structure of the catalytic fragment of the human brain 2′,3′-cyclic-nucleotide 3′-phosphodiesterase (hCNP-CF) was determined by Kozlov *et al* (454). The authors measured the dissociation constants (K_D) obtained by NMR titrations, and demonstrated a preference for 3′-AMP (K_D 0.57 ± 0.04) over 2′-AMP (K_D 1.49 ± 0.14) and 5′-AMP (K_D 1.68 ± 0.04); this was consistent with the measured competitive inhibition constants of 0.239 ± 0.013, 0.417 ± 0.012, and 1.10 ± 0.14, respectively. In addition, ATP was a very poor inhibitor with a K_I ~13 mM. The authors also compared the binding of $NADP^+$ (K_D 5.38 ± 0.55) and NAD^+ (K_D 21.19 ± 0.72), and determined that the phosphate group of $NADP^+$ significantly improved binding affinity. The binding affinity of the oligonucleotide, A6, for hCNP-CF was also examined because the

enzyme binding site resembles RNA-binding proteins in that it contains several aromatic (Tyr-168, Phe-172, Phe-235, and Tyr-352) and positively charged (Lys-214, Lys-234, R307) residues which are located on β-sheets. Furthermore, similar enzymes from this 2H phosphodiesterase family bind RNA and/or are active in RNA-processing pathways. Kozlov *et al.* (454) was surprised to find that the A6 RNA was a relatively weak inhibitor of hCNP-CF, with a KI of ~0.8, and that the chemical shift changes were smaller than with 3′-AMP or 5′-AMP, indicating weaker binding than the nucleoside phosphates. The authors do note that a 3′- or 5′- terminal phosphate might be important for binding since positively charged arginine and lysine residues are frequently present in CoA-binding sites. Certainly, determining the kinetic activity of the CoA isomers and derivatives with the hCNP-CF would be very interesting.

Crystal structure of the human CNP-catalytic fragment. The crystal structure for the catalytic fragment of human brain 2′,3′-cyclic-nucleotide 3′-phosphodiesterase (hCNP-CF) complexed with a phosphate ion at 1.8 Å resolution was recently published. In this report, Sakamoto *et al.* (455) suggests that the enzyme's narrow V-shaped active site cleft could accommodate only an extended single-stranded oligonucleotide or a mononucleotide. The small size of this enzyme's active site cleft effectively excludes double-stranded RNAs and RNAs containing secondary structures, such as tRNA, as potential substrates. A structural-homology search performed on this enzyme indicated that bacterial

RNA ligase and plant CPDase, which both belong to the 2H phosphoesterase superfamily, have similar topologies as hCNP-CF. A comparison of the electrostatic surface potentials of these three similar enzymes indicated that hCNP-CF is most similar to plant CPDase in terms of the size of the active site cleft and the array of positive charges surrounding it. Surprisingly, the physiological substrate for plant CPDase is the recently discovered small molecule, ADP-ribose 1”,2”-cyclic phosphate (Appr>p), shown in Figure 38, Panel B. This discovery certainly raises the possibility that hCNP-CF might act on other small nucleotide phosphates, such as CoA and or CoA-derivatives.

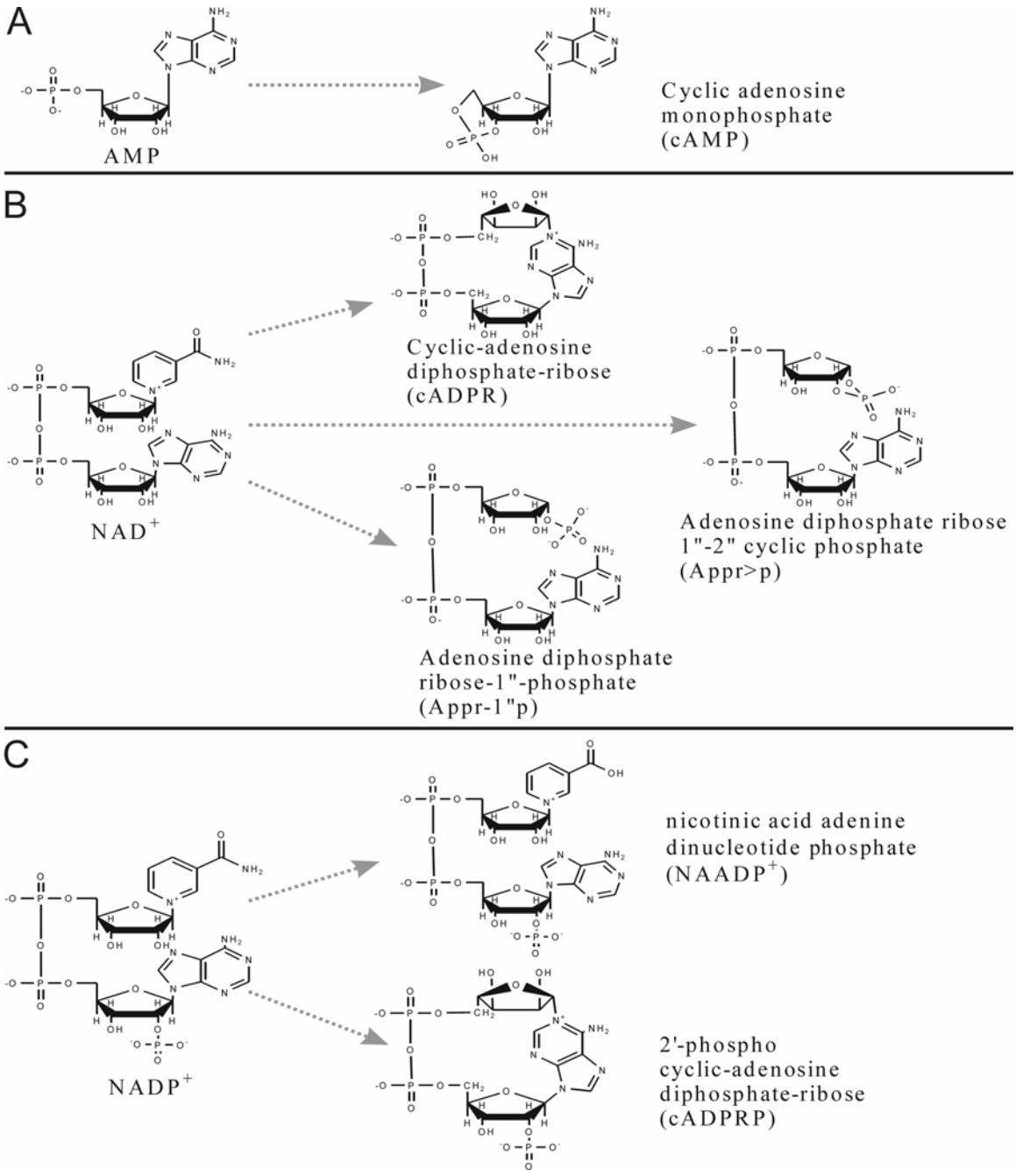

Figure 38. Nucleotide Phosphate Derivatives Known or Suggested to have Activity as Second Messengers in Cellular Signal Transduction.

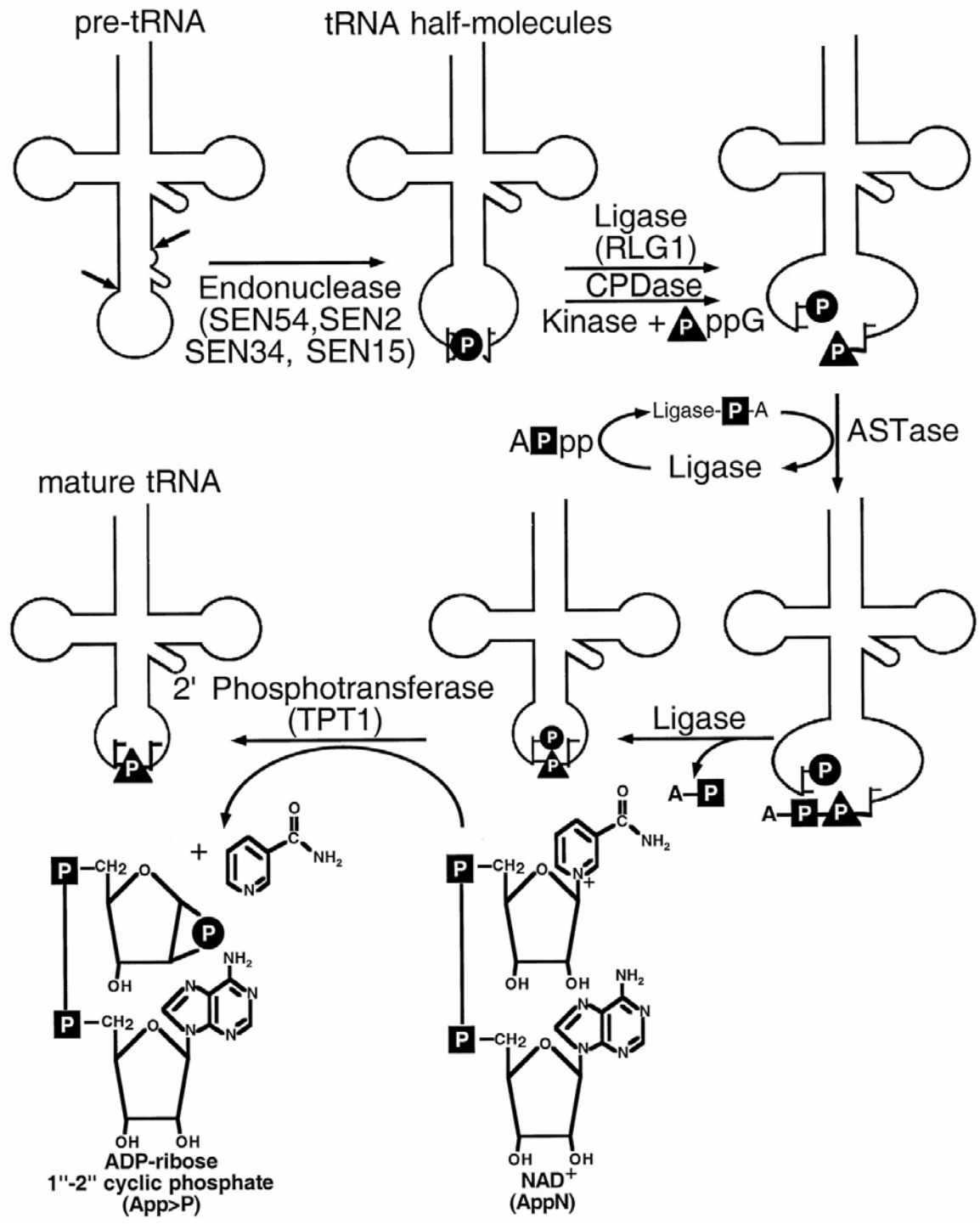

Figure 39. The tRNA Splicing Pathway of Yeast. Gene names are given in parenthesis for the proteins of the pathway. CPDase, cyclic phosphodiesterase; ASTase, adenylyl synthetase. Reproduced from Abelson *et al* (456).

Novel Substrates for the CPDase Enzyme Family. A specific class of enzymes in the CPDase family (known as Cpd1p in yeast) have been discovered, which catalyze the hydrolysis of ADP-ribose 1",2"-cyclic phosphate (Appr>p) generating ADP-ribose 1" phosphate (Appr-1"p) (455,457,458). Appr>p, shown in Figure 38, Panel B, was first identified *in vivo* in *Zenopus* oocytes by Culver *et al.* (459) in 1993, and is presumed to be a by-product of tRNA splicing (459,460). As illustrated in Figure 39, the Appr>p generated during the final step of tRNA splicing, in both plants (458,460,461) and yeast (457,462), is produced in equimolar quantities to the tRNA spliced. Deletion mutants of yeast CPDase (Cpd1p), prepared by Nasr and Filipowicz (457), established that all *in vivo* Appr>p hydrolyzing activity originated with the Cpd1p enzyme. When Appr>p was first discovered in 1993 Culver *et al.* (459) speculated that there may be some other cellular capacity for Appr>p. This speculation has been promoted in the literature (457,460-464) by two key points. First, this unique tRNA splicing pathway is conserved in vertebrates (457,459,465), although vertebrates preferentially splice tRNA using another RNA ligase; thus this pathway could function as a redundant tRNA splicing pathway or as a mechanism to generate Appr>p or its metabolites (457). Second, Appr>p is produced in yeast during each tRNA splicing event which is estimated to occur with up to 500,000 molecules of tRNA per generation (462). Furthermore, recent evidence suggests that baseline levels of Appr-1"p may be maintained by the cellular

environment because generation of Appr-1”p exceeds the rate of removal by the Poa1p-specific catabolic enzyme (462).

In contrast, studies of deletion mutants of Cpd1p performed by Nasr and Filipowicz (457), and Poa1p (the specific phosphatase that acts on Appr-1”p generating ADP-ribose *in vitro*) performed by Shull *et al.* (462), indicated that these deletion mutants grew normally and did not exhibit any unusual phenotype. These reports suggest that Appr>p and Appr-1”p do not play a critical role *in vivo*. Additionally, overexpression of Cpd1p to levels which should deplete Appr>p generate no change in the growth profile of yeast cells in standard media (457). Furthermore, Genschik *et al.* (461) found that neither Appr>p nor Appr-1”p had any affect on cADPR induced calcium release in sea urchin egg homogenates. Although these results tend to suggest that Appr>p and Appr-1”p are non-essential and do not mediate calcium release, unknown functions of these unique metabolites may still exist and are still under investigation (462).

Second Messengers. In spite of initial strong criticism from the scientific community, the concept of second messengers like cyclic-adenosine monophosphate (cAMP), which Sutherland (466) explored in the late fifties and received the 1971 Nobel Prize in Physiology or Medicine, is now an established concept in biochemistry. Indeed, an entire host of small molecules, such as cGMP and inositol-1,4,5-triphosphate (IP_3), were discovered in subsequent years and established to be involved as second

messengers in multiple molecular pathways. In the late eighties, while researching the effect of Ca^{++} mobilization on sea urchin egg microsomes, Lee and Coworkers (467) discovered that pyridine nucleotide metabolites could release nearly as much Ca^{++} as the well established calcium mediator IP_3. Extensive further studies have indicated that the NAD^+ metabolite, cyclic-ADP-ribose (cADPR) (468), as well as the $NADP^+$ metabolites, nicotinic acid adenine dinucleotide phosphate ($NAADP^+$) (469-471) and 2′-phospho-cyclic ADP-ribose (cADPRP) (472,473), shown in Figure 38, appear to act as second messengers which ultimately mediate Ca^{++} mobilization. Several experimentally established and proposed pathways for the generation of pyridine nucleotide phosphate derivatives are illustrated in Figure 40.

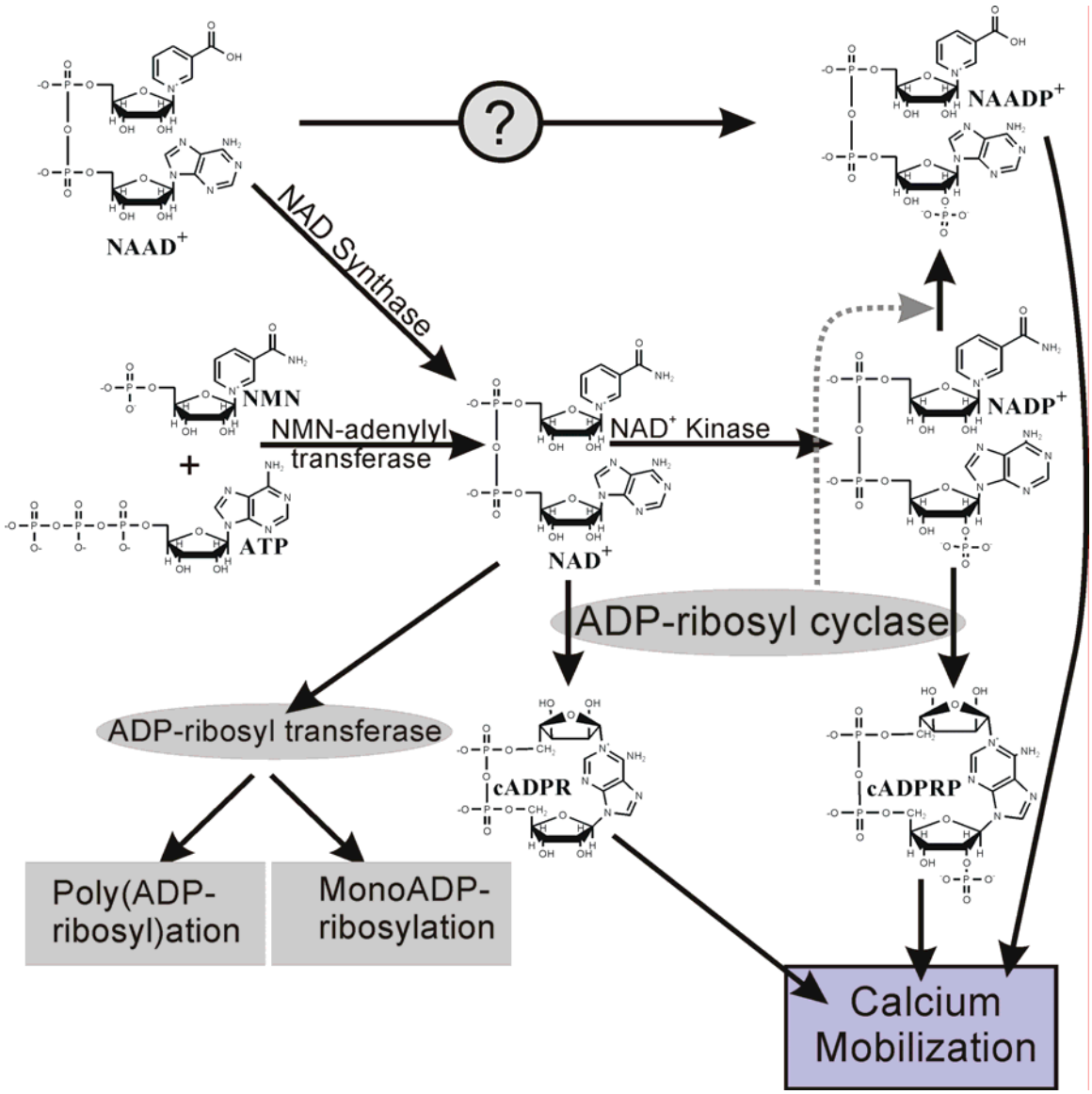

Figure 40. NAD^+-dependent Signaling Pathways generating Pyridine Nucleoside Diphosphate Derivatives (474).

Recently Discovered Second Messengers: cADPR and cADPRP.

The first discovered and most extensively studied of these new second messengers is cADPR (467,468) which has been shown to mediate calcium mobilization by acting on the ryanodine receptors (RYRs) (475); moreover, release of Ca^{++} from intracellular stores has been demonstrated in 50 different cell types from various phyla and species (475) suggesting widespread importance of this second messenger. The structurally similar NADPH metabolite cADPRP (2'-phospho-cyclic ADP-ribose) which was first identified in 1996 by Vu and coworkers (472,473) occurs naturally in mammalian tissues (473) and utilizes the same binding site and exhibits the same affinity as cADPR. Both cADPR and cADPRP elicit identical Ca^{++} mobilizing activity in rat brain microsomes (472,474,476), and Jurkat and HPB.ALL T-lymphocyte cell lines (477). In contrast, cADPRP exhibited no Ca^{++} releasing activity in sea urchin egg homogenates (478); this indicates a difference between higher and lower eukaryotes (479).

Considering the wealth of information presently available and currently in progress for the activity of cADPR there is comparatively little research into cADPRP. The similarities between cADPR and cADPRP in higher eukaryotes seems to have discouraged researchers from further investigating cADPRP. This dearth of information regarding cADPRP is discouraging in view of the importance of NADP(H) in reductive biosynthesis and the added energetic expense for NADP(H) biosynthesis (480). Frivolous biosynthesis of cADPRP seems odd since lower eukaryotes

putatively cannot utilize this substrate and higher eukaryotes would receive equal benefit from using NAD to produce cADPR. Certainly, further studies regarding the 2'-phosphate derivative of cADPR, cADPRP, are warranted.

Nicotinic Acid Adenine Dinucleotide Phosphate (NAADP). Within a two week time-span in 1995, two groups published the discovery of NAADP (nicotinic acid adenine dinucleotide phosphate), shown in Figures 18 and 19 (469,481). NAADP is derivative of $NADP^+$ and is reported to mobilize Ca^{++} from intracellular stores in approximately 50 different cell (475) types ranging from plants to humans (482). NAADP, which differs from NADP only in the exchange of $NADP^+$'s amide for a carboxylic acid group, apparently functions via a mechanism independent of either the IP_3 receptors or the ryanodine receptors, which bind cADPR (469,481). Current research indicates the presence of a novel, as yet uncharacterized Ca^{++} channel receptor for NAADP. Research shows that NAADP binds a site on sea urchin eggs with a K_D of 300 pM (483) and reports indicate that the Ca^{++} channels are located on novel lysosomal-like Ca^{++} stores (484,485) instead of the endoplasmic reticulum. Further investigations also revealed a requirement for phospholipids for NAADP receptor binding (485). Interestingly, studies of NAADP analogues have revealed that NAAD is functionally inactive; this indicates that the ribose-phosphate of NAADP is important to activity. However, both 3'-NAADP and 2',3'-cyclic-NAADP exhibit activity suggesting that the position of the ribose phosphate is not critical but that a

phosphate must be present on the ribose moiety for activity. Moreover, the reduced form of $NAADP^+$, NAADPH, has been shown to be functionally inactive at the NAADP receptor. Billington *et al.* (486) suggests that this may be a mechanism for inactivating the second messenger $NAADP^+$ *in vivo*. While NAADP research is in its infancy, it is ongoing and future studies into this novel second messenger may reveal entirely new pathways of signal transduction.

While the role of $NADP^+$ as a redox facilitator has been established for most of the century, the role of $NADP^+$ metabolites had been overlooked until the last few decades. It is clear that the potential significance for these metabolites is substantial. Possibly, this research will be crucial to elucidating the machinery of signaling pathways in a similar manner to Sutherland's pioneering work with cAMP and the once controversial second messengers.

Could CoA Derivatives Exist In vivo In a Regulatory Capacity. Given the relatively recent discovery of the $NADP^+$ metabolites, it is certainly sensible to consider the possibility that derivatives of CoA might exist *in vivo*, potentially acting in a regulatory capacity. The chemical structures of CoA and $NADP^+$ both contain an adenosine diphosphate moiety, as shown in Figures 2 and 10, but the structures differ in that CoA contains the pantothenic acid and mercaptoethylamine groups while $NADP^+$ possesses the nicotinamide ribose moiety. Despite obvious

structural dissimilarities, the CoA and $NAD(P)^+$ biosynthetic schemes, detailed in Figures 21 and 22, demonstrate that the biosynthesis of CoA does not necessarily consume more energy (in terms of ATP equivalents) than does the biosynthesis of $NADP^+$. This suggests that the likelihood of *in vivo* CoA derivatives is similar to the probability of $NAD(P)^+$ metabolites. In the case of CoA, shown in Figure 41, biosynthesis from pantothenate requires the conversion of 3 ATP to 3 ADP and the consumption of one ATP with liberation of pyrophosphate yielding a net consumption of 5 ATP equivalents. The situation with $NAD(P)^+$, illustrated in Figure 42, is somewhat more complex because two pathways are possible. When nicotinate or quinolinate are the starting materials, $NADP^+$ biosynthesis entails consumption of one ATP, and conversion of 3 ATP to 1 ADP and 2 AMP yielding a net consumption of 7 ATP equivalents (like the activation reaction in β-oxidation of fatty acids, conversion of each ATP to AMP consumes 2 ATP equivalents). If on the other hand $NADP^+$ biosynthesis begins with nicotinamide, a net of 5 ATP will be consumed—1 ATP consumed, and 2 ATP converted to 1 AMP (2ATP equivalents) and 1 ADP. Therefore, it is clear from the studies presented here that there is no inherent energetic advantage to utilizing metabolites of $NADP^+$ rather than CoA and that a derivative of CoA, such as iso-CoA, cyclic-CoA or a metabolite, might possibly be present *in vivo*. Nevertheless, it still remains to be determined if metabolites of CoA such as iso-CoA or cyclic CoA actually do exist *in vivo*.

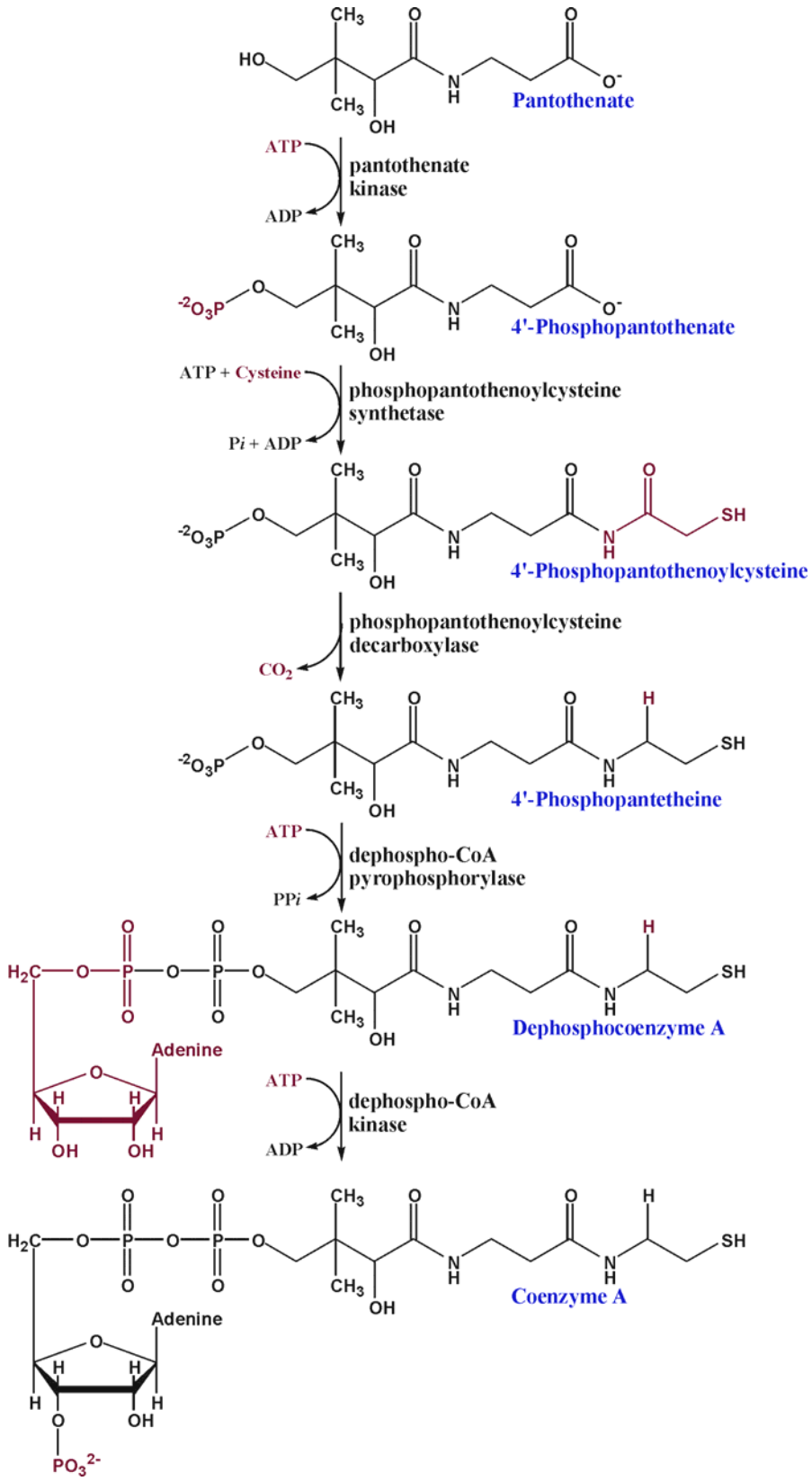

Figure 41. Biosynthesis of Coenzyme A. Reproduced from Voet and Voet (487).

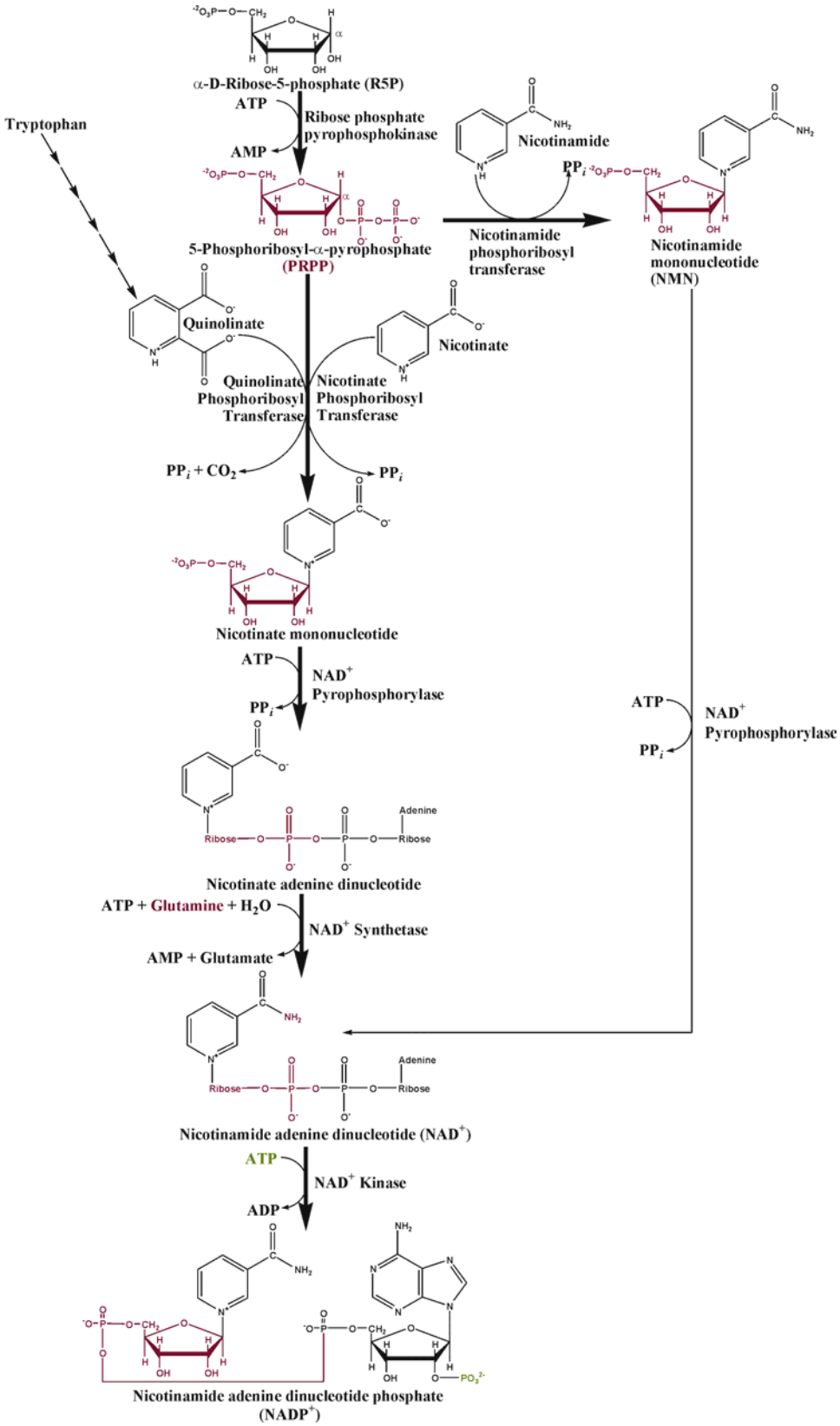

Figure 42. Biosynthesis of NAD(P)H. Modified from Voet and Voet (488).

While the biological significance of iso-CoA is presently unknown, the potential for this class of isomeric compounds is clearly significant. Iso-CoA isoforms have potential as pseudosubstrates, inhibitors, and as probes for investigating CoA binding to the extensive class of CoA-utilizing enzymes. We anticipate that our investigation, in addition to generating the first reports of enzymes that perform acyl-transfer reactions with iso-CoA isomers, will provide the necessary methodology for future studies into iso-CoA and acyl-iso-CoA compounds.

CHAPTER 10

ISO-COENZYME A: CONCLUSION

Herein we have reported the first structural analysis of iso-CoA, which was accomplished by 1D NMR, 2D NMR, MS, and MS/MS analyses of HPLC-purified samples. The isomers of acetyl-CoA, acetoacetyl-CoA, and β-hydroxybutyryl-CoA were also identified by HPLC-MS. These isomers were found to be good substrates for the enzymes β-ketothiolase, acetoacetyl-CoA reductase, and PHB synthase, which are the first enzymes shown to catalyze acyl transfer reactions with the 2'-phospho isomers of their natural compounds. We report the first HPLC method that separates a series of iso-CoA-containing isomers with baseline resolution, and this methodology was used to detect the presence of the 2'-phospho isomers in commercial preparations of CoA, acetyl-CoA, acetoacetyl-CoA and b-hydroxybutyryl-CoA. A novel regioselective synthesis of iso-CoA from CoA or cyclic-CoA is reported which uses β-cyclodextrin in high salt to produce iso-CoA in high yield. The generation of iso-CoA from CoA in the presence of strong acid is established, and this route is proposed as plausible mechanism, which may account for the presence of the iso-CoA isoforms in commercial preparations. Finally, we discuss the biological significance of the iso-CoA-containing molecules

in vivo, *in vitro* as probes for exploring enzyme binding, and as potential model compounds for the rational design of pseudosubstrates or inhibitors.

CHAPTER 11

SELENIUM REDOX CYCLING: INTRODUCTION

The biological role of selenium and selenium-containing compounds has been a subject of intense current interest. Selenium has been recognized for its antioxidant properties for at least 40 years (489). Selenium-containing compounds and proteins have been implicated in the amelioration of oxidative stress, which results from either a relative excess of pro-oxidants and/or a dearth of antioxidants (489). As many as thirty seleno-proteins have been identified (489) and many small molecular weight organoselenium compounds, including selenomethionine and ebselen (2-phenyl-1,2-benzisoselenazole-3(2H)-one), have been shown to exhibit antioxidative properties (489).

Peroxynitrite. Peroxynitrite is one of the major endogenous prooxidant and nitrating species (490,491). This cytotoxic compound is generated *in vivo* via the diffusion-limited reaction between superoxide anion and nitric oxide as shown in Figure 43 (489).

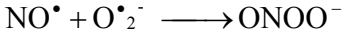

Figure 43. The Formation of Peroxynitrite

Peroxynitrite is highly reactive and overproduction of this species is believed to be involved in the pathways mediating tissue damage and inflammation (492). Several oxidation and nitration events within the body are known to be initiated by peroxynitrite, including lipid peroxidation, oxidation of sulfur groups such as sulfhydryls and methionine, tyrosine nitration, and the generation of single- and double-strand breaks in DNA supercoils (492).

Glutathione. Glutathione is an important endogenous antioxidant, which also acts as a general cellular reductant and is involved in metabolism of toxins (492). The so-called antioxidant status of the cell is in part maintained by glutathione. Glutathione can react *in vivo* with peroxynitrite. The reaction of glutathione with peroxynitrite can follow either a two-electron oxidation or a one-electron pathway, the latter reaction generating a sulfur-centered radical which then undergoes further metabolism (492,493). Glutathione can also protect against peroxynitrite-mediated oxidative damage via the action of the selenoprotein, glutathione peroxidase (GPx), as shown in Figure 44 where GSH is reduced glutathione and GSSG is the disulfide dimer of glutathione (492).

$$ONOO^- + 2GSH \xrightarrow{GPx} NO_2 + H_2O + GSSG$$

Figure 44: The Reaction of Peroxynitrite with Reduced Glutathione.

Organoselenium Compounds. Small organoselenium compounds, including selenomethionine, selenocystine, and ebselen have been found to be effective antioxidants against peroxynitrite-mediated damage (494,495). A study by Sies and coworkers (496) reported that the selenoorganic compounds, selenomethionine, selenocystine, and ebselen, are capable of protecting DNA from peroxynitrite-mediated single-strand breaks. The putative mechanism of DNA protection by organoselenium compounds is via the reaction of the selenium-compound with peroxynitrite to yield the corresponding organoselenoxide and nitrite as shown in Figure 45 (494). Selenoxides formed from a reaction with peroxynitrite can be reduced back to the corresponding selenides by the action of reduced glutathione (GSH). This ability of glutathione to reduce selenoxides can generate a catalytic cycle, which effectively increases the available quantity of selenium. Recycling with GSH does not occur with sulfur-containing compounds, as GSH does not reduce sulfoxides to sulfides.

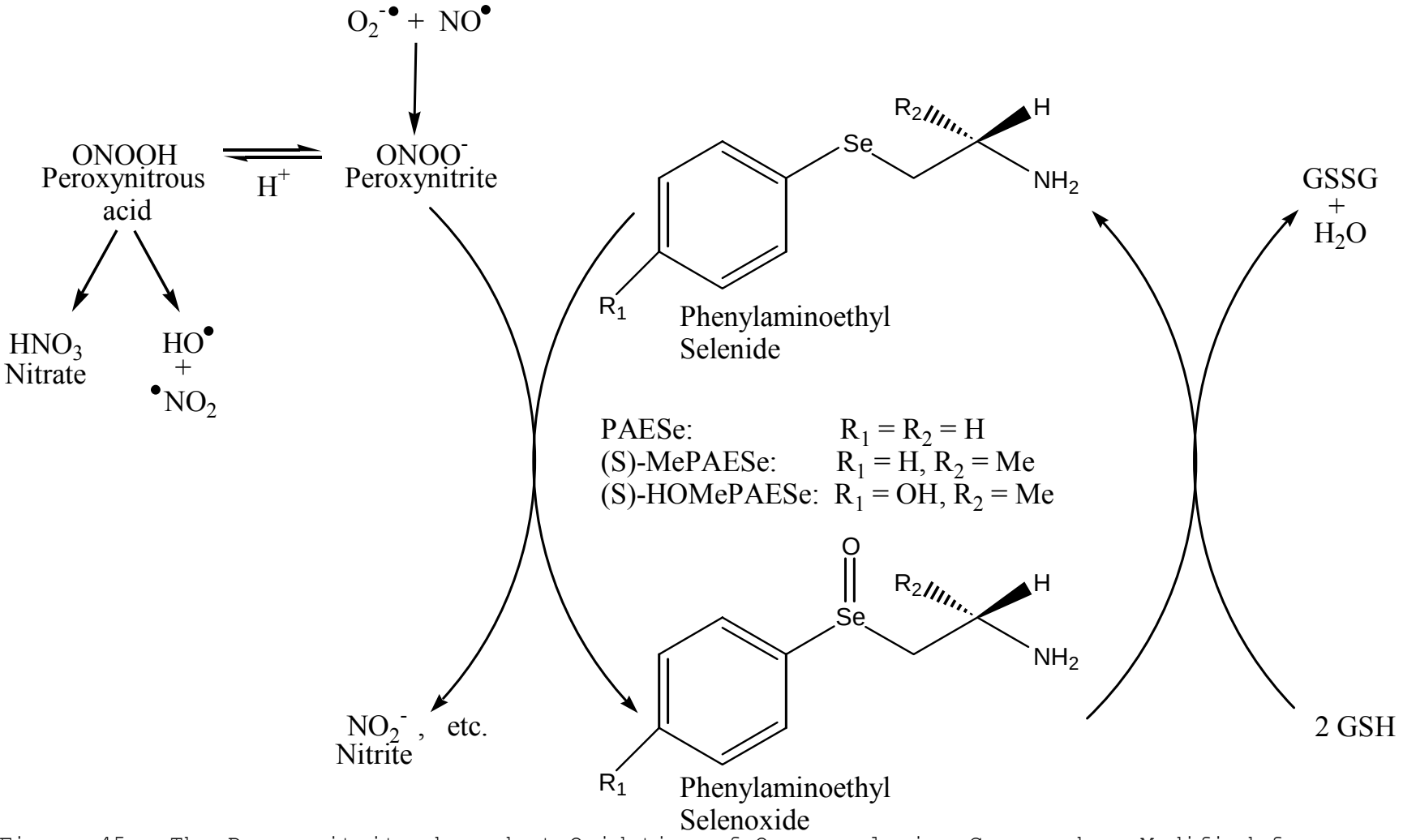

Figure 45. The Peroxynitrite-dependent Oxidation of Organoselenium Compounds. Modified from Masumoto and Sies (494)

Phenylaminoethyl Selenides. Recently, this laboratory demonstrated that phenylaminoethyl selenides (PAESe), which were developed as inhibitors of dopamine-β-monooxygenase, react efficiently with peroxynitrite to yield the selenoxide as the sole selenium-containing product (See Figure 45) (497). In addition, the second order rate constants for the reaction of PAESe and (S)-HOMePAESe with peroxynitrite are comparable to those of selenomethionine and the major metabolite of ebselen, 2-(methylseleno)benzanilide, measured at pH 7.0 and 25 C (497). Consequently, it seems reasonable to anticipate that these compounds could protect against oxidative damage and may have future pharmacological potential.

Herein we report that phenylaminoethyl selenide compounds protect DNA from peroxynitrite-mediated single-strand breaks (1). Moreover, these organoselenium compounds protect DNA more effectively than their sulfur analogues. Additionally, the ability of glutathione to enhance the protective effects of the selenium-containing compounds against peroxynitrite-induced DNA damage suggests that a selenium redox cycle, in which the peroxynitrite-generated selenoxide is recycled back to a selenide via glutathione, has been established. The mechanism of protection against peroxynitrite mediated DNA damage was investigated by HPLC for the selenium- and corresponding sulfur-containing compounds. HPLC analysis shows that phenylaminoethyl selenides are quickly oxidized by peroxynitrite forming

selenoxides as the sole selenium-containing product. Moreover, in the presence of reduced glutathione, the selenide to selenoxide ratio was higher suggesting the establishment of a glutathione-mediated catalytic redox cycle. Phenylaminoethyl sulfide (PAES) was, likewise, shown to react slowly with peroxynitrite to form a small quantity of the sulfoxide as the main product but no redox cycle could be established with the sulfur analogues (1). Finally, the unique chemistry of the reaction between peroxynitrite and HOMePAES was investigated using HPLC and HPLC/MS.

CHAPTER 12

SELENIUM REDOX CYCLING: EXPERIMENTAL

Reagents. Hydrogen peroxide and diethylenetriamine pentaacetic acid were obtained from Aldrich Chemical Co. (Milwaukee, WI). Reduced glutathione was obtained from Sigma Chemical Co.(St. Louis, MO). Selenomethionine was purchased from Acros Organics(Morris Plains, NJ). All other chemicals and solvents were purchased from standard commercial sources and were of the highest grade available. HPLC columns(C-8) were obtained from Alltech.

Synthesis of selenides and sulfides. (S)-HOMePAESe [(S)-1-(4'-hydroxyphenylseleno)-2-aminoethane] (498), PAESe[1-(phenylseleno)-2-aminopropane] (499) and the sulfur analogs HOMePAES (500,501) and PAES (501) were synthesized as described previously.

Synthesis of the selenoxides. Hydrogen peroxide oxidation of the selenides and was performed as previously described (497,498). Briefly, the hydrochloride salt of each selenide was dissolved in H_2O and reacted with a 30% solution of H_2O_2 in a 1:1 mole ratio. The reactions were monitored by HPLC and, once

complete, lyophilized overnight. Each phenyl-2-aminoethyl selenoxide product was recrystallized (methanol/ether) and characterized as follows:

HOMePAESeO: mp 76 C (dec.); ^{1}H NMR(D_2O) δ7.55(m, 2H), 7.0(m, 2H), 3.7-3.6(m, 2H), 3.0-3.4(m, 2H), 1.35-1.25(dd, 2H); IR(KBr) strong Se=O stretch at 795 cm^{-1}.

PAESeO: mp 95-96 C; ^{1}H NMR(D_2O) δ7.65(d, 2H), 7.55(m, 3H), 3.1-3.45(m, 4H); IR(KBr) strong Se=O stretch at 815 cm^{-1}.

Synthesis of HOMePAES Oxide. [(±)1-(4'-Hydroxyphenylthio)-2-aminopropane] hydrochloride(HOMePAES) (221.5 g, 1.0 mmol) was dissolved in 12.5 ml of H_2O on ice and mixed with 10 ml of $TiCl_4$(2 mmol, 88 mM) followed by the dropwise addition of 971 μL of 30% H_2O_2 (10 mmol). The reaction was quenched after 20 s with MnO_2. The mixture was basified (pH 12), filtered and the pH adjusted to 8.9. After extraction with brine/THF (12 x 100 ml) the combined extracts were dried ($MgSO_4$) and filtered. The resulting oil was dissolved in acidified H_2O and the precipitate removed by filtration the remaining supernatant was evaporated by vacuum centrifugation. A brown oil was recovered, dissolved in ethanol, filtered, and recrystallized(ethanol/ether) resulting in a white crystalline solid. (77 mg, 32%): mp 209 C (dec.); ^{1}H NMR (D_2O) δ 6.94-7.56(d,d 4H), 3.22-2.83(m, 3H), 1.20(d, 3H). Anal. ($C_9H_{13}NO_2S$ HCl) C: calcd., 45.86; found, 44.13; H: calcd., 5.98; found, 5.83. IR: S=O str. 1033cm^{-1}.

Synthesis of PAES Oxide. [2-(Phenylthio)ethylamine Hydrochloride] (PAES) (189.6 mg, 0.97 mmol) was dissolved in 3 ml of H_2O on ice, mixed with 0.225 g of $NaIO_4$ (1.05 mmol) and allowed to react at 4 C overnight. The resulting solution was filtered, the pH adjusted to 12, and extracted with chloroform/water (4 x 25 ml). The combined extracts were dried($MgSO_4$) and filtered. The resulting yellow oil was dissolved in acidified methanol and recrystallized(methanol/ether) as a white crystalline solid. (191 mg, 93%): mp 160-162 C(lit. mp156-158 C); ^1H NMR (D_2O) δ 7.369(m, 5H), 3.20-3.31(m, 4H). Anal. ($C_9H_{13}NO_2S$ HCl) C: calcd, 46.71; found, 46.66; H: calcd, 5.89; found, 5.90.IR: S=O str. 1039cm^{-1}.

Synthesis of Peroxynitrite. Peroxynitrite was synthesized by the autooxidation of 10 mM hydroxylamine in 0.5 M aqueous NaOH solution containing 100 μM DTPA, as previously described (497,502,503). Oxygen was bubbled through the solution (200 mL) for 3 h at room temperature. The resulting yellow solution was treated with granular MnO_2 to remove excess H_2O_2, filtered, and concentrated by freeze fractionation at −20 C. Peroxynitrite concentration was determined spectrophotometrically at 302 nm (ε_{302}=1670 $M^{-1}cm^{-1}$) (497,504) in 0.5 M sodium hydroxide with a Hewlett Packard Model 8453 diode array spectrophotometer.

Plasmid DNA Reaction System. pUC 19 plasmid (25 μg/ μl) was incubated with peroxynitrite (0.5 mM) in the presence and absence

of various sulfur- and selenium-containing compounds (0.5 mM) in 200 mM phosphate buffer, pH 6.8, for 3 min at room temperature. The DNA bands were resolved by agarose gel electrophoresis and scanned with a Molecular Dynamics Laser densitometer. The band intensities were determined using the ImageQuaNT analysis program. % Damaged DNA = (Open Circular DNA + Linear DNA)/ (Open Circular DNA + Linear DNA + Supercoiled DNA) x100 %. Each percentage was corrected for the level of damage in pUC 19 plasmid DNA in the absence of peroxynitrite. The level of damage caused by peroxynitrite in the absence of sulfur- and selenium-containing compounds was set to 100 %. The DNA gel electrophoresis experiments were performed by Ms. Veronica De Silva.

Reaction system. Typically, 250 μM of peroxynitrite was added to a solution of sulfide or selenide (250 μM) in 200 mM sodium phosphate buffer pH 8.0 and vortexed at room temperature. In appropriate experiments, 250 μM of reduced glutathione was added prior to peroxynitrite addition. Following a standard incubation time of at least 3 minutes the samples were injected on to a C-8 reverse phase HPLC column and analyzed. Peroxynitrite and its reduction product eluted in the void peak.

HPLC Analysis. Samples (10 μM) were injected into a C-8 reverse phase column (RP Allsphere Octyl C8, 5μ). Separation was performed in isocratic mode with a mobile phase containing 20% of

acetonitrile, 80% water, and 0.1% trifluoroacetic acid on a LDC/Milton Roy ConstaMetric III metering pump at a flow rate of 1.5 mL/min. Compounds were monitored with an Analytical SpectroMonitor 3100 variable wavelength UV Detector at 236 nm for HOMePAESe, 254 nm for HOMePAES and 238 nm for PAES. Quantification of the concentrations of the reaction products was carried out based on calibration curves calculated using peak height verses concentration of authentic selenide and selenoxide samples. The identities of the selenide and sulfide peaks as well as their corresponding oxides were confirmed by retention time and by spiking with authentic samples.

CHAPTER 13

SELENIUM REDOX CYCLING: RESULTS AND DISCUSSION

Phenylaminoethyl Selenides Protect Against Peroxynitrite-induced DNA damage. The electrophoresis results shown in Figure 46 clearly indicate that the phenylaminoethyl selenide and phenylaminoethyl sulfide compounds protect plasmid DNA against peroxynitrite-mediated nicking. The phenylaminoethyl selenium compounds protect plasmid DNA at a level comparable to selenomethionine and are significantly more effective than the corresponding phenylaminoethyl sulfide analogues. Quantitative results indicate that under these experimental conditions as much as 46% of the DNA damage generated by peroxynitrite could be prevented by selenomethionine. The reduction in the quantity of DNA damage for PAESe, HOMePAESe was 31 and 38%, respectively, while PAES, HOMePAES, and methionine could only decrease DNA damage by 15, 11, and 27% respectively. For further discussion please refer to De Silva *et al* (1).

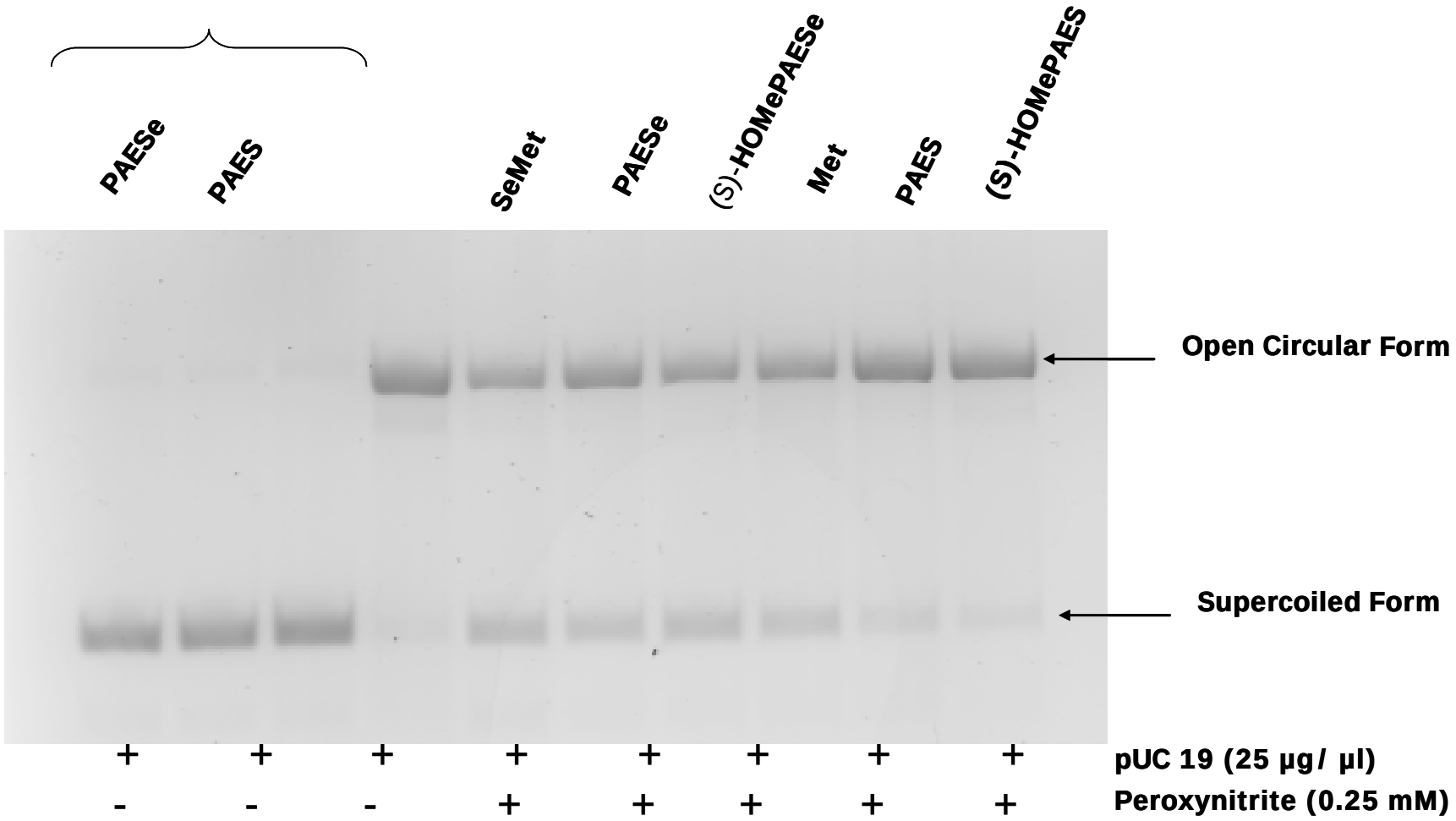

Figure 46. Selenium and Sulfur-Containing Compounds protect pUC19 plasmid DNA from Peroxynitrite-mediated Single Strand Nicks. Unnicked pUC19 plasmid DNA, which is in the Supercoiled form, undergoes single strand nicking via peroxynitrite to generate the open circular form that is detected by electrophoresis. Data obtained by Ms. Veronica De Silva (1).

HPLC Analysis of the Phenylaminoethyl Selenide Compounds. The plasmid DNA reaction system was investigated by HPLC analysis as shown in Figure 47. In the case of the reactions with phenylaminoethyl selenide compounds, quantitative HPLC confirmed stoichiometric formation of the phenylaminoethyl selenoxide by peroxynitrite and that the selenoxide was the sole selenium-containing moiety, as illustrated in Panel B. The locations of the selenide and selenoxide peaks were identified by HPLC spiking experiments with authentic selenoxide and by retention times.

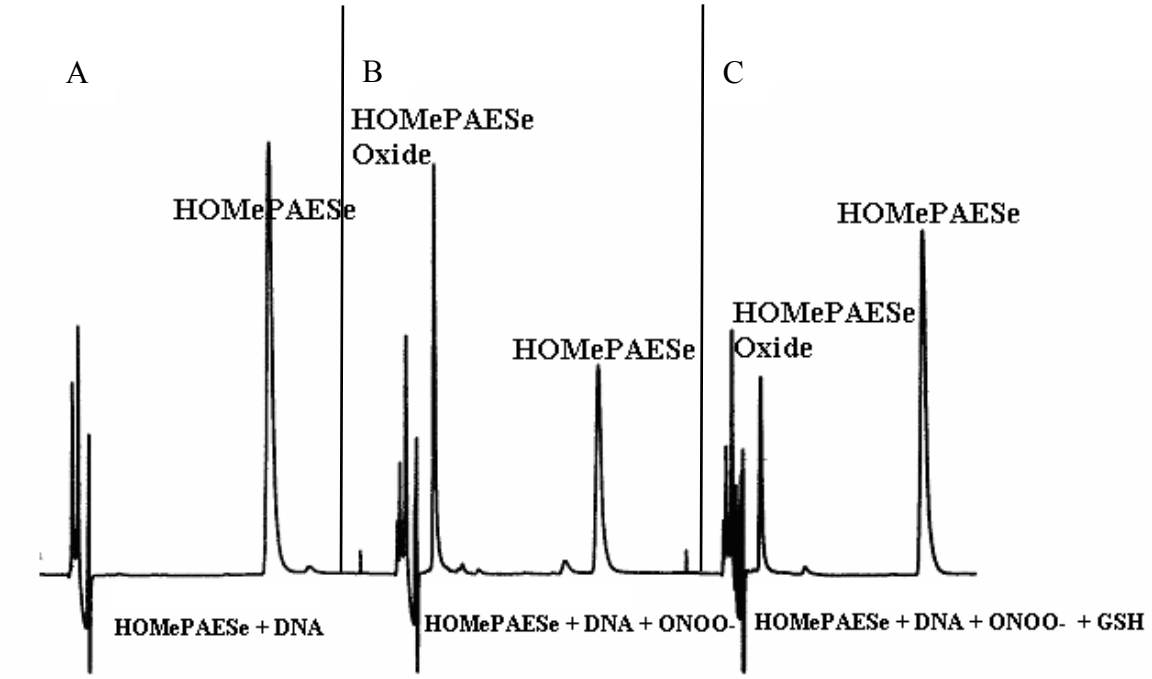

Figure 47. HPLC Chromatograms Illustrating the Protective Effects of HOMePAESe against Peroxynitrite-mediated DNA Damage. Panel A: Reaction Mixture containing 250 •M HOMePAESe, 25 ng/uL pUC19 plasmid DNA. Panel B: Reaction mixture containing 250 •M HOMePAESe, 25 ng/•L pUC19 plasmid DNA, 250 •M peroxynitrite. Panel C: Reaction mixture containing 250 •M HOMePAESe, 25 ng/•L pUC19 plasmid DNA, 250 •L peroxynitrite, 250 •M GSH (1). HPLC performed as detailed in the text.

The HPLC results further suggest that reduced glutathione, GSH, can reduce and/or prevent formation of the selenoxide; thus, maintaining quantitatively higher levels of the selenide moiety, as shown in Panel C. As previously discussed, quantitative HPLC gel electrophoresis experiments showed that HOMePAESe was capable of decreasing the peroxynitrite-mediated damage to DNA by 31%. Moreover, the addition of GSH to this reaction mixture results in a further statistically significant enhancement of protection of up to 14.5% (1). This HPLC evidence coupled with the enhancement of protection of plasmid DNA from peroxynitrite mediated damage as measured by gel electrophoresis suggests that GSH is capable of propagating a catalytic redox cycle, similar to that illustrated in Figure 48, which may enhance the protective effects of phenylaminoethyl selenides against peroxynitrite-induced DNA damage.

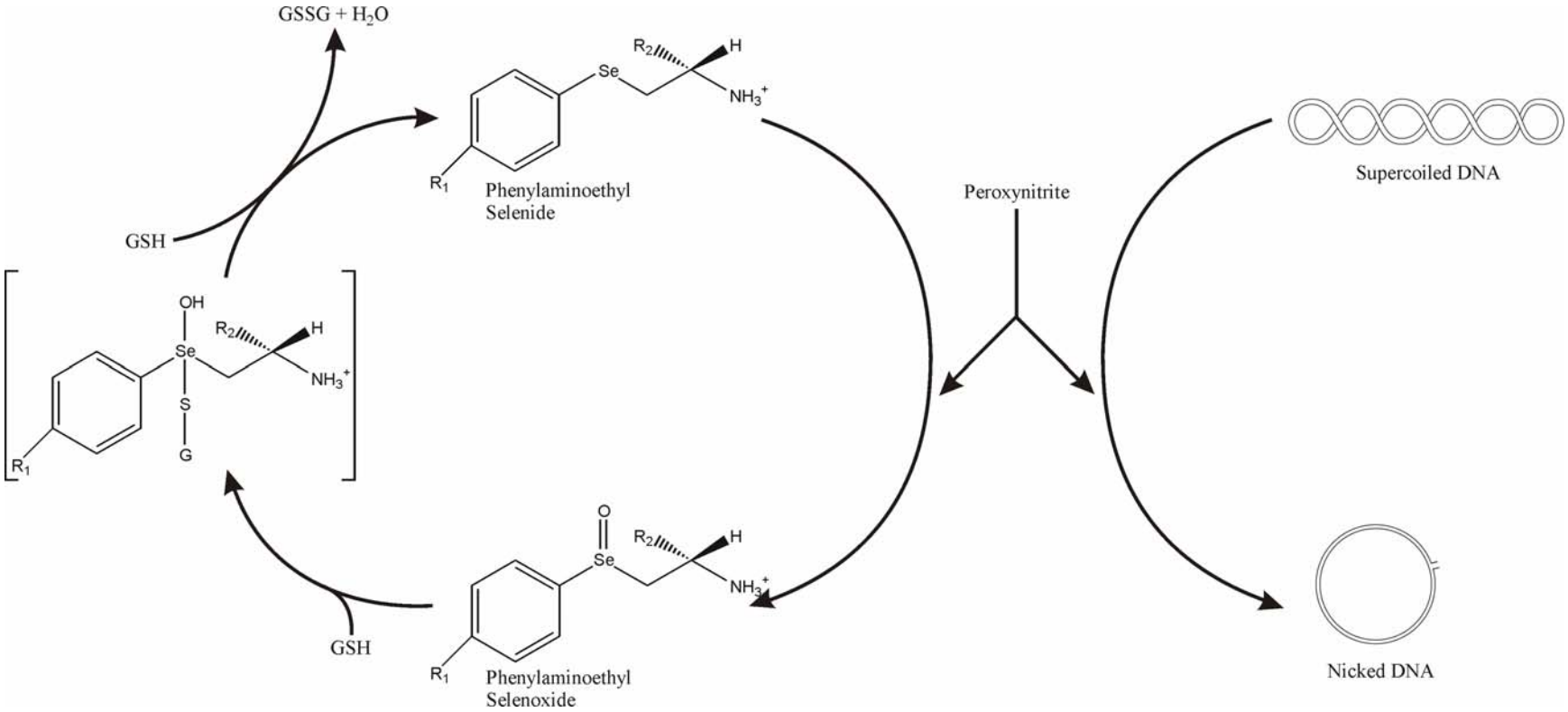

Figure 48. Catalytic Redox Cycle Established with reduced Glutathione and Phenylaminoethyl Selenides can Protect DNA from Peroxynitrite-induced Damage.(1)

HPLC Analysis of the Phenylaminoethyl Sulfide Compounds. In the course of our experiments, HPLC analysis was performed on the phenylaminoethyl sulfide compounds as well as the selenium-containing compounds. While the sole sulfur-containing compound generated by reaction of PAES with peroxynitrite was the corresponding sulfoxide, PAESO, unusual results were obtained with HOMePAES. As shown in Figure 49, Panel 2, HPLC analysis of a reaction mixture containing 250 µM HOMePAES and 250 µM of peroxynitrite generated not only the expected HOMePAES oxide peak but also an additional two peaks of unknown composition. Peak 1 in Figure 49, Panel B has been identified as HOMePAES Oxide by spiking experiments and by comparing the retention time at 2 min 40 s to authentic HOMePAES Oxide and Peak 2 at 4 min 20 s is clearly the reagent HOMePAES, in which a control is shown in Panel A for comparison. Peaks 3 and 4 in Panel B were investigated further using electrospray HPLC-MS experiments.

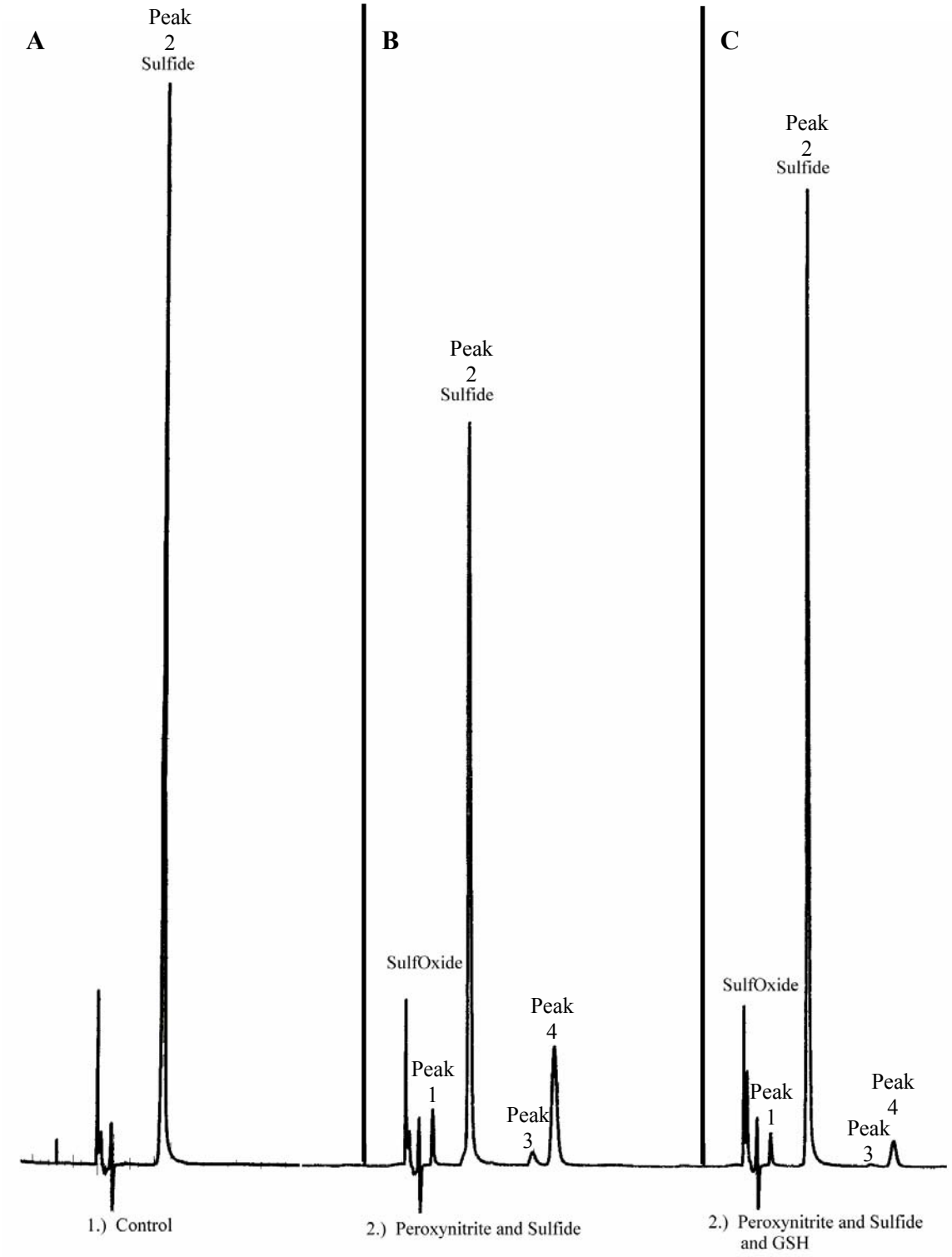

Figure 49. HPLC Chromatograms of the Reactions between HOMePAES, Peroxynitrite, and GSH. Panel A: Authentic HOMePAES. Panel B: Reaction mixture containing 250 •M of peroxynitrite and 250 •M HOMePAES. Panel C: Reaction mixture containing 250 •M peroxynitrite, 250 •M HOMePAES, and 250 •M GSH. HPLCs performed as detailed in text.

Electrospray HPLC/MS Analysis of the Products of the Reaction between HOMePAES and Peroxynitrite. The identity of the unidentified peaks, 3 and 4 in Figure 49, was tentatively determined using electrospray LC/MS analysis. Electrospray analysis of Figure 49, Peak 2 revealed the expected molecular ion m/z 184, which corresponds to the molecular weight of HOMePAES, and a decomposition product was observed with m/z 167, which would suggest the loss of ammonia from the HOMePAES compound during electrospray analysis. Analysis of Peak 3 showed a compound with a molecular ion 368 m/z, which likely results from the formation of a HOMePAES dimer as shown in Figure 50. Electrospray analysis of Peak 4 revealed a molecular ion m/z 230. We suggest that this is the nitration product of HOMePAES which we tentatively designate as 3-nitro-HOMePAES as shown in Figure 50. The formation of 3-nitro-HOMePAES is further supported by the observed decomposition product in the electrospray analysis, which exhibited a molecular ion m/z 213; this corresponds to the loss of ammonia and parallels the observed loss of ammonia for HOMePAES.

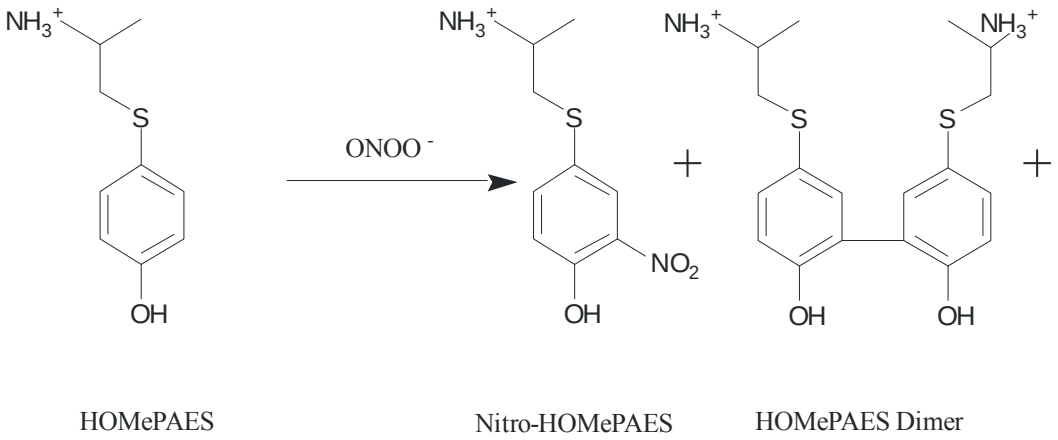

Figure 50. Proposed reaction between HOMePAES and $ONOO^-$ Producing Nitro-HOMePAES and a HOMePAES dimer.

Tyrosine Nitration as a Model for the Reaction of HOMePAES with Peroxynitrite. The reaction of tyrosine with peroxynitrite has been shown to produce 3-nitro-tyrosine as well as a dimer of tyrosine as shown in Figure 51. This reaction is well characterized and is known to occur with free tyrosine as well as with tyrosine that is incorporated into a protein (505,506). We suggest that the electronic configuration of the phenyl ring in HOMePAES is similar to that of tyrosine and that this results in the nitration and dimerization of HOMePAES in a reaction analogous to tyrosine nitration and dimerization. Moreover, HPLC analysis of PAES (data not shown) does not show evidence of nitration; this supports the contention that the *p*-hydroxy moiety of the phenyl ring is important to activate the ring to nitration and dimerization by peroxynitrite.

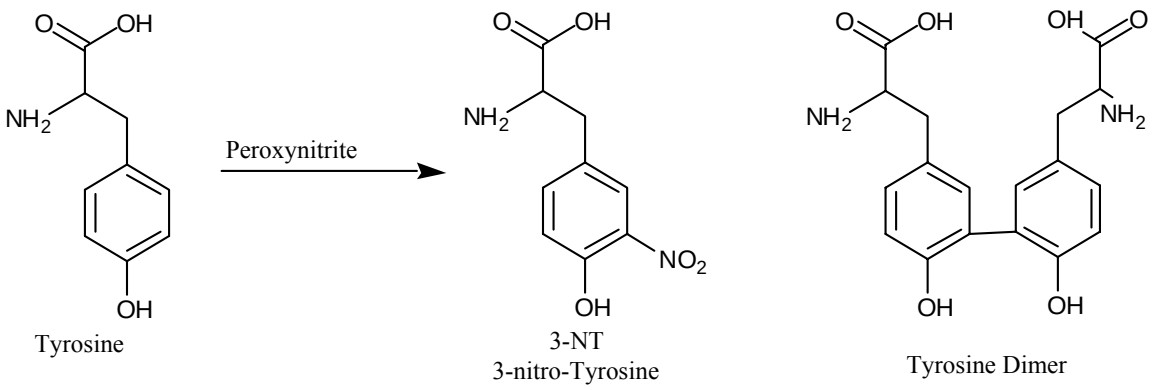

Figure 51. Nitration and Dimerization of Tyrosine in the Presence of Peroxynitrite.

HPLC analysis of the reaction between HOMePAES and peroxynitrite in the presence of GSH, shown in Figure 49, Panel C, revealed a reduction in the nitrated and dimer peaks (Peaks 3 and 4). Further experiments indicated that GSH is unable to react with either of the reaction products, the nitro-HOMePAES or the HOMePAES dimer. Consequently, we propose that in the presence of GSH, peroxynitrite reacts more quickly with GSH (to form GSSG) than with HOMePAES; thus, less of the nitro-HOMePAES or HOMePAES dimer are formed as seen in Figure 49, Panel C.

CHAPTER 14

CYCLOOXYGENASE INHIBITORS

Prostaglandin H Synthase. Prostaglandin H Synthase (PGH Synthase; PGHS) catalyzes the first step in the so-called cyclic pathway of eicosanoid metabolism. The eicosanoids are a class of C_{20} compounds (Greek: eikosi, twenty) which include prostaglandins, prostacyclins, thromboxanes, leukotrienes, and lipoxins, and which act like localized paracrine hormones in that they act by binding G-protein-coupled receptors, which are mediated by the cAMP cascade. Eicosanoid metabolism follows two main pathways; the linear pathway, shown in Figure 52, which generates the leukotrienes and HPETEs, and the cyclic pathway, shown in Figure 53, which generates the prostacyclins, prostaglandins and thromboxanes, and is named for the formation of the cyclopentane ring which is characteristic of the prostaglandins (247).

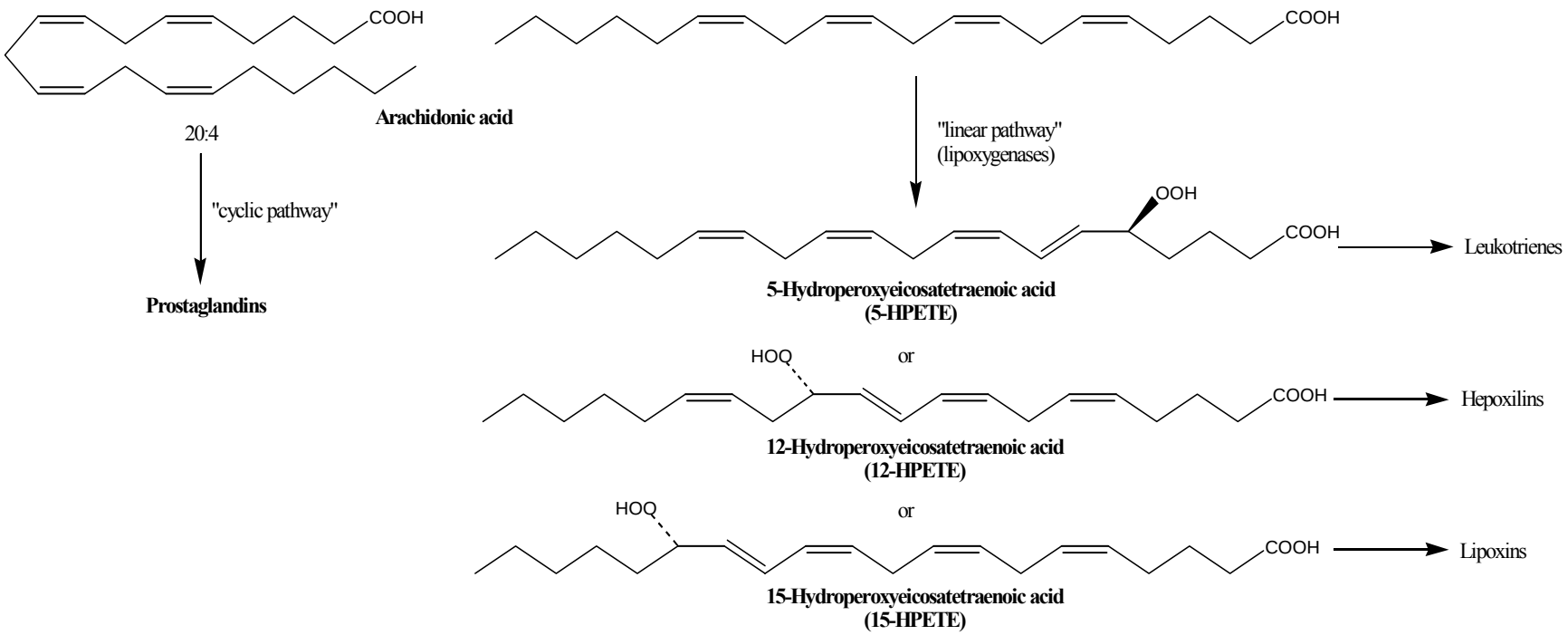

Figure 52. The Cyclic and Linear Pathways of Arachidonic Acid Metabolism. Reproduced from Voet and Voet (247).

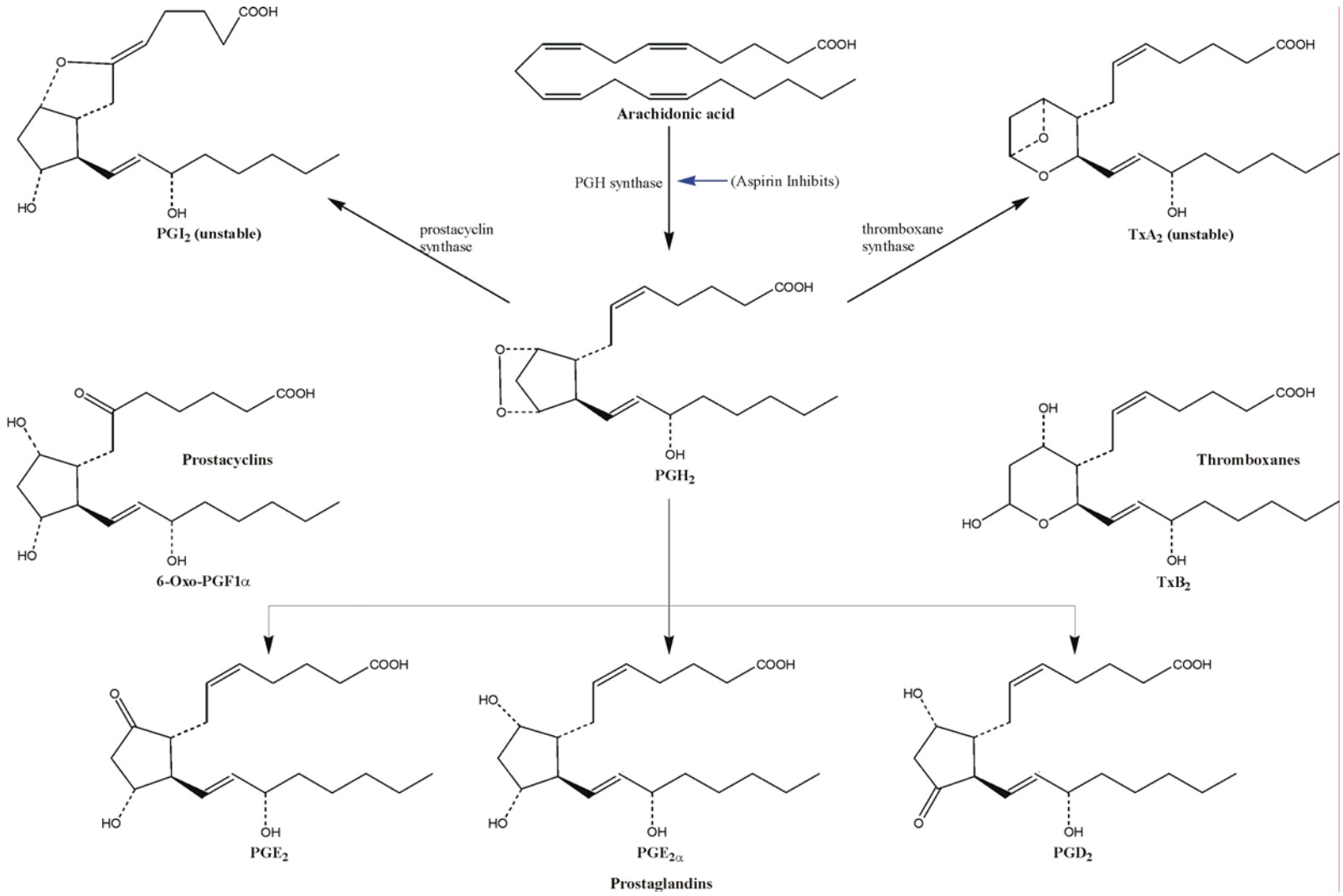

Figure 53. The Cyclic Pathway of Arachidonic Acid Metabolism. Modified from Voet and Voet (247).

Catalytic Function of Prostaglandin H Synthase.

Prostaglandin H Synthase is a heme-containing bifunctional enzyme which contains both cyclooxygenase and peroxidase activities. As Figure 54 illustrates, the cyclooxygenase activity of Prostaglandin H Synthase catalyzes the tyrosyl-radical-mediated addition of two O_2 to arachidonic acid, a major prostanoid precursor, which generates PGG_2 and it is this functionality, which lends the name COX to the enzyme. The peroxidase activity of Prostaglandin H Synthase is responsible for converting the hydroperoxy moiety of PGG_2 to a hydroxyl group, which yields the final product PGH_2 (247).

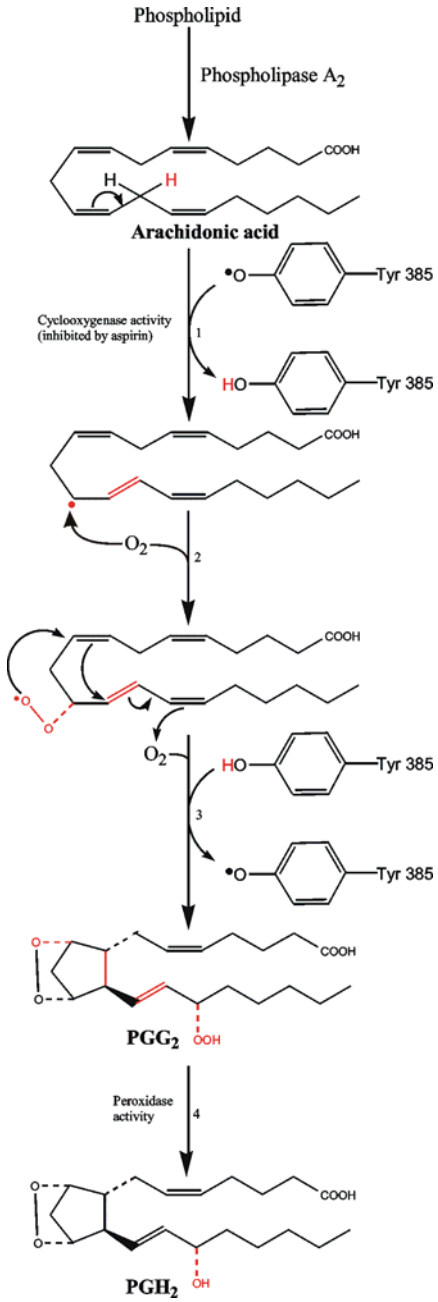

Figure 54. The Reactions Catalyzed by PGH Synthase (PGHS). The enzyme contains two activities: a cyclooxygenase, which catalyzes steps 1 to 3 and is inhibited by aspirin, and a peroxidase, which catalyzes Step 4. 1.) A radical at Tyr-385 that is generated by the enzyme's heme cofactor stereospecifically abstracts a hydrogen atom from C13 of arachidonic acid, which then rearranges so that the radical is on C11. 2.) The radical reacts with O_2 to yield a hydroperoxide radical. 3.) The radical cyclizes and reacts with a second O2 molecule at C15 to yield a peroxide in a process that regenerates the tyrosyl radical. 4.) The enzyme's peroxidase activity converts the peroxide at C15 to a hydroxyl group. Reproduced from Voet and Voet (247).

Discovery and Function of COX Isozymes. In 1991 a second isozyme of PGHS, designated as COX-II, was discovered. COX-II is a stimulus inducible enzyme, which is involved in pathogenic processes such as pain, inflammation, and cancer. COX-I is constitutively expressed in many cell types and acts in a house keeping manner *in vivo* (507,508). The similarities and differences between COX-I and COX-II are summarized in Table 20. A third isozyme of COX, COX-III, has also been tentatively proposed in the literature but currently no consensus regarding the validity of this isozyme has been reached. The proposed COX-III isozyme is a splice variant of COX-I and appears to be expressed mainly in the central cortex of mammals (509).

Table 20. Overview of the Activities and Active Sites of COX-I and COX-II (510).

	COX-I	COX-II
Activity	Constituitive (constant inhibition can cause gastric ulceration)	Inducible (Desirable target for inhibition)
Cyclooxygenase Activity	V_{max} ~3500 mol/min of arachidonate/mol of dimer K_M arachidonate ~ 5μM K_M O_2 5μM	Cyclooxygenase activity activated at 10x lower hydroperoxide concentrations thus permits COX-II to out compete COX-I.
1° Structure	576 aa	587aa (18aa inserted 6 residues in from C terminus)
2° Structure	Homodimers which independently catalyze reactions	
	N-glycosylated at 3 sites which is required for enzyme binding so problems w enzyme production	Variably glycosylated at 2-4 sites. Expressed in baculovirus systems.
Peroxidase Activity	Catalyzes heterolytic $2e^-$ reduction of hydroperoxidase substrates	Catalyzes 60% $2e^-$ and 40% $1e^-$ reductions
	Slower	Faster rates of formation of oxyferryl group + protoporphyrin IX
	Preference for secondary alkyl hydroperoxides	
Cyclooxygenase Active Site	Smaller	Larger More Accommodating
	Exhibits negative allosterism at low arachiodonate concentrations	No allosterism
	Global catalytic domain contains a 25 Å, 25 residue, hydrophobic channel that originates at the membrane binding domain, where the substrate/NSAID and O_2 enters, and protrudes into the globular domain core where the substrate/NSAID binds. The NSAID binding site involves the upper half of the channel from Arg-120 to Tyr-385. [Only 3 polar residues line the channel Arg-120, Ser-353, Ser-530 (Aspirin Acetylation site)]	

Table 20 Continued

--	*Binding site is 20% larger than COX-I which leads to greater substrate flexibility
Ile 523	Val-523 produces a small side pocket adjacent to the active site channel
Ile 434	Val-434 further increases side pocket size; induces a movement of Phe518 which further increases the size
His513	Arg-513 alters the chemical environment of the side pocket forming a stable positive charge in the center of the pocket; interacts with the 4-methylsulfonyl substituents of COX-II inhibitors; gives rise to the time-dependent inhibition displayed by this class of inhibitors. Helix D is cantilevered upward to provide a larger opening and displace Arg-120.

Similarities between COX-I and COX-II. COX-I and COX-II share 60% sequence identity and are integral membrane proteins, which reside in the ER and perinuclear envelopes. The COX isozymes have homologous and superimposable crystal structures with both enzymes existing as homodimers. Three structural domains make up the COX monomer; a membrane-binding domain, a catalytic binding domain that is located on the luminal side and contains a heme-binding site, and an N-terminal epidermal growth factor (EGF)-like domain. The COX active site lies between the helices of the membrane-binding site, and it is proposed that this site undergoes significant conformational changes to allow for substrate binding and release (507). The isozymes also have similar cyclooxygenase turnover numbers, K_M values for arachidonate and O_2, and the key residues for catalysis are conserved (511).

Structure of the COX Active Site. The COX-I and COX-II monomer binding site is located at the upper end of a 25 Å hydrophobic channel, which begins at the membrane binding site and reaches toward the heme in the globular domain. The hydrophobic active site is lined by 24 amino acid residues beginning with Arg-120 and ending at Tyr-385. Substrates bind the hydrophobic COX active site in an L-shaped formation with Tyr-385 positioned to perform tyrosal-radical mediated catalysis (510).

Differences between the COX-I and COX-II Active Site. The COX-II active site is approximately 20% larger than in COX-I. This is due to three notable variations in the structures between the COX-I and COX-II active sites. The residues Ile-523, Ile-434, and His-513 in COX-I are replaced by Val-523, Val-434, and Arg-513 in COX-II, respectively. The replacement of the COX-I residues Ile-523 and Ile-434 with Val in COX-II create a small side pocket in COX-II; this generates the larger COX-II binding site. In addition, the substitution of His-513 in COX-I with the Arg-513 in COX-II substantially alters the chemical environment inside the COX-II side pocket; this effectively forms a stable positive charge in the center of the COX-II side pocket. Arg-120 is an important residue for binding to the carboxylate groups of fatty acids and many NSAIDS in both COX-I and COX-II. In COX-II Arg-120 is displaced somewhat since helix D is cantilevered upward; this provides a larger opening in the membrane binding domain (510).

Rationale for Selective COX-II Inhibitors. The differences between the COX-I and COX-II binding site have been exploited in the design of selective COX-II NSAID inhibitors. Approximately 1% of all patients receiving chronic treatment with traditional NSAIDS develop serious gastrointestinal complications such as ulcers. COX-I is the major cyclooxygenase isozyme present in the lining of the stomach and inhibition of this isozyme has been historically implicated in the promotion of gastrointestinal

complications and ulcerogenesis (508). Consequently, the COX-II hypothesis (512) suggests that selective NSAID inhibition of COX-II, the inducible isozyme involved in inflammation and disease sates, without inhibition of the constitutive Cox I isozyme, would provide the same anti-inflammatory, analgesic, and antipyretic qualities as traditional, nonselective NSAIDS without the possibility of serious GI complications (510).

Questions Regarding the Safety and Efficacy of Selective COX-II inhibitors. The clinical picture regarding the success of the selective NSAIDS has certainly been mixed. The first COX-II selective NSAIDS reached market in 1999 (513) and are shown in Figure 55. These new drugs were marketed heavily and through direct to the public advertising, which quickly elevated them to so-called blockbuster status (513). However, in September 2004, Merck, Sharp and Dohme Limited (MSD) withdrew rofecoxib following evidence of an increased risk of cardiovascular disease in the preliminary results of the APPROVe trial (513). Then in 2005, the FDA asked Pfizer to voluntarily withdraw valdecoxib from the market (514). The FDA has also called into question the cardiovascular risk of all NSAIDS which includes over the counter and prescription drugs (514).

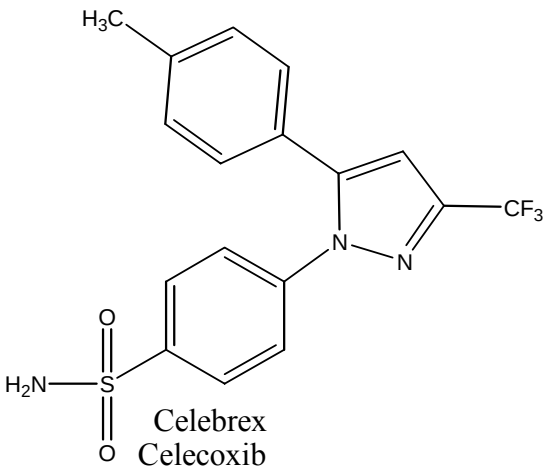

Celebrex
Celecoxib
(G.D. Searle LCC, Pfizer)

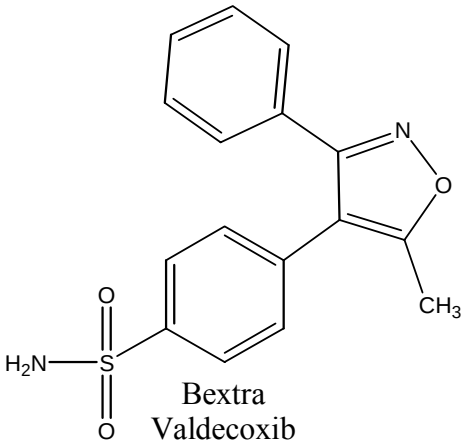

Bextra
Valdecoxib
(G.D. Searle LCC, Pfizer)

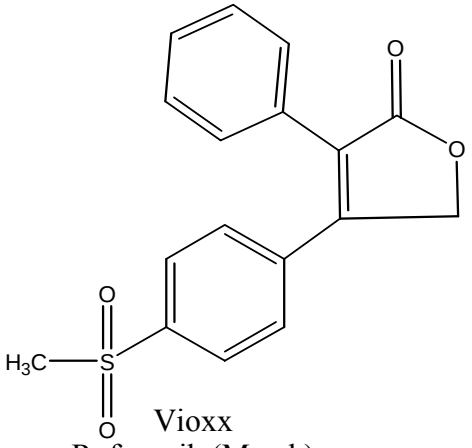

Vioxx
Rofecoxib (Merck)

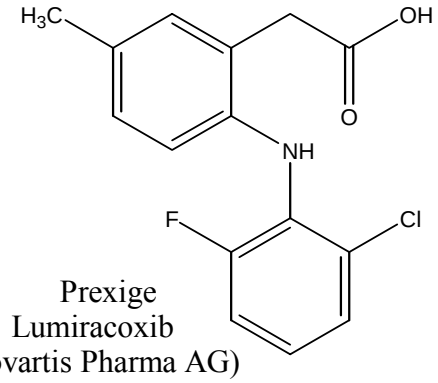

Prexige
Lumiracoxib
(Novartis Pharma AG)
(Approved in UK, ETA US 2005)

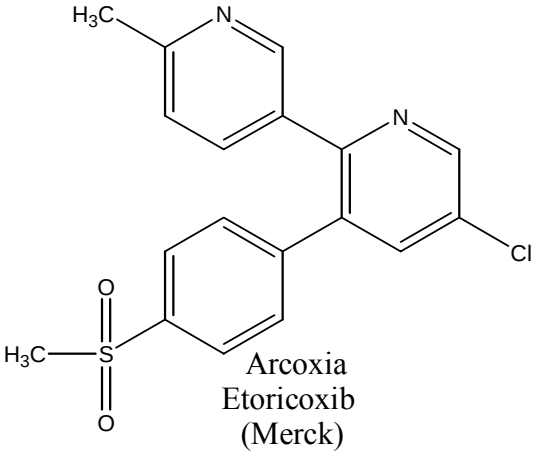

Arcoxia
Etoricoxib
(Merck)
(Approved in UK, Currently at FDA)

Figure 55. Selective COX-II Inhibitors that have been or are currently commercially available.

The Fitzgerald Hypothesis for the Increased Risk of Cardiovascular Disease with Selective COX-II Inhibitors. The increased risk for cardiovascular disease, which prompted removal of several selective COX-II NSAIDS from the market, seems to be a direct result of the mechanism of this class of drugs instead of a spurious side effect of the individual drugs themselves. The Fitzgerald hypothesis suggests that inhibition of COX-II sans COX-I inhibition is doubly detrimental to the cardiovascular system (513). As summarized in Table 21 (513), COX-I negatively effects the endothelium by inducing production of thromboxane A2 which facilitates platelet aggregation, vasoconstriction, and smooth muscle proliferation. COX-II acts beneficially on the endothelium by facilitating the production of prostacyclin which counterbalances COX-I by opposing the effects of thromboxane A2 (512). Consequently, NSAIDS, which inhibit the beneficial effects of COX-II on the endothelium without inhibiting the detrimental effects on the endothelium produced by COX-I, can result in an increased risk of cardiovascular disease in susceptible individuals (513). Nevertheless, the absolute risk of a detrimental cardiovascular outcome while taking a selective COX-II NSAID is quite low. Specifically, a 1.1% chance of any cardiovascular event was observed with rofecoxib in contrast to 0.47% for naproxen (Alleve). We note that it does seem reasonable to consider treatment with COX-II selective NSAIDS for select populations with low cardiovascular risk factors.

Table 21. The Fitzgerald Hypothesis. A single mechanism, blockage of COX-II, could explain increased cardiovascular risk. Reproduced from Hazleman *et al*. (513)

Mechanism	Outcome
COX-I induction via thromboxane A2	Platelet aggregation, vasoconstriction and vascular smooth muscle proliferation
COX-II induction via prostacyclin	Vasodilatation, inhibition of vascular smooth muscle proliferation, inhibition of platelet aggregation
Inhibition of COX-II	Elevation of blood pressure, acceleration of atherogenesis, predisposes to an exaggerated thrombotic response

Modalities of COX-Mediated Inhibition. Three modes of NSAID-mediated COX inhibition have been reported and the particular mode of inhibition appears to be dependent on the chemical structure of the specific NSAID (510,515). The first mode of inhibition is a rapid, reversible binding followed by covalent modification of Ser-530. This classic mode of suicide inhibition of COX occurs with compounds containing an acetyl-moiety like aspirin, which is the only commercial inhibitor of this type. Aspirin's irreversible, suicide inhibition of COX-I is believed to be responsible for it's ability to prevent COX-I-mediated thromboxane-induced platelet aggregation, because mature platelets are essentially non-nucleated thus are incapable of generating fresh COX-I enzymes after inhibition with aspirin (515).

A second method of COX inhibition is the rapid and reversible binding, which is characteristic of ibuprofen; this is likely the most common mode of binding COX to traditional NSAIDs. A third mode of inhibitor binding is the rapid, lower affinity, reversible binding followed by time-dependent, higher affinity, slowly reversible binding; this is the binding mode for the traditional NSAID, flurbiprofen. The mechanism of binding for this mode of inhibition with traditional COX inhibitors is not clearly understood and likely dependent on the individual drug structure.

The COX-II selective inhibitors bind COX-I via the previously discussed, rapid, competitive, reversible mechanism,

but inhibition of COX II occurs via the third mode, a time-dependent pseudoirreversible mechanism. With selective COX-II inhibitors that contain a sulfonamide or a methylsulfone moiety, the time-dependent pseudoirreversible inhibition of COX-II is believed to be due to the interaction with the Arg-513 side group, and rarely with Arg-120 (510).

The Development of a Selective Terphenyl COX Inhibitor. In 1998 May, Pollock, and Coworkers (508) published a study which evaluated a novel arylacetic acid, 1-(carboxymethyl)-3,5-diphenyl-2-methylbenzene (CDB), which is shown in Figure 56. CDB was shown to inhibit carrageenan edema in rat hind paws in a dose dependent manner (ED_{50} of 41 mg/kg at 3 h) (508). The compound also inhibited hind paw inflammation (70%) and arthogram scores in rats with adjuvant-induced arthritis. Moreover, CDB possessed significant analgesic activity in mice (70% inhibition with 50 mg/kg). Studies suggest that the pharmacological activity observed in the study is a direct result of CDB's inhibition of COX-I activity ($IC_{50} \approx 17$ μM); the compound inhibited PAM and COX-II only weakly. The terphenyl scaffold of CDB is attractive since the increased stability and the lipophilicity may enhance absorption and distribution. While CDB is certainly of interest for the treatment of anti-inflammatory diseases, a more desirable compound would have more potent and selective COX-II activity. We are now working to turn this meta-terphenyl scaffold into a

selective COX-II inhibitor. Herein we report the development of novel CDB derivatives, which are selective COX-II inhibitors.

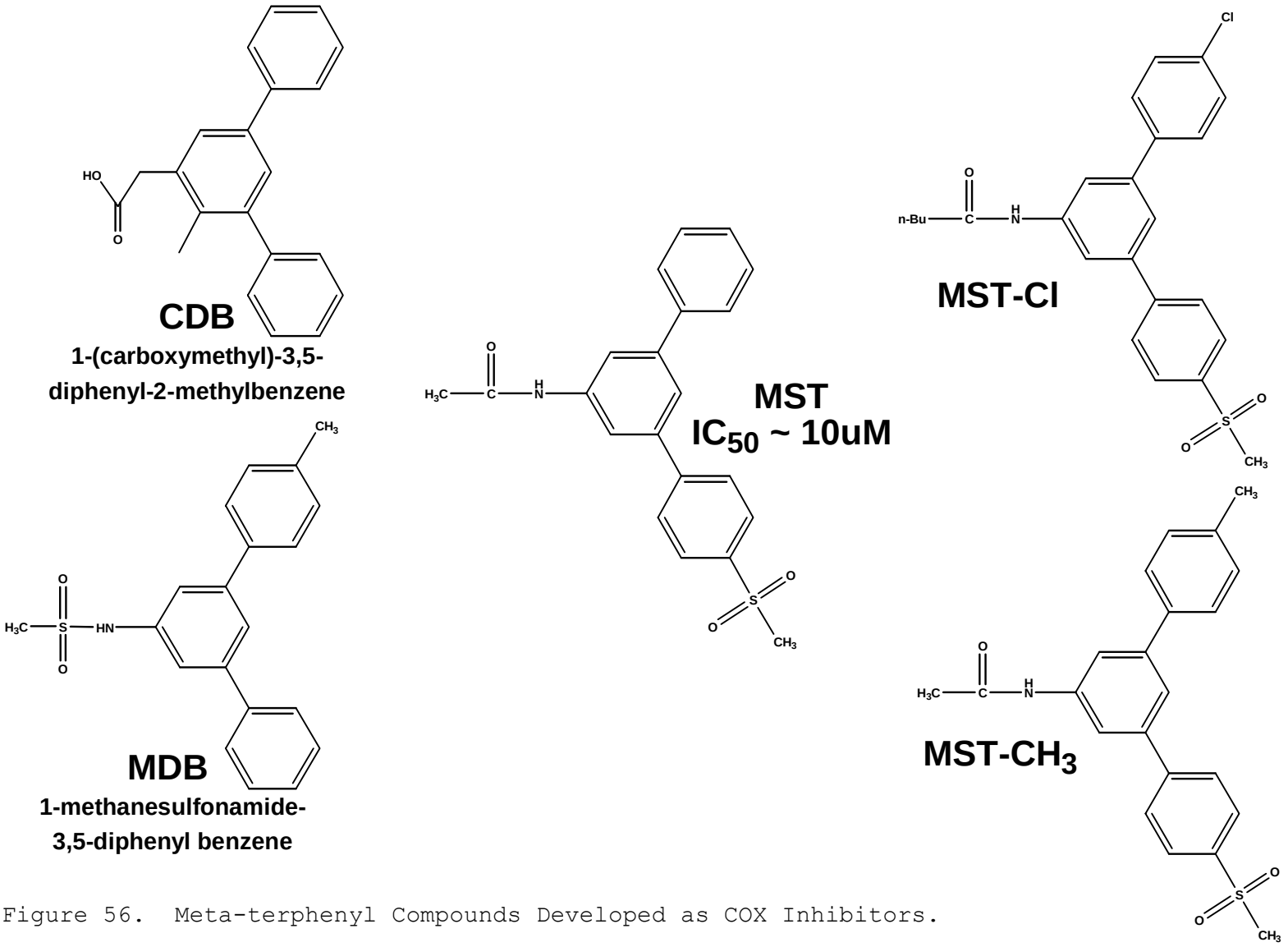

Figure 56. Meta-terphenyl Compounds Developed as COX Inhibitors.

The Design of Selective COX-II Inhibitors. The CDB derivatives developed in this study are shown in Figure 56. An optimized synthesis illustrated in Figure 57 was used to generate these meta-terphenyl derivatives. This synthesis is efficient and convenient and from this basic MDB scaffold, a variety of derivatives can be generated as shown in Figure 56. Functional groups can be added onto the terminal phenyl groups by placing electron withdrawing groups on the benzaldehyde precursor and electron donating groups on the acetophenone precursor prior to the cyclization reaction. Nothing can be done with the nitrile groups except for hydrolysis. However, the free amine on the aniline compound can be converted to several moieties via reactions like the Sandmeyer reaction.

Our meta-terphenyl compounds have a more open orientation than the commercial COX-II inhibitors, which would be more analogous to an ortho-orientation. Furthermore, the sulfonamide moiety is on the center phenyl of MDB instead of on the terminal phenyl moieties as is nearly always seen with COX-II selective inhibitors. The sulfonamide position is considered critical for enzyme binding selectivity because it forms an electrostatic interaction with the Arg-513 residue. Consequently, a series of compounds, designated as MST (methylsulfone terphenyl) in Figure 56, were designed with a methylsulfone moiety at the para position on the outer phenyl ring.

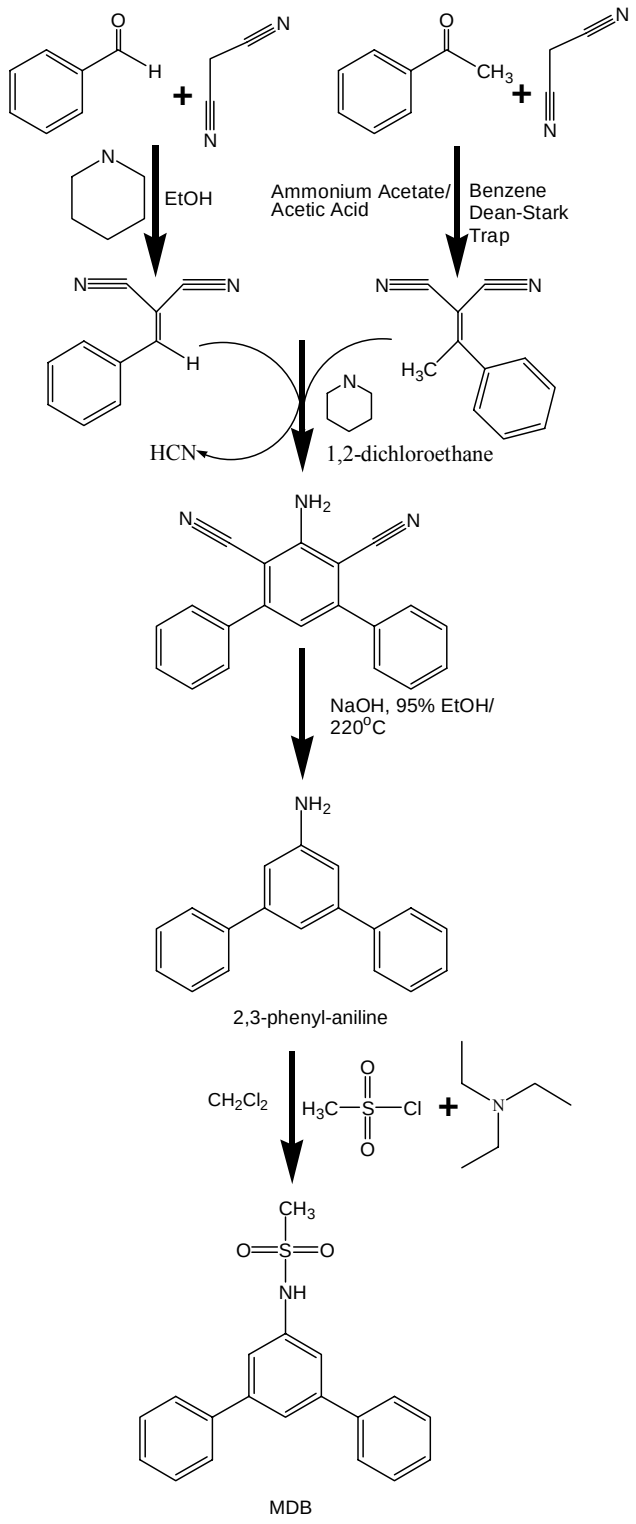

Figure 57. Synthesis of MDB as a Scaffold for other Meta-terphenyl Derivative Compounds.

Experimental Setup for Assaying COX Inhibitors. The compounds investigated in this study were screened for the ability to inhibit COX-I and COX-II *in vitro* using the Colorimetric COX (ovine) Inhibitor Screening assay from Cayman Chemical as directed. This assay utilizes the peroxidase activities of COX-I and COX-II, which are colorimetrically assayed by monitoring the appearance of oxidized N,N,N',N'-tetramethyl-*p*-phenylenediamine at 590 nm.

Whole Blood ELISA Assay Promising compounds were also screened for and COX-2 activity in whole blood using the following procedure. Whole blood, 25 mL, from a volunteer predosed with aspirin was collected in heperinzed tubes, pooled, and 0.5 mL of whole blood was transferred to microcentrifuge tubes containing 2 µL of inhibitor in DMSO or DMSO only; the inhibitors were set up in triplicate. The blood was incubated for 15 min at 37 C in the presence of the inhibitor or vehicle and then 10 µL of lipopolysaccharide (LPS) was added to induce Cox-II activity. The blood was then incubated for 24 hours.

The blood samples were then assayed using an Enzyme-Linked Immunosorbent Assay (ELISA) for the quantitative analysis of Prostaglandin E_2 (See Figure 53) levels using a kit from Oxford Biomedical Research. This assay operated on the basis of competition between the enzyme-PGE_2 horseradish peroxidase conjugate and the PGE_2 in the sample for a limited number of binding sites on the antibody-coated plate. In this situation the extent of color development, measured at 650 nm. is

inversely proportional to the amount of PGE_2 in the sample or standard; thus a stronger the inhibitor would generate less PGE_2 which would generate more color development.

Results of the In Vitro Colorimetric Inhibitor Screening. Of the compounds assayed with the *in vitro* colorimetric inhibitor screen, the MST derivatives show the most promise. As shown in Figure 58, MST appears to be a selective inhibitor of COX-II and does not inhibit COX-I at the measured concentrations. The results of the control compounds indomethacin, which is a non-selective COX- inhibitor, and celecoxib, which is a selective COX-II inhibitor, were somewhat less clear. Celecoxib (illustrated in Figure 59) completely inhibited COX-1 at both measured concentrations and inhibited COX-II in a dose dependent manner. The results with indomethacin are unclear, inhibition of COX-I is clearly observed at 0.1 µM but a dose response curve is not observed since the inhibition at 0.1 µM is less that at 0.1 µM. Finally, the results with MST-Cl and MST-CH_3 cannot be interpreted, as there is simply too much error involved with the results of this assay.

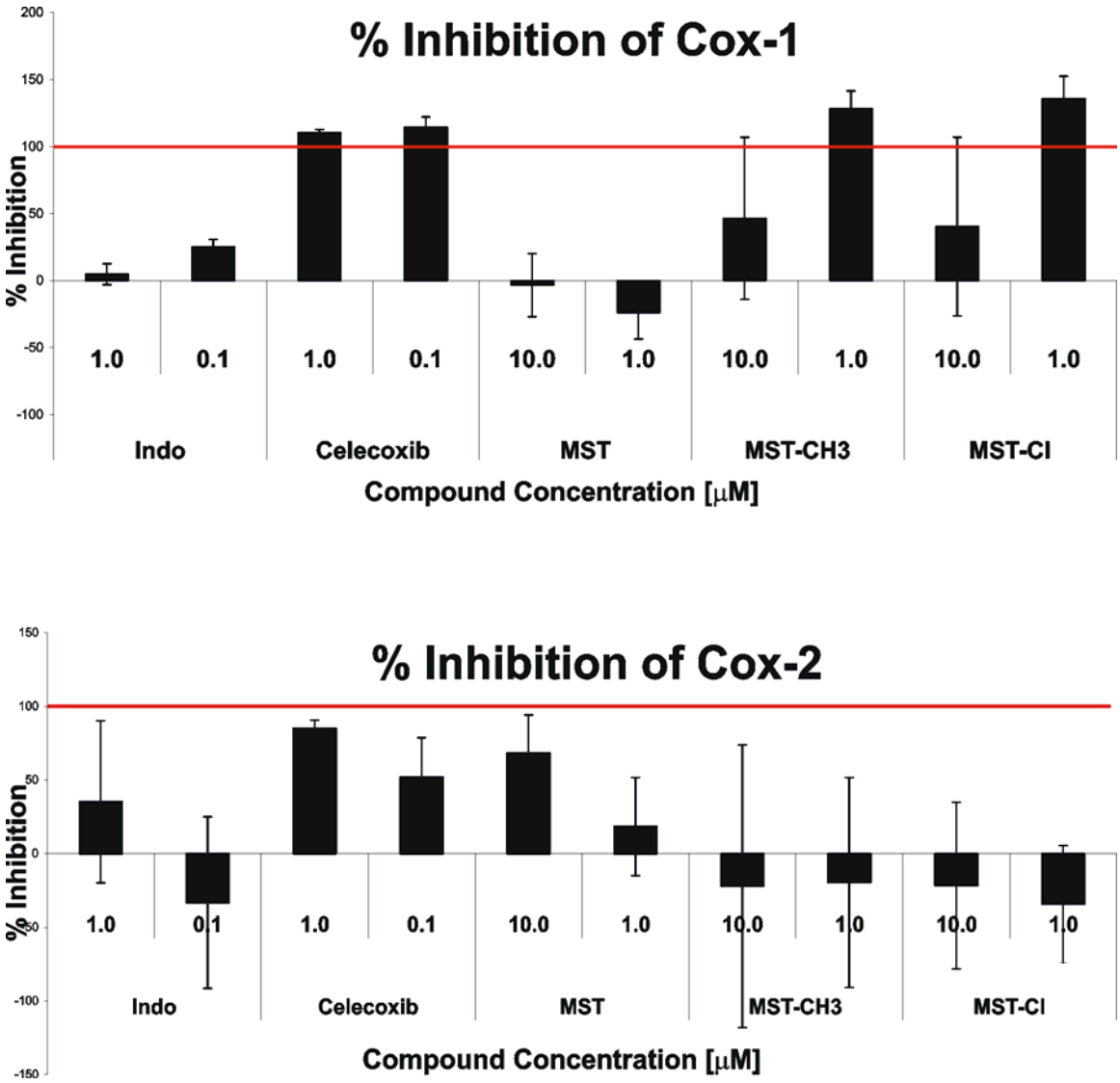

Figure 58. Percent Inhibition of COX-I and COX-II *In Vitro*. Results were determined using the Colorimetric COX (ovine) Inhibitor Screening assay from Cayman Chemical, which was used as per the instructions.

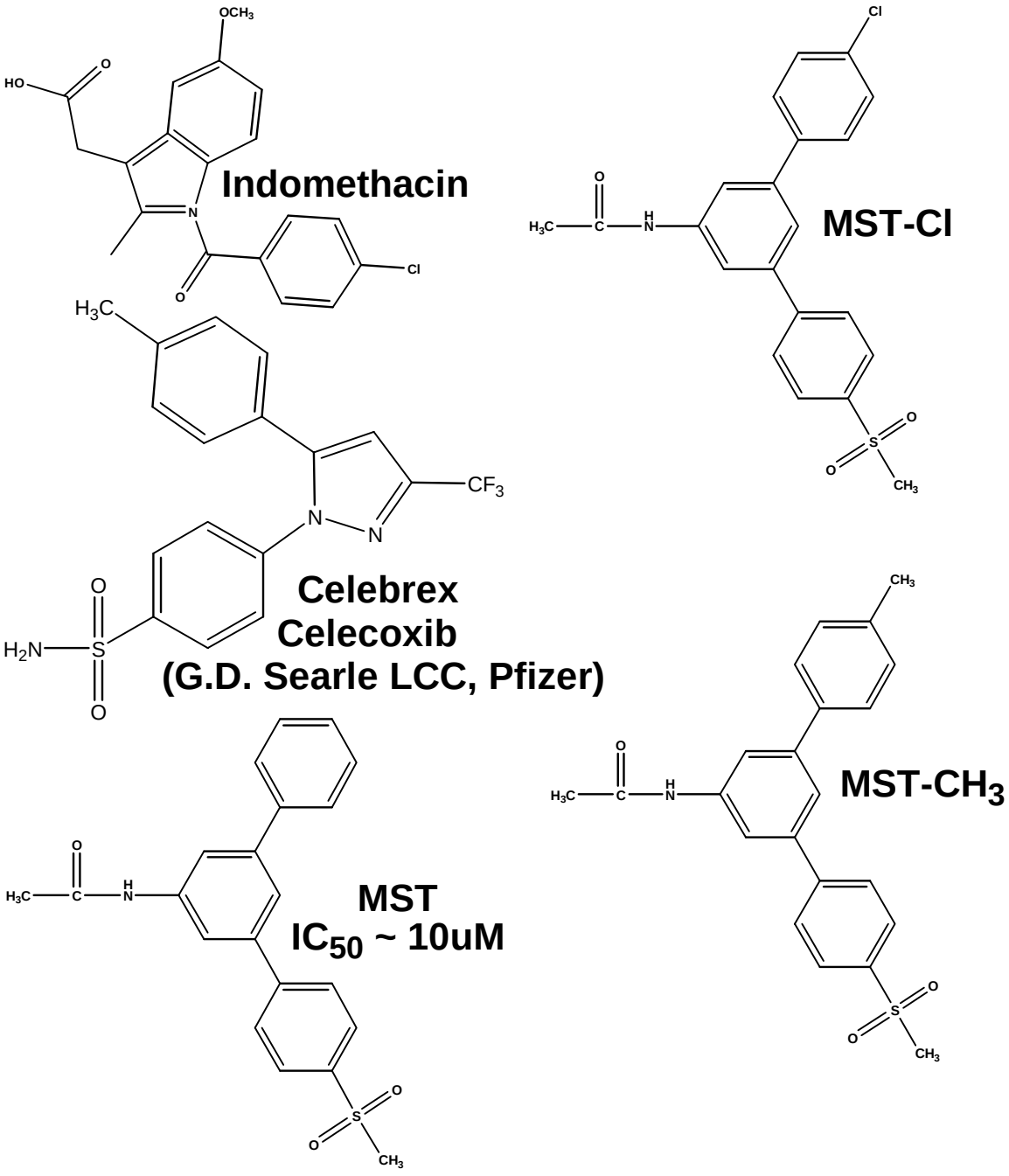

Figure 59. Meta-terphenyl Derivatives Assayed for the Ability to Inhibit COX-I and Cox-II in an *In Vitro* Colorimetric Assay.

Results of the Whole Blood ELISA Screening. The results of the *in vitro* colorimetric inhibitor screen (Figure 58) indicate that MST is a selective inhibitor of COX-II. Consequently, we investigated the ability of this compound to inhibit COX-II in whole blood using the procedure described above. The results shown in Figure 60 clearly indicate that MST is indeed an inhibitor of COX-II in whole blood cells. The magnitude of the inhibition observed with the control inhibitors, celecoxib and indomethacin, is a function of concentration; both compounds have low IC_{50}'s so all COX-II activity is inhibited at the measured concentrations.

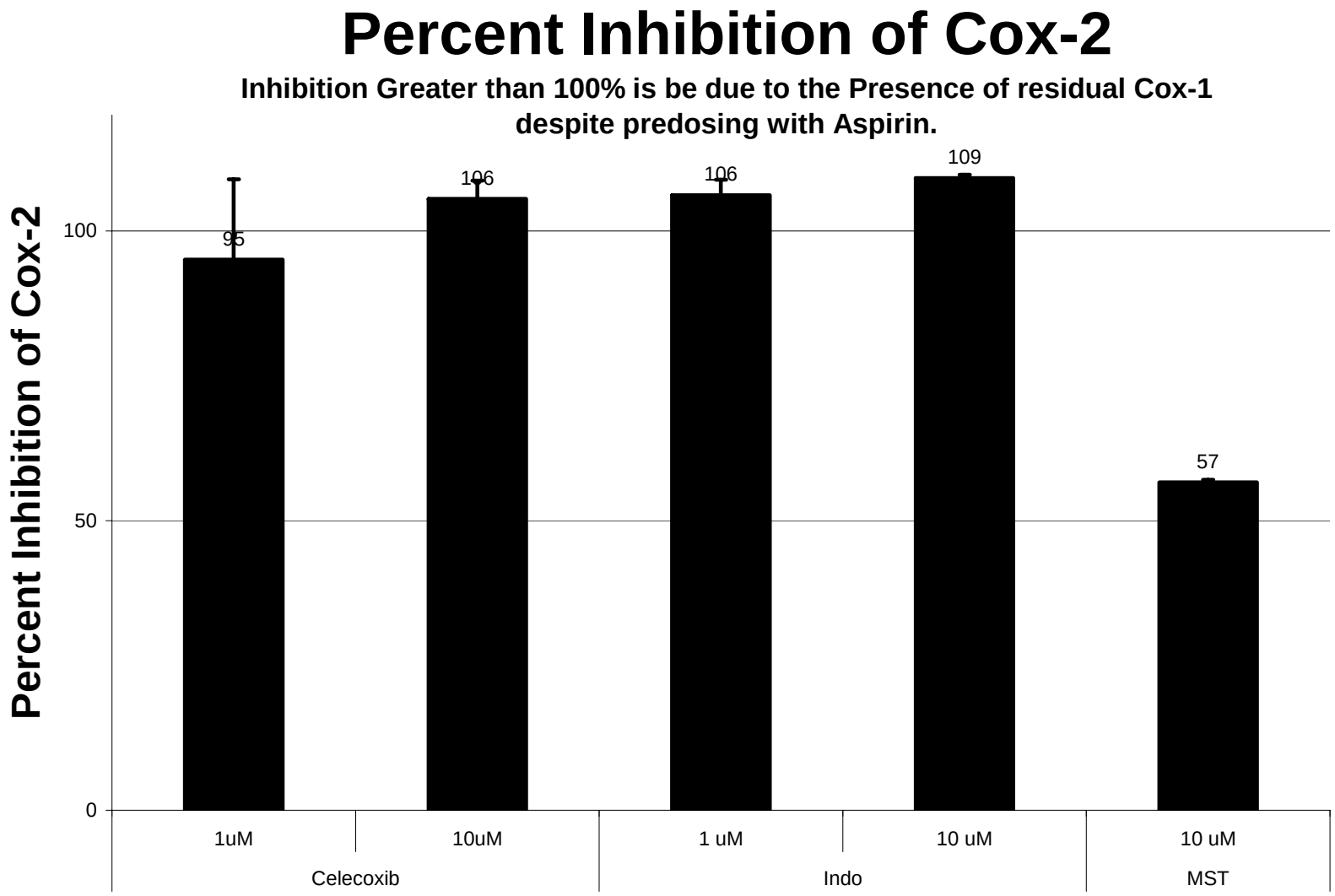

Figure 60. Percent Inhibition of COX-II in Whole Blood.

Herein we report the development of a novel selective COX-II inhibitor. MST inhibits COX-II but not COX-I in the *in vitro* colorimetric inhibitor screen and MST inhibits COX-II in the whole blood ELISA assay. The ability of MST to inhibit COX I in whole blood is being investigated. The presence and location of the methylsulfone moiety on MST likely facilitates the inhibition of COX-II by allowing an electrostatic interaction to form between the MST inhibitor and the Arg-513 residue of COX-II. Further experiments are currently underway to examine modifications in the MST scaffold such at generating a meta-sulfone moiety on the terminal phenyl group and modifying the amide moiety on the central ring.

APPENDIX 1: PHB MODEL

This is the first structured kinetic metabolic model developed using *in vitro* data of metabolite concentrations, which simulates the *in vitro* biosynthesis of PHB. The equations for the β-ketothiolase and PHB synthase reaction were based on the work of Leaf and Srienc (190), while the equation for the Acetoacetyl-CoA Reductase enzyme was from Daae *et al* (191). Kinetic and thermodynamic parameters used in this model were gathered from the literature, from laboratory analysis, by fitting the simulation to the time course data, and by calculations based on the kinetic rate and Haldane equations.

β-ketothiolase. β-ketothiolase has been shown to proceed via a bi bi ping-pong mechanism as described by the following integrated rate equation:

$$v_o = \frac{V_f V_r \left([\mathrm{A}][\mathrm{B}] - [\mathrm{P}][\mathrm{Q}]/K_{eq}\right)}{\begin{aligned} &K_b V_r[\mathrm{A}] + K_a V_r[\mathrm{B}] + V_r[\mathrm{A}][\mathrm{B}] + K_q V_f[\mathrm{P}]/K_{eq} + K_p V_f[\mathrm{Q}]/K_{eq} \\ &+ V_f[\mathrm{P}][\mathrm{Q}]/K_{eq} + K_q V_f[\mathrm{A}][\mathrm{P}]/K_{ia}K_{eq} + K_a V_r[\mathrm{B}][\mathrm{Q}]/K_{iq} \end{aligned}}$$

Equation 1: The integrated rate equation for the reversible bi bi ping-pong mechanism, where the reaction substrates [A] and [B] are acetyl-CoA, and [P] and [Q] are the products, CoA and acetoacetyl-CoA, respectively. The rate constants for the four compounds are K_a, K_b, K_p and K_q and the inhibition constants are K_{ia}, K_{ib}, K_{ip}, and K_{iq}. V_f and V_r are respectively the maximal velocities in the forward and reverse directions, and K_{eq} is the equilibrium constant.

Equation 1 can be solved at the initial rate, v_o, by assuming there are no products (i.e. [P]=[Q]=0); this simplification yields the equation:

$$v_o = \frac{V_f V_r [\mathrm{A}][\mathrm{B}]}{K_b V_r [\mathrm{A}] + K_a V_r [\mathrm{B}] + V_r [\mathrm{A}][\mathrm{B}]}$$

Equation 2: Initial rate equation for the bi bi ping-pong mechanism with zero initial product quantities.

Table 22. Kinetic and Thermodynamic Parameters for the β-ketothiolase, Acetoacetyl-CoA Reductase and PHB Synthase Reactions. The values listed in blue were gathered from the literature; those determined by simulated fit are in red. Values calculated from the Haldane or laboratory equilibrium data are in green. The ratios were calculated based on the data from Haywood *et al.* and laboratory data and are listed in pink and underlined in blue.

Kinetic parameters	***β-ketothiolase***	***Acetoacetyl-CoA Reductase***	***PHB Synthase***
K_{eq}	4×10^{-5}	2.16×10^{9}	---
V_r (µM/s)	2924	135.09	---
V_f (µM/s)	9.75	1486	0.309
Ratio	$V_r/V_f = 300$	$V_f/V_r = 11$	---
$K_{M\ (AcCoA)}$ µM	0.158	---	---
$K_{M\ (AcCoA)}$ µM	1237.84	---	---
$K_{M\ (CoA)}$ µM	16	---	---
$K_{M\ (AcAcCoA)}$ µM	44	5	---
$K_{M\ (NADPH)}$ µM	---	19	---
$K_{M\ (HBCoA)}$ µM	---	16.5	103
$K_{M\ (NADP^+)}$ µM	---	31	---
$K_{I\ (AcCoA)}$ µM	46.74	---	---
$K_{I\ (AcCoA)}$ µM	1237.84	---	---
$K_{I\ (CoA)}$ µM	15.78	---	108
$K_{I\ (AcAcCoA)}$ µM	0.1467	28.83	---
$K_{I\ (NADPH)}$ µM	---	50	---
$K_{I\ (HBCoA)}$ µM	---	5	---
$K_{I\ (NADP^+)}$ µM	---	47.15	---

Literature
Simulated fit
Calculated from the Haldane equations or with equilibrium data
Generated from the model and literature data.
Laboratory data

The kinetic constants for β-ketothiolase reaction are presented in Table 22. In the case of β-ketothiolase, further simplifications are made because the reaction substrates are the same, i.e. [A]=[B]=[acetyl-CoA].

$$v_o = \frac{V_f V_r [\mathrm{A}]^2}{(K_b + K_a) V_r [\mathrm{A}] + V_r [\mathrm{A}]^2} = \frac{V_f [\mathrm{A}]}{K_b + K_a + [\mathrm{A}]}$$

Equation 3: Initial rate equation for the bi bi ping-pong mechanism with zero initial product and identical reaction substrates.

We note that even though the reactants, [A] and [B], are the same, the rate constants and inhibition constants for the reactants are not the same, so $K_a \neq K_b$ and $K_{ia} \neq K_{ib}$. However, we can state that $K_a + K_b = K_{sum}$, and the measured rate K_{sum} for acetyl-CoA is 1.238 mM (160). Under these considerations, the initial rate equation collapses to into the form of a simple Michaelis-Menten equation:

$$v_o = \frac{V_f [\mathrm{A}]}{K_{sum} + [\mathrm{A}]}$$

Equation 4. Simplified initial rate equation for the bi bi ping-pong mechanism with zero initial product and assuming that $K_a + K_b = K_{sum}$.

Accordingly, this relationship and the five known Haldane relationships (Equation 5) were utilized to calculate the kinetic constants that were not reported in the literature.

$$K_{eq} = \frac{K_{ip}K_{iq}}{K_{ia}K_{ib}} = \frac{V_f K_{ip}K_q}{V_r K_{ia}K_b} = \frac{V_f K_p K_{iq}}{V_r K_a K_{ib}} = \frac{V_f^{\,2} K_p K_q}{V_r^{\,2} K_a K_b} = \frac{1/K_b - 1/K_{ib}}{1/K_{ip} - 1/K_p}$$

Equation 5: Haldane equations for the reversible bi bi ping-pong mechanism.

Four of the kinetic constants, K_q, K_p, K_{ip}, and K_{eq} are known from the literature, and the ratio V_r/V_f was determined by comparing the modeled data against the data gathered from the initial rate plot from Haywood *et al*. (348), which is shown in Figure 61.

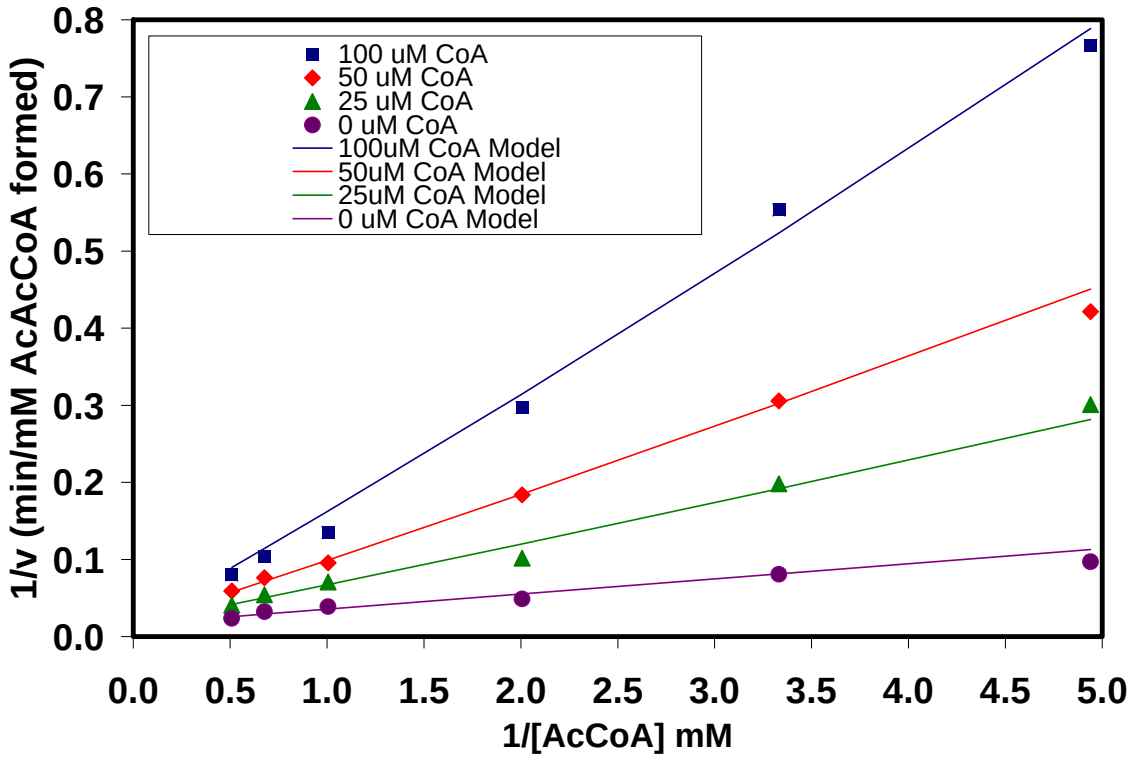

Figure 61. Initial Rate Plots for Inhibition of the Condensation Reaction by CoA. Plots were generated by inserting the values from Table 22 into Equation 1 and taking the concentration of acetoacetyl-CoA, [Q], to be zero. The data points gathered from Haywood *et al*. (348) are shown next to the solid lines which were generated by the model in accord with Leaf *et al*.

Equation 5, combined with the known quantities for K_q, K_p, K_{ip}, K_{eq} and V_r/V_f yield direct solutions to the remaining unknown parameters. These equations are listed below for convenience.

$$K_a = \frac{\left(K_{sum} \pm \sqrt{K_{sum}{}^2 - 4\left(\frac{V_f}{V_r}\right)^2 \frac{K_p K_q}{K_{eq}}} \right)}{2}$$

Equation 6: The quadratic equation is used here to determine K_a.

$$K_b = K_{sum} - K_a$$

Equation 7: Relationship used in the Determination of K_b.

$$K_{ia} = \left(\frac{V_f}{V_r}\right)\left(\frac{K_{ip} K_q}{K_{eq} K_b}\right)$$

Equation 8: Haldane Relationship used in the determination of K_{ia}.

$$K_{ib} = \frac{K_{ip} K_p K_b}{K_b K_{eq}\left(K_{ip} - K_p\right) + K_{ip} K_p}$$

Equation 9: Haldane Relationship used in the Determination of K_{ib}.

$$K_{iq} = \frac{K_{eq} K_{ia} K_{ib}}{K_{ip}} = \left(\frac{V_r}{V_f}\right)\left(\frac{K_{eq} K_a K_{ib}}{K_p}\right)$$

Equation 10: Haldane Relationship used in the determination of K_{iq}.

Acetoacetyl-CoA Reductase. The kinetic mechanism for acetoacetyl-CoA reductase from *C. necator* has not been determined. However, the corresponding enzyme in *Z. ramigeria* purportedly proceeds via an ordered bisubstrate mechanism:

$$v_o = \frac{V_f V_r([A][B] - [P][Q]/K_{eq})}{K_{ia}K_b V_r + V_r K_b[A] + V_r K_a[B] + V_f K_q[P]/K_{eq} + V_f K_p[Q]/K_{eq} + V_r[A][B] + V_f K_q[A][P]/K_{eq}K_{ia} + V_f[P][Q]/K_{eq} + V_r K_a[B][Q]/K_{iq} + V_r[A][B][P]/K_{ip} + V_f[B][P][Q]/K_{ib}K_{eq}}$$

Equation 11. Integrated rate equation for the reversible ordered bi substrate reaction. [A] = NADPH, [B] = acetoacetyl-CoA, [P] = β-hydroxybutyryl-CoA, [Q] = $NADP^+$ and the rate constants for the four compounds are K_a, K_b, K_p, and K_q and the inhibition constants are K_{ia}, K_{ib}, K_{ip}, and K_{iq}.

Kinetic parameters utilized in the simulation for the reaction catalyzed by acetoacetyl-CoA reductase are provided in Table 22 and the known Haldane relationships are:

$$K_{eq} = \left(\frac{V_f}{V_r}\right)^2\left(\frac{K_{ip}K_q}{K_a K_{ib}}\right) = \left(\frac{V_f}{V_r}\right)\left(\frac{K_p K_{iq}}{K_{ia}K_b}\right)$$

Equation 12: Haldane equations for the reversible ordered bisubstrate mechanism.

Acetoacetyl-CoA reductase displays significant substrate inhibition; however, this behavior was not included in the simulation because it introduces unnecessary complexity

considering the very low *in vitro* and *in vivo* concentrations observed for this metabolite.

The combined equilibrium for the β-ketothiolase and acetoacetyl-CoA reductase reactions was obtained from the HPLC data at t = 10 min for the two-enzyme system at equilibrium:

$$K_{eq\ combined} = \frac{\left([\mathrm{CoA}][\mathrm{HBCoA}][\mathrm{NADP^+}]\right)}{\left([\mathrm{AcCoA}]^2[\mathrm{NADPH}]\right)} = \left(K_{eq\ \beta-ketothiolase}\right) \bullet \left(K_{eq\ Acetoacetyl-CoA\ \mathrm{Re}ductase}\right)$$

Equation 13: Combined equation for the equilibrium constant, which is reached in the presence of β-ketothiolase and acetoacetyl-CoA reductase.

From this combined equilibrium constant and the known equilibrium constant for β-ketothiolase, which was reported in the literature (190), the acetoacetyl-CoA equilibrium constant was calculated. This calculated value is approximately one-half of the literature value for the acetoacetyl-CoA reductase equilibrium constant, which correlates relatively well, and this is most likely due to differing experimental conditions.

PHB Synthase. PHB synthase, in this simulation, is represented by the simple irreversible one-substrate Michaelis-Menten equation exhibiting product inhibition as shown in Equation 14. The pertinent kinetic parameters are listed in Table 22.

$$v_o = \left(\frac{V_{Max}[\mathrm{S}]}{K_M(1+([\mathrm{I}]/K_I))+[\mathrm{S}]} \right)$$

Equation 14: Integrated rate equation for the irreversible one substrate Michaelis-Menten mechanism. K_M is the Michaelis-Menten constant; [S] and [I] are the concentrations of the substrate, β-hydroxybutyric acid, and the inhibitor, CoA, respectively. V_{Max} is the maximal velocity of the reaction upon saturation of the enzyme by the substrate.

APPENDIX 2: PHB LABORATORY

Production of poly-3-hydroxybutyrate using *Cupriavidus necator*

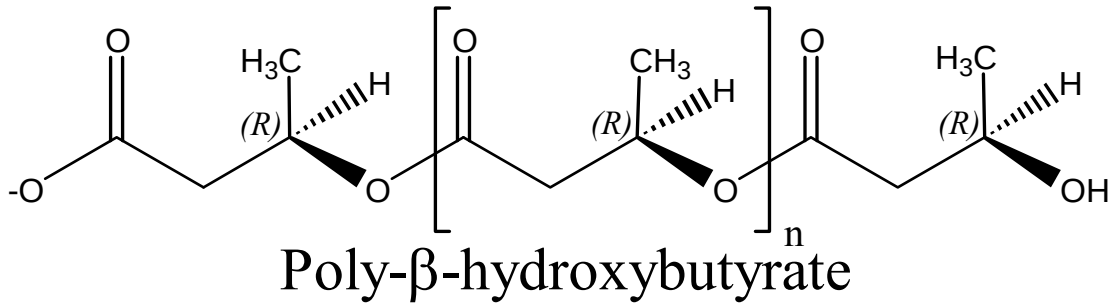

Poly-β-hydroxybutyrate

Figure 62. The Chemical Structure of Poly-β-hydroxybutyrate.

Poly-3-hydroxybutyrate (PHB), shown in Figure 62, is an intracellular polymer that accumulates in the cytoplasm of bacterial cells if a carbon source is provided, and if at least one nutrient, such as nitrogen, is limited. Because it is a biodegradable polyester, there is much interest in its production. In addition to being biodegradable, PHB possesses piezoelectric properties and has characteristics similar to polypropylene, making it suitable for a wide range of applications in surgery, medicine, agriculture, the food industry, and environmental protection.

Cupriavidus necator is one of many bacterial species that will produce PHB under nitrogen-limiting conditions. It has been

reported in the literature that *C. necator* is able to produce up to 60% of its biomass in the form of PHB when using fructose as the carbon source.

The purpose of this experiment is to familiarize the student with the production of PHB using *C. necator*, and to provide a biopolymer sample that can be characterized and compared with other types of polymers.

Initial Growth of *C. necator*

1. Remove vial labeled *C. necator* H16 from the freezer and rapidly thaw cells at 30 °C.

2. Place 35mL of *C. necator* growth medium (Table 23) in a 125mL Erlenmeyer flask. Inoculate the media by adding 250μL of the *C. necator* cells to the nutrient broth.

Table 23. Components of *C. necator* Growth Medium

Media component	**Mass (g/L)**
Nutrient Broth	16.0
Yeast Extract	10.0
Ammonium Sulfate	5.0
The nutrient broth should have a pH of 6.4 upon completion and should need no further pH adjustment.	

3. Incubate the flask in a small shaking incubator at 30 °C and 325 RPM.

4. (This step should take about 12 hours.) When the turbidity of the medium becomes significant, aseptically remove a 1mL aliquot from the shake flask and measure the optical density at 600 nanometers (OD_{600}) by UV-Vis. If the measured absorbance is greater than 1, appropriately dilute the solution and calculate the OD_{600} by multiplying the absorbance of the diluted sample by the dilution factor. Repeat this step until the calculated OD_{600} is 15-16. (After this step, cells may be refrigerated for up to two days.)

5. At this point, the cells are ready to transfer to the Nitrogen-Limited medium. Harvest the cells by centrifugation at 13,800 x g for 5 min. The cells will form a pellet at the bottom of the sterile 50mL centrifuge tube. Decant the nutrient broth and save the pellet. This is the harvested *C. necator* cell paste.

Preparation of Nitrogen-Limited Media

Table 24. Components of Nitrogen-Limited Media

Compound (Parentheses denote volume needed for 1L)		***Mass (g/L)***	***Final Media Concentration***
Solution #1:	Phosphates (1 L)		
	KH_2PO_4	2.8687	19.50mM
	Na_2HPO_4	4.1385	26.97mM
Solution #2:	Magnesium (25mL)		
	$MgSO_4 \cdot 7H_2O$	213.1521	20.00mM
Solution #3:	Iron (5mL)		
	Ferric Ammonium Citrate	5.1420	91 μM
	$CaCl_2$	1.4300	60 μM
Solution #4:	Trace Elements (1mL)		
	$NaMoO_4 \cdot 2H_2O$	0.0057	0.024μM
	$MnCl_2 \cdot 4H_2O$	0.0050	0.023μM
	$ZnSO_4 \cdot 6H_2O$	0.0874	0.300μM
	H_3BO_3	0.0648	0.970μM
	$CuSO_4 \cdot 5H_2O$	0.1295	0.480μM
	$CoCl_2 \cdot 6H_2O$	0.1543	0.600μM
		0.1352	0.250μM
$Cr_2(SO_4)_3 \cdot 6H_2O$			
	$NiCl_2 \cdot 6H_2O$	0.1927	0.750μM
Solution #5:	Fructose (50mL)		
	Fructose	300	15

1. The pH of solution #1 (Table 24) should be pH 6.9, adjust as necessary with NaOH or H_3PO_4.

2. Autoclave, separately, 35mL of solution #1 in a 125mL Erlenmeyer, and also a stock solution of #2.

3. Individually, sterile filter stock solutions #3, #4, and #5.

4. When autoclaved solutions #1 and #2 are cool, add the following quantities to solution #1(Phosphate):

   875μL of solution #2 (Magnesium);

   175μL of solution #3 (Iron);

   35μL of solution #4 (Trace);

   1.75mL of solution #5 (Fructose).

   ***Note: To avoid precipitation, solutions #1 and #2 must be cool. ***

PHB Production Stage of Bacterial Growth

1. Resuspend the harvested *C. necator* cell paste by aseptically adding approximately 15mL of the pre-prepared nitrogen-limited medium to the cell pellet in the centrifuge tube. Gently swirl or shake the capped centrifuge tube until the cell pellet is fully resuspended.
2. Transfer the resuspended *C. necator* cells to the 125mL Erlenmeyer flask containing nitrogen-limited media.
3. Incubate the flask for 24 hours in a small shaking incubator at 30 °C and 325 RPM. Incubation may continue for up to 48 hours.
4. When cell growth is complete, record the OD_{600} as described above. The OD_{600} should reach 30-40 within 24 hours. These cells can be stored in the refrigerator for as long as a week or two.

This is the beginning of the Laboratory Experiment.

SDS Extraction of PHB

Procedure Overview:

SDS, a common detergent, is used in this procedure to extract the PHB from the bacterial cells. Essentially, SDS dissolves away everything except the PHB. Initially, a small aliquot of cell suspension is removed, centrifuged, the supernatant is discarded and the cell pellet allowed to dry in an oven to obtain the dry cell weight of the *C. necator* cells. Then the remaining cell suspension is centrifuged, resuspended in water, SDS and EDTA are added, and the mixture is autoclaved. After autoclaving, the PHB is pelleted by centrifuging, resuspended in water, and then centrifuged again to remove all the SDS and any residual cellular debris. Finally, the crude PHB pellet is acetone dried by vacuum filtration yielding the crude PHB.

1. Each Erlenmeyer flask contains PHB-laden *C. necator* cells in 35mL of nitrogen-limited media.
2. To a pre-weighed 15mL polypropylene centrifuge tube, add a 10mL aliquot of the *C. necator* cells. Set this aliquot aside; it will be used later to determine the dry cellular

weight. To ensure that the aliquot is a good representation of the entire cell sample, be sure to swirl the Erlenmeyer flask so that the cell mixture becomes homogeneous before removing this aliquot.

3. Harvest the remaining 25mL of *C. necator* cells by transferring the cells to a 50mL centrifuge tube and centrifuging at 3440 x g for 5 min. Decant the media and save the pellet.
4. Add 25mL of deionized water to the cell pellet and resuspend by shaking vigorously.
5. To the resuspended *C. necator* cells, add 0.2g SDS and 0.18g EDTA. Cap the centrifuge tube and shake to mix the ingredients.
6. Remove the cap from the centrifuge tube, and autoclave for 30 min.
7. While the cells are autoclaving, centrifuge the 10mL aliquot (set aside in Step 2) of *C. necator* cells at 3200 x g for 10 min. Decant the supernatant, save the pellet, and allow the cell pellet to dry overnight in a 60°C oven. The weight of the pellet will be determined during the next lab period.
8. After autoclaving the 25mL of *C. necator* cells, centrifuge the cell suspension at 13800 x g for 10 min. Decant the supernatant and save the pellet.

9. To remove residual SDS, add 25mL of deionized water to the centrifuge tube and resuspend PHB pellet by stirring with a wooden applicator stick and then shaking vigorously.
10. Centrifuge the PHB/SDS mixture at 13800 x g for 10 min, decant the supernatant, and save the crude PHB pellet.
11. Resuspend the PHB pellet in a minimal amount of deionized water (not more than 2mL) to create a white PHB slurry. Add approximately 10mL of acetone to the PHB slurry. This will induce aggregation of the PHB to facilitate filtering.
12. Filter the PHB/Acetone/Water mixture, under vacuum, with a Buchner funnel containing a Whatman #1 filter. Rinse the centrifuge tube with additional acetone to remove all PHB.
13. Rinse the PHB, by adding approximately 5mL of deionized water to the PHB on the filter to ensure removal of all SDS.
14. Rinse the PHB with acetone and allow PHB to dry under vacuum. This is the crude purification of PHB.

Chloroform Purification of PHB

Procedure Overview:

In this procedure, the PHB is extracted and filtered three times with chloroform. The filtrate, containing the PHB, is collected after each extraction. The PHB solution is concentrated by boiling off some of the chloroform and the PHB is precipitated by addition of methanol. The purified PHB is collected on a Whatman #1 filter paper.

1. Place the crude PHB in a clean Erlenmeyer flask. Add approximately 30mL of chloroform and a wooden boiling stick to the Erlenmeyer flask, and carefully allow the chloroform to come to a boil on a hot plate. Gentle swirling and addition of the boiling stick will help prevent bumping. WARNING! Handle hot glass with a paper towel to prevent burns.
2. After boiling the mixture for about 1 min, remove the flask from the heat and add two scoopulas of celite filtering agent. Filter this mixture under vacuum with a Buchner funnel containing a Whatman #1 filter. Remember that the filtrate, collected in the filter flask, contains the desired PHB.

3. Scrape the residual PHB and celite from the filter paper back into the 125mL Erlenmeyer flask. Add another 30mL of chloroform, boil, and then filter (as performed in step 2) to extract the residual PHB.
4. Repeat step 3, so that a total volume of 90mL is used for the PHB extraction.
5. Rinse the Erlenmeyer flask twice with a total of 10mL of chloroform to remove any residual PHB.
6. Remove the filtration flask from the vacuum system, and concentrate the PHB/chloroform mixture by boiling on a hot plate until approximately 30mL of chloroform remains. The solution will become slightly more viscous. Be careful to stop boiling the sample when 30mL of the chloroform/PHB mixture remains or the polymer will stick and burn on the bottom of the flask.
7. Briefly cool the concentrated PHB/chloroform mixture, and then precipitate the PHB with 150mL of methanol. Up to 300mL of methanol may be necessary depending on the PHB concentration. The PHB should precipitate as a white floc.
8. Collect the precipitated PHB by filtering, under vacuum, with a Buchner funnel containing a Whatman #1 filter. Gently scrape the filter to impede the formation of a PHB mat, which clogs the filter. Do not allow the filter to dry out and clog, or another filter will be necessary.

9. When the filtration is nearly complete, rinse the walls of the filtration unit with a small volume of acetone. Allow the PHB to form a mat on the filter paper.
10. When adequately dry, remove the filter paper containing the PHB mat from the filtration unit. Then carefully remove the PHB by peeling the paper away from the PHB mat.
11. Air-dry the PHB overnight. The PHB will appear as a clear to white sheet of stiff plastic.

PHB Production Workup: To be performed during the next lab period

1. Obtain the weight of the PHB. This is the final yield of PHB.
2. Obtain the weight of the dry cell pellet. This is the DCW of 10mL of *C. necator* cells.
3. Determine the percent of PHB obtained per gram dry cellular weight of *C. necator* cells using the following formula:

$$\text{Percent of PHB/Gram Dry Cell Weight} = \left(\frac{\text{PHB Final Yield}}{\text{Dry Cellular Weight of Pellet} \times \left(\frac{35\ \text{mL}}{10\ \text{mL}} \right)} \right) \times 100$$

Equation 15. Determination of the Percent of PHB per Gram DCW.

REFERENCES

1. De Silva, V., Woznichak, M. M., Burns, K. L., Grant, K. B., and May, S. W. (2004) *J Am Chem Soc* **126**(8), 2409-2413

2. Kirk, O., Borchert, T. V., and Fuglsang, C. C. (2002) *Curr Opin Biotechnol* **13**(4), 345-351

3. Payen, A., and Persoz, J. F. (1833) *Ann. Chim. (Phys.)* **53**, 73-92

4. Voet, D., and Voet, J. G. (2004) Chapter 13-1 Introduction to Enzymes: Historical Perspective. In: Harris, D., and Fitzgerald, P. (eds). *Biochemistry 3rd Edition*, John Wiley & Sons, Hoboken, NJ

5. Kirk, O., Damhus, T., Borchert, T. V., Fuglsang, C. C., Olsen, H. S., Hansen, T. T., Lund, H., Schiff, H. E., and Nielsen, L. K. (2004) *Industrial Enzyme Applications*,

6. Galante, Y. M., and Formantici, C. (2003) *Current Organic Chemistry* **7**, 1399-1422

7. (2001) *Enzymes at Work*, (available as pdf file from www.novozymes.com).

8. Otten, L. G., and Quax, W. J. (2005) *Biomol Eng* **22**(1-3), 1-9

9. Wolfson, W. (2005) *Chemistry & Biology* **12**, 503-505

10. Palackal, N., Brennan, Y., Callen, W. N., Dupree, P., Frey, G., Goubet, F., Hazlewood, G. P., Healey, S., Kang, Y. E., Kretz, K. A., Lee, E., Tan, X., Tomlinson, G. L., Verruto, J., Wong, V. W., Mathur, E. J., Short, J. M., Robertson, D. E., and Steer, B. A. (2004) *Protein Sci* **13**(2), 494-503

11. Gavrilescu, M., and Chisti, Y. (2005) *Biotechnol Adv* **23**(7-8), 471-499

12. Ahuja, S. K., Ferreira, G. M., and Moreira, A. R. (2004) *Crit Rev Biotechnol* **24**(2-3), 125-154

13. Hibbert, E. G., Baganz, F., Hailes, H. C., Ward, J. M., Lye, G. J., Woodley, J. M., and Dalby, P. A. (2005) *Biomol Eng* **22**(1-3), 11-19

14. Schoemaker, H. E., Mink, D., and Wubbolts, M. G. (2003) *Science* **299**(5613), 1694-1697

15. Burns, K. L., and May, S. W. (2003) *J Chromatogr B Analyt Technol Biomed Life Sci* **797**(1-2), 175-190

16. Lorenz, P., and Eck, J. (2005) *Nat Rev Microbiol* **3**(6), 510-516

17. (Jul 1, 2002) *The Application of Biotechnology to Industrial Sustainability: A Primer*, http://www.oecd.org/dataoecd/61/13/1947629.pdf

18. (Nov, 16 2001) *The Application of Biotechnology to Industrial Sustainability*, http://www.oecdbookshop.org/oecd/display.asp?TAG=XKB708XX59X99X9929KWNK&CID=&LANG=EN&SF1=DI&ST1=5LMQCR2K94XV

19. (2003) *White Biotechnology: Gateway to a More Sustainable Future*, http://www.europabio.org/articles/article_320_EN.pdf

20. Agterberg, F.-.-C., Butler, J.-.-B., Carrez, D.-.-E., Gómez, M.-.-B., Iden, R.-.-B., Kessenich, E.-.-B., Laane, C.-.-D., McWhinnie, S.-.-R. S. o. C., Mills, R.-.-D. E., and Sommer, K.-.-B. (2005) *The Vision for 2005 and Beyond: A European Technology Platform for Sustainable Chemistry*, http://www.suschem.org/media/document/38_2170ctp_final.pdf?PHPSESSID=031699eb232ff88bbdb9c769bdf28b6f

21. (2002) *Roadmap: For Biomass Technologies in the United States*, http://www.bioproducts-bioenergy.gov/pdfs/finalbiomassroadmap.pdf

22. Jenck, J. F., Agterberg, F., and Droescher, M. J. (2004) *Green Chemistry* **6**, 544-556

23. Patel, R., Hanson, R., Goswami, A., Nanduri, V., Banerjee, A., Donovan, M. J., Goldberg, S., Johnston, R., Brzozowski, D., Tully, T., Howell, J., Cazzulino, D., and Ko, R. (2003) *J Ind Microbiol Biotechnol* **30**(5), 252-259

24. Rouhi, A. M. (2003) *Chemical & Engineering News* **81**(18), 56-61

25. Rouhi, A. M. (2004) *Chemical & Engineering News* **82**(24), 47-62

26. Bruggink, A., Roos, E. C., and Vroom, E. d. (1998) *Organic Process Research & Development* **2**, 128-133

27. Schroen, C. G., Nierstrasz, V. A., Moody, H. M., Hoogschagen, M. J., Kroon, P. J., Bosma, R., Beeftink, H. H., Janssen, A. E., and Tramper, J. (2001) *Biotechnol Bioeng* **73**(3), 171-178

28. Rhee, D. K., Lee, S. B., Rhee, J. S., Ryu, D. D., and Hospodka, J. (1980) *Biotechnol Bioeng* **22**(6), 1237-1247

29. Wegman, M. A., van Langen, L. M., van Rantwijk, F., and Sheldon, R. A. (2002) *Biotechnol Bioeng* **79**(3), 356-361

30. Erickson, B. (2002) *The Application of Industrial Biotechnology to Pollution Prevention*, http://www.bio.org/ind/background/pollutionprevn2.asp?id=2

31. Tzanov, T., Andreaus, J., Guebitz, G., and Cavaco-Paulo, A. (2003) *Protein Interactions in enzymatic processes in Textiles*, http://www.ejbiotechnology.info/content/vol6/issue3/full/8

32. Ramachandran, T., and Karthik, T. (2004) Application of Genetic Engineering and Enzymes in Textiles. In. *Textile Engineering*

33. Poliakoff, M., Fitzpatrick, J. M., Farren, T. R., and Anastas, P. T. (2002) *Science* **297**(5582), 807-810

34. Anastas, P. T., and Kirchhoff, M. M. (2002) *Acc Chem Res* **35**(9), 686-694

35. (2002) *Green Chemistry Program Fact Sheet*, http://www.epa.gov/greenchemistry/whats_gc.html

36. *12 Principles of Green Chemistry*, http://www.epa.gov/greenchemistry/principles.html

37. (2005) *Presidential Green Chemistry Challenge Award for Alternative Synthetic Pathways: Archer Daniels Midland Company & Novozymes: NovaLipid™: Low Trans Fats and Oils Produced by Enzymatic Interesterification of Vegetable Oils Using Lipozyme®*, http://www.epa.gov/greenchemistry/aspa05.html

38. Ritter, S. K. (2005) *Chemical & Engineering News* **83**(26), 40-43

39. *FDA Acts to Provide Better Information to Consumers on Trans Fats*, http://www.fda.gov/oc/initiatives/transfat/

40. Stevens, E. S. (2003) *BioCycle* **44**(3), 24-27

41. Stevens, E. S. (2002) *BioCycle* **43**(12), 42-45

42. (1999) *Presidential Green Chemistry Challenge Award for Alternative Solvents/Reaction Conditions Award: Nalco Chemical Company: The Development and Commercialization of ULTIMER®: The First of a New Family of Water Soluble Polymer Dispersions*, http://www.epa.gov/greenchemistry/ascra99.html

43. (2005) *biopolymer*, http://www.merriam-webster.com

44. Steinbuchel, A. (2001) *Macromolecular Bioscience* **1**, 1-24

45. *ASTM D 6400-4 Standard Specification for Compostable Plastics*, http://www.astm.org/cgi-bin/SoftCart.exe/DATABASE.CART/REDLINE_PAGES/D6400.htm?L+mystore+owsu2461

46. *ASTM D 6002-96 Standard Guide for Assessing the Compostability of Environmentally Degradable Plastics*, http://www.astm.org/cgi-bin/SoftCart.exe/DATABASE.CART/HISTORICAL/D6002-96.htm?L+mystore+owsu2461

47. *ASTM D 6868-03 Standard Specification for Biodegradable Plastics Used as Coatings on Paper and Other Compostable Substrates*, http://www.astm.org/cgi-bin/SoftCart.exe/DATABASE.CART/REDLINE_PAGES/D6868.htm?L+mystore+owsu2461

48. *ASTM D 6954-04 Standard Guide for Exposing and Testing Plastics that Degrade in the Environment by a Combination of Oxidation and Biodegradation*, http://www.astm.org/cgi-bin/SoftCart.exe/DATABASE.CART/REDLINE_PAGES/D6954.htm?L+mystore+owsu2461

49. Klemchuk, P. P. (1990) *Polymer Degradation and Stability* **27**, 183-202

50. Bonhomme, S., Cuer, A., Delort, A.-M., Lemaire, J., Sancelme, M., and Scott, G. (2003) *Polymer Degradation and Stability* **81**, 441-452

51. Scott, G. (2000) *Polymer Degradation and Stability* **68**, 1-7

52. Gross, R. A., and Kalra, B. (2002) *Science* **297**(5582), 803-807

53. Loeker, F. C., Duxbury, C. J., Kumar, R., Gao, W., Gross, R. A., and Howdle, S. M. (2004) *macromolecules* **37**(7), 2450-2453

54. Perez, J., Munoz-Dorado, J., de la Rubia, T., and Martinez, J. (2002) *Int Microbiol* **5**(2), 53-63

55. Kim do, Y., Lutke-Eversloh, T., Elbanna, K., Thakor, N., and Steinbuchel, A. (2005) *Biomacromolecules* **6**(2), 897-901

56. Scott, G., and Wiles, D. M. (2001) *Biomacromolecules* **2**(3), 615-622

57. Weiland, M., and David, C. (1994) *Polymer Degradation and Stability* **45**, 371-377

58. Jakubowicz, I. (2003) *Polymer Degradation and Stability* **80**, 39-43

59. Chiellini, E., Corti, A., and Swift, G. (2003) *2003* **81**, 341-351

60. Mecking, S. (2004) *Angew Chem Int Ed Engl* **43**(9), 1078-1085

61. Moore, C. J., Moore, S. L., Leecaster, M. K., and Weisberg, S. B. (2001) *Mar Pollut Bull* **42**(12), 1297-1300

62. Kubota, M., Takayama, K., and Namimoto, D. (2005) *Appl Microbiol Biotechnol* **67**(4), 469-476

63. Thompson, R. C., Olsen, Y., Mitchell, R. P., Davis, A., Rowland, S. J., John, A. W. G., McGonigle, D., and Russell, A. E. (2004) *Science* **304**, 838

64. Derraik, J. G. (2002) *Mar Pollut Bull* **44**(9), 842-852

65. Ryan, P. G., and Moloney, C. L. (1993) *Nature* **361**, 23

66. Eilperin, J. (2004) Plastic Debris Found in Oceans; Bits of Refuse on Beaches and Ocean Floor, Study Reveals. In. *The Washington Post*, Washington, D.C.

67. Baker, A. (2005) New York Garbage Adapts To Life After Fresh Kills. In. *The New York Times*, Late Edition Ed., New York

68. Johnson, K. (2002) Throwaway Societies of Yesteryear; Past Decades Were the Golden Ages for Waste, Scientist Says. In. *The New York Times*, New York

69. Gottberg, A., Morris, J., Pollard, S., Mark-Herbert, C., and Cook, M. (2005) *Sci Total Environ*

70. Okuwaki, A. (2004) *Polymer Degradation and Stability* **85**, 981-988

71. Uela, K., and Koizumi, H. (2001) *Environment* **Nov 1, 2001**, 22-32

72. Lehmann, M. A. (2004) *2004* **28**, 435-449

73. Braunegg, G., Bona, R., Schellauf, F., and Wallner, E. (2004) *Polymer-Plastics Technology and Engineering* **43**(6), 1755-1767

74. (2005) *Recycling Facts and Figures*, http://www.epa.gov/epaoswer/non-hw/muncpl/recycle.htm

75. Gerngross, T. U., and Slater, S. C. (2000) *Scientific American* **August**, 37-41

76. Caruso, G. (2005) When Will World Oil Production Peak. In. *10th Annual Asia Oil and Gas Conference*, Energy Information Administration, Kuala Lumpur, Malaysia

77. Perlack, R. D., Wright, L. L., Turhollow, A. F., Graham, R. L., Stokes, B. J., and Erbach, D. C. (2005) Biomass as Feedstock for a Bioenergy and Bioproducts Industry: The Technical Feasibility of a Billion-Ton Annual Supply. In: Agriculture, U. S. D. o., and Energy, U. S. D. o. (eds).

78. Chen, E. (2005) Bush Signs Overhaul of U.S. Energy Policy. In. *Los Angeles Times*, Home Edition Ed., Los Angeles

79. Kinti, E. (2005) *Science* **309**, 863

80. (2005) *Energy Policy Act of 2005*, http://www.govtrack.us/data/us/bills.text/109/h6.pdf

81. Gerngross, T. U. (1999) *Nature Biotechnology* **17**, 541-544

82. Kurdikar, D., Fournet, L., Slater, S. C., Paster, M., Gruys, K. J., Gerngross, T. U., and Coulon, R. (2001) *Journal of Industrial Ecology* **4**(3), 107-122

83. Nonato, R. V., Mantelatto, P. E., and Rossell, C. E. (2001) *Appl Microbiol Biotechnol* **57**(1-2), 1-5

84. Akiyama, M., Tsuge, T., and Doi, Y. (2003) *Polymer Degradation and Stability* **80**, 183-194

85. Kim, S., and Dale, B. E. (2005) *Biopolymers* **10**(3), 200-210

86. Hocking, P. J. a. M., R. H. (1998) Polyhydroxyalkanoates. In: Kaplan, D. L. (ed). *Biopolymers from Renewable Resources*, Springer-Verlag, Berlin, Heidelberg, New York

87. Cherry, J. R., and Fidantsef, A. L. (2003) *Curr Opin Biotechnol* **14**(4), 438-443

88. MacDonald, E. (2005) *Forbes* **March 28**

89. Selke, S. E. P. (2000) Plastics Recycling and Biodegradable Plastics. In: Harper, C. A. (ed). *Modern Plastics Handbook*, McGraw-Hill

90. Herrick, T. (2004) *The Wall Street Journal* **October 12, 2004**

91. Vink, E. T., Rabago, K. R., Glassner, D. A., Springs, B., O'Connor, R. P., Kolstad, J., and Gruber, P. R. (2004) *Macromol Biosci* **4**(6), 551-564

92. Steinbüchel, A. (ed) (2004) *Polyesters I: Biological Systems and Biotechnological Production: Biodegradable aliphatic-aromatic polyesters: "Ecoflex®"*, Wiley-VCH

93. Auras, R., Harte, B., and Selke, S. (2004) *Macromol Biosci* **4**(9), 835-864

94. Vink, E. T. H., Rabago, K. R., Glassner, D. A., and Gruber, P. R. (2003) *Polymer Degradation and Stability* **80**, 403-419

95. Tullo, A. (2005) *Chemical & Engineering News* **83**(5), 11

96. Company, D. C. (2005) Form 10-K. In: Commission, U. S. S. a. E. (ed).

97. Katsnelson, A. (2005) *Nat Biotechnol* **23**(6), 638

98. Tullo, A. (2005) *Chemistry & Engineering News: Business* **83**(9), 26

99. Kharif, O. (2005) *Business Week Online* **2/22/2005**, 00

100. (2005) BASF Builds Second Biodegradable Plastics Plant. In. *Chemical Week*

101. (2005) *Chemical & Engineering News* **83**(18), 12-13

102. Jaiimsin, A. (2004) BASF, Thai Agency Discuss New Biodegradable-Polymers Venture. In. *Bangkok Post*, BangKok, Thailand

103. (2005) BASF: BASF Increases Capacity for Biodegradable Plastic Ecoflex. In. *M2 Presswire*

104. Bastioli, C. (1998) *Polymer Degradation and Stability* **59**(1-3), 263-272

105., http://www.metabolix.com/sustainable%20solutions/energybalance.html

106. (1996) *Chemistry & Engineering News: Business*, 11

107. *Mater-Bi*, http://www.materbi.com/ing/html/prodotto/tecnologie/indextecnologie.html

108. (2000) *Chemical & Engineering News* **78**(16), 13-14

109. Kurian, J. V. (2005) *Journal of Polymers and the Environment* **13**(2), 159 - 167

110. *Dupont™ Sorona(R): Frequently Asked Questions*, http://www.dupont.com/sorona/faqs.html#21

111. Ritter, S. K. (2008) *Chemical & Engineering News* **81**(26), 30-35

112. (2003) *Presidential Green Chemistry Challenge Award for Alternative Solvents/Reaction Conditions Award: DuPont: Microbial Production of 1,3-Propanediol*, http://www.epa.gov/greenchemistry/ascra03.html

113. Nakamura, C. E., and Whited, G. M. (2003) *Curr Opin Biotechnol* **14**(5), 454-459

114. Chen, G. Q., and Wu, Q. (2005) *Appl Microbiol Biotechnol* **67**(5), 592-599

115. Khanna, S., and Srivastava, A. K. (2005) *Process Biochemistry* **40**, 607-619

116. Lenz, R. W., and Marchessault, R. H. (2005) *Biomacromolecules* **6**(1), 1-8

117. Noda, I., Green, P. R., Satkowski, M. M., and Schechtman, L. A. (2005) *Biomacromolecules* **6**(2), 580-586

118. Lenz, R. W., Farcet, C., Dijkstra, P. J., Goodwin, S., and Zhang, S. (1999) *Int J Biol Macromol* **25**(1-3), 55-60

119. *The Nobel Prize in Chemistry 1953: "for his discoveries in the field of macromolecular chemistry" Hermann Staudinger*, http://nobelprize.org/chemistry/laureates/1953/index.html

120. Reddy, C. S., Ghai, R., Rashmi, and Kalia, V. C. (2003) *Bioresour Technol* **87**(2), 137-146

121. United States. Congress. Office of Technology Assessment. (1993) *Biopolymers: Making Materials Nature's Way*, The Office: For sale by the U.S. G.P.O., Supt. of Docs., Washington, DC

122. Poirier, Y. (1999) *Nat Biotechnol* **17**(10), 960-961

123. Nawrath, C., Poirier, Y., and Somerville, C. (1994) *Proc Natl Acad Sci U S A* **91**(26), 12760-12764

124. (2001) *Metabolix Purchases BioPol Assets from Monsanto*, http://www.metabolix.com/publications/pressreleases/PRbiopol.html;
http://www.monsanto.co.uk/news/ukshowlib.phtml?uid=5082

125. Fidler, S., and Dennis, D. (1992) *FEMS Microbiol Rev* **9**(2-4), 231-235

126. Miller, M. (2004) *Metabolix and ADM Enter Strategic Alliance to Commercialize PHA Natural Polymers*, http://www.metabolix.com/publications/pressreleases/PRnov2004ADM.html

127. Tullo, A. (2005) *Chemical & Engineering News* **83**(13), 9

128. Barber, J. (2005) *BP and Metabolix Agree to a Joint Development Program for Renewable Plastics*, http://www.metabolix.com/publications/pressreleases/PRmar2005BP.html;
http://www.innovene.com/innovene/T_A1_press_release_10.html

129. Plant Fact Sheet: Switchgrass. In: Agriculture, U. S. D. o. (ed). USDA NRCS Plant Materials Program

130. Steinbuchel, A., and Valentin, H. E. (1995) *FEMS Microbiology Letters* **128**, 219-228

131. Chen, G. Q., and Wu, Q. (2005) *Biomaterials* **26**(33), 6565-6578

132. Cozier, M. (2004) *European Chemical News* **80**(2094), 25

133. Lutke-Eversloh, T., Bergander, K., Luftmann, H., and Steinbuchel, A. (2001) *Microbiology* **147**(Pt 1), 11-19

134. Lutke-Eversloh, T., Fischer, A., Remminghorst, U., Kawada, J., Marchessault, R. H., Bogershausen, A., Kalwei, M., Eckert, H., Reichelt, R., Liu, S. J., and Steinbuchel, A. (2002) *Nat Mater* **1**(4), 236-240

135. Gerngross, T. U., and Martin, D. P. (1995) *Proc Natl Acad Sci U S A* **92**(14), 6279-6283

136. Burns, K. L., Lane, J., Thompson, J., Lubarsky, M., and May, S. W. (2003) *In Vitro* Enzymatic Synthesis of Poly-(β)-hydroxybutyric acid. In. *Abstracts, 55th Southeast Regional Meeting of the American Chemical Society*, American Chemical Society, Washington, D. C., Atlanta, GA, United States

137. Hocking, P. J., and Marchessault, R. H. (1998) Polyhydroxyalkanoates. In: Abe, A., Monnerie, L., Shibaev, V., Suter, U. W., Tiorrell, D., and Ward, I. M. (eds). *Biopolymers from Renewable Resources*, Springer-Verlag, Berlin, Heidelberg, New York

138. Potter, M., and Steinbuchel, A. (2005) *Biomacromolecules* **6**(2), 552-560

139. Saegusa, H., Shiraki, M., Kanai, C., and Saito, T. (2001) *J Bacteriol* **183**(1), 94-100

140. York, G. M., Lupberger, J., Tian, J., Lawrence, A. G., Stubbe, J., and Sinskey, A. J. (2003) *J Bacteriol* **185**(13), 3788-3794

141. Schwartz, E., Henne, A., Cramm, R., Eitinger, T., Friedrich, B., and Gottschalk, G. (2003) *J Mol Biol* **332**(2), 369-383

142. Potter, M., Muller, H., Reinecke, F., Wieczorek, R., Fricke, F., Bowien, B., Friedrich, B., and Steinbuchel, A. (2004) *Microbiology* **150**(Pt 7), 2301-2311

143. Numata, K., Kikkawa, Y., Tsuge, T., Iwata, T., Doi, Y., and Abe, H. (2005) *Biomacromolecules* **6**(4), 2008-2016

144. Abe, H., and Doi, Y. (2002) *Biomacromolecules* **3**(1), 133-138

145. Akmala, D., Azizanc, M. N., and Majid, M. I. A. (2003) *Polymer Degradation and Stability* **80**(2), 513-518

146. Marchessault, R. H., C. J. Monasterios, C. J., and Jesudason, J. J. (1994) *Polymer Degradation and Stability* **45**(2), 187-196

147. *Metabolix: Fermentation*, http://www.metabolix.com/biotechnology%20foundation/fermentation.html

148. Wieczorek, R., Pries, A., Steinbuchel, A., and Mayer, F. (1995) *J Bacteriol* **177**(9), 2425-2435

149. Stubbe, J., and Tian, J. (2003) *Nat Prod Rep* **20**(5), 445-457

150. Qi, Q., Steinbuchel, A., and Rehm, B. H. (2000) *Appl Microbiol Biotechnol* **54**(1), 37-43

151. York, G. M., Stubbe, J., and Sinskey, A. J. (2002) *J Bacteriol* **184**(1), 59-66

152. Potter, M., Madkour, M. H., Mayer, F., and Steinbuchel, A. (2002) *Microbiology* **148**(Pt 8), 2413-2426

153. York, G. M., Stubbe, J., and Sinskey, A. J. (2001) *J Bacteriol* **183**(7), 2394-2397

154. York, G. M., Junker, B. H., Stubbe, J. A., and Sinskey, A. J. (2001) *J Bacteriol* **183**(14), 4217-4226

155. Maehara, A., Taguchi, S., Nishiyama, T., Yamane, T., and Doi, Y. (2002) *J Bacteriol* **184**(14), 3992-4002

156. Brown, D. M., and Todd, A. R. (1951) *J. Chem. Soc.*, 2952

157. Stern, J. R., and Ochoa, S. (1951) *J Biol Chem* **191**(1), 161-172

158. Merrick, J. M., and Doudoroff, M. (1961) *Nature* **189**, 890-892

159. Saito, T., Fukui, T., Ikeda, F., Tanaka, Y., and Tomita, K. (1977) *Arch Microbiol* **114**(3), 211-217

160. Haywood, G. W., Anderson, A. J., Chu, L., and Dawes, E. A. (1988) *FEMS Microbiology Letters* **52**, 259-264

161. Haywood, G. W., Anderson, A. J., and Dawes, E. A. (1989) *FEMS Microbiology Letters* **57**, 1-6

162. Gerngross, T. U., Snell, K. D., Peoples, O. P., Sinskey, A. J., Csuhai, E., Masamune, S., and Stubbe, J. (1994) *Biochemistry* **33**(31), 9311-9320

163. Jossek, R., Reichelt, R., and Steinbuchel, A. (1998) *Appl Microbiol Biotechnol* **49**(3), 258-266

164. Muh, U., Sinskey, A. J., Kirby, D. P., Lane, W. S., and Stubbe, J. (1999) *Biochemistry* **38**(2), 826-837

165. Zhang, S., Yasuo, T., Lenz, R. W., and Goodwin, S. (2000) *Biomacromolecules* **1**(2), 244-251

166. Su, L., Lenz, R. W., Takagi, Y., Zhang, S., Goodwin, S., Zhong, L., and Martin, D. P. (2000) *Macromolecules* **33**, 229-231

167. Song, J. J., Zhang, S., Lenz, R. W., and Goodwin, S. (2000) *Biomacromolecules* **1**(3), 433-439

168. Zhang, S., Kolvek, S., Lenz, R. W., and Goodwin, S. (2003) *Biomacromolecules* **4**(3), 504-509

169. Zhang, S., Kamachi, M., Takagi, Y., Lenz, R. W., and Goodwin, S. (2001) *Appl Microbiol Biotechnol* **56**(1-2), 131-136

170. Kamachi, M. Z., Shiming, Goodwin, S., and Lenz, R. W. (2001) *Macromolecules* **34**(20), 6889 -6894

171. Zhang, S., Kolvek, S., Goodwin, S., and Lenz, R. W. (2004) *Biomacromolecules* **5**(1), 40-48

172. Yuan, W., Jia, Y., Tian, J., Snell, K. D., Muh, U., Sinskey, A. J., Lambalot, R. H., Walsh, C. T., and Stubbe, J. (2001) *Arch Biochem Biophys* **394**(1), 87-98

173. Pantazaki, A. A., Tambaka, M. G., Langlois, V., Guerin, P., and Kyriakidis, D. A. (2003) *Mol Cell Biochem* **254**(1-2), 173-183

174. Hiraishi, T., Kikkawa, Y., Fujita, M., Normi, Y. M., Kanesato, M., Tsuge, T., Sudesh, K., Maeda, M., and Doi, Y. (2005) *Biomacromolecules* **6**(5), 2671-2677

175. Matsumoto, K., Matsusaki, H., Taguchi, K., Seki, M., and Doi, Y. (2002) *Biomacromolecules* **3**(4), 787-792

176. Sudesh, K., Gan, Z., Matsumot, K., and Doi, Y. (2002) *Ultramicroscopy* **91**(1-4), 157-164

177. Sudesha, K., Ganb, Z., Maeharac, A., and Doi, Y. (2002) *Polymer Degradation and Stability* **77**(1), 77-85

178. Nobes, G. A. R., Jurasek, L., Marchessault, R. H., Martin, D. P., Putaux, J. L., and Chanzy, H. (2000) *Macromolecular Rapid Communications* **21**(1), 77 - 84

179. Jossek, R., and Steinbuchel, A. (1998) *FEMS Microbiol Lett* **168**(2), 319-324

180. Liu, S. J., and Steinbuchel, A. (2000) *Appl Microbiol Biotechnol* **53**(5), 545-552

181. Satoh, Y., Tajima, K., Tannai, H., and Munekata, M. (2003) *J. Biosci. Bioeng.* **95**(4), 335-341

182. Satoh, Y., Murakami, F., Tajima, K., and Munekata, M. (2005) *J Biosci Bioeng* **99**(5), 508-511

183. Kameda, A., Shiba, T., Kawazoe, Y., Satoh, Y., Ihara, Y., Munekata, M., Ishige, K., and Noguchi, T. (2001) *J Biosci Bioeng* **91**(6), 557-563

184. Kim, Y. R., Paik, H. J., Ober, C. K., Coates, G. W., and Batt, C. A. (2004) *Biomacromolecules* **5**(3), 889-894

185. Paik, H. J., Kim, Y. R., Orth, R. N., Ober, C. K., Coates, G. W., and Batt, C. A. (2005) *Chem Commun (Camb)* (15), 1956-1958

186. Lee, S. J., Park, J. P., Park, T. J., Lee, S. Y., Lee, S., and Park, J. K. (2005) *Anal Chem* **77**(17), 5755-5759

187. Tajima, K., Satoh, Y., Nakazawa, K., Tannai, H., Erata, T., and Munekata, M. (2004) *Macromolecules* **37**, 4544-4546

188. Kaihara, S., Osanai, Y., Nishikawa, K., Toshima, K., Doi, Y., and Matsumura, S. (2005) *Macromol Biosci* **5**(7), 644-652

189. van Wegen, R. J., Lee, S. Y., and Middelberg, A. P. (2001) *Biotechnol Bioeng* **74**(1), 70-80

190. Leaf, T. A., and Srienc, F. (1998) *Biotechnology and Bioengineering* **57**(5), 557-570

191. Daae, E. B., Dunnill, P., Mitsky, T. A., Padgette, S. R., Taylor, N. B., Valentin, H. E., and Gruys, K. J. (1999) *Metab Eng* **1**(3), 243-254

192. Heinzle, E., and Lafferty, R. M. (1980) *European J. Appl. Microbiol. Biotechnol.* **11**, 8-16

193. Mulchandani, A., Luong, J. H. T., and Groom, C. (1989) *Appl. Microbiol. Biotechnol.* **30**, 11-17

194. Beun, J. J., Heijnen, J. J., and van Loosdrecht, M. C. (2001) *Biotechnol Bioeng* **75**(1), 82-92

195. Beun, J. J., Paletta, F., Van Loosdrecht, M. C., and Heijnen, J. J. (2000) *Biotechnol Bioeng* **67**(4), 379-389

196. Beun, J. J., Verhoef, E. V., Van Loosdrecht, M. C., and Heijnen, J. J. (2000) *Biotechnol Bioeng* **68**(5), 496-507

197. Dircks, K., Beun, J. J., van Loosdrecht, M., Heijnen, J. J., and Henze, M. (2001) *Biotechnol Bioeng* **73**(2), 85-94

198. Katoh, T., Yuguchi, D., Yoshii, H., Shi, H., and Shimizu, K. (1999) *J Biotechnol* **67**(2-3), 113-134

199. Kurja, J., Zirkzee, H. F., de Koning, G. M., and Maxwell, I. A. (1995) *Macromol. Theory Simul.* **4**, 839-855

200. Schuler, A. J., Jenkins, D., and Ronen, P. (2001) *Water Sci Technol* **43**(1), 173-180

201. Yoo, S., and Kim, W.-S. (1994) *Biotechnol. Bioeng.* **43**, 1043-1051

202. Yu, J., Si, Y., and Wong, W.-K. R. (2002) *Process Biochemistry* **37**, 731-738

203. Yu, J., and Wang, J. (2001) *Biotechnol Bioeng* **73**(6), 458-464

204. Carlson, R., Fell, D., and Srienc, F. (2002) *Biotechnol Bioeng* **79**(2), 121-134

205. Gadkar, K. G., Doyle, F. J., 3rd, Crowley, T. J., and Varner, J. D. (2003) *Biotechnol Prog* **19**(5), 1487-1497

206. Guisasola, A., Pijuan, M., Baeza, J. A., Carrera, J., Casas, C., and Lafuente, J. (2004) *Biotechnol Bioeng* **85**(7), 722-733

207. Lynen, F., and Ochoa, S. (1953) *Biochim Biophys Acta* **12**(1-2), 299-314

208. Pratt, S., Yuan, Z., and Keller, J. (2004) *Biotechnol Bioeng* **88**(2), 135-147

209. Third, K. A., Newland, M., and Cord-Ruwisch, R. (2003) *Biotechnol Bioeng* **82**(2), 238-250

210. Third, K. A., Sepramaniam, S., Tonkovic, Z., Newland, M., and Cord-Ruwisch, R. (2004) *Water Sci Technol* **50**(10), 171-180

211. Yagci, N., Artan, N., Cokgor, E. U., Randall, C. W., and Orhon, D. (2003) *Biotechnol Bioeng* **84**(3), 359-373

212. Gruys, K. J., Mitsky, T. A., Kishore, G. M., Slater, S. C., Padgette, S. R., and Stark, D. M. (1999) Methods of optimizing substrate pools and biosynthesis of hydroxybutyrate-hydroxyvalerate copolymer in bacteria and plants. In., Monsanto Company, St. Louis, Mo., US

213. Slater, S., Houmiel, K. L., Tran, M., Mitsky, T. A., Taylor, N. B., Padgette, S. R., and Gruys, K. J. (1998) *J Bacteriol* **180**(8), 1979-1987

214. Bradford, M. M. (1976) *Anal Biochem* **72**, 248-254

215. Davis, J. T., Moore, R. N., Imperiali, B., Pratt, A. J., Kobayashi, K., Masamune, S., Sinskey, A. J., Walsh, C. T., Fukui, T., and Tomita, K. (1987) *J Biol Chem* **262**(1), 82-89

216. Fukui, T., Yoshimoto, A., Matsumoto, M., Hosokawa, S., and Saito, T. (1976) *Arch Microbiol* **110**(23), 149-156

217. Mendes, P. (1993) *Comput Appl Biosci* **9**(5), 563-571

218. Mendes, P. (1997) *Trends Biochem Sci* **22**(9), 361-363

219. Mendes, P., and Kell, D. (1998) *Bioinformatics* **14**(10), 869-883

220. Ploux, O., Masamune, S., and Walsh, C. T. (1988) *Eur J Biochem* **174**(1), 177-182

221. Gilbert, H. F., Lennox, B. J., Mossman, C. D., and Carle, W. C. (1981) *J Biol Chem* **256**(14), 7371-7377

222. Burns, K. L., Gelbaum, L. T., Sullards, M. C., Bostwick, D. E., and May, S. W. (2005) *J Biol Chem* **280**(17), 16550-16558

223. King, M. T., and Reiss, P. D. (1985) *Anal Biochem* **146**(1), 173-179

224. Boynton, Z. L., Bennett, G. N., and Rudolph, F. B. (1994) *Applied and Environmental Microbiology* **60**(1), 39-44

225. Norwood, D. L., Bus, C. A., and Millington, D. S. (1990) *J. Chromatogr., B: Anal. Technol. Biomed. Life Sci.* **527**(2), 289-301

226. DeBuysere, M. S., and Olson, M. S. (1983) *Anal Biochem* **133**(2), 373-379

227. Claessens, H. A., vanStraten, M. A., and Kirkland, J. J. (1996) *Journal of Chromatography A* **728**(1-2), 259-270

228. Killenberg, P. G., and Dukes, D. F. (1976) *J Lipid Res* **17**(5), 451-455

229. Baker, F. C., and Schooley, D. A. (1979) *Anal Biochem* **94**(2), 417-424

230. Ingebretsen, O. C., Normann, P. T., and Flatmark, T. (1979) *Anal Biochem* **96**(1), 181-188

231. Corkey, B. E., Brandt, M., Williams, R. J., and Williamson, J. R. (1981) *Anal Biochem* **118**(1), 30-41

232. Abbott, D. A., Schlarman, D. E., Patrick, P. H., Tal, D. M., and Elliott, W. H. (1985) *Anal Biochem* **146**(2), 437-441

233. Takeyama, N., Takagi, D., Adachi, K., and Tanaka, T. (1986) *Anal Biochem* **158**(2), 346-354

234. Dugan, R. E., Schmidt, M. J., Hoganson, G. E., Steele, J., Gilles, B. A., and Shug, A. L. (1987) *Anal Biochem* **160**(2), 275-280

235. Norwood, D. L., Bus, C. A., and Millington, D. S. (1990) *J Chromatogr* **527**(2), 289-301

236. Yamato, S., Nakajima, M., Wakabayashi, H., and Shimada, K. (1992) *J Chromatogr* **590**(2), 241-245

237. HermansLokkerbol, A., vanderHeijden, R., and Verpoorte, R. (1996) *J Chromatogr A* **752**(1-2), 123-130

238. Tachibana, A., Yano, Y., Otani, S., and Taniguchi, M. (1998) *J Ferment Bioeng* **86**(5), 523-526

239. Ingebretsen, O. C., and Farstad, M. (1980) *J Chromatogr* **202**(3), 439-445

240. Burns, J. A., Butler, J. C., Moran, J., and Whitesides, G. M. (1991) *Journal of Organic Chemistry* **56**, 2648-2650

241. Anderson, V. E., Bahnson, B. J., Wlassics, I. D., and Walsh, C. T. (1990) *J Biol Chem* **265**(11), 6255-6261

242. Thompson, S., Mayerl, F., Peoples, O. P., Masamune, S., Sinskey, A. J., and Walsh, C. T. (1989) *Biochemistry* **28**(14), 5735-5742

243. Wakil, S. J., Green, D. E., Mii, S., and Mahler, H. R. (1954) *J. Biol. Chem.* **207**(2), 631-638

244. Nobes, G. A. R., Jurasek, L., Marchessault, R. H., Martin, D. P., Putaux, J. L., and Chanzy, H. (2000) *Macromol Rapid Commun.* **21**, 77-84

245. Masamune, S., Walsh, C. T., Sinskey, A. J., and Peoples, O. P. (1989) *Pure & Applied Chemistry* **61**(3), 303-321

246. Satoh, Y., Tajima, K., Tannai, H., and Munekata, M. (2003) *J. Biosci. Bioeng.* **95**(4), 335-341

247. Voet, D., and Voet, J. G. (2004) Chapter 25 Lipid Metabolism. In: Harris, D., and Fitzgerald, P. (eds). *Biochemistry 3rd Edition*, John Wiley & Sons, Hoboken, NJ

248. Voet, D., and Voet, J. G. (2004) Chapter 26 Amino Acid Metabolism. In: Harris, D., and Fitzgerald, P. (eds). *Biochemistry 3rd Edition*, John Wiley & Sons, Hoboken, NJ

249. Yao, K. W., and Schulz, H. (1996) *J Biol Chem* **271**(30), 17816-17820

250. Schlegel, H. G., Gottschalk, G., and Von Bartha, R. (1961) *Nature* **191**, 463-465

251. Meier-Schneiders, M., Weikmann, W., Grosshans, U., Busch, C., and Steinbuchel, A. (1995) *Canadian Journal of Microbiology* **41**(Suppl. 1), 267-273

252. Repaske, R., and Mayer, R. (1976) *Appl Environ Microbiol* **32**(4), 592-597

253. Repaske, R., and Repaske, A. C. (1976) *Appl Environ Microbiol* **32**(4), 585-591

254. Cho, K. S., Ryu, H. W., Lee, E. G., and Chang, Y. K. (2000) *Biotechnol Prog* **16**(2), 238-243

255. Ryu, H. W., Cho, K. S., Lee, E. G., and Chang, Y. K. (2000) *Biotechnol Prog* **16**(4), 676-679

256. Choi, J., and Lee, S. Y. (1999) *Biotechnol Bioeng* **62**(5), 546-553

257. Hahn, S. K., Chang, Y. K., Kim, B. S., and Chang, H. N. (1994) *Biotechnology and Bioengineering* **44**, 256-261

258. Anderson, A. J., and Dawes, E. A. (1990) *Microbiol Rev* **54**(4), 450-472

259. Hahn, S. K., Chang, Y. K., and Lee, S. Y. (1995) *Appl Environ Microbiol* **61**(1), 34-39

260. Holmes, P. A., and Lim, G. B. (1990) Separation process. In., Imperial Chemical Industries PLC (London, GB), United States

261. Ling, Y., Wong, H. H., Thomas, C. J., Williams, D. R., and Middelberg, A. P. (1997) *Bioseparation* **7**(1), 9-15

262. Berger, E., Ramsay, B. A., Ramsay, J. A., and Chavarie, C. (1989) *Biotechnology Techniques* **3**(4), 227-232

263. Ramsay, J. A., Berger, E., Ramsay, B. A., and Chavarie, C. (1990) *Biotechnology Techniques* **4**, 221-226

264. Kim, M., Cho, K. S., Ryu, H. W., Lee, E. G., and Chang, Y. K. (2003) *Biotechnol Lett* **25**(1), 55-59

265. Moffatt, J. G., and Khorana, H. G. (1959) *J. Am. Chem. Soc.* **81**(5), 1265-1265

266. Moffatt, J. G., and Khorana, H. G. (1961) *J. Am. Chem. Soc.* **83**, 663-675

267. Khym, J. X., Doherty, D. G., and Cohn, W. E. (1954) *J. Am. Chem. Soc.* **76**(21), 5523-5530

268. D'Ordine, R. L., Paneth, P., and Anderson, V. E. (1995) *Bioorg. Chem.* **23**, 169-181

269. Lipmann, F. (1964) Development of the acetylation problem: a personal account. In. *Nobel Lecture, Physiology or Medicine 1942-1962*, Elsevier Publishing Company, Amsterdam

270. Novelli, G. D. (1953) *Fed Proc* **12**(3), 675-681

271. Lipmann, F. (1945) *Journal of Biological Chemistry* **160**, 173-190

272. Lipmann, F., Kaplan, N. O., Novelli, G. D., Tuttle, L. C., and Guirard J., B. M. (1947) *Journal of Biological Chemistry* **167**, 869-870

273. Lipmann, F., Kaplan, N. O., Novelli, G. D., Tuttle, L. C., and Guirard, B. M. (1950) *J. Biol. Chem.* **186**(1), 235-243

274. Novelli, G. D., Kaplan, N. O., and Lipmann, F. (1950) *Federation Proceedings* **9**(1), 209-209

275. Snell, E. E., Brown, G. M., Peters, V. J., Craig, J. A., Wittle, E. L., Moore, J. A., McGlohon, V. M., and Bird, O. D. (1950) *Journal of the American Chemical Society* **72**(11), 5349 - 5350

276. Baddiley, J., and Thain, E. M. (1951) *Journal of the Chemical Society* **SEP**, 2253-2258

277. Wang, T. P., Shuster, L., and Kaplan, N. O. (1952) *J. Am. Chem. Soc.* **74**(12), 3204-3205

278. Wang, T. P., and Kaplan, N. O. (1954) *J. Biol. Chem.* **206**(1), 311-325

279. Shuster, L., and Kaplan, N. O. (1953) *J Biol Chem* **201**(2), 535-546

280. Baddiley, J., Thain, E. M., Novelli, G. D., and Lipmann, F. (1953) *Nature* **171**(4341), 76

281. Voet, D., and Voet, J. G. (2004) Chapter 21 Citric Acid Cycle. In: Harris, D., and Fitzgerald, P. (eds). *Biochemistry 3rd Edition*, John Wiley & Sons, Hoboken, NJ

282. Michelson, A. M. (1961) *Biochim. Biophys. Acta* **50**(3), 605-607

283. Michelson, A. M. (1964) *Biochim. Biophys. Acta* **93**(1), 71-77

284. Shimizu, M., Nagase, O., Okada, S., Hosokawa, Y., and Tagawa, H. (1965) *Chem. Pharm. Bull.* **13**(9), 1142-1144

285. Shimizu, M., Nagase, O., Okada, S., Hosokawa, Y., and Tagawa, H. (1967) *Chem. Pharm. Bull.* **15**(5), 655-662

286. Hashimoto, M., and Mukaiyama, T. (1972) *Chem. Lett.* **7**, 595-598

287. Taguchi, Y., Nishimura, N., Kakimoto, T., and Mushika, Y. (1976) *Bull. Chem. Soc. Jpn.* **49**(4), 1122-1125

288. Michenfelder, M., and Retey, J. (1986) *Angew. Chem., Int. Ed.* **25**(4), 366-367

289. Michenfelder, M., and Retey, J. (1986) *Angew. Chem.* **98**(4), 337-338

290. Michenfelder, M., Hull, W. E., and Retey, J. (1987) *Eur. J. Biochem.* **168**, 659-667

291. Brendelberger, V. G., Retey, J., Ashworth, D. M., Reynolds, K., Willenbrock, F., and Robinson, J. A. (1988) *Angew. Chem.* **100**, 1122-1124

292. Brendelberger, G., and Retey, J. (1988) *Angew. Chem. Int. Ed. Engl.* **27**(8), 1089-1090

293. Brendelberger, V. G., and Retey, J. (1989) *Isr. J. Chem.* **29**, 195-200

294. Wagner, A. P., and Retey, J. (1991) *Eur. J. Biochem.* **195**(3), 699-705

295. Zhao, Y., Michenfelder, M., and Retey, J. (1994) *Can. J. Chem.* **72**, 164-169

296. Stewart, C. J., and Wieland, T. (1978) *Liebigs Ann. Chem.* **1**, 57-65

297. Ciardelli, T. L., Stewart, C. J., Seeliger, A., and Wieland, T. (1981) *Liebigs Ann. Chem.* **5**, 828-841

298. Thorpe, C., Ciardelli, T. L., Stewart, C. J., and Wieland, T. (1981) *Eur. J. Biochem.* **118**, 279-282

299. Nikawa, J., Numa, S., Shiba, T., Stewart, C. J., and Wieland, T. (1978) *FEBS Lett.* **91**(1), 144-148

300. Guenther, W. H., and Mautner, H. G. (1965) *J. Am. Chem. Soc.* **87**, 2708-2716

301. Miller, T. L., Rowley, G. L., and Steward, C. J. (1966) *J. Am. Chem. Soc.* **88**(10), 2299-2304

302. Minkler, P. E., Anderson, V. E., Maiti, N. C., Kerner, J., and Hoppel, C. L. (2004) *Anal. Biochem.* **328**(2), 203-209

303. Shimizu, M., Suzuki, T., Hosokawa, Y., Nagase, O., and Abiko, Y. (1970) *Biochim. Biophys. Acta* **222**(2), 307-319

304. Mukai, J. I., Sy, J., and Lipmann, F. (1983) *Proc. Natl. Acad. Sci. U. S. A.* **80**(10), 2899-2901

305. Rossier, J. (1977) *Biochem. J.* **165**(2), 321-326

306. Frerman, F. E., Miziorko, H. M., and Beckmann, J. D. (1980) *J. Biol. Chem.* **255**(23), 11192-11198

307. Wu, D., and Hersh, L. B. (1995) *J. Biol. Chem.* **270**(49), 29111-29116

308. Banns, H., Hebb, C., and Mann, S. P. (1977) *J. Neurochem.* **29**(3), 433-437

309. Kumar, S., and Porter, J. W. (1971) *J. Biol. Chem.* **246**(24), 7780-7789

310. Poulose, A. J., and Kolattukudy, P. E. (1982) *Int J Biochem* **14**(6), 445-448

311. Bhatnagar, R. S., Schall, O. F., Jackson-Machelski, E., Sikorski, J. A., Devadas, B., Gokel, G. W., and Gordon, J. I. (1997) *Biochemistry* **36**(22), 6700-6708

312. Tracy, J. W., and Kohlhaw, G. B. (1975) *Proc. Natl. Acad. Sci. U. S. A.* **72**(5), 1802-1806

313. (1960) The Enzymes. In: Boyer, P. D., Lardy, H., and Myrback, K. (eds). *Prosthetic Groups and Cofactors (Part B)*, Academic Press, New York and London

314. Velikodvorskaia, V. V., Rabinkov, A. G., Kopelevich, V. M., Tolosa, E. A., Bulanova, L. N., and Gunar, V. I. (1990) *Biokhimiia* **55**(6), 1018-1024

315. Wang, T. P., Shuster, L., and Kaplan, N. O. (1954) *J. Biol. Chem.* **206**(1), 299-309

316. Rosenfeld, S. (1997) *J. Am. Chem. Soc.* **199**(35), 8395

317. Cobas, J. C., and Sardina, F. J. (2003) *Concept. Magn. Reson.* **19A**, 80-96

318. Mieyal, J. J., Webster, L. T., Jr., and Siddiqui, U. A. (1974) *J. Biol. Chem.* **249**(8), 2633-2640

319. Wilson, G. E., Jr., Bazzone, T. J., Kuo, C. H., and Rinaldi, P. L. (1975) *J. Am. Chem. Soc.* **97**(10), 2907-2908

320. Lee, C.-H., and Sarma, R. H. (1975) *J. Am. Chem. Soc.* **97**(5), 1225-1236

321. Patel, S. S., and Walt, D. R. (1988) *Anal. Biochem.* **170**(2), 355-360

322. Vogel, K. W., Stark, L. M., Mishra, P. K., Yang, W., and Drueckhammer, D. G. (2000) *Bioorg. Med. Chem.* **8**(10), 2451-2460

323. Voet, D., and Voet, J. G. (2004) Chapter 13 Introduction to Enzymes. In: Harris, D., and Fitzgerald, P. (eds). *Biochemistry 3rd Edition*, John Wiley & Sons, Hoboken, NJ

324. Ragg, E., Scaglioni, L., Mondelli, R., Carelli, I., Casini, A., and Tortorella, S. (1991) *Biochim Biophys Acta* **1076**(1), 49-60

325. Sogin, D. C. (1976) *J. Neurochem.* **27**(6), 1333-1337

326. BRENDA. *Brenda: The Comprehensive Enzyme Information System*, http://www.brenda.uni-koeln.de/

327. Nojiri, T., Tanaka, F., and Nakayama, I. (1971) *J. Biochem. (Tokyo, Jpn.)* **69**(4), 789-801

328. Chohan, S. N., and Copeland, L. (1998) *Appl Environ Microbiol* **64**(8), 2859-2863

329. Belova, L. L., Sokolov, A. P., Sidorov, I. A., and Trotsenko, Y. A. (1997) *FEMS Microbiology Letters* **156**, 275-279

330. Madan, V. K., Hillmer, P., and Gottschalk, G. (1973) *Eur. J. Biochem.* **32**(1), 51-56

331. Bhaskar, B., DeMoll, E., and Grahame, D. A. (1998) *Biochemistry* **37**(41), 14491-14499

332. Ramer, S. E., Raybuck, S. A., Orme-Johnson, W. H., and Walsh, C. T. (1989) *Biochemistry* **28**(11), 4675-4680

333. Raybuck, S. A., Bastian, N. R., Orme-Johnson, W. H., and Walsh, C. T. (1988) *Biochemistry* **27**(20), 7698-7702

334. Hovik, R., and Osmundsen, H. (1003) *Biochem. J.* **290**(Pt 1), 97-102

335. Peterson, K. L., and Srivastava, D. K. (1997) *Biochem J* **325 (Pt 3)**, 751-760

336. Hamilton, G. A., and Buckthal, D. J. (1982) *Bioorg. Chem.* **11**, 350-370

337. Kozlov, I. A., Milgrom, Y. M., Saburova, L. A., and Sobolev, A. (1984) *Eur. J. Biochem.* **145**(2), 413-416

338. Myrback, K., Hoek, J. B., and Ernster, L. (1976) Nicotinamide Nucleotide Transhydrogenases. In: Boyer, P. D. (ed). *The Enzymes*, Academic Press, New York and London

339. Rydstrom, J. (1972) *Eur J Biochem* **31**(3), 496-504

340. Harris, D. R., Ward, D. E., Feasel, J. M., Lancaster, K. M., Murphy, R. D., Mallet, T. C., and Crane, E. J. I. (1995) *FEBS Journal* **272**(5), 1189-1200

341. delCardayre, S. B., Stock, K. P., Newton, G. L., Fahey, R. C., and Davies, J. E. (1998) *J Biol Chem* **273**(10), 5744-5751

342. Harris, D. R., Ward, D. E., Feasel, J. M., Lancaster, K. M., Murphy, R. D., Mallet, T. C., and Crane, E. J., 3rd. (2005) *Febs J* **272**(5), 1189-1200

343. Little, C., Olinescu, R. M., and O'Brien, P. J. (1970) *Biochem. Biophys. Res. Commun.* **41**(2), 287-293

344. Mautner, H. G., Pakula, A. A., and Merrill, R. E. (1981) *Proc. Natl. Acad. Sci. U. S. A.* **78**(12), 7449-7452

345. Shimizu, M., Suzuki, T., Hosokawa, Y., Nagase, O., and Abiko, Y. (1970) *Biochem Biophys Res Commun* **38**(3), 385-392

346. Rasche, M. E., Smith, K. S., and Ferry, J. G. (1997) *J Bacteriol* **179**(24), 7712-7717

347. Iyer, P. P., and Ferry, J. G. (2001) *J. Bacteriol.* **183**(14), 4244-4250

348. Haywood, G. W., Anderson, A. J., Chu, L., and Dawes, E. A. (1988) *FEMS Microbiology Letters* **52**, 91-96

349. Tiralongo, J., Schmid, H., Thun, R., Iwersen, M., and Schauer, R. (2000) *Glycoconjugate J.* **17**(12), 849-858

350. Cebrat, M., Kim, C. M., Thompson, P. R., Daugherty, M., and Cole, P. A. (2003) *Bioorg. Med. Chem.* **11**(15), 3307-3313

351. Thauer, R. K., Kirchniawy, F. H., and Jungermann, K. A. (1972) *Eur. J. Biochem.* **27**(2), 282-290

352. Della Ragione, F., Erwin, B. G., and Pegg, A. E. (1983) *Biochem. J.* **213**(3), 707-712

353. Kelley, M., and Vessey, D. A. (1990) *J. Biochem. Toxicol.* **5**(2), 125-135

354. Day, P. J., Lewendon, A., and Shaw, W. V. (1988) *Biochem. Soc. Trans.* **16**(5), 715-716

355. Hinderer, W., and Seitz, H. U. (1985) *Arch. Biochem. Biophys.* **240**(1), 265-272

356. Hinderer, W., and Seitz, H. U. (1986) *Arch. Biochem. Biophys.* **246**(1), 217-224

357. Khalil, E. M., De Angelis, J., Ishii, M., and Cole, P. A. (1999) *Proc. Natl. Acad. Sci. U. S. A.* **96**(22), 12418-12423

358. Bhatnagar, R. S., Jackson-Machelski, E., McWherter, C. A., and Gordon, J. I. (1994) *J Biol Chem* **269**(15), 11045-11053

359. Boyer, P. D., Lardy, H., and Myrback, K. (1960) The Enzymes. In: Boyer, P. D. (ed). *Prosthetic Groups and Cofactors (Part B)*, Academic Press, New York and London

360. Vogel, H. J., and Bridger, W. A. (1981) *J Biol Chem* **256**(22), 11702-11707

361. Kloster, G., and Eggerer, H. (1975) *Anal. Biochem.* **65**(1-2), 389-395

362. Miernyk, J. A., and Trelease, R. N. (1981) *Phytochemistry (Elsevier)* **20**(12), 2657-2663

363. Miziorko, H. M., Clinkenbeard, K. D., Reed, W. D., and Lane, M. D. (1975) *J Biol Chem* **250**(15), 5768-5773

364. Middleton, B. (1972) *Biochem J* **126**(1), 35-47

365. Halvorsen, O., and Skrede, S. (1982) *Eur. J. Biochem.* **124**(1), 211-215

366. Fisher, M. N., Robishaw, J. D., and Neely, J. R. (1985) *J. Biol. Chem.* **260**(29), 15745-15751

367. Vallari, D. S., Jackowski, S., and Rock, C. O. (1987) *J Biol Chem* **262**(6), 2468-2471

368. Quadri, L. E., Weinreb, P. H., Lei, M., Nakano, M. M., Zuber, P., and Walsh, C. T. (1998) *Biochemistry* **37**(6), 1585-1595

369. McAllister, K. A., Peery, R. B., Meier, T. I., Fischl, A. S., and Zhao, G. (2000) *J Biol Chem* **275**(40), 30864-30872

370. Whitty, A., Fierke, C. A., and Jencks, W. P. (1995) *Biochemistry* **34**(37), 11678-11689

371. Dimroth, P., Loyal, R., and Eggerer, H. (1977) *Eur. J. Biochem.* **80**(2), 479-488

372. Buckel, W., Dorn, U., and Semmler, R. (1981) *Eur. J. Biochem.* **118**(2), 315-321

373. Damuni, Z., and Reed, L. J. (1987) *J. Biol. Chem.* **262**(11), 5133-5138

374. Yamakawa, N., Shimeno, H., Soeda, S., and Nagamatsu, A. (1990) *Biochim. Biophys. Acta* **1037**(3), 302-306

375. Mukai, J. (1984) *Nucleic Acids Symp Ser* (15), 77-80

376. Anke, H., and Spector, L. B. (1975) *Biochem. Biophys. Res. Commun.* **67**(2), 767-773

377. Banns, H., Hebb, C., and Mann, S. P. (1978) *J. Neurochem.* **30**(4), 915-916

378. Biriukov, A. I., Zhukov Iu, N., Kopelevich, V. M., Bulanova, L. N., and Gunar, V. I. (1993) *Bioorg Khim* **19**(9), 905-911

379. Tanaka, T., Hosaka, K., and Numa, S. (1981) *Methods Enzymol.* **71 Pt C**, 334-341

380. Hosaka, K., Mishina, M., Kamiryo, T., and Numa, S. (1981) *Methods Enzymol.* **71**, 325-333

381. Tanaka, T., Hosaka, K., Hoshimaru, M., and Numa, S. (1979) *Eur. J. Biochem.* **98**(1), 165-172

382. Cha, S. (1969) *Methods Enzymol.* **13**, 62-69

383. Cha, S., Cha, C. J., and Parks, R. E., Jr. (1967) *J Biol Chem* **242**(11), 2577-2581

384. Siewecke, H. J., and Leistner, E. (1991) *Z. Naturforsch., C: J. Biosci.* **46**, 585-590

385. Scrutton, M. C. (1974) *J. Biol. Chem.* **249**(22), 7057-7067

386. Lent, B. A., and Kim, K. H. (1983) *Arch. Biochem. Biophys.* **225**(2), 964-971

387. Nikawa, J.-i., Tanabe, T., Ogiwara, H., Shiba, T., and Numa, S. (1979) *FEBS Letters* **102**(2), 223-226

388. Griebel, R., Smith, Z., and Merrick, J. M. (1968) *Biochemistry* **7**(10), 3676-3681

389. Liebergesell, M., Sonomoto, K., Madkour, M., Mayer, F., and Steinbuchel, A. (1994) *Eur J Biochem* **226**(1), 71-80

390. Istvan, E. S., and Deisenhofer, J. (2000) *Biochim Biophys Acta* **1529**(1-3), 9-18

391. Istvan, E. S., Palnitkar, M., Buchanan, S. K., and Deisenhofer, J. (2000) *Embo J* **19**(5), 819-830

392. Barycki, J. J., O'Brien, L. K., Strauss, A. W., and Banaszak, L. J. (2000) *J Biol Chem* **275**(35), 27186-27196

393. Djordjevic, S., Pace, C. P., Stankovich, M. T., and Kim, J. J. (1995) *Biochemistry* **34**(7), 2163-2171

394. Kim, J. J., and Wu, J. (1988) *Proc Natl Acad Sci U S A* **85**(18), 6677-6681

395. Kim, J. J., Wang, M., and Paschke, R. (1993) *Proc Natl Acad Sci U S A* **90**(16), 7523-7527

396. Tiffany, K. A., Roberts, D. L., Wang, M., Paschke, R., Mohsen, A. W., Vockley, J., and Kim, J. J. (1997) *Biochemistry* **36**(28), 8455-8464

397. Hall, P. R., Wang, Y. F., Rivera-Hainaj, R. E., Zheng, X., Pustai-Carey, M., Carey, P. R., and Yee, V. C. (2003) *Embo J* **22**(10), 2334-2347

398. Govindasamy, L., Pedersen, B., Lian, W., Kukar, T., Gu, Y., Jin, S., Agbandje-McKenna, M., Wu, D., and McKenna, R. (2004) *J Struct Biol* **148**(2), 226-235

399. Jogl, G., and Tong, L. (2003) *Cell* **112**(1), 113-122

400. Iyer, P. P., Lawrence, S. H., Luther, K. B., Rajashankar, K. R., Yennawar, H. P., Ferry, J. G., and Schindelin, H. (2004) *Structure (Camb)* **12**(4), 559-567

401. Kursula, P., Ojala, J., Lambeir, A. M., and Wierenga, R. K. (2002) *Biochemistry* **41**(52), 15543-15556

402. Modis, Y., and Wierenga, R. K. (2000) *J Mol Biol* **297**(5), 1171-1182

403. Modis, Y., and Wierenga, R. K. (1999) *Structure Fold Des* **7**(10), 1279-1290

404. Kursula, P., Sikkila, H., Fukao, T., Kondo, N., and Wierenga, R. K. (2005) *J Mol Biol* **347**(1), 189-201

405. Wang, X. G., Olsen, L. R., and Roderick, S. L. (2002) *Structure (Camb)* **10**(4), 581-588

406. Clements, A., Rojas, J. R., Trievel, R. C., Wang, L., Berger, S. L., and Marmorstein, R. (1999) *Embo J* **18**(13), 3521-3532

407. Lin, Y., Fletcher, C. M., Zhou, J., Allis, C. D., and Wagner, G. (1999) *Nature* **400**(6739), 86-89

408. Becker, A., and Kabsch, W. (2002) *J Biol Chem* **277**(42), 40036-40042

409. Ferrer, J. L., Jez, J. M., Bowman, M. E., Dixon, R. A., and Noel, J. P. (1999) *Nat Struct Biol* **6**(8), 775-784

410. Jez, J. M., Ferrer, J. L., Bowman, M. E., Dixon, R. A., and Noel, J. P. (2000) *Biochemistry* **39**(5), 890-902

411. Wolf, E., Vassilev, A., Makino, Y., Sali, A., Nakatani, Y., and Burley, S. K. (1998) *Cell* **94**(4), 439-449

412. Bhatnagar, R. S., Futterer, K., Farazi, T. A., Korolev, S., Murray, C. L., Jackson-Machelski, E., Gokel, G. W., Gordon, J. I., and Waksman, G. (1998) *Nat Struct Biol* **5**(12), 1091-1097

413. Beaman, T. W., Blanchard, J. S., and Roderick, S. L. (1998) *Biochemistry* **37**(29), 10363-10369

414. Russell, R. J., Ferguson, J. M., Hough, D. W., Danson, M. J., and Taylor, G. L. (1997) *Biochemistry* **36**(33), 9983-9994

415. Russell, R. J., Gerike, U., Danson, M. J., Hough, D. W., and Taylor, G. L. (1998) *Structure* **6**(3), 351-361

416. Smith, C. V., Huang, C. C., Miczak, A., Russell, D. G., Sacchettini, J. C., and Honer zu Bentrup, K. (2003) *J Biol Chem* **278**(3), 1735-1743

417. Yun, M., Park, C. G., Kim, J. Y., Rock, C. O., Jackowski, S., and Park, H. W. (2000) *J Biol Chem* **275**(36), 28093-28099

418. Olsen, L. R., and Roderick, S. L. (2001) *Biochemistry* **40**(7), 1913-1921

419. Parris, K. D., Lin, L., Tam, A., Mathew, R., Hixon, J., Stahl, M., Fritz, C. C., Seehra, J., and Somers, W. S. (2000) *Structure Fold Des* **8**(8), 883-895

420. Reuter, K., Mofid, M. R., Marahiel, M. A., and Ficner, R. (1999) *Embo J* **18**(23), 6823-6831

421. Ricagno, S., Jonsson, S., Richards, N., and Lindqvist, Y. (2003) *Embo J* **22**(13), 3210-3219

422. Thoden, J. B., Zhuang, Z., Dunaway-Mariano, D., and Holden, H. M. (2003) *J Biol Chem* **278**(44), 43709-43716

423. Benning, M. M., Taylor, K. L., Liu, R. Q., Yang, G., Xiang, H., Wesenberg, G., Dunaway-Mariano, D., and Holden, H. M. (1996) *Biochemistry* **35**(25), 8103-8109

424. Benning, M. M., Haller, T., Gerlt, J. A., and Holden, H. M. (2000) *Biochemistry* **39**(16), 4630-4639

425. Mancia, F., Keep, N. H., Nakagawa, A., Leadlay, P. F., McSweeney, S., Rasmussen, B., Bosecke, P., Diat, O., and Evans, P. R. (1996) *Structure* **4**(3), 339-350

426. Gulick, A. M., Starai, V. J., Horswill, A. R., Homick, K. M., and Escalante-Semerena, J. C. (2003) *Biochemistry* **42**(10), 2866-2873

427. Fraser, M. E., James, M. N., Bridger, W. A., and Wolodko, W. T. (1999) *J Mol Biol* **285**(4), 1633-1653

428. Wolodko, W. T., Fraser, M. E., James, M. N., and Bridger, W. A. (1994) *J Biol Chem* **269**(14), 10883-10890

429. Pan, H., Tsai, S., Meadows, E. S., Miercke, L. J., Keatinge-Clay, A. T., O'Connell, J., Khosla, C., and Stroud, R. M. (2002) *Structure (Camb)* **10**(11), 1559-1568

430. Sugantino, M., and Roderick, S. L. (2002) *Biochemistry* **41**(7), 2209-2216

431. Stenmark, P., Gurmu, D., and Nordlund, P. (2004) *Biochemistry* **43**(44), 13996-14003

432. Beaman, T. W., Sugantino, M., and Roderick, S. L. (1998) *Biochemistry* **37**(19), 6689-6696

433. Burns, K. L., Gelbaum, L. T., Sullards, M. C., Bostwick, D. E., and May, S. W. (2005) *Iso-coenzyme A(Book)*

434. Ingebretsen, O. C., Normann, P. T., and Flatmark, T. (1979) *Anal. Biochem.* **96**(1), 181-188

435. Wang, H. Y., Baxter, C. F., Jr., and Schulz, H. (1991) *Arch. Biochem. Biophys.* **289**(2), 274-280

436. Hermans-Lokkerbol, A., Heijden, R., and Verpoorte, R. (1996) *J. Chromatogr., A* **752**, 123-130

437. Tachibana, A., Yano, Y., Otani, S., and Taniguchi, M. (1998) *J. Ferment. Bioeng.* **86**(5), 523-526

438. Shimazu, M., Vetcher, L., Galazzo, J. L., Licari, P., and Santi, D. V. (2004) *Anal. Biochem.*

439. Sawata, S., and Komiyama, M. (1992) *J. Phys. Org. Chem.* **5**, 502-506

440. Komiyama, M., Sawata, S., and Takeshige, Y. (1992) *J. Am. Chem. Soc.* **114**(3), 1070-1074

441. Shuster, L., and Kaplan, N. O. (1955) *J. Biol. Chem.* **215**(1), 183-194

442. Oivanen, M., and Lonnberg, H. (1989) *J. Org. Chem.* (54), 2556-2560

443. Oivanen, M., Schnell, R., Pfleiderer, W., and Lonnberg, H. (1990) *J. Org. Chem.* **56**, 3623-3628

444. Mikhailov, S. N., Oivanen, M., Oksman, P., and Lonnberg, H. (1992) *J. Org. Chem.* **57**, 4122-4126

445. Buyske, D. M., Handschumacher, R. E., Higgins, H., King, T. E., Strong, F. M., Cheldelin, V. H., Teply, L. J., and Mueller, G. C. (1951) *J. Biol. Chem.* **193**(1), 307-316

446. Beinert, H., Von Korff, R. W., Green, D. E., Buyske, D. A., Handschumacher, R. E., Higgins, H., and Strong, F. M. (1952) *J. Am. Chem. Soc.* **74**, 854-855

447. Stadtman, E. R., and Kornberg, A. (1953) *J. Biol. Chem.* **203**(1), 47-54

448. Beinert, H., Von Korff, R. W., Green, D. E., Buyske, D. A., Handschumacher, R. E., Higgins, H., and Strong, F. M. (1953) *J. Biol. Chem.* **200**(1), 385-400

449. Kurooka, S., Hosoki, K., and Yoshimura, Y. (1967) *Chem. Pharm. Bull.* **15**(7), 944-948

450. Mitsugi, K., Nakazawa, E., Takahash, M., and Yamada, H. (1964) *Agricultural and Biological Chemistry* **28**(12), 859

451. Mitsugi, K., Takahashi, M., Yamada, H., and Nakazawa, E. (1964) *Agricultural and Biological Chemistry* **28**(8), 571

452. Lee, J., Gravel, M., Gao, E., O'Neill, R. C., and Braun, P. E. (2001) *J. Biol. Chem.* **276**(18), 14804-14813

453. Mazumder, R., Iyer, L. M., Vasudevan, S., and Aravind, L. (2002) *Nucleic Acids Res.* **30**(23), 5229-5243

454. Kozlov, G., Lee, J., Elias, D., Gravel, M., Gutierrez, P., Ekiel, I., Braun, P. E., and Gehring, K. (2003) *J. Biol. Chem.* **278**(46), 46021-46028

455. Sakamoto, Y., Tanaka, N., Ichimiya, T., Kurihara, T., and Nakamura, K. T. (2005) *J Mol Biol* **346**(3), 789-800

456. Abelson, J., Trotta, C. R., and Li, H. (1998) *J Biol Chem* **273**(21), 12685-12688

457. Nasr, F., and Filipowicz, W. (2000) *Nucleic Acids Res* **28**(8), 1676-1683

458. Tyc, K., Kellenberger, C., and Filipowicz, W. (1987) *J Biol Chem* **262**(27), 12994-13000

459. Culver, G. M., McCraith, S. M., Zillmann, M., Kierzek, R., Michaud, N., LaReau, R. D., Turner, D. H., and Phizicky, E. M. (1993) *Science (Washington, DC, U. S.)* **261**(5118), 206-208

460. Culver, G. M., Consaul, S. A., Tycowski, K. T., Filipowicz, W., and Phizicky, E. M. (1994) *J Biol Chem* **269**(40), 24928-24934

461. Genschik, P., Hall, J., and Filipowicz, W. (1997) *J Biol Chem* **272**(20), 13211-13219

462. Shull, N. P., Spinelli, S. L., and Phizicky, E. M. (2005) *Nucleic Acids Res* **33**(2), 650-660

463. Schwer, B., Sawaya, R., Ho, C. K., and Shuman, S. (2004) *Proc Natl Acad Sci U S A* **101**(9), 2788-2793

464. Culver, G. M., McCraith, S. M., Consaul, S. A., Stanford, D. R., and Phizicky, E. M. (1997) *J Biol Chem* **272**(20), 13203-13210

465. Zillman, M., Gorovsky, M. A., and Phizicky, E. M. (1992) *J Biol Chem* **267**(15), 10289-10294

466. *Press Release: The 1971 Nobel Prize in Physiology or Medicine*, http://nobelprize.org/medicine/laureates/1971/press.html

467. Clapper, D. L., Walseth, T. F., Dargie, P. J., and Lee, H. C. (1987) *J Biol Chem* **262**(20), 9561-9568

468. Lee, H. C., Walseth, T. F., Bratt, G. T., Hayes, R. N., and Clapper, D. L. (1989) *J. Biol. Chem.* **264**(3), 1608-1615

469. Lee, H. C., and Aarhus, R. (1995) *J. Biol. Chem.* **270**(5), 2152-2157

470. Billington, R. A., Thuring, J. W., Conway, S. J., Packman, L., Holmes, A. B., and Genazzani, A. A. (2004) *Biochem. J.* **378**(Pt 1), 275-280

471. Churamani, D., Carrey, E. A., Dickinson, G. D., and Patel, S. (2004) *Biochem. J.* **Pt**

472. Vu, C. Q., Lu, P. J., Chen, C. S., and Jacobson, M. K. (1996) *J. Biol. Chem.* **271**(9), 4747-4754

473. Vu, C. Q., Coyle, D. L., and Jacobson, M. K. (1997) *Biochem. Biophys. Res. Commun.* **236**(3), 723-726

474. Ziegler, M. (2000) *Eur J Biochem* **267**(6), 1550-1564

475. Galione, A., and Churchill, G. C. (2002) *Cell Calcium* **32**(5-6), 343-354

476. Zhang, F.-J., Gu, Q.-M., Jing, P., and Sih, C. J. (1995) *Bioorganic & Medicinal Chemistry Letters* **5**(19), 2267-2272

477. Guse, A. H., da Silva, C. P., Weber, K., Armah, C. N., Ashamu, G. A., Schulze, C., Potter, B. V., Mayr, G. W., and Hilz, H. (1997) *Eur J Biochem* **245**(2), 411-417

478. Aarhus, R., Graeff, R. M., Dickey, D. M., Walseth, T. F., and Lee, H. C. (1995) *J Biol Chem* **270**(51), 30327-30333

479. Guse, A. H., Cakir-Kiefer, C., Fukuoka, M., Shuto, S., Weber, K., Bailey, V. C., Matsuda, A., Mayr, G. W., Oppenheimer, N., Schuber, F., and Potter, B. V. (2002) *Biochemistry* **41**(21), 6744-6751

480. Voet, D., and Voet, J. G. (2004) Chapter 23-4 The Pentose Phosphate Pathway. In: Harris, D., and Fitzgerald, P. (eds). *Biochemistry 3rd Edition*, John Wiley & Sons, Hoboken, NJ

481. Chini, E. N., Beers, K. W., and Dousa, T. P. (1995) *J Biol Chem* **270**(7), 3216-3223

482. Patel, S. (2004) *Biol Cell* **96**(1), 19-28

483. Cancela, J. M., Charpentier, G., and Petersen, O. H. (2003) *Pflugers Arch* **446**(3), 322-327

484. Churchill, G. C., Okada, Y., Thomas, J. M., Genazzani, A. A., Patel, S., and Galione, A. (2002) *Cell* **111**(5), 703-708

485. Churamani, D., Dickinson, G. D., and Patel, S. (2005) *Biochem J* **386**(Pt 3), 497-504

486. Billington, R. A., Thuring, J. W., Conway, S. J., Packman, L., Holmes, A. B., and Genazzani, A. A. (2004) *Biochem J* **378**(Pt 1), 275-280

487. Voet, D., and Voet, J. G. (2004) Chapter 28 Nucleotide Metabolism. In: Harris, D., and Fitzgerald, P. (eds). *Biochemistry 3rd Edition*, John Wiley & Sons, Hoboken, NJ

488. Voet, D., and Voet, J. G. (2004) Chapter 28 Nucleotide Metabolism. In: Harris, D., and Fitzgerald, P. (eds). *Biochemistry 3rd Edition*, John Wiley & Sons, Hoboken, NJ

489. Arteel, G. E., and Sies, H. (2001) *Environmental Toxicology and Pharmacology* **10**, 153-158

490. Klotz, L. O., and Sies, H. (2003) *Toxicol Lett* **140-141**, 125-132

491. Ducrocq, C., Blanchard, B., Pignatelli, B., and Ohshima, H. (1999) *Cell Mol Life Sci* **55**(8-9), 1068-1077

492. Arteel, G. E., Briviba, K., and Sies, H. (1999) *FEBS Lett* **445**(2-3), 226-230

493. Quijano, C., Alvarez, B., Gatti, R. M., Augusto, O., and Radi, R. (1997) *Biochem J* **322 (Pt 1)**, 167-173

494. Masumoto, H., and Sies, H. (1996) *Chem Res Toxicol* **9**(1), 262-267

495. Briviba, K., Roussyn, I., Sharov, V. S., and Sies, H. (1996) *Biochem J* **319 (Pt 1)**, 13-15

496. Roussyn, I., Briviba, K., Masumoto, H., and Sies, H. (1996) *Arch Biochem Biophys* **330**(1), 216-218

497. Woznichak, M. M., Overcast, J. D., Robertson, K., Neumann, H. M., and May, S. W. (2000) *Arch Biochem Biophys* **379**(2), 314-320

498. May, S. W., Wang, L., Gill-Woznichak, M. M., Browner, R. F., Ogonowski, A. A., Smith, J. B., and Pollock, S. H. (1997) *J Pharmacol Exp Ther* **283**(2), 470-477

499. May, S. W., Herman, H. H., Roberts, S. F., and Ciccarello, M. C. (1987) *Biochemistry* **26**(6), 1626-1633

500. Herman, H. H., Pollock, S. H., Fowler, L. C., and May, S. W. (1988) *J Cardiovasc Pharmacol* **11**(5), 501-510

501. May, S. W., and Phillips, R. S. (1980) *Journal of the American Chemical Society* **102**(18), 5981 - 5983

502. Koppenol, W. H., Kissner, R., and Beckman, J. S. (1996) *Methods Enzymol* **269**, 296-302

503. Hughs, M. N., and Nicklin, H. G. (1971) *Journal of the Chemical Society A: Inorganic, Physical, Theoretical*, 164-168

504. Benton, D. J., and Moore, P. (1970) *J. Chem. Soc., A*, 3179-3182

505. Zhang, H., Joseph, J., Feix, J., Hogg, N., and Kalyanaraman, B. (2001) *Biochemistry* **40**(25), 7675-7686

506. Beckman, J. S. (1996) *Chem Res Toxicol* **9**(5), 836-844

507. Murakami, M., and Kudo, I. (2004) *Prog Lipid Res* **43**(1), 3-35

508. Cutler, S. J., DeWitt Blanton, C., Jr., Akin, D. T., Steinberg, F. B., Moore, A. B., Lott, J. A., Price, T. C., May, S. W., and Pollock, S. H. (1998) *Inflamm Res* **47**(7), 316-324

509. Warner, T. D., and Mitchell, J. A. (2004) *Faseb J* **18**(7), 790-804

510. Smith, W. L., DeWitt, D. L., and Garavito, R. M. (2000) *Annu Rev Biochem* **69**, 145-182

511. Smith, W. L., Garavito, R. M., and DeWitt, D. L. (1996) *J Biol Chem* **271**(52), 33157-33160

512. Grosser, T., Fries, S., and FitzGerald, G. A. (2006) *J Clin Invest* **116**(1), 4-15

513. Ostor, A. J., and Hazleman, B. L. (2005) *Inflammopharmacology* **13**(4), 371-380

514. Rainsford, K. D. (2005) *Inflammopharmacology* **13**(4), 331-341

515. Smith, W. L., and Langenbach, R. (2001) *J Clin Invest* **107**(12), 1491-1495